Anaerobic digestion of algal biomass for bioenergy production- a feasibility study

MSc Thesis

Compiled by: Alister Edward Inglesby

Supervisors: Dr R P van Hille and Prof S T L Harrison

2011

[1]Department of Chemical Engineering, University of Cape Town, Rondebosch, South Africa

Declaration:

The work described in this dissertation was carried out in the Department of Chemical Engineering, University of Cape Town, between January 2010 and September 2010. It is the original and independent work of the author, except where specifically acknowledged in the text. Neither the present dissertation, nor any part thereof, has been submitted to any other university. This dissertation contains 45 320 words.

Alister Edward Inglesby Department of Chemical Engineering, University of Cape Town, February 2011

Acknowledgements:

I wish to acknowledge my supervisor, Dr Rob van Hille, and co-supervisor, Prof Sue Harrison, for all their help, support and guidance during my MSc. Their efforts are much appreciated. Furthermore, I acknowledge my colleagues in the CeBER group; Ms Fran Poccok, Ms Sue Jobson, Mr Gary Dicks and Dr Seun Oyekola for all their input to my project.

Finally, I would like to express my gratitude to the Nation Research Foundation and the Department of Chemical Engineering for providing financial support.

Abstract

In the post-fossil era, biomass, a renewable storehouse of unlimited solar power, presents the only organic carbon source available as raw material for production of various fuels. Apart from the ever more decreasing level of available fossil fuels, interest in renewable energies has been kindled by the threat of global warming and related potential mitigation of carbon dioxide emissions through the use of non-fossil energy resources. Chang et al. (2010) highlight the need for sustainable development such that new solutions are identified to decrease today's rapid consumption of non-renewable resources (petroleum, natural gas, coal and minerals).

Biomass can be derived from cultivation of dedicated energy crops; by harvesting forestry and other plant residues; and from biomass wastes. Microalgae have emerged as a potential source for biomass due to their productivity, lipid content and CO_2 fixation ability. They have been shown to be more photosynthetically efficient than higher plants and can be grown in a simple salts medium on a large scale. Algal biomass can be used directly, converted into ethanol, methanol, hydrogen, methane, or lipids extracted to produce fuel oils.

AD technology is well developed, cost efficient and can be easily implemented in developing countries. Biogas production has become a very topical subject, with many European nations introducing initiatives to increase biogas production. AD of algal biomass was studied in detail during the 1980's, however, with the current drive toward cleaner technology processes, there has been a renewed interest in the technology.

This study investigated the feasibility of using algal biomass as a feedstock for AD. Batch digestion studies were conducted as a data gathering tool and the information obtained implemented in the initiation of a semi-continuous anaerobic digester. The strains that were identified for investigation were the microalga *Scenedesmus spp.* and the cyanobacterium *Spirulina spp. Scenedesmus* was selected as it has been identified as a potential source of lipids for biodiesel production, while *Spirulina* has been successfully cultivated at industrial scale, where its structure and physiology provide advantages in terms of provision of carbon for growth and ease of harvesting. In addition, previous work using *Spirulina* has resulted in the highest methane yields amongst microalgal substrates tested.

Four key areas of study were identified and experimentally investigated. These were the feasibility of anaerobic digestion of the aforementioned algal strains, the effect of mechanical pre-treatment on the efficiency of digestion, the feasibility of digesting the residue that remains after direct transesterification

(DT) of *Scenedesmus* for biodiesel production and finally the development of an integrated algal anaerobic digestion system using *Spirulina* as the sole feedstock.

Mesophilic batch phase digestion of whole cell *Spirulina* conducted in 1 L digesters for a period of 64 days resulted in a higher productivity and final yield of methane (maximum yield 113 m^3 CH_4/ton VS and productivity 0.175 L $CH_4/L_{reactor}$.day) compared to the digestion of whole cell *Scenedesmus* (max yield 55 m^3 CH_4/ton VS and 0.067 L $CH_4/L_{reactor}$.day). This was a direct result of the amount of acetic acid produced by acetogenic organisms and its subsequent conversion to methane. The increased acetic acid available for consumption by methanogens in the *Spirulina*-fed digesters was influenced by the structure and composition of the cell wall.

The disruption studies showed that *Spirulina* cells disrupted more easily than *Scenedesmus* cells. This was attributed the sensitivity of *Spirulina* cells to osmotic shock, the composition of the cell wall and the filamentous nature of the biomass. *Scenedesmus* cells required an extended period to disrupt, as the rigid cell has a wall is made up of biopolymers (primarily cellulose) that are resistant to degradation. The final methane yields (m^3 CH_4/ton VS) obtained from digestion with the inclusion of mechanical pre-treatment showed a 47% increase for *Spirulina* compared to 76% for *Scenedesmus*-fed digesters.

Batch phase digestion of the residue remaining from DT of *Scenedesmus* proved to have poor reproducibility. Only one digester could be used in results analysis. The poor reproducibility was attributed to the sensitivity of the anaerobic consortia to toxic compounds potentially remaining after DT. The methane yield obtained from the DT residue digester (75 m^3 CH_4/ton VS) was lower than the ruptured cell digesters, but higher than the whole cell digesters, due to the partial disruption of cells during DT. It is recommended that further research be conducted into the feasibility of digesting the residual biomass after DT for an optimised DT process.

The concept of developing an integrated, algal anaerobic digestion system using *Spirulina* as the feed stock was proven. Based on the experimental data, the following operating conditions were recommended for semi-continuous digestion of *Spirulina*: S_0 = 5 kg/m^3, retention period 30 days and OLR 0.8 g $VS/L_{reactor}$.day. Under these conditions, a lower production of VFA's is expected, but for an extended period of time. This would reduce the possibility of VFA accumulation (pH reduction) and excessive ammonia and sulphide release, thereby reducing inhibition of the methanogenic consortia. The temperature should be maintained in the mesophilic range as thermophilic anaerobic microbial consortia have been reported to be very sensitive and so relatively more prone to inhibition.

The net energy yields in terms of GJ/ha.year from anaerobic digestion of whole cell *Spirulina* were greater than that of *Scenedesmus*. This originated from the higher methane, faster productivity (75 tons DW/ ha.year) as well as the ease at which *Spirulina* can be harvested (low energy input for biomass generation estimated at less than 20 GJ/ha.year). To compete with first generation energy crops, *Spirulina* productivity needed to exceed 75 ton DW/ha.year at an energy input less than 20 GJ/ha.year.The result for *Scenedesmus* was less encouraging and particularly given the challenges associated with harvesting unicellular organisms as well as CO_2 provision through direct gas liquid mass transfer. This suggests bioenergy

production through AD of whole cell *Scenedesmus* is not energetically favourable. However, microalgae offer several additional benefits associated with their intrinsic characteristics (CO_2 fixation, use of non-arable land etc. (Sialve et al., 2009)). These properties may allow for lower net energy productivities to be acceptable.

The projected net energy productivity, in terms of GJ/ha.year, for anaerobic digestion of ruptured *Spirulina* remained greater than that of ruptured *Scenedesmus*. This is accounted for by the higher methane yields (m^3 CH_4/ton VS), the greater productivity (tons DW/ ha.year) and the reduced energy required for disruption.

The projected net energy productivity of anaerobic digestion of *Scenedesmus*, as a stand-alone technology, was lower than that of the integrated biodiesel-AD system. It is recommended that a full experimental analysis be conducted on the two processes and a detailed energy evaluation be made to arrive at a final conclusion as to whether or not biodiesel and biogas production should be integrated or whether biogas production should stand-alone as bioenergy production process. The beneficiation of the residual biomass is critical in making microalgal biodiesel production energetically feasible, so obtaining a full understanding of all potential issues that relate to its digestion requires attention.

In summary it can be said that *Spirulina* definitely has the opportunity to be utilised in an AD process to produce a competitive amount of energy relative to traditional and second generation energy crops. This study has shown that with the high growth yields, high CO_2 sequestrations, easy harvesting methods an energy efficient process can be designed using the algae as the sole feed stock.

Contents

List of Figures

List of Tables

Nomenclature

Symbol	Description	Units
COD	Chemical oxygen demand	mg COD/L
OLR	Organic loading rate	g VS/$L_{reactor}$.day
HRT	Hydraulic retention time	days
SRT	Solid retention time	days
Y_{NH_3-N}	Ammonia nitrogen yield	mg/g TS
Y_{CH_4}	Theoretical Methane yield	m^3CH_4 / kg VS
VSd/deg	Volatile solids degraded	kg
pK_a	Acid dissociation constant	Dimensionless
C_i	Concentration of compound i	g/L
IA	Integrated area	mV or AU/minute
ΔH_{vap}	Heat of vaporisation	J/ mol or kJ/kmol
LHV	Lower heating value	MJ/m^3 or MJ/kg
DS	Dry solids	kg
B_0	Ultimate methane yield	m^3CH_4 / kg TS
S_0	Initial substrate loading	g/L or kg VS/m^3
SMY	Specific methane yield	m^3CH_4 / ton VS
p_i	Partial pressure	KPa or Bar
V	Volume	m^3 or L or mL
E	Energy recovery	MJ/kg VS

Abbreviations

Symbol	Description
AD	Anaerobic digestion
MP	Methane producers
rpm	Revolutions per minute
SRB	Sulphate reducting bacteria
TS	Total solids
UTEX	University of Texas
VS	Volatile solids

Glossary

Term	Description
Anaerobic:	The absence of oxygen
Biogenic:	Derived from biological as opposed to fossil sources
Biomass:	Lignocellulosic plant or algal material i.e. wood agricultural residues and energy crops
Chemical oxygen demand (COD):	COD expresses the amount of oxygen originating from potassium dichromate that reacts with the oxidisable substances contained in 1 l of a specific liquid sample. The value is representative of the amount of potential degradable organic compounds solubilised in the liquid phase.
Combined heat and power:	The concomitant generation of electricity and heat
Energy yield:	Ratio of amount of energy produced by the process relative to that required by the process
First generation biofuels:	Biofuels which are produced from a single storage product of the plant. (e.g. seed oil)
Flame ionisation detection (FID):	A device in which the measured change in conductivity of a standard flame (hydrogen) due to the insertion of another gas vapour is used to detect the gas or vapour.
Gas chromatography (GC):	Chromatography in which the substance to be separated into its components is diffused with a carrier gas through a liquid or solid adsorbent for differential adsorption.
High performance liquid chromatography (HPLC):	A form of column chromatography in which the column holds chromatographic packing material (stationary phase). Mobile phase moves through the column and a detector shows the retention time of the molecules. Retention time varies depending on the interaction between stationary phase molecules and solvent.
Lower heating value:	Amount of energy released on combustion of a fuel, after returning the products to 150°C, combustion products are CO_2 and H_2O in the vapour phase.
Lignocellulosic:	Plant biomass that is composed of cellulose, hemicellulose, and lignin

Term	Description
Osmotic shock	A sudden change in the solute concentration around a cell, causing a rapid change in the movement of water across its cell membrane and so osmotic pressure
Second generation biofuels:	Biofuels which are produced from lignocellulosic material, algae or biogenic waste streams
Transesterification	The process of exchanging the organic group R" of an ester with the organic group R' of an alcohol. These reactions are often catalyzed by the addition of an acid or base catalyst. The reaction can also be accomplished with the help of enzymes (biocatalyst), particularly lipases
Volatile solids:	The organic fraction of a biogenic stream which can be degraded by microbial action. These solids are lost on ignition at 550°C

Chapter 1

Introduction

The history of energy production has passed through the pre-fossil era to the current short-oil fossil era (Chang et al., 2010). It has been stated that we now have to prepare for the arrival of the post-fossil era, when fossil fuel will no longer play an important role in the energy sector (Figure 1.1).

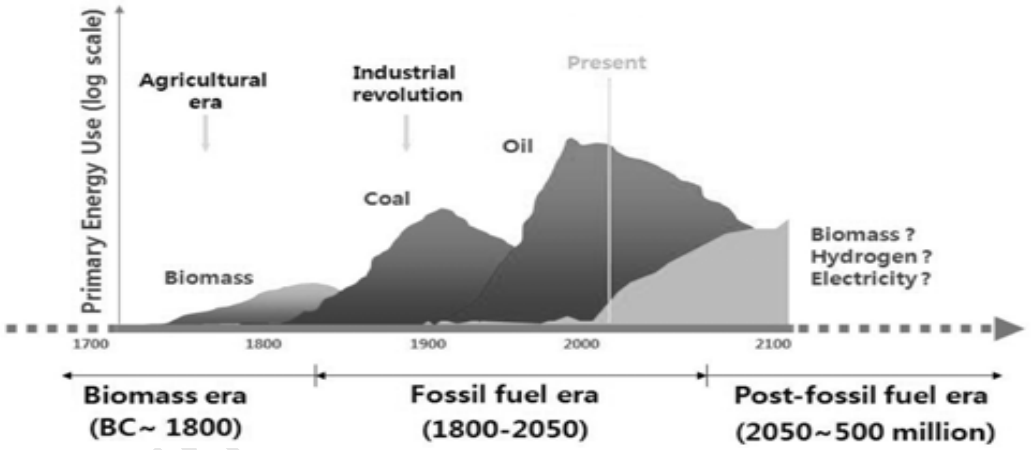

Figure 1.1: History of energy resources use (Chang et al., 2010)

In the post-fossil era, biomass, a renewable storehouse of unlimited solar power, presents the only organic carbon source available as raw material for production of various fuels. Apart from the ever more decreasing level of available fossil fuels, interest in renewable energies has been kindled by the threat of global warming and related potential mitigation of carbon dioxide emissions through the use of non-fossil energy resources. Chang et al. (2010) highlight the need for sustainable development such that new solutions are identified to decrease today's rapid consumption of non-renewable resources (petroleum, natural gas, coal and minerals).

The amount of energy potential from renewable technologies far exceeds the annual energy consumption (Table 1.1). The major task, however, is to make these renewable energies economically viable.

Table 1.1: Global exergy flow (Chang et al., 2010)

Renewables			Non-renewables		
Source	Potential (TW)	Current use (TW)	Source	Potential (ZJ)	Current use (TW)
Solar	86,000	0.016	Coal	270	3.6
Wind	870	0.06	Oil	110	5.0
Biomass	90 (65 from terrestrial, 25 from ocean)	traditional: 1.2 biofuel: 0.15	Natural gas	50	3.2
Hydro-electricity	5.4	0.36	Methane hydrate	200	–
Others	Ocean-tides 3.5 Geothermal: 32	Ocean-tides: 0.0005 Geothermal: 0.03	Others	Uranium (U):1,000 Lithium: 3,100 Thorium (Th): 300 Seawater-U: 360,000 Deuterium 10^{10}	Uranium: 1 Thorium: little

Solar 162, 000 ZJ/year, 1ZJ = 10^{21} J, the current global exergy use is 30 TW, which is equal to 1 ZJ/year. Exergy is the useful portion of energy that allows us to do work and perform energy services. We gather exergy from energy-carrying substances in the natural world we call energy resources. While energy is conserved, the exergenic portion can be destroyed when it undergoes an energy converion.

Currently some 80 % of the world's overall energy supply of about 0.4 ZJ per year (using the conversion of 30 TW=1 ZJ/year, this relates to 12 TW) is derived from fossil fuels (Beurskens et al., 2010; Braun et al., 2010). Roughly 15% of this demand is covered by biomass resources, making biomass by far the most important renewable energy source used to date. Other major contributors to renewable energy are hydropower, geothermal, wind, solar and marine energy (Beurskens et al., 2010). On average, biomass in the industrialised countries contributes 3-12% to the total energy supplies. In developing countries this contribution can be as high as 50-90% of the total energy supply.

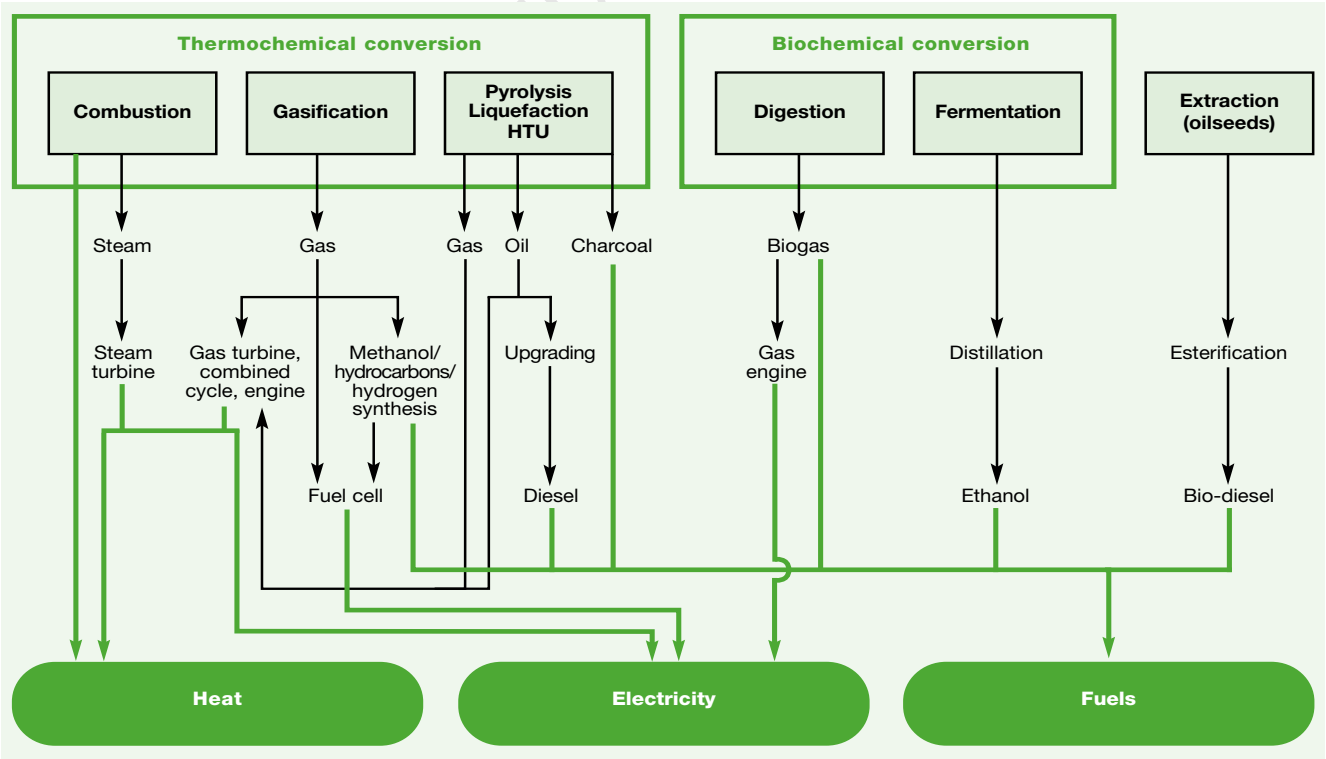

Figure 1.2: Main biomass energy conversion routes, taken from Beurskens et al. (2010)

Various conversion routes are possible for energy generation from biomass (Figure 1.2). Combustion is currently responsible for 90% of the energy production from secondary energy carriers. Liquid biofuels such as biodiesel, bioethanol etc., cover only a small part of this supply. Biogas (from anaerobic digestion) plays a smaller, but steadily growing role. The production of biogas was initially as a result of sewage sludge and industrial wastewater treatment and regarded as a beneficiary by-product, however is becoming a well established energy resource through the use of renewable biomass (Braun et al., 2010). Selection of the product and technology for its formation is governed both by the desirability of a product range and the characteristics of the starting material e.g. moisture content, digestibility (Burton et al., 2008; Dowling, 2009).

Chapter 2

Literature Review

2.1 Introduction

Biomass can be derived from cultivation of dedicated energy crops; by harvesting forestry and other plant residues; and from biomass wastes (Amin, 2009). Microalgae have emerged as a potential source for biomass due to their productivity, lipid content and CO_2 fixation ability (Cheng et al., 2006; De Schamphelaire and Verstraete, 2009; Chisti, 2007). They have been shown to be more photosynthetically efficient than higher plants and can be grown in a simple salts medium on a large scale (Illman et al., 2000). Algal biomass can be used directly, converted into ethanol, methanol, hydrogen, methane, or lipids extracted to produce fuel oils (Illman et al., 2000).

2.1.1 Microalgal production

Microalgae can be cultivated in a large number of systems (Greenwell et al., 2010). For large-scale cultivation, algae can be grown in either open culture systems or closed systems (Chaumont, 1993). Open ponds can be grouped into natural water (lake, lagoons, ponds) and artificial ponds or containers. The most common systems are shallow large ponds, tanks, circular ponds and raceway ponds (constant circulation supplied from a paddle wheel) (Greenwell et al., 2010). Closed system tubular photobioreactors are suitable for outdoor mass cultures. The reactors are generally constructed out of either plastic or glass and recirculated either by a pump or an air-lift system (Amin, 2009). The closed system reactors minimise contamination through surface exposure to air and so maximise stability in large-scale cultivation. Tube diameters of the photobioreactors are kept small to maximise light penetration through the dense cultures.

2.1.2 Harvesting and processing algal biomass

Microalgae can be harvested by using various techniques. Centrifugation, flocculation, autoflocculation, sedimentation and filtration have all proven successful in recovery of concentrated biomass (Amin, 2009). Processing algae to recover the lipid content is required for the transesterification process. Methods such as pressing, solvent extraction (benzene, hexane), enzymatic extraction (enzymes degrade cell walls making fractionation easier), osmotic shock (disruption of cells by a sudden change in osmotic pressure)

and supercritical CO_2 solvent extraction have been proven to be successful in recovering the oil content of algae (Amin, 2009).

2.1.3 Energy Production

Eight possible technologies investigated in previous studies have been highlighted as potential solutions for the harnessing energy from microalgae. These are presented in Figure 2.1 and discussed below.

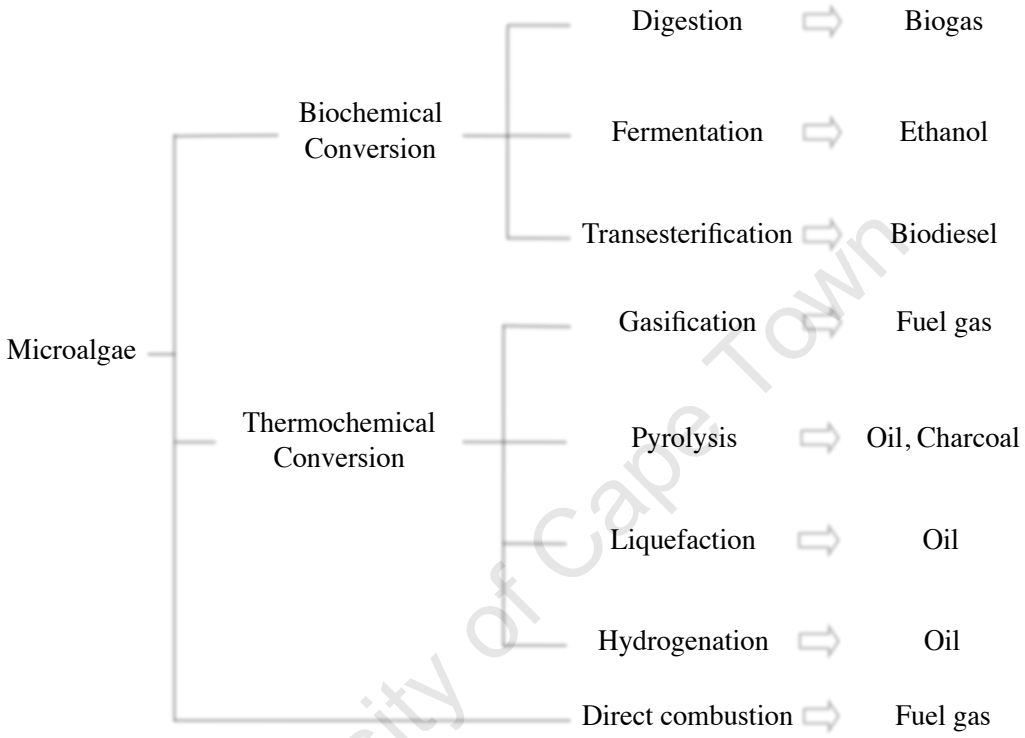

Figure 2.1: Energy conversion processes for microalgae, adapted from Amin (2009)

Anaerobic digestion (AD)

AD incorporates series of processes in which microorganisms break down biodegradable material in the absence of oxygen (McKendry, 2002b). AD technology is widely used to harness energy from renewable sources. This process produces methane (65-70%) and carbon dioxide (30-35%) rich biogas suitable for energy production, as an alternative to fossil fuels (Gunaseelan, 1997; McKendry, 2002b). The biogas produced from anaerobic digestion can be utilised directly or indirectly to derive energy in a number of processes. Examples of these processes are: Use in a combined heat and power unit (CHP) where the gas is combusted to produce heat and electricity; directly compressed or liquefied to produce a transport fuel (De Schamphelaire and Verstraete, 2009) or purified and used in the production of more traditional transport fuels such as petroleum or diesel (De Schamphelaire and Verstraete, 2009). Maximum obtainable energy yields from AD of algae are discussed further in this review.

Combustion

Combustion of algae in the presence of excess oxygen is a complex process that involves simultaneous coupled mass and heat transfer with both homogeneous and heterogeneous reactions (Nussbaumer, 2003; Jenkins et al., 1998). The mechanism takes place via 4 major process steps: drying of biomass, devolitisation, char combustion and gas phase oxidation (Nussbaumer, 2003; Werther et al., 2000). These phases do overlap especially in the case of larger fuel particle size (Nussbaumer, 2003).

Fermentation

Fermentation of algae for ethanol production consists of cultivation, harvesting, slurry preparation, fermentation and ethanol separation stages. Starch of microalgae is released from the cells with the aid of equipment or an enzyme (disruption of cells to liberate carbohydrates). As the cells degrade, *Sacharomycess cerevisiae* yeast is added to the biomass to begin fermentation. Ethanol produced is drained from the reactor and pumped to a holding tank to be fed to a distillation unit (Amin, 2009). Fermentation by-products included acetate, hydrogen and carbon dioxide. Ethanol can be used directly as a fuel (100% alcohol) or as a hybrid with gasoline (90% gasoline and 10% ethanol). The energy of ethanol is 31.1 MJ/kg compared to regular gasoline of 44.4 MJ/kg and the hybrid fuel of 33.7 MJ/L.

Gasification

Gasification constitutes the incomplete combustion, which results in the production of combustible gases, known collectively as syngas. This gas mixture contains the following compounds: carbon monoxide (CO), carbon dioxide (CO_2), hydrogen (H_2), and hydrocarbon gases (Bridgwater, 2003). Gasification is induced by a sub-stoichiometric supply of oxygen and proceeds via four distinct phases to yield syngas rich in CO and H_2. These are; drying of fuel, pyrolysis (devolitisation at approx. 300-500°C), followed by combustion and gasification (partial oxidation at ca. 700-900°C) (McKendry, 2002a,b; Burton et al., 2008; Rajvanshi, 1986). The syngas produced can be used to synthesise products such as methanol, ethanol, naphta, gasoline, wax kerosene, diesel, hydrogen and methane. The gas can also be used directly for electricity generation in a fuel cell.

Hydrogenation

Hydrogenation is a catalytic process, where hydrogen (H_2) is added to the double bonds of a unsaturated organic molecule, through a chemical reaction. The result of the process is the conversion of solid organic compounds to long chain liquid hydrocarbons, or oils. Reported temperatures of operation are 400-430 °C at pressures of 7-14 MPa in the presence of a cobalt molybdate catalyst (Amin, 2009). Hydrocarbon rich gas is a by-product of the process. Oil yields of 46.7 wt% (based on algae loaded) have been reported (FAO, 2009). The oil produced can be used for further synthesis of transport fuels.

Liquefaction

Direct hydrothermal liquefaction in sub-critical water conditions converts wet biomass to liquid fuel. The liquefaction is conducted in aqueous salt solutions at ca. 300°C and 10 MPa with or without the presence of alkali catalysts. Solvent extraction followed by evaporation is used to recover the oil produced. The heavy oil produced consists of carbon (73%), hydrogen (9%), nitrogen (5%) and oxygen (13%) (Amin, 2009). The lower heating value (LHV) of the oil has been reported as 34.7 MJ/kg. The higher nitrogen content in the oil necessitates treatment of flue gas to prevent formation of nitrous compounds (NO_x's) (Amin, 2009; Yang et al., 2004). Yang et al. (2004) reported an oil yield of 33% (organic basis) by direct hydrothermal liquefaction of algae. The by-products of liquefaction are CH_4 and CO_2 gases, solid residue (unconverted algae and catalyst) as well as an aqueous phase waste stream (from washing of solvent used for extraction).

Pyrolysis

Slow pyrolysis is the conversion of biomass to biofuel, charcoal and gas fraction by slow heating of the biomass in the absence of air to around 500°C, using long residence times (Amin, 2009; Uzun et al., 2006). Fast or flash pyrolysis is conducted in the presence of a catalyst at a high heating rate with short gas residence times. Pyrolysis requires a dry feed stock with a low moisture content. Microalgal pyrolysis would require harvesting and drying of biomass before pyrolysis could be initiated. The bio-oil product of pyrolysis can be used in engines and turbines and as a feed stock for refineries (McKendry, 2002a; Amin, 2009). The oil has a higher heating value (HHV) of ca. 17 MJ/kg. Miao et al. (2004) reported a higher heating value of 29 MJ/kg for bio-oil produced by fast pyrolysis of *Chllorella protothecoides* and *Microcystis aeruginosa* microalgae. The HHV, density (1.16 g/L) and viscosity (0.1 Pa.s) of bio-oil from microalgae make it more suitable for fuel oil use than fast pyrolysis oils from lignocellulosic materials. The liquid fuels from fast pyrolysis of microalgae can be used as a conventional fuel or as a source of chemicals (Miao et al., 2004).

Transesterification

Transesterification is process of exchanging the organic group R" of an ester with the organic group R' of an alcohol. These reactions are often catalyzed by the addition of an acid or base catalyst. The reaction can also be accomplished with the help of enzymes (biocatalyst) particularly lipases (Amin, 2009). Transesterification of lipids or oils derived from biomass is usually the conversion of triglycerides to fatty acid methyl esters (FAME) and glycerol. FAMEs or biodiesel are the desired product of the process. Conversion efficiencies in excess of 98% have been reported. While the production of biodiesel from the oil component of algae is technically feasible, economic feasibility, as a stand-alone technology, has not been proven (Chisti, 2007).

Summary

The technologies described above all show great potential for bioenergy production from microalgae. The feasibility biomethanation through anaerobic fermentation of an algal substrate has been identified as a

possible conversion technology, however there has been limited research in recent years. The process is thus investigated further through a full literature review and experimental analysis.

2.2 Anaerobic digestion in general

2.2.1 Process stages

The digestion process (Figure 2.2) begins with hydrolysis of the input materials in order to break down insoluble organic polymers such as carbohydrates and make them available for anaerobic bacteria. Extracellular enzymes catalyse this hydrolysis step (Angelidaki et al., 1999). Acidogenic bacteria then convert the sugars, fatty acids and amino acids into carbon dioxide, hydrogen, ammonia, alcohols and organic acids. Acetogenic bacteria convert these resulting organic substrates into acetic acid, with co-products ammonia, hydrogen, and carbon dioxide. Finally methanogens convert these products to methane and carbon dioxide (Angelidaki et al., 1999).

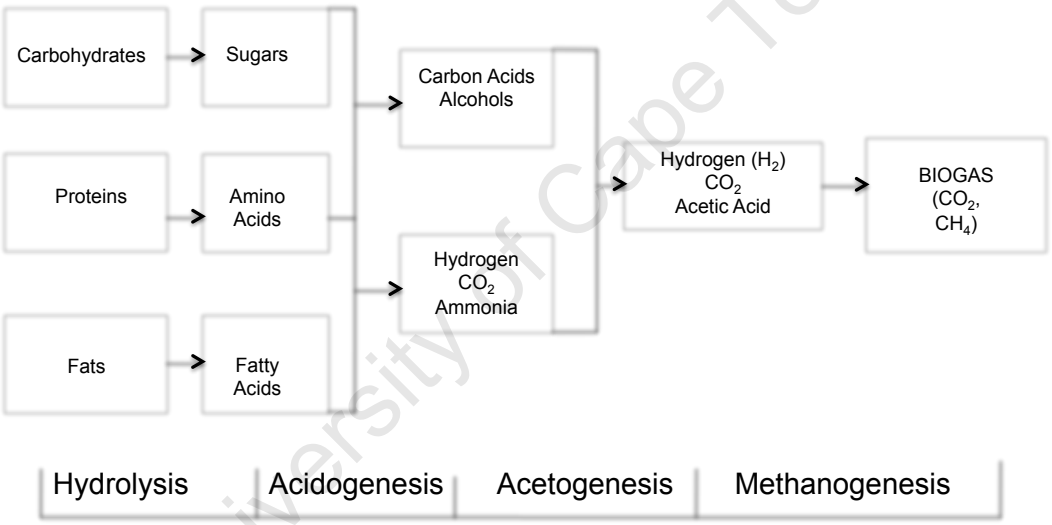

Figure 2.2: Anaerobic digestion process scheme, adapted from Lau (2008)

2.2.2 Reactor configurations

There are many different reactor configurations available for anaerobic digestion, selected to maximise the production of methane based on the type of organic substrate digested (Speece, 1983). In the simplest single stage, fed batch or continuously stirred tank reactors (CSTR) all stages (Figure 2.2) take place at the given operating conditions. This configuration may lead to inefficiencies in the process since metabolic rates of different microbial species vary in the bioreactor. In order to decouple hydraulic and solid retention times and allow multiple species to be maintained in the absence of commensalism or mutualism, reactor configurations have been proposed to enhance the biomass retention. Examples of these are anaerobic filters (attachment of biomass to a solid support material) and the upflow anaerobic sludge blanket (USAB) reactor (microbes induce floc formation thereby retaining biomass in the absence of a solid support). Further configurations such as anaerobic baffled reactors (ABR) and covered lagoons (plug

flow) can also increase retention times of the biomass. Following these configurations are two-stage and two-phase reactors. In the two-stage digester, the residual substrate from the first stage can be reduced at the second-stage digester, carrying out the same reactions as the first but running at different retention times and solution conditions (Gunaseelan, 1997). For quickly fermentable wastes the two-stage digester could have a lower overall retention time than the one stage. The two-phase digester process separates hydrolysis, acidogenisis and acetogenisis from methanogenisis by using different retention times and operating conditions (Gunaseelan, 1997). Two-phase digesters often result in considerably lower retention times and increased biogas production rates due to the potential to optimise conditions for sets of microbes independently (Ghosh et al., 1975; Gunaseelan, 1997).

2.2.3 Operating conditions

Temperature effect

Temperature of AD controls the microbial growth and substrate degradation rates within the bioreactor. Anaerobic microorganisms can be selected to give optimum metabolic rates in either a mesophilic (25-40°C, preferably 35°C) or a thermophilic (50-65°C, preferably $<$ 55°C) range (Buekens, 2005). Thermophilic digestion allows higher loading rates, and so smaller reactors with shorter retention times. It also achieves a more complete pathogen destruction and degradation efficiency of the substrate, however, it is more sensitive to toxins (ammonia) and changes in the environment and less attractive from an energetic point of view (Gunaseelan, 1997; Poulsen, 2003). Mesophilic bacteria can withstand greater changes to their immediate environment increasing the process stability. Mesophilic operations are currently the most popular as this stability is essential (Buekens, 2005).

pH

Methanogens function optimally in a pH range from 6.7 to 7.4 (Gunaseelan, 1997). Acid producing bacteria have much lower optima than methanogens with respect to the pH, but are not as sensitive as the methanogens to change (Poulsen, 2003). A falling pH can result from acid accumulation, indicative of an overload of volatile solids in the digester. Under these conditions the acidogenic bacteria thrive, producing larger amounts of organic acids and so lowering the pH to a level fatal to methanogens. The decrease in methanogen concentration within the bioreactor leads to further acid accumulation. Conversely, excessive methanogenesis can result in a higher concentration of ammonia, increasing the pH above 8.0 and reducing acidogenesis. This is overcome by adding fresh feedstock, promoting acidogenesis and acid formation (Buekens, 2005; Poulsen, 2003; Speece, 1983). Start-up poses difficulties for maintaining pH, since fresh waste must undergo acid forming stages before the methanogens can produce methane. To aid the start-up, calcium carbonate or sodium hydroxide (NaOH) can be added to the digester (Buekens, 2005).

Hydraulic retention time (HRT) and solid retention time (SRT)

The HRT refers to the time that liquid phase substrate remains in the digester where SRT refers to the time that solid phase substrate is retained in the digester. HRT defines the time in which the anaerobic microbes

can consume the soluble organic load (Speece, 1983). The longer a substrate is kept under appropriate reaction conditions, the more complete degradation will be. The rate of reaction does however decrease with a rising residence time. Ideally the solid retention time (SRT) should be higher than that of the HRT to facilitate greater organic load reductions, owing to a high biomass concentration (Speece, 1983). If the HRT is too short the organic material is not fully degraded resulting in low gas yields and possible inhibition of the process. Short retention time can also result in washout of the methanogens if the retention time is less than their rate of multiplication (Speece, 1983). Hydraulic retention times generally vary between 3 and 40 days, depending on the type of substrate and amount loaded into the digesters (Gunaseelan, 1997). The optimal value varies according to technology, process details, temperature and waste composition (Buekens, 2005).

Carbon/Nitrogen (C/N) ratio

The C/N ratio influences the potential methane yield of anaerobic digestion. A low C/N ratio can cause ammonia to accumulate from mass digestion of nitrogenous matter, which inhibits the methanogens. Additionally, the quality of the compost resulting from the digestate decreases with ammonia production (Buekens, 2005). Yen and Brune (2007) reported after co-digestion of algae with waste paper that a C/N ratio between 20 and 25 was optimal. Chen (1987) reported a range between 25 and 35. Additional reading suggests an optimal ratio between 20 and 30 (Parkin and Owen, 1986; Buekens, 2005).

Solids content

The solids content determines, amongst other things, the retention times required. This originates from the time bacteria need to access the liquid substrate, which has been hydrolysed from the solid biomass. Typical solid loading is in the substrate ranges from 3-8% but can be as high as 25%(Gunaseelan, 1997).

Organic loading rate

The organic loading rate (OLR) determines the amount of volatile solids loaded into the digester. If the OLR is too high, the acidogenic bacteria multiply, causing a decrease in pH and a low biogas production rate. Various OLR have been reported in literature based on the amount of volatile solids (VS) per litre of material fed. The OLR is selected according to the type of substrate (e.g. low for high nitrogen organics) and reactor configuration (Speece, 1983). Typical ranges seen are 1.4-3.5 g VS/$L_{reactor}$.day (Golueke et al., 1957; Chen, 1987; Chandra et al., 2006; Antonopoulou and Lyberatos, 2009).

2.2.4 Inhibition of anaerobic digestion

The most important and influential inhibitory compounds, which result from the substrates and the process, are discussed below:

Ammonia

Ammonia is produced by the biological degradation of nitrogenous matter i.e. proteins (Kayhanian and Rich, 1995). The yield of ammonia expected from the anaerobic digestion of a given substrate can be estimated in a number of ways. During anaerobic digestion the proteins are digested and ammonia accumulates in the liquid phase. The pH value determines the distribution between ammonium ions (NH_4^+) and free ammonia (NH_3). The non-ionised hydrophobic (non-polar) form of ammonia is able to diffuse passively across the cell membranes where it expresses its toxicity by causing a proton imbalance or potassium deficiency (Sialve et al., 2009; Gallert et al. 1998). According to Sialve et al. (2009) research has shown that the acetoclastic methanogens are of the most sensitive to ammonia inhibition. Inhibition of ammonia becomes significant between 1.7 and 14.0 g/l and depends on several factors such as the acclimatisation period, nature of substrate and inoculum and operating conditions (Angelidaki and Ahring, 1993). Ammonia inhibition can be mitigated by various techniques, such as pH, temperature and antagonistic cations (Na^+, Ca^{2+}, K^{2+}, Mg^{2+}) (Chen et al., 2008).

Sulphur and Sulphide

In anaerobic digesters, sulphate is reduced to sulphide by the sulphate reducing bacteria (SRB) (Chen et al., 2008). Inhibition occurs in two stages: initially from competition for organic substrates between SRB and methanogens and secondly as a result of sulphide toxicity (Harada et al., 1994; Anrderson et al., 1982). Many studies have determined the parameters involved with the competition between SRB and methanogens. Factors such as COD/SO_4^{2-} ratios (Choi, 1991), methanogen:SRB ratios (Stefanie et al., 1994) and temperature (Colleran and Pender, 2002) play an important role in determining the significance of competitive inhibition. A COD/SO_4^{2-} ratio below 1.7 will cause SRB to dominate, whilst ratios above 2.7 allow for MP to dominate. At temperatures of 37°C, SRB may dominate, whilst temperatures in excess of 55°C allow for MP to dominate.

Sulphide toxicity has been shown to inhibit cellular activity by denaturing of proteins, interfering with coenzyme sulphide linkages and affecting assimilatory sulphide metabolism (Zehnder, 1998). MP (archae) are the most susceptible to sulphide toxicity as sulphur is required as a nutrient for methanogens (Chen et al., 2008). The toxic sulphide concentration causing a 50% decrease in methanogenic activity over a fixed period of exposure time (IC50) ranges from 50 to 250 mg H_2S/L depending on the distribution between HS^- and H_2S affected by the pH of the system (Chen et al., 2008).

Light metal ions

Light metal ions (Ca^{2+}, Mg^{2+}, Na^+, K^+) may occur in an anaerobic digestion system as a result of their presence in the substrate, release from digestion or as a pH control additive (Chen et al., 2008). If the concentrations of the ions become too high they become inhibitory to the anaerobic microbes. The calcium (Ca) and magnesium (Mg) ions are particularly detrimental as they affect the system by precipitating out of useful nutrients phosphate and carbonate which results in the loss of these essential nutrients as well as buffering capacity (Keenan et al., 1993; van Langerak et al., 1998; Chen et al., 2008). Sodium (Na)

is typically more toxic than Mg and Ca, but Mg and Ca reduce nutrient availability. Toxic levels vary widely in literature due to the nature of the processes tested. A review conducted by Chen et al. (2008) has shown a range of inhibitory concentrations, IC50, of 0.15 to 29 g/L for K and 5.6 to 53 g/L for Na ions.

Heavy metal ions

The metals of concern in terms of inhibition are chromium (Cr^{3+}), iron (Fe^{2+}), copper (Cu^{2+}), zinc (Zn^{2+}), cadmium (Cd^{2+}) and nickel (Ni^{2+}) (Jin et al., 1998). Heavy metals can accumulate within the cells to acutely toxic levels (Sterritt and Lester, 1980). The toxicity of heavy metals originates from their impact on enzyme function and structure. The inhibition of heavy metals is controlled by factors such as speciation of metal, pH and redox potential (Chen et al., 2008). Methanogens are most sensitive to heavy metal inhibition and have a relative sensitivity of Cd > Cu > Cr> Zn > Pb > Ni.

Organic compounds

Non-polar organic compounds that accumulate within the microbial membranes inhibit the anaerobic digestion process. This can lead bacterial cell lysis. Inhibitory compounds include: chlorophenols, halogenated aliphatics, N-substituted aromatics, long chain fatty acids and lignin related compounds (Chen et al., 2008).

2.3 Anaerobic digestion of algae

2.3.1 Properties of algae

Spirulina spp. (cyanobacteria) and *Scenedesmus spp.* (microalgae) have been chosen as the algae to be investigated in this study.

Spirulina spp. is a microscopic blue-green alga in the shape of a spiral coil, living both in sea and fresh water. *Spirulina* is the common name for human and animal food produced primarily from two species of cyanobacteria: *Arthrospira platensis*, and *Arthrospira maxima.* Though referred to as algae because they are aquatic organisms capable of photosynthesis, cyanobacteria are not related to any of the various eukaryotic algae (Ciferri, 1983). *Arthrospira* are free-floating filamentous cyanobacteria characterized by cylindrical, multicellular trichomes in an open left-hand helix (Venkataraman, 1997). They occur naturally in tropical and subtropical lakes with high pH (above 9.5) and high concentrations of carbonate and bicarbonate (above 20 g/L). These species were once classified in the genus *Spirulina*. There is now agreement that they are in fact *Arthrospira*; nevertheless, the older term *Spirulina* remains in use for historical reasons (Ciferri, 1983). Most cultivated *Spirulina* is produced in open-channel raceway ponds, with paddle-wheels used to agitate the water (Venkataraman, 1997).

Scenedesmus spp. is a small, nonmotile colonial green alga consisting of cells aligned in a flat plate.

The cells are usually cylindrical but may be more lunate, ovoid, or fusiform. Each cell contains a single parietal, plate-like chloroplast with a single pyrenoid (Oilgae (2010) original source Meyen (1820)). The cell walls may be covered in bumps or reticulations that are best viewed with scanning electron microscopy. *Scenedesmus spp.* is commonly found in the plankton of freshwater rivers, ponds, and lakes. Growth of the microalgae typically takes place in closed photobioreactors in at pH 7 and through direct gas liquid mass tranfer of carbon dioxide (Hartig et al., 1988).

The macro-composition of a given substrate can help to determine the digestion potential in terms of methane yields (Sialve et al., 2009). It also enables the C:N:P nutrient ratio available to the anaerobic microbes to be determined. The composition of nutrients within algal cells is dependent on the environment in which it has grown (Sialve et al., 2009). A gross average of composition for the chosen algal substrates has been adapted from Becker (2007) are presented in Table 2.1 along with the calculated empirical formulae.

Table 2.1: Algal substrate composition and empirical formulae

Substrate	Proteins (avg %)	Carbohydrates (avg %)	Lipids (avg %)	Empirical formula[b] ($C_aH_bO_cN_d$)
Scenedesmus spp.	50-56	10-17	12-14	$C_{3.7}H_{7.0}O_{1.7}N_{0.6}S_{0.01}$
Spirulina spp.	46-63	8-14	4-9	$C_{3.5}H_{6.7}O_{1.8}N_{0.6}S_{0.01}$

*All data taken directly from Becker (2007) and Heaven et al. (2010) for *Scenedesmus obliquus* and *Spirulina platentis* respectively, [a] assumed 100% removal of lipid from extraction, [b] Assuming the material is entirely composed of protein, lipid and carbohydrate, in the relative proportions shown (i.e. on a VS basis)

2.3.2 Theoretical and reported methane and ammonia production

According to Angelidaki and Sanders (2004), the theoretical yield of methane and ammonia can be calculated for any substrate from the organic composition. This allows predictions of methane yield to be made as well as the efficiency of the digester determined. Angelidaki and Sanders (2004) based their calculations on the formula (given by Equation 2.1) derived by Symons and Buswell (1933) to calculate methane potential when fermenting carbohydrates.

$$C_aH_bO_cN_d + (\frac{4a-b-2c+3d}{4})H_2O \longrightarrow (\frac{4a+b-2c-3d}{8})CH_4 + (\frac{4a-b+2c+3d}{8})CO_2 + dNH_3 \quad (2.1)$$

From Equation 2.1, the specific methane yield in terms of litres CH_4 per gram of total solids (TS), B_0 can be calculated as follows:

$$B_0 = \frac{4a+b-2c-3d}{8(12+b+16c+14d)} * V_m \quad (2.2)$$

Where V_m is the molar volume of methane and a,b,c,d are the atomic coefficients in the empirical formula.

Similarly, the ammonia yield can similarly be calculated as follows:

$$Y_{N-NH_3(mg/mgTS)} = \frac{d * 17 * 100}{12a + b + 16c + 14d} \tag{2.3}$$

Sialve et al. (2009) note that this method of determining the yield does not account for cell maintenance and anabolism.

An influential factor impacting the CH_4 composition in the biogas is that of pH. The pH controls the speciation of the carbonate system and the release of CO_2 as well as the activity of both acidogens and methanogens(Angelidaki and Sanders, 2004). The oxidation state of the biomass that drives the proportion of released methane influences the quality of the biogas. Equation 2.4, derived by Harris and Adams (1979), allows one to calculate the ratio (r_G) of methane to carbon dioxide in the biogas from the average carbon oxidation state (n) in the substrate.

$$r_G = \frac{4 - n}{4 + n} \tag{2.4}$$

where:

$$n = \frac{-b + 2c + 3d}{a} \tag{2.5}$$

Using Equations 2.2-2.5 and the empirical formula for each substrate from Becker (2007), Table 2.2 was prepared for the given biomass substrates used in this study. Based on the empirical formula alone, theoretically *Scenedesmus spp.* is expected to result in a slightly higher methane yield per kg of total or volatile solid. This theoretical yield does not take the biodegradability of the orgainc source into account.

Table 2.2: Theoretical methane yield, ammonia yield, and biogas composition of biomass substrates

Substrate	Empirical formula ($C_aH_bO_cN_d$)[a]	B_0 [b] (m^3/kg TS)	Y_{CH_4} [c] (m^3/kg VS)	$Y_{N\text{-}NH_3}$ (mg/g TS)	CH_4 (vol%)
Scenedesmus spp.	$C_{3.7}H_{7.0}O_{1.7}N_{0.6}S_{0.01}$	0.46	0.53	42	68
Spirulina spp.	$C_{3.5}H_{6.7}O_{1.8}N_{0.6}S_{0.01}$	0.43	0.50	89	68

[a] Assuming the material is entirely composed of protein, lipid and carbohydrate, in the relative proportions shown (i.e. on a VS basis),[b] Calculated from theoretical methane yields for protein, lipid and carbohydrate multiplied by the percentage of each constituent present in the material (i.e. TS basis), [c] Calculated from empirical formula using equation 2.2; equal to value in the previous column × 100% / (protein% + lipid% + carbohydrate%) (i.e. VS basis). 'Minimum' values,

This both allows prediction of theoretical values and their comparison to yields achieved in previous studies (Table 2.3). The key process parameters and reactor set-up influence the achievable yields. Most of the studies conducted on AD of algae have resulted in a methane yield lower than the predictions made using the macro-composition. This suggests that the maximum achievable conversion is not reached on AD of whole cell algae. Therefore methods to enhance AD of algae need to be investigated.

Table 2.3: Results obtained from previous studies conducted on anaerobic digestion of algae, adapted from Sialve et al. (2009)

Reactor	Substrate	T (°C)	HRT (d)	Loading Rate (g VS/ L.j)	Y_{CH_4} (m^3/kg VS)	CH_4 (vol%)	Ref
Batch 11 L	*Chlorella-Scenedesmus*	35-50	3-30	1.44-2.89	0.17-0.32	62-64	1
Batch 11 L[a]	*Chlorella-Scenedesmus*	45	20	2.7	0.6	71	2
Semi-cont 10 L	*Spirulina maxima*	35	33	0.97	0.26	68-72	3
Fed Batch 2 L	*Spirulina maxima*	15-32	4-40	0.93-1.2	0.25-0.34	46-76	4
Batch 11 L	Algal biomass	35	28	1	0.43	72	5
	Spirulina	35	28	0.91	0.32-0.31		
	Dunaliella	35	28	0.91	0.44-0.45		
CSTRs 2-5 L	*Tetraselmis* (fresh)	35	14	2	0.31	72-74	6
	Tetraselmis (dry)	35	14	2	0.26	72-74	
	Tetraselmis (dry)+NaCl 35 g/L	35	14	2	0.25	72-74	
CSTR 4L	*Chlorella-Scenedesmus*	35	10	2-6	0.09-0.136	69	7
Semi-cont 8 L[a]	*Chlorella, Pseudokirchneriella, Chlamydomonos*	35	-	0.015	0.49	65	8

[1] Golueke et al. (1957), [2] Golueke and Oswald (1959), [3] Samson and LeDuy (1982), [4] Samson and LeDuy (1986), [5] Chen (1987), [6] Asinari Di San Marzano et al. (1982), [7] Yen and Brune (2007), [8] De Schamphelaire and Verstraete (2009), [a]Closed-loop systems

2.4 Increasing the efficiency of anaerobic digestion of algae

The average total energy content of algae is around 25.1 J/g(Chen and Oswald, 1998). During anaerobic digestion an optimised mesophilic system recovers around 60% of this energy (Golueke et al., 1957). The remaining 40% is typically resistant to release during digestion because of substrate properties such as degradation resistant biopolymers contained within the cell walls (Blokker et al., 1998).

2.4.1 Pre-treatment

A pre-treatment of lignocellulosic material is essential for the removal of lignin and hemicelluloses, which can enhance hydrolysis of cellulose and thus improve yields (Sun and Cheng, 2002; Wyman et al., 2005). The cell walls of algal biomass protect the cell from enzymes produced by the anaerobic microbe, reducing the cells' biodegradability and so creating a strong resistance to hydrolysis. Golueke et al. (1957) and Sanchez and Travieso (1993) reported the presence of whole cells in their digesters after long periods of time, confirming the resistance to degradation.

Physical factors that influence the hydrolysis of cellulose have been identified. These include the porosity (accessible surface area) of materials, cellulose fibre crystallinity, and the lignin and hemicellulose content (Himmel and Overend, 1994). Therefore the removal of lignin and hemicelluloses, reduction of cellulose crystallinity and increase of porosity during pre-treatment is expected to have positive effects on the hydrolysis efficiency of enzymes such as cellulases (Sun and Cheng, 2002). Algal biomass is typically characterised by a relatively high ($> 10\%$) hemicellulose content. Ververis et al. (2007) investigated cellulose, hemicellulose, lignin and ash contents for various organic materials (Table 2.4). The results emphasised the high content of hemicellulose (average 16.3%).

Table 2.4: Cellulose, hemicellulose, lignin and ash contents of organic materials (Ververis et al., 2007)

Materials	Chemical components			
	Cellulose (%)	hemicellulose (%)	lignin (%)	ash (%)
Algal biomass[a]	7.1	16.3	1.52	1.80
Orange peels	13.61	6.1	2.1	1.5
Lemon peels	12.72	5.3	1.73	1.92

[a] Algal biomass comprised of filamentous species *Ulothrix sp.*, *Microspora sp., Stigeoclonium sp.* and *Oedogonium sp.* along with *Chlorella sp.* and *Scenedesmus sp.* (ellipsoidal cells). Cyanobacteria were represented by *Hydrocoleus sp.* and *Oscillatoria sp.* whereas diatoms were represented by *Nitzschia sp.* and *Gomphonema sp.*

Hydrolysis of cellulose does occur in digestion, but is difficult and may be rate limiting if present in high concentrations (Yen and Brune, 2007). This makes investigation into cell disruption relevant. A number of technologies exist for the disruption of cell walls for the release of proteins, lipids, nucleic acids and carbohydrates (Doucha and Livansky, 2008). Of all the available technologies the following have been investigated for algal biomass pre-treatment: Physical (ultrasonification, Samson and LeDuy, 1983b), thermal (hot water hydrolysis, Chen and Oswald, 1998; Samson and LeDuy, 1983b) and thermo-chemical (heating with addition of NaOH, Chen and Oswald, 1998; Samson and LeDuy, 1983b) pre-treatments, results summarised in Table 2.5.

Table 2.5: Impact of pre-treatments applied to algal biomass prior to anaerobic digestion for methane production

Species	Method of Pre-treatment	Parameters Investigated	Result	Conclusion	Reference
Mixed consortia	Thermal and Themochemical	Temperature, duration of treatment, concentration of substrate, sodium hydroxide addition	Increased methane specific production, a maximum increase of 33%	Temperature has the greatest impact, Optimal- 100°C for 8h, 3.5% solids conc and no NaOH addition	1
Spirulina maxima	Mechanical and Thermochemical	Ultrasonic disintegration-10 min, Temperature and pH	Pre-treatment increased solubility of biomass and positive effect on the activity of the acidogenic bacteria but not on that of the methanogens	Severe thermo-chemical treatment has inhibitory effects on methanogens due to high sodium levels. Optimum pre-treatment- 150°C at pH=11	2

[1] Chen and Oswald (1998), [2] Samson and LeDuy (1983b)

No consideration has been provided in the literature on whether the extra energy put into the process through the pre-treatment increased the overall energy recovery to provide a net increase in energy harnessed.

2.4.2 Metabolically increasing biochemical methane potential of algae

Variation in composition of algae is related directly to growth conditions. Nitrogen limitation leads to the reduction of protein content, resulting in lower ammonia release (inhibitor) and increased theoretical

methane potential (Sialve et al., 2009). This condition also results in an increase in intracellular lipid accumulation enhancing the overall calorific value of the algae. However, growth rates of algae are negatively affected by this condition (Sialve et al., 2009). The potential energetic added value when digesting algae using the metabolic approach to increase lipid content is summarised in Table 2.6.

Table 2.6: Energetic content of algae (Illman et al. (2000),Heaven et al. (2010))

Species	Growth Conditions	Oil Content (%)	**Case 1:** Anaerobic digestion of the whole algal biomass	Energetic added value with high lipid content
			Methane[a] (kJ/g VS)	Additional Energy (kJ/g VS)
C.vulgaris	Balanced	18	18.6	
C.vulgaris	Low N	40	23.7	5.1
C. emersonii	Balanced	21	21.6	
C. emersonii	Low N	29	28.8	7.2

[a] Values calculated from methane yields based on the percentage of protein, lipid and carbohydrate and a conversion factor of 35.6 MJ/CH_4 as used in Sialve et al. (2009).

The results cited by Heaven et al. (2010) show that when digesting a cell with high lipid content, greater theoretical methane yields are expected. Low N cells also have a decreased protein content and so the theoretical ammonia yield is decreased. These two important results may improve both the conversion efficiency and the stability of the digestion process (Sialve et al., 2009). Where the lipid is removed from the algal cell for biodiesel production, a high protein residue remains which may pose issues with ammonia release and low methane efficiency. Therefore co-digestion with high carbon wastes has been recommended (Yen and Brune, 2007).

2.4.3 Co-digestion

Co-digestion has been identified as a potential method to enhance methane recovery during anaerobic digestion through optimising influent substrate composition. The composition is enhanced through adaption of the C/N ratio enabling better control and thus optimum methane yields can be realised.

Additionally, co-digestion is reported to stimulate enzymatic synthesis that can also improve methane yields. Cellulases are inducible enzymes, synthesised and mostly secreted into the environment by microorganisms during growth on cellulosic materials. Yen and Brune (2007) showed an increase in cellulase activity when co-digesting algal biomass with waste paper. It was suggested that the paper addition induced cellulase excretion by the anaerobic bacteria. This had a positive effect on the digestion of the algal cell walls and final methane yields. Co-digestion also assists in diluting certain toxic compounds, found in either one of the substrates, which mitigates potential adverse effects on methane recovery via AD (Sialve et al., 2009).

The major studies conducted to determine the impact of anaerobic co-digestion of algal biomass with high carbon containing compounds to produce methane are those of Yen and Brune (2007), Samson and LeDuy (1983a) and Chen (1987). The optimum results obtained from each study are summarised in Table 2.7. The impact of co-digestion is significant resulting in methane yields increasing three fold. The generally accepted optimum C/N ratio lies between 20 and 30.

Table 2.7: Impact of anaerobic co-digestion of algal biomass with high carbon containing wastes

Co-digestive	Substrate	Ratio[a]	C:N Ratio	Result	Reference
Waste paper	*C.vulgaris*	60%	20-25	Methane production rate 1.77 L CH_4/L.day compared to 0.57 CH_4 L/L.day for algae only	1
Sewage sludge	*Spirulina maxima*	50%	6.2	Methane yield and productivity increased over two fold	2
Canning facility effluent	*Spirulina maxima*	25%	25-35	Methane yield increased by 33%	3

[1] Yen and Brune (2007), [2] Samson and LeDuy (1983a), [3] Chen (1987); [a] Ratio of co-digestive to substrate

2.4.4 Summary

From the results for the three available techniques it appears that the highest methane productivity has been reported with co-digestion. However co-digestion does not eliminate the need to increase the biodegradability of the algal cell prior to digestion. Treatment to release and/or solubilise key compounds within the algal cells is expected to further increase methane productivitiy. Further rigorous analysis on algal biodegradability with and without prior cell envelope disruption have not been reported. High temperature for lengthy time periods (100°C for 8 hours plus) are simply not energetically feasible and even with heat integration could not be realised (Sialve et al., 2009). For these reasons it is imperative to develop a method of mechanical treatment whereby a low energy process can be implemented with positive release and or/ solubilisation of key organic compounds.

Methods adapted to cell rupturing prior to lipid extraction for biodiesel production have shown positive results (Pernet and Tremblay, 2003) and compared to thermal and thermo-chemical pre-treatments are less energy intensive. The correct choice of algae is also of great importance (Sialve et al., 2009). Certain microalgae such as *Scenedesmus spp.* and *Chlorella spp.* have strong, thick recalcitrant cell walls and so are more resistant to hydrolysis (Okuda, 2002). Conversely more filamentous algae such as *Spirulina spp.* are easier to rupture and so their biodegradability would be higher (Samson and LeDuy, 1983b). With regards to metabolically increasing the theoretical methane potential, the impact of increased lipid content must be weighed against the reduced biomass productivity on the overall system to understand its potential advanatage. Introducing a time factor into the results obtained by Sialve et al. (2009) will produce a more comparable analysis.

2.5 Bioenergy production from anaerobic digestion of microalgae as a stand-alone technology versus as an integrated process in biodiesel production

AD of the residual biomass after extraction or direct esterification of the lipids (tryglycerides) results in a potential for energy recovery (Chisti, 2007). However with the nature of the AD process, that is being

able to have a feed with high moisture content and the high productivity of algae a new question arises: should anaerobic digestion be used as a stand-alone technology, or should it be integrated into the biodiesel production process?

The determination of which combination results in the most economical and energetically feasible process can be initially estimated using the results obtained from previously conducted experiments, inherent properties (LHV) and theoretical predictions based on macro-composition (Sialve et al., 2009). So far most of the initial predictions made on the impact of AD in the biodiesel production process have only considered the energy of the products for each case (De Schamphelaire and Verstraete, 2009; Sialve et al., 2009). This is a good initial indication, however investigation of the total energy required for each process should provide a more accurate comparison. A study conducted by Illman et al. (2000) investigated increasing the lipid content of microalgae by limiting nitrogen availability. Heaven et al. (2010) utilised their results to determine the impact on overall energy potential through AD of the microalgae with increased lipid content (case 1, Table 2.8). Heaven et al. (2010) also predicted the energy potential of the products following lipid extraction for biodiesel production i.e. using the remaining residue as a substrate for AD (case 2, Table 2.8).

Table 2.8: Energy recovery with AD as an integrated process (Heaven et al., 2010; Illman et al., 2000)

Species	Growth Conditions	**Case 1:** Anaerobic digestion of the whole algal biomass	**Case 2:** anaerobic digestion of algal residues			Energetic added value with lipid recovery
		Methane (kJ/g VS)	Methane[a] (kJ/g VS)	Lipids[b] (kJ/g VS)	Du Long equation Total CV (kJ/g VS)[c]	Additional Energy (kJ/g VS)
C.vulgaris	Balanced	18.6	12.2	6.5	21.3	2.7
C.vulgaris	Low N	23.7	9.2	14.4	25.5	1.8
C. emersonii	Balanced	21.6	11.1	10.5	24.4	2.8
C. emersonii	Low N	28.8	6.1	22.7	31.3	2.5

[a] Computed with a methane calorific value of 35.6 MJ/t ; [b] Computed with the calorific value of rapeseed crude oil; 36.87 MJ/t; [c] Higher heat value MJ/kgVS = (34.1C + 102H + 6.3N + 19.1S−9.85O)/100

This preliminary energy balance, only taking the products' energy potential into account, suggests that an integrated process is more efficient than AD as a stand-alone technology. However, the impact on the growth rate associated with increased lipid content remains to be considered. A comparison between AD and AD with lipid recovery by merely comparing the energy potential of the products is flawed. While nitrogen limitation does increase lipid content, the content of tryglycerides in specific algae needs to be highlighted. A more accurate and useful energetic comparison requires investigation of these specific lipids to assign a conversion to biodiesel. Using this and assigning a calorific value to biodiesel would enhance quality of data for comparison..

De Schamphelaire and Verstraete (2009) investigated AD as a stand-alone technology. They cited a

number of advantages of a biogas production process over a biodiesel process, summarised in Table 2.9.

Table 2.9: General advantages of biogas production over biodiesel production (De Schamphelaire and Verstraete, 2009)

Biogas Production Advantages	Biodiesel Disadvantages
Can be obtained from wastes such as manure	Requires cultivation of specific crops (e.g. rapeseed)
All components of biomass can be digested	Only lipid content of biomass utilised
Biogas more efficient-71,000 km out of transport fuel per ha	Less efficient 18,500 km out of transport fuel per ha
Biogas separates spontaneously from reactor	Higher energy required for fuel separation

Chisti (2008) investigated the theoretical ratio of renewable energy produced per unit of fossil energy input for a microalgal biomass process. This was conducted for both the integrated biodiesel-AD system and for AD as a stand-alone process. Using a basis of 82 ton/ha.year of algal biomass produced and an average lipid content of 20% of dry weight in the biomass the following results were obtained.

Table 2.10: Summary of results obtained by Chisti (2008) comparing various bioenergy conversion routes

System	Ratio[a]	Additional information
Integrated system	2.8	Total energy 1444 GJ/ha.year, 57% from AD
AD alone	2.4	Assumed conversion of 50%
Integrated+ recuperation of nutrients set free during AD	3.3	closed-loop algal growth-AD system
AD alone+ recuperation of nutrients set free during AD	2.9	closed-loop algal growth-AD system

[a] ratio of the renewable energy produced versus fossil energy input

These results suggest that both systems are relatively similar in yield. Chisti (2008) concludes on the integrated system as the best option. However, in the integrated process AD contributes some 57% of the total energy output and with its simplicity and low energy input requirement it appears that the study may have been bias towards algal biodiesel production.Chisti (2008) did conclude that biogas production is key to make the biodiesel system sufficiently energetically and economically viable. De Schamphelaire and Verstraete (2009) again suggest that the one-step digestion has the advantage of a lower complexity process and the production of a single type of energy carrier, which can be either combusted or employed as biofuel.

From the results seen in the three studies it can be concluded that AD as a stand-alone technology appears to represent a positive alternative renewable energy system.

2.6 Creating an integrated algal anaerobic digestion system for bioenergy production

Section 2.5 introduced the topic of using AD as a stand-alone technology for harnessing bioenergy from algae. When Golueke and Oswald (1959), the pioneers of this technology, first investigated this potential process, they focused on creating a closed-loop system to convert solar energy into bioenergy using a three-unit process. The first was an algal growth unit, the second an AD unit and the third an activated

sludge unit to aerobically digest the AD effluent for recycle into the algal growth system. The ctivated sludge unit was included to break down the residual organic matter in the digester effluent before returning it to the algal growth unit. However, this unit did not perform its function and was eventually bypassed (Golueke and Oswald, 1959).

A new closed-loop system was proposed and investigated De Schamphelaire and Verstraete (2009). In this system a Microbial Fuel Cell (MFC) was included in place of the activated sludge unit. The purpose of the MFC remains to break down organic material in the AD effluent before recycle into the algal growth unit, with the added benefit of producing bioelectricity in small amounts. In this MFC system, a fresh stream from the algal growth unit flows past the cathode of the MFC to provide oxygen as an electron acceptor whilst organic compounds in the digester effluent are oxidised by bacteria in the anodic chamber releasing electrons that are transported by the bacteria to the anode (De Schamphelaire and Verstraete, 2009). The electron moves to the cathode through an external circuit so drawing a current. De Schamphelaire and Verstraete (2009) had success with the MFC in terms of breaking down the organic content of the digester effluent, but not in terms of generating electricity. In the MFC, 37% of the COD, 70% of Volatile Fatty Acids (VFAs) and 10-60% of the ammonia (NH_4^+-N) were removed, but the MFC only achieved a columbic efficiency of 40%.

Hence the most important results of the closed-loop system centre on improvement in terms of algal productivity, digester methane productivity and/or yield. The increase is due to implementation the recycling and polishing of the digester effluent as well has continuous harvesting of the algal growth unit. A summary of these results can be seen in Table 2.11.

Table 2.11: Energy potential of a closed-loop sunlight-to-bioenergy conversion system

Substrate	Growth Rate (ton DW/ha.year)	Y_{CH_4} (m^3/kg VS)	Power potential (kW/ha)	Conversion efficiency (%)	Reference
Chlorella-Scenedesmus	-	0.6	high	2-3	1
Chlorella, Pseudokirchneriella, Chlamydomonos	24-30	0.5	9-23	2	2

[1] Golueke and Oswald (1959), [2] De Schamphelaire and Verstraete (2009)

It is difficult to compare the two due to variations in algal substrate species, reactor set-up, retention times, temperatures etc. However purely based on the methane yield of the digester unit, a greater conversion was achieved by Golueke and Oswald (1959). Comparing these results with those previously reported for direct digestion or growth of algae it can be concluded that the closed-loop system has increased the methane yield. A value of 0.6 m^3/kg VS is the highest value reported in literature. That takes into account all studies conducted on codigestion and pre-treatment.

2.7 Energy potential of an integrated algal AD system

To evaluate overall energy production potential of the process is considered, reference must be made to the ultimate energy source and how this can be converted in a closed system. This approach has been adapted from that taken by De Schamphelaire and Verstraete (2009). Solar irradiation within the world generally varies between a yearly 700 and 2,500 kWh/m^2, with 1000 kWh/ m^2.year obtained in a temperate region (De Schamphelaire and Verstraete, 2009). A theoretical photosynthetic conversion efficiency of 9% is cited by Wijffels (2008) for conversion of this solar energy to biomass, suggesting production of 130-160 on DW/ha.year of biomass in a temperate climate. However more realistic values of 50–60 ton DW/ha year (Carlsson et al., 2007; Moheimani and Borowitzka, 2006) have been shown to be achievable. Using this and an average calorific value of algae at 20–25 kJ/g (Illman et al., 2000; Kube, 2006; Renaud et al., 2002), a complete transformation into energy-rich biogas would produce 400 MWh/ha.year. This value based on a theoretical maximum conversion will be diminished through cell maintenance and growth as well as substrate recalcitrance (Chen and Oswald, 1998).

As shown in this review, about 40–60% of algal volatile matter is transformed into biogas (Chen and Oswald, 1998; Oswald and Goluke, 1960). With a biogas production of 0.5 m^3 biogas/ kg VS, methane concentration of 65%, and corresponding heat of combustion of 25 MJ/N m^3 biogas, approximately 200 MWh of gross energy production per hectare is attainable annually, which represents a power plant with an annual capacity of 23 kW/ha.

2.8 Work done

2.8.1 Problem statement and objectives

There are a number of technologies available for harnessing energy from algal biomass. Anaerobic digestion has been identified as a technology with great potential. This study aims to observe and compare the methane produced from two algal species: *Spirulina spp.* and *Scenedesmus spp.* Key constraints which hinder the production and concentration of methane yielded per kilogram of volatile solids degraded (or COD consumed) are indentified. Constraints are realised using tested variables, which were monitored during the course of experimentation.

In a parallel study, the influence of mechanical pre-treatment of the algal biomass on the anaerobic digestion was investigated. Mechanical pre-treatment has been identified as the most feasible technique to increase the efficiency of AD of algal biomass, hence its impact is determined.

As stated in a number of studies (Chisti, 2007, 2008; Sialve et al., 2009), anaerobic digestion of algal filter cake is a necessary step for economically viable microalgal biodiesel production. An investigation into the feasibility of digesting the filter cake remaining after lipid extraction through direct transeserification was conducted. From previous studies conducted on microalgal biodiesel, the microalgae *Scenedesmus spp* has proven to be of particular relevance due to its high lipid storage capabilities and good growth rate. For this reason it is used in conducting this investigation. Using the results obtained from these experiments

and those from AD experiments of whole cell algal biomass (includes lipids) a comparison can be made on the benefit of utilising AD in an integrated process with microalgal biodiesel production and using it as a stand-alone technology. This can be further informed by the net energy production in terms of GJ/ha.year.

The stand-alone anaerobic digestion of *Spirulina spp.* is predicted to be an energetically feasible technology. The relative degradability and resultant methane productivity of *Scenedesmus spp.* and *Spirulina spp.* is compared. Further investigation into creating a integrated algal anaerobic digestion system with *Spirulina spp.* as the feedstock will be conducted.

2.8.2 Hypotheses

Anaerobic digestion of Spirulina spp. and Scenedesmus spp.

- Anaerobic digestion of *Spirulina spp* will result in a greater specific methane yield than *Scenedesmus spp.*. This can be attributed to the ease at which the *Spirulina spp.* cells undergo hydrolysis to provide readily consumable organic compounds
- The net energy yield from open pond algal cultivation and anaerobic digestion of *Spirulina spp.* will be greater than *Scenedesmus spp.*. This stems from the higher methane yields, greater productivity in unaerated open raceway ponds as well as the ease with which *Spirulina spp.* can be harvested (low energy input for biomass generation).

Impact of mechanical pre-treatment on the efficiency of anaerobic digestion of Spirulina spp. and Scenedesmus spp.

- Rupturing of the algal cells prior to digestion will enhance AD and thus productivity and yield of methane, relative to whole cell substrate, as it will allow for release and/or solubilisation of key compounds.
- Mechanical disruption of *Scenedesmus spp.* will increase the productivity and yield of methane, relative to the whole cell digesters, to a greater extent than will the disruption on *Spirulina spp.* This can be assigned to the fact that the *Spirulina spp.* cells easily undergo disruption and are disrupted in both digesters within a short period of time.
- The net energy productivity from anaerobic digestion of ruptured *Spirulina spp.* will be greater than that of ruptured *Scenedesmus spp.* This stems from the higher expected methane yields the faster growth productivity and from the ease at which the cells are disrupted.

Bioenergy production from anaerobic digestion of microalgae as a stand-alone technology versus as an integrated process with algal biodiesel production

- The total net energy for anaerobic digestion of *Scenedesmus spp.* as a stand-alone technology will be greater than that of the integrated biodiesel-AD system. This results from the simplicity of the lower energy digestion process. Both complex downstream and upstream processing for biodiesel production will result in an energy requirement that will decrease the total net energy production to levels lower than that of the stand-alone AD process.

2.8.3 Statement of key questions

Anaerobic digestion of Spirulina spp. and Scenedesmus spp.

- Which algal substrate will have the highest methane yield and average methane production rate when digested under the same operating conditions?
- Which algal substrate will yield a biogas with the highest methane content?
- Which algal substrate when anaerobically digested will result in the highest net energy production (GJ/ha.year) taking into account growth production in tons DW/ha.year

Impact of mechanical pre-treatment on the efficiency of anaerobic digestion of Spirulina spp. and Scenedesmus spp.

- Will rupturing of algal cells result in higher yields and production rates of methane relative to un-ruptured substrates when digested under the same operating conditions?
- Which algal substrate will require the highest energy input for complete cell disruption?
- Will rupturing of algal cells result in a biogas with higher methane content?

Bioenergy production from anaerobic digestion of microalgae as a stand-alone technology versus as an integrated process with algal biodiesel production

- Will the catalyst and solvent used in direct transesterification hinder anaerobic digestion of the remaining algal residue?
- Will the direct transesterification process result in cell rupturing and, if so, to what extent?
- Will anaerobic digestion as a stand-alone technology result in a greater net energy productivity than that of the integrated biodiesel-AD system?

Creating an integrated algal anaerobic digestion system from Spirulina spp.

- Will the concept of creating an integrated system using *Spirulina spp.* biomass as the sole feed stock prove feasible?

Chapter 3

Materials and Methods

3.1 Introduction

The following chapter presents a detailed description of the materials and methods used for the algal growth, batch digestion and semi-continuous digestion experiments.

3.2 Materials

3.2.1 Cultures

Algal stock cultures

Scenedesmus spp.

Stock cultures of the microalga *Scenedesmus spp.* (obtained from African Bioproducts algal ponds) were maintained at ambient temperature in 500 mL flasks, sparged (2 L/min) with air and illuminated with three fluorescent bulbs (120 μmol photon/m^2.s at the surface) from one side of the flask. All *Scenedesmus spp.* cultures were grown on *Botryococcus* media comprising of: nutrients (0.75 g/L $NaNO_3$, 0.075 g/L K_2HPO_4, 0.175 g/L KH_2PO_4, 0.025 g/L $CaCl_2.2H_2O$ and 0.025 g/L NaCl) and a metal solution (0.75 g/L Na_2EDTA, 0.017 g/L $FeCl_3.6H_2O$, 0.041 $MgCl_2.4H_2O$, 0.005 g/L $ZnCl_2$, 0.002 g/L $CoCl_2.6H_2O$, and 0.004 g/L $Na_2MoO_4.2H_2O$) at a concentration of 6 mL/L. The cultures were further inoculated into airlift photobioreactors (3.2 L) and a raceway pond (50 L) for generation of the required masses for digestion.

Spirulina spp.

Stock cultures of the cyanobacterium *Spirulina spp.* (obtained from the Environmental Biotechnology Research Unit, Rhodes University) were maintained at ambient temperature in 2 L flasks, continuously mixed with a magnetic stirrer and illuminated with three fluorescent bulbs (120 μmol photon/m^2.s at the surface) from one side of the flask. All *Spirulina spp.* cultures were grown on Zarrouk's media comprising of: nutrients (18 g/L $NaHCO_3$, 2.5 g/L $NaNO_3$, 0.5 g/L K_2HPO_4, 1 g/L K_2SO_4, 0.04 g/L $CaCl_2.2H_2O$, 1 g/L NaCl, 0.2 g/L $MgSO_4.7H_2O$, 0.01 $FeSO_4.7H_2O$ and 0.08 g/L EDTA), metal solution A5 (2.86 g/L H_3BO_3, 1.81 g/L $MnCl_2.4H_2O$, 0.22 g/L $ZnSO_4.7H_2O$, 0.08 g/L $CuSO_4.5H_2O$ and 0.0124 g/L Na_2MoO_4)

at a concentration of 1 mL/L and metal solution B6 (56.6 mg/L K_2CrO_7, 47.8 mg/L $NiSO_4.7H_2O$ and 4.2 mg/L $CoSO_4.7H_2O$) at a concentration of 1 mL/L. The cultures were further inoculated into airlift photobioreactors (3.2 L) and a raceway pond (50 L) for generation of the required masses for digestion.

Anaerobic digestion inocula

Two different inocula in were used to provide the required anaerobic microbes in all anaerobic digesters. The first inoculum was obtained from an anaerobic digester treating brewery effluent, located at South African Breweries (SAB), Newlands, Cape Town, South Africa. The second component if the inoclum was obtained from a 1 L stock reactor maintained on *Spirulina spp.*. The stock reactor was inoculated with 20% (vol/vol) activated sewerage sludge. The stock digester was operated in fed batch mode with intermittent loading of *Spirulina spp.*. Gas production and composition were monitored to ensue that the digester was operating efficiently. The digester was harvested when necessary and the volume gradually increased back to the operating volume of 1 L by addition of *Spirulina spp.* slurries. The method of inoculation utilised in this study ensured a relatively consistent initial population of microorganisms in each digester.

3.2.2 Photobioreactors

A portion of the algal biomass used for batch digestion studies was generated in 3.2 L glass and stainless steel, internal loop airlift reactors.

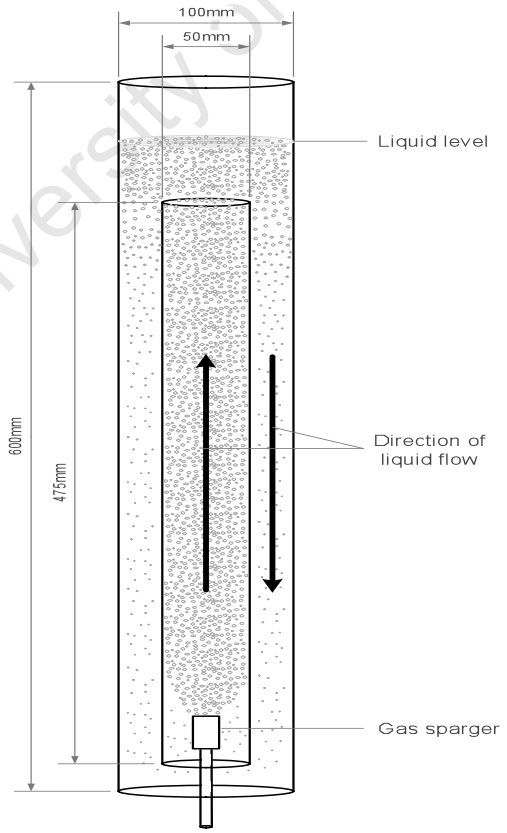

Figure 3.1: Schematic diagram of the experimental set-up for the algal photobioreactors (Langley et al., 2010)

The photobioreactors (Figure 3.1) consisted of a 600 mm high, 100 mm outside diameter (OD) column and a 50 mm OD draught tube. For *Spirulina spp.* air and for *Scenedesmus spp.* air enriched (2900 ppm) with CO_2 were sparged into the column through a 0.22 μm stainless steel HPLC inlet filter located at the base of the draught tube. Air and CO_2 flow rates were controlled with a Brooks 5850S Thermal Mass Flow Controller. The two gas streams were then sent through an inline mixer and fed to each column at a flow rate of 2 L/min. Light was supplied continuously by three Osram 18 watt cool white fluorescent bulbs at a distance of 3 cm from the column surface, providing 300 μmol photon/m^2.s.

3.2.3 Raceway pond

A 50 l Perspex raceway pond (Figure 3.2) with a paddle wheel was used for larger-scale algal cultivation. *Scenedesmus spp.* cultures were sparged with air (25 L/min) through a 6.35 mm stainless steel tube, with 1 mm holes drilled every 20 cm, positioned on the reactor floor. No sparging was required during growth of *Spirulina spp.* as the primary carbon source was bicarbonate (HCO_3^-), not CO_2. Circulation of the media was achieved using a four bladed paddle at 20 rpm for *Scenedesmus spp.* and at 10 rpm for *Spirulina spp.*. The liquid depth was 10 cm and the total surface area was 0.51 m^2. Six 58 watt and two 36 watt fluorescent bulbs provided continuous light to the cultures.

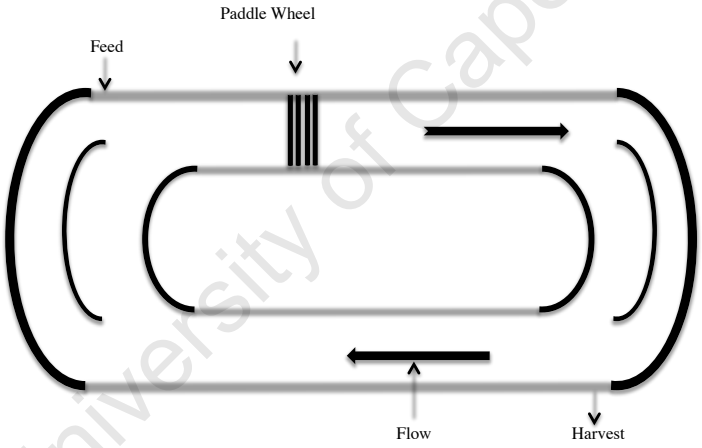

Figure 3.2: Schematic digram of the experimental set-up for the algal raceway pond

3.2.4 Bead mill

Batch phase bead milling was used as the mechanical pre-treatment to rupture the algal cells. The bead mill was agitated, at 900 rpm, using a 20 mm diameter Rushton turbine and mixing was enhanced by four 10 mm wall baffles. The mill (Figure 3.3) was loaded with glass beads (1 mm diameter) at 35% vol/vol for the smaller *Scenedesmus spp.* and with larger beads (4 mm diameter) at the same loading for the filamentous *Spirulina spp.* algal cells. The mill ran for a time period that allowed for complete disruption of the algal cells.

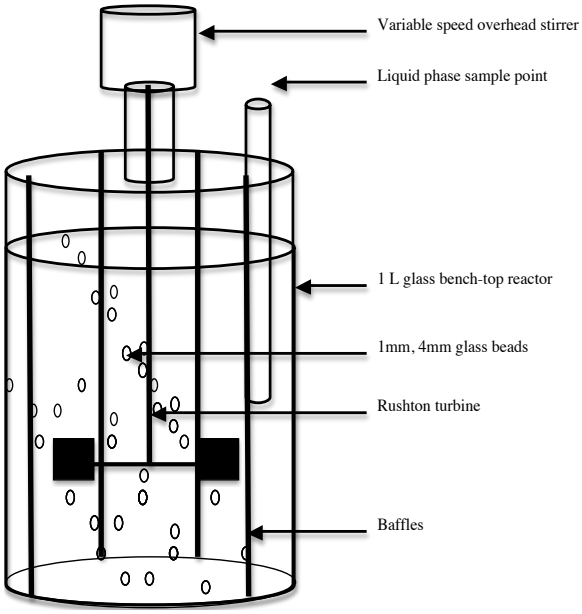

Figure 3.3: Schematic diagram of the experimental set-up for the algal cell bead mills

3.2.5 Anaerobic bench-top batch reactors

The digestion experiments were carried out in continuously mixed bench-top batch reactors (Figure 3.4).

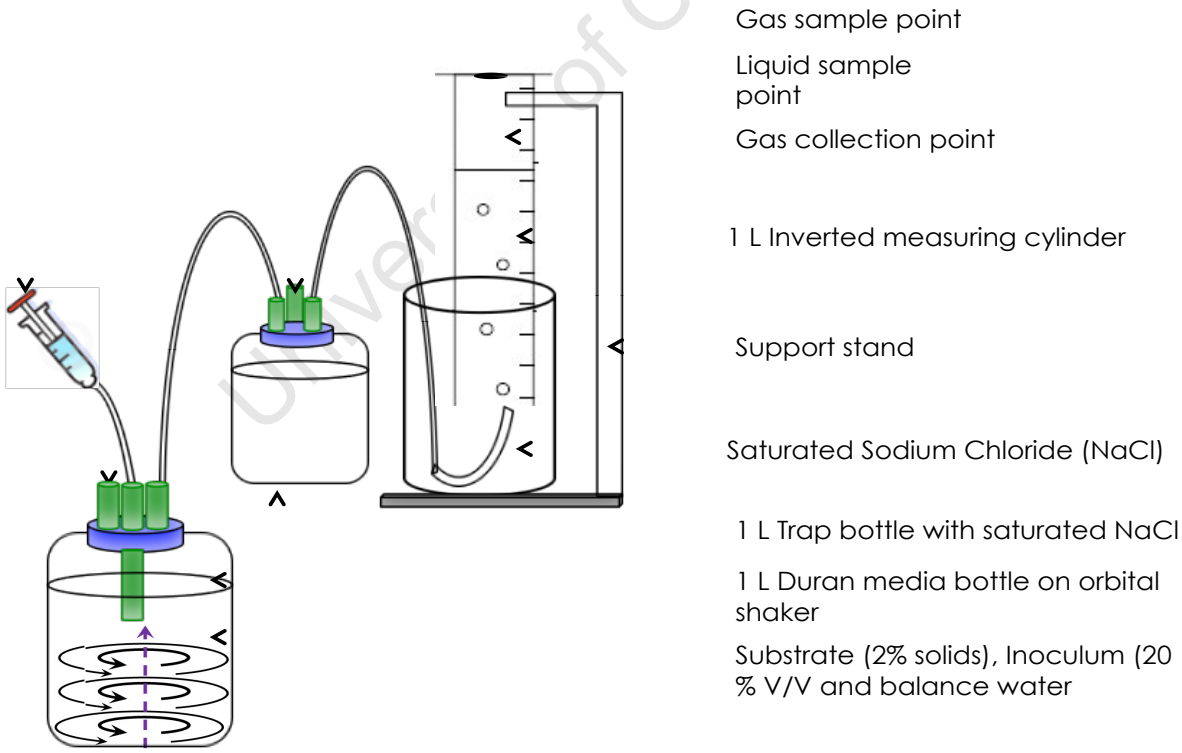

Figure 3.4: Schematic diagram of the 1-L digesters used for batch digestion of algal biomass

* *Scenedesmus spp.* DT residue digesters were 500 mL Duran Schott bottle

The reactors were constructed from 1 L Duran Schott bottles and were operated with minimal headspace. The lid of the reactor was modified to include three ports. The first port was used for biogas collection, the

second for liquid sampling and third for biogas sampling to determine composition. The units were placed in a controlled environment room at 37 ± 2^{o}C, and were continuously mixed on an orbital shaker (140 rpm). Biogas was collected using water displacement vessels filled with saturated sodium chloride (NaCl) solution to minimise the dissolution of CO_2. To prevent any backflow of NaCl into the reactors 1 L trap bottles were inserted on all biogas lines. These trap bottles were fitted with a secondary biogas sampling point. The volume of biogas produced was corrected for normal temperature and pressure (STP). The digester pH could be controlled by injecting 5 M sodium hydroxide (NaOH).

3.2.6 Integrated algal anaerobic digestion system

The integrated algal anaerobic digestion system comprised of four major processes: algal biomass (*Spirulina spp.*) generation, continuous harvesting, semi-continuous anaerobic digestion and continuous CO_2 scrubbing. The design of the integrated system is shown in Figure 3.5. This study presents a detailed investigation into the first three stages whilst the CO_2 scrubbing process results are presented in detail in the thesis and papers by Langley et al. (2010).

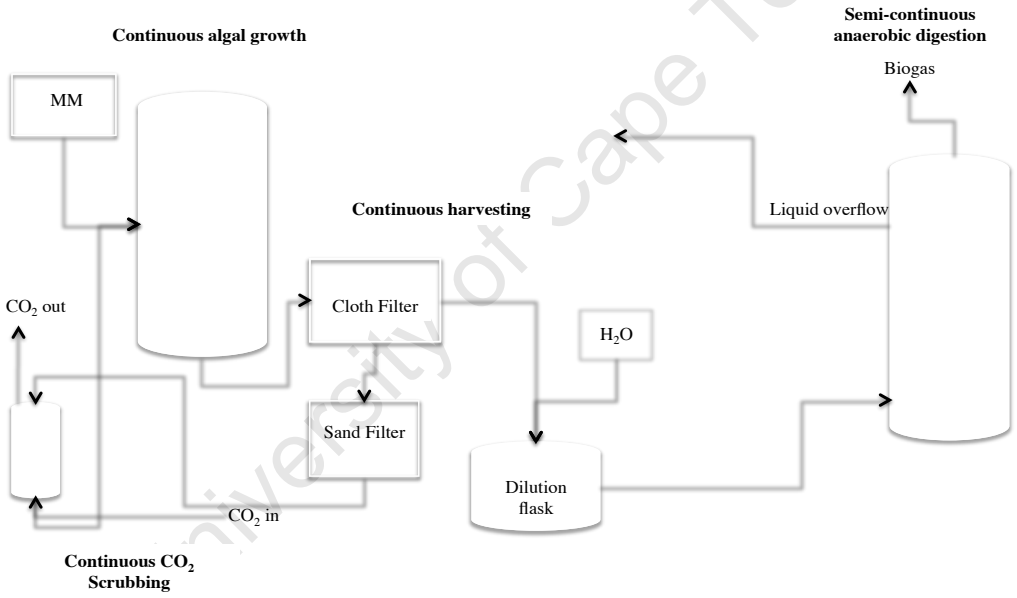

Figure 3.5: Schematic diagram of the experimental set-up for the integrated algal anaerobic digestion system

Algal growth unit

The algal growth unit consisted of a 65 L raceway pond, similar to that described in Section 3.2.3. The make up media consisted of all key components of the Zarrouk media except for the $NaHCO_3$, which was recovered in the filtrate recycle.

Continuous harvesting

Spirulina spp. harvesting was carried out continuously using nylon cloth filtration (pore size 100 μm). Filtrate was further filtered through a sand filter (650×150 (ID) mm), scrubbed against CO_2 and recycled

back into the raceway pond with fresh make-up media (MM). The biomass that collected on the cloth filter was removed once a day. All continuous flow was produced using lab-scale peristaltic pumps.

Semi-continuous anaerobic digestion

The semi-continuous digester utilised in the integrated system was specifically designed (Figure 3.6). The reactor consisted of: a 10 mm thick Perspex tube ((1) 640×100(ID) mm) fitted with an overflow ((2) 510 mm from base) and continuous feed ((3) 5 mm from base) port. The continuous feed port was fitted in anticipation of further continuous studies being conducted. The positioning of the overflow port allowed for a 4 L liquid volume and 1 L headspace volume. The Perspex tube was machined and glued into a solid Perspex base (120 ×120×12 mm). The inner lining of the Perspex tube was fitted with four (640×1×10 mm wide) Perspex strips, which acted as baffles increasing mixing. The top of the tube was flanged such that a lid (5) could be screwed on with four butterfly nut and bolts. The lid was sealed with a 105 mm outer diameter silicone o-ring (6), which was placed in a special grove that had been machined into the base of the lid. The lid was fitted with four ports. The first port had a stainless steel tube (510×8 mm) running through to a ball valve (10 bar specified) for substrate feeding. The second port was fitted with a 12.7 mm check valve (3 bar cracking pressure) to serve as the safety relief valve. The third port was fitted with a 3.18 mm pressure gauge (4 bar rating) for headspace pressure readings. The fourth port was fitted with a ball valve (10 bar specified) for gas collection and sampling. Continuous mixing was also supplied using a magnetic stirrer.

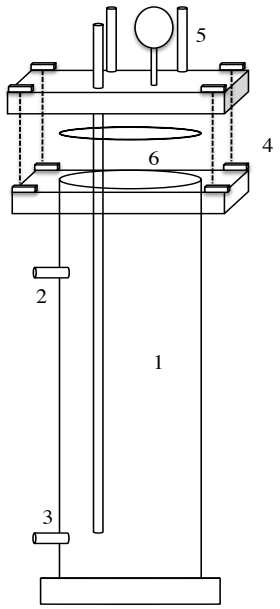

Figure 3.6: Schematic representation of the semi-continuous anaerobic digestion unit of the integrated algal anaerobic digestion system

CO_2 Scrubbing

The filtrate from the sand filter was scrubbed against 95% CO_2 in a counter current packed bed column. A full decription of the materials used can be found in the thesis presented by (Langley et al., 2010).

3.3 Methods

3.3.1 Analytical techniques

Alkalinity

Alkalinity was determined using a modification of the titration method (2320 B) described in the Standard Methods for the Examination of Water and Wastewater (APHA, 1999). An appropriate volume of sample (10-20 mL) was added to a 250 mL Erlenmeyer flask and the pH recorded. If the pH was greater than pH 8.3 the solution was titrated against a standard solution of sulphuric acid until the pH reached pH 8.3, the equivalence point for bicarbonate. The alkalinity calculated to this point is termed the phenolphthalein alkalinity as the original method used indicators, rather than pH measurement. The volume of acid added was recorded. The solution was titrated further to pH 4.5, the equivalence point for carbonic acid (dissolved CO_2). This value is termed methyl orange alkalinity.

The alkalinity, in mg/L $CaCO_3$ equivalents is determined according to the following equation:

$$Alkalinity,\, mg\, CaCO_3/L = \frac{A \times N \times 50000}{mL\, Sample}$$

Where: A is mL of standard acid used

and N is the normality of the standard assay

The contribution to total alkalinity of the various alkaline species was determined according to the Table 3.1.

Table 3.1: Calculation of composition of the total alkalinity. P = phenolphthalein alkalinity and MO = methyl orange (total) alkalinity.

Result of titration	Hydroxide alkalinity	Carbonate alkalinity	Bicarbonate alkalinity
Initial pH 8.3 < 4.5	0	0	MO
P < 0.5 MO	0	2P	MO-(2P)
P = 0.5 MO	0	MO	0
P > 0.5 MO	2P-MO	2(MO-P)	0
P = MO	MO	0	0

Conversion of values from mg/L $CaCO_3$ equivalent to sodium bicarbonate were made, based on relative molecular mass and charge of the anionic species, by multiplying by 84 and dividing by 50.

Ammonium ions

Ammonium ion concentration was determined by HPLC using a Waters Breeze 2.0 system equipped with a Hamilton PRP-X200 Polymeric cation exchange column (4.1 × 150 mm) and a conductivity detector. The system was run isocratically using a 4mM nitric acid in 30% methanol mobile phase. The HPLC was run at ambient temperatures with a mobile phase flow rate of 1 mL/min. The pressure in the column did not exceed 1600 psi. Sample injection volumes of 100 µL were used. To quantify the ion concentration,

standard solutions (50, 100, 500 and 1000 mg NH_4^+/L) were prepared using NH_4Cl. The standard curve is shown in Appendix A (Figure 8.2).

Biomass concentration using optical density

Biomass concentration was determined daily by measuring optical density at 750 nm with a Helios spectrophotometer and converting these to dry mass concentration using a calibration curve (Appendix A-Figures 8.4 and 8.5). The sample was first diluted to ensure that the absorbance measured did not exceed 1. The final concentration was adjusted using this dilution factor.

Biomass concentration using dry weight

Biomass dry weight was measured by filtration of a 5 mL sample through a pre-weighed 0.22 μm filter paper, which was then dried at 80°C overnight before being re-weighed.

Methane

The methane content of the biogas was determined using flame ionisation detection gas chromatography (FID GC). All FID GC measurements were conducted on a Perkin Elmer Autosystem Gas Chromatograph using a Supelco wax column (1.2 mm× 37 m). The FID detector was set at 280°C, whilst an oven temperature of 50°C was used. Nitrogen, at a flow rate of 1.5 mL/min, was used as the carrier gas. 100 μL of gas was injected into the chromatograph. The chromatograph was calibrated with a standard gas containing 52.8% CH_4 vol/vol.

Nitrates and Phosphates

Aqueous nitrate and phosphate ion concentrations were measured by HPLC using a Waters Breeze 2.0 system equipped with a Waters IC-Pak A HR (Anion High resolution) column and a conductivity detector. The system was run isocratically using a sodium borate-gluconate mobile phase (Table 3.2) at a flow rate of 1 mL/min.

Table 3.2: Sodium borate-gluconate solution for anion detection HPLC mobile phase component make-up

Component	Amount added to 1 L
Sodium Borate-Gluconate Concentrate	
Sodium gluconate	16 g
Boric acid	18 g
Sodium tetraborate decahydrate	25 g
Glycerine	250 mL
dH_2O	Balance (mL)
Mobile phase	
Sodium Borate-Gluconate Concentrate	20 mL
Butanol	20 mL
Acetonitrile	120 mL
dH_2O	Balance (mL)

The HPLC was run at ambient temperatures with a mobile phase flow rate of 1 mL/min. The pressure in the column did not exceed 2000 psi. Sample injection volumes of 100 µL were used. To quantify the ion concentrations standard solutions (50, 100, 500 and 1000 mg NO_3^- and PO_4^{3-}/L) were prepared using sodium nitrate ($NaNO_3$) and potassium dihydrogen phosphate (KH_2PO_4) respectively. The resulting standard curves are shown in Appendix A (Figure 8.8)

pH

All pH testing was done on a Cyberscan 2500 micro pH meter. The meter was calibrated daily using standard (pH of 4.0 and 7.0) buffer solutions.

Soluble, solid and total COD

All COD measurements were carried out using the Merk reagent test protocol for high (1500 - 10000 mg/L) concentrations. The method is based on the oxidation of the sample with a hot sulphuric acid solution containing potassium dichromate, with silver sulphate as the catalyst. The chloride is masked with mercury sulphate. The concentration of unconsumed yellow $Cr_2O_7^{2-}$ ions or green Cr^{3+} ions is then determined photometrically and used to quantify oxygen demand. The specific method for determining the solid, soluble and total COD concentrations is typically not described in literature so the detailed protocol is described in Apeendix A. To quantify the COD concentrations, standard solutions (0, 2500, 5000, 7500 and 10000 mg COD/L) were prepared using potassium hydrogen phthalate. The resulting standard curve is shown in Appendix A (Figure 8.6)

Sulphide

Aqueous sulphide was quantified using the colorimetric DMDP method. The principle of the method is reaction of aqueous sulphide with N,N-dimethyl-p-phenylene diamine, catalysed by ferric ions, to produce methylene blue. An appropriate volume of sample (10 µL – 4800 µL) is added to 200 µL of 1% zinc acetate. The volume is made up to 5 mL with deoxygenated water, after which 500 µL of 0.4% N,N-dimethyl-p-phenylene diamine (in 6 M HCl) and 500 µL of 1.6% ferric chloride (in 6 M HCl) are added. The sample is mixed well and left to react for a minimum of 5 minutes after which the absorbance is read at 670 nm and the concentration determined relative to a standard curve. The assay has a maximum detection limit of just over 1 mg/L so significant dilution is required. This is typically achieved by using a small volume (20-50 µL) of sample. The standard curve for the assay is shown in Appendix A (Figure 8.3).

Volatile fatty acids (VFAs)

A full volatile fatty acids (VFA) analysis was conducted to quantify the concentration of lactic, acetic, propionic, iso-butyric, butyric, iso-valeric and valeric acids present in all digesters over the duration of digestion. The concentration of each VFA was determined using HPLC on a Waters Breeze 2 HPLC system equipped with a Bio-Rad Organics Acids ROA column and a UV (210 nm wavelength) detector. The system was run isocratically using a mobile phase of 0.01 M H_2SO_4 at a flow rate of 0.6 mL/min.

The pressure in the column did not exceed 2000 psi. Sample injection volumes of 100 µL were used. To quantify the VFA concentrations standard solutions (50, 100, 500 and 1000 mg/L for each acid) were prepared. The resulting standard curves are shown in Appendix A (Figure 8.10)

Volatile solids

Volatile solids were quantified using the standard method. The sample (1 mL) was filtered through a pre-weighed 25 mm diameter Glass Fibre Acetate (GFA) filter. The filter was placed in a furnace at 105°C over night to determine the moisture content. The filter was heated further at 550°C for two hours. The amount of ash left behind was quantified by re-weighing the filter. From this the total mass of volatile solids was calculated and a relative % VS determined. All VS testing was done in triplicate to quantify the error associated with the method.

3.3.2 Molecular analysis of the inoculum

The inoculum loaded into each of the anaerobic digesters was made up of comprised of an equal volume from two separate sources. Characterisation of the different inocula involved DNA extraction and quantitative polymer chain reaction (qPCR) using domain specific primer sets. The testing aimed to determine the ratio between bacteria and archae. The DNA extraction method was adapted from the standard method for extracting DNA from biomining samples and is described Appendix A.

Quantitative polymerase chain reaction

The concentration of DNA in the samples extraction was calculated using the nanodrop ND-2000 Spectrophotometer (Thermo Scientific). The domain specific forward and reverse primer sequences are presented in Table 3.3.

Table 3.3: Primer sequence used in QPCR

Name	Primer Sequence	Orientation
UniBactF336	gactcctacgggaggcagca	forward
UniBactR937	ttgtgcgggcccccgtcaat	reverse
UniArchF343	acggggigcaicaggcg	forward
UniArchR932	tgctcccccgccaattcc	reverse

Each qPCR reaction included, 1 µL template DNS (10 µg/µl), 7.2 µL mastermix (Kax Biotech), 6.2 µL molecular grade dH_2O, 0.3 µL of each primer (0.25 mM). The real time PCR reactions were carried out using a Corbett Roto-gene 6000 as follows; 95°C for 5 minutes (melt), followed by 35 cycles of 60°C for 20 seconds (annealing of primers), 72°C (extension). Upon completion of the amolification cycles a melt curve was generated by heating from 72°C to 95°C in increments of 0.2°C. The proportion of bacteria and acrchae were determined from specific standard curves.

3.3.3 Algal biomass harvesting

The *Scenedesmus spp.* loaded into the batch digesters was harvested by centrifugation at 7000 rpm. *Spirulina spp.* biomass utilised in the batch digesters and integrated system was harvested using cloth

filtration (pore size 100μm).

3.3.4 Algal cell disruption

Bead milling was used to physically rupture both *Scenedesmus spp.* and *Spirulina spp.* cells. The method involved loading 1 L of concentrated algae slurry into the bead mill and operating continuously for a period of time that would allow for complete disruption. The algal cells were disrupted at concentrations of 40 g/L and 20 g/L. Two 2 mL samples were taken every 30 min for *Spirulina spp.* disruption and hourly for *Scenedesmus spp.* disruption. The samples were spun down at 12000 rpm for 10 minutes. The supernatant was decanted and utilised for optical density, soluble COD, pH and VFA analyses. The solid pellet remaining was diluted to 2 mL using dH_2O and used for solid COD analysis. Photographs taken, using a diluted 20 μL volume, through a 100X objective lens were used to obtain confirmation of cell disruption and for determination of complete disruption. The mill ran for a time period that allowed for complete disruption of the algal cells.

3.3.5 Direct transesterification

This study utilised an alternate technique, developed by Griffiths et al. (2010), to extract the lipids from the algal biomass in prefernece to conventional solvent extraction methods. Rather than extracting the lipids, the transesterification reaction was performed using whole cells. The residue was then recovered from the reaction solution using centrifugation and evaporation.

The tranesterification reaction involved using the sequential use of base, followed by acid catalysis as follows: A 5% sodium hydroxide (NaOH) in methanol (CH_3OH) solution was added to the samples (15 mL/ g of dry algae), the samples mixed briefly by vortexing and placed in an 80°C incubator, shaking at 300 rpm for 20 min. They were then cooled for 5 min to room temperature and a 2% hydrochloric acid (HCl) in methanol solution (15 mL/g of dry algae) added before repeating the incubation period. After cooling to room temperature, dH_2O and hexane (C_6H_{14}) (extracts the fatty acid methyl esters (FAME)) were added (5 mL/g of dry algae) and contents mixed well by vortexing. The samples were then centrifuged at 4000 rpm for 1 min and the upper hexane layer, containing the FAME extract removed. The remaining mixture, containing the algal residue and excess reaction compounds underwent evaporation at 60℃ to recover the DT residue used in subsequent digestions.

3.3.6 Microscopy

Microscopy was performed using an OLYMPUS BX 40 microsope, fitted with a colourview 11 digital camera. Images were captured using the analySIS Five (Soft Imaging Solutions) software package.

3.4 Experimental Protocol

3.4.1 Substrate preparation

Whole cell slurry

To obtain the desired slurry concentration for addition to the anaerobic digesters the following process was followed. A sufficient mass (wet weight) of algal cells were harvested. The dry mass of a fraction of the wet algae was determined to allow for the calculation of the moisture content. Once the moisture content of the wet algae had been determined, sufficient wet mass was diluted with dH_2O to obtain the desired dry weight slurry concentration. The accuracy of the process was calculated by performing a dry mass determination of a fraction of the slurry. This procedure was applied to both *Scenedesmus spp.* and *Spirulina spp.* algal slurries.

Ruptured cell slurry

For the digesters loaded with ruptured biomass the same initial procedure was followed. This produced an unruptured algal slurry with the correct biomass concentration. After this had been done the slurry was loaded into the bead mill and operation initiated. Once complete disruption had occurred the slurry was separated from the beads using sedimentation and cloth filtration (100 μm pore size).

Direct Transesterified slurry

For the digesters loaded with DT residue the same initial procedure was followed to obtain the desired amount of biomass. An extra amount (10 %) of biomass (22 g/L) was harvested in anticipation of the lipid removal decreasing the amount of solid biomass in the slurries. DT was then performed on the wet algae. After the final evaporation stage the residue that remained was diluted with dH_2O to yield the desired amount of DT algal residue slurry to be loaded into the digesters.

3.4.2 Batch digestion studies

Protocol

The following experimental protocol was followed for all batch digestion experiments. The digesters were loaded with 20 g DW of the appropriate substrate. The substrate was either in the form of wet biomass or as a slurry of ruptured cells with an initial loading of 20 g DW. Tap water was added to a total volume of 800 mL. The reactor was inoculated with 100 mL of the *Spirulina spp.* stock inoculum and 100 mL of the SAB inoculum. The reactor was made airtight using a custom cast silicone seal, which fitted inside the screw cap. The sampling and gas collection port were connected and the reactor prepared for anaerobic operation by sparging with nitrogen for 5 min. All ports, with the exclusion of the gas exhaust port that was positioned into the gas collection system, were sealed. The reactors were loaded onto an orbital shaker rotating at 140 rpm in a temperature controlled room at 37℃.

Sample protocol and preparation

The sampling protocol for all batch digesters involved daily gas phase sampling whereby a 100 µL Hamilton syringe to sample directly from the digester headspace. Every second day 2 mL of liquid sample was removed from the digesters via the liquid phase sampling port. The sample was separated into two 2 mL Eppendorf tubes (1 mL of sample in each). One of the tubes was used for pH analysis and immediately stored at -20℃ for future sampling, if necessary. The second sample was spun down at 12 000 rpm for 10 minutes. The supernatant was decanted from the solid pellet. A 400 µL sample of the supernatant was further diluted to 2 mL, filtered through a 0.22 µm Millipore filter and used for all HPLC analysis. A further 400 µL sample of the supernatant was diluted to 1400 mL and used in the COD analysis. The solid pellet remaining was diluted to 2 mL and used for COD analysis. Note all dilutions were conducted using dH_2O.

Sample testing frequency

For all batch digester units the following variables were tested with the given frequency:

Table 3.4: Variables tested and frequency of sampling for batch digestion units

Variable	Frequency
Biogas production	daily
Biogas composition	daily
pH	every 2nd day
Solid COD	every 2nd day
Soluble COD	every 2nd day
VFAs	every 2nd day
VS	beginnig and end

3.4.3 Integrated algal anaerobic digestion system studies

Algal growth unit

Sample protocol and preparation

The sampling protocol for the continuous algal growth unit involved taking three 5 mL samples every second day. Each sample was filtered through a pre-weighed GFA filter. The filtrate was used for all soluble phase analytical methods, whilst the filter cake remaining was used in dry weight and VS analyses. A 2 mL sample was also taken, spun down at 12 000 rpm for 10 minutes and the solid pellet used for solid COD analysis. Note all dilutions were conducted using dH_2O.

Sample testing frequency

For the algal growth unit the following variables were tested with the given frequency:

Table 3.5: Variables tested and frequency of sampling for the semi-coninuous digestion unit of the integrated algal AD system

Stream	Tests	Frequency
Algal growth unit effluent	VS	Every 2 days
	Solid and Soluble COD	Every 2 days
	Dry weight conc.	Daily
	OD	Daily
	pH	Daily
	Nitrates conc.	Every 2 days
	Phosphates conc.	Every 2 days

Continuous harvesting

All sampling was conducted on the harvested biomass with the following frequency:

Table 3.6: Variables tested and frequency of sampling for the semi-coninuous digestion unit of the integrated algal AD system

Stream	Tests	Frequency
Filter Cake	Wet Weight	Daily
	Dry weight	Daily
	VS	Every 2 days

Semi-continuous AD unit

The AD unit was first set-up in a batch phase mode to allow for acclimatisation of the microbial consortia after which semi-continuous flow commenced.

Batch phase acclimatisation and semi-continuous feeding

The digester was loaded with 80 g DW of whole cell *Spirulina spp.* biomass. Tap water was added to a total volume of 3.2 L. The reactor was inoculated with 400 mL of the *Spirulina spp.* stock inoculum and 400 mL of the SAB inoculum. The reactor was made airtight using a custom cast silicone o-ring, which fitted on an inner groove machined into the reactor lid. The lid was set in place by tightening the four butterfly screws (as shown in Figure 3.6). The sampling and gas collection ports were closed and the reactor prepared for anaerobic operation by sparging with nitrogen for 5 min. The reactor was loaded onto magnetic stirrer plate. The reactor was secured to a stand and placed in an ambient environment, until it was later moved into a temperature control room at 37℃. After the initial batch phase acclimatisation period (6 weeks), semi-continuous operation was initiated by feeding 286 mL of diluted biomass into the reactor whilst recovering 286 mL from the overflow port. Feeding was done at the same time everyday to ensure a constant retention time of the digester. The real time tracking of key parameters such as VFA production, aqueous sulphide concentration, solid and soluble COD, VS etc. allowed for the operating conditions to be varied between retention times to try and optimise the efficiency of digestion. Table 3.7 depicts the conditions that were used for each 14 day retention period of digestion. The organic loading rate was controlled by the amount of wet biomass that was diluted to 286 mL and fed into the digester.

The temperature was controlled by moving the entire digester into a 37 ± 2℃ temperature controlled room.

Table 3.7: Operating conditions investigated in AD unit of integrated system

Retention period	OLR (g VS/$L_{reactor}$.day)	Temperature (℃)	Added miscellaneous changes
1	1.72	Ambient	None
2	1.15	Ambient	None
3	1.15	37 ± 2	Addition of 7 g Sodium Molybdtae and 286 mL of SAB inoculum
4	0.48	37 ± 2	None

Sample protocol

The sampling protocol for the semi-continuous digester involved daily gas phase sampling whereby all the gas produced was released into a collection bag by opening of the gas exhaust. A 100 µL Hamilton gas syringe was then used to sample directly from the collection bag. The bag was emptied into a water displacement gas measuring unit, similar to that used for the batch digesters, to confirm the volume determined from the pressure gauge reading. Every day 286 mL of effluent was recovered from the digester overflow port. Every second day 2 mL of the effluent was stored at -20℃ for future sampling, if necessary. A further 26 mL sample was spun down at 12 000 rpm for 10 minutes in 2 mL Eppendorf tubes. The supernatant was filtered through a 0.22 µm Millipore filter and used for alkalinity, sulphide, HPLC and COD analysis. One of the solid pellets from the 2 mL samples spun down, was diluted back to 2 mL and used for solid COD analysis. A further 6 mL of effluent was first used for pH analysis and then for TS and VS analysis (2 mL done in triplicate). Note all dilutions were conducted using dH_2O.

Sample testing frequency

The following variables were tested with the given frequency:

Table 3.8: Variables tested and frequency of sampling for the semi-continuous digestion unit of the integrated algal AD system

Stream	Tests	Frequency
AD Feed	pH	Every 2 days
	Ammonium ions	Every 2 days
	VS	Every 2 days
	COD	Every 2 days
	Nitrates	Every 2 days
	Phosphates	Every 2 days
AD Liquid Effluent	pH	Every 2 days
	Ammonium ions	Every 2 days
	VS content	Every 2 days
	Soluble and Solid COD	Every 2 days
	Alkalinity	Every 2 days
	VFA's	Every 2 days
	Sulphide	Every 2 days
	Nitrates	Every 2 days
	Phosphates	Every 2 days
AD Gas Effluent	Composition	Daily
	Volume	Daily

3.5 Experimental Design

3.5.1 Introduction

The overall experimental design of this study included the following components:

1. Batch digestion studies on whole cell *Scenedesmus spp.* and *Spirulina spp.* biomass.
2. Batch digestion studies on ruptured *Scenedesmus spp.* and *Spirulina spp.* biomass.
3. Batch digestion studies on direct transesterification residue following biodiesel extraction from *Scenedesmus spp.* biomass
4. Evaluation of operating conditions and potential of the integrated algal anaerobic digestion system focussing on the continuous harvesting and anaerobic digestion of *Spirulina spp.* biomass.

3.5.2 Batch digestion studies

The batch phase digestion studies were conducted in triplicate. Where possible two replicates were run in parallel and the third in a separate run to better evaluate reproducibility. The experimental design is summarised in Table 3.9. In all cases the digesters were set up and sampled as described in Section 3.2.5 and 3.4.2.

Table 3.9: Experimental design of batch digestion experiments

Reactor	Substrate	Substrate pre-treatment	Running period
1-3	*Spirulina spp.*	none	R1: 19/4/2010 - 25/6/2010 (64 days) R2-3: 19/5/2010 - 22/6/2010 (64 days)
4-6	*Spirulina spp.*	bead milling	R4: 19/4/2010 - 25/6/2010 (64 days) R5-6: 19/5/2010 - 22/6/2010 (64 days)
7-9	*Scenedesmus spp.*	none	R7-8:19/4/2010 - 9/6/2010 (48 days) R9: 28/6/2010 - 10/08/2010 (48 days)
10-12	*Scenedesmus spp.*	bead milling	R10-11: 19/4/2010 - 9/6/2010 (48 days) R12: 28/6/2010 - 10/08/2010 (48 days)
13-15	*Scenedesmus spp.* DT residue	direct transesterification	R13-15: 3/8/2010 - 20/09/2010 (48 days)
16	Inoculum (control)	none	A control ran for each of the above time periods
17	Stock inoculum	none	19/4/2010 - 3/8/2010

3.5.3 Integrated algal anaerobic digestion system

Table 3.10 summarises the experimental investigations carried out over the integrated system and the time period over which they were performed. The integrated system was configured and operated as described in Sections 3.2.6 and 3.4.3.

Table 3.10: Experimental design for the integrated system

Operation	Running period
Batch phase acclimatisation of digester	1/6/2010 - 14/7/2010 (42 days)
Initialisation of continuous biomass harvesting, scrubbing and recycle of media	14/7/2010 - 3/9/2010 (56 days)
Beginning of phase 1: continuous biomass harvesting, semi-continuous feeding of AD unit and characterising of AD effluent-Retention period 1	14/7/2010 - 27/7/2010 (14 days)
Retention period 2	27/7/2010 - 3/8/2010 (14 days)
Retention period 3	9/8/2010 - 22/7/2010 (14 days)
Retention period 4	22/8/2010 - 3/10/2010 (14 days)

Chapter 4

Anaerobic digestion of *Spirulina spp.* and *Scenedesmus spp.*: batch studies on whole cells, ruptured cells and direct transesterification residue

4.1 Introduction

In this chapter the analysis of batch anaerobic digestion of *Spirulina spp.* and *Scenedesmus spp.* is presented. Most studies conducted on AD of algal biomass have used a semi-continuous system in which feed is added to the digesters at a specific load of volatile matter and desired retention period. However, few studies consider fundamental batch data before proceeding to operate a semi-continuous or continuous mode digester. Studies that have conducted batch phase digestion have typically not used a sufficiently rigorous analytical protocol to gather adequate fundamental data for analysis to inform continuous AD process design. Therefore, the main aim of the batch studies conducted in the current study was to gather a data set which was both broad and detailed enough to inform an assessment of the potential of using algal biomass as a substrate for AD.

This chapter presents a detailed aqueous phase analysis of the digester contents and relates this to trends observed in the gaseous product. Key variables analysed were VFA production and consumption, soluble COD and the contribution of VFAs to COD. Indicator VFAs were also investigated to seek possible causes of inhibition in the system. The gaseous phase results focused on methane production and associated this with the VFA dynamics in the system. Dynamics represent the fluctuations observed in the concentration profiles of the various parameters.

In Section 4.4 the impact of mechanical disruption, as a pre-treatment, on the overall digestibility of the specific algal substrates is discussed. Key aqueous phase profiling and characterisation of the gaseous product again inform this analysis. This approach was also used to determine the feasibility of anaerobic digestion of *Scenedesmus spp.* lipid extraction residue (Section 4.5).

4.2 Methodology

The results presented in this chapter refer to the experimental design detailed in Section 3.5.2. All the results represent the mean values from triplicate digesters, with the exception of the DT residue digester where data from only one digester is presented. A full work-up of the data presented in all Figures and Tables can be found in Appendix B.

4.3 Whole cell digestion

4.3.1 Substrate analysis

The most important characteristics of each algal substrate are summarised in Table 4.1. The components of the substrates are key in identifying their digestibility (Sialve et al., 2009). By quantifying the carbohydrate, lipid and protein contents of the substrate important predictions can be made (Section 4.3.2). It also allows for a better understanding of the system's progress and explanation of certain products forming which may impact digester efficiency (Ahring et al., 1995).

Table 4.1: Properties and characteristics of *Scenedesmus spp.* and *Spirulina spp.* algal biomass

Constituent	*Scenedesmus spp.*		*Spirulina spp.*	
	mg/g TS	mg/L[a]	mg/g TS[a]	mg/L
Proteins[b]	500-560	10000-11200	600-700	12000-14000
Carbohydrates[c]	100-170	2000-3400	60-70	1200-1400
Lipids[d]	120-140	2400-2800	130-160	2600-3200
Volatile Solids	850	16500	860	16800
Total VFAs	-	1000	-	1350
Alkalinity[e]	-	-	55	2000
C	462	9230	410	8190
H	71	1428	61	1218
O	427	8542	450	9000
N	40	800	77	1536
P	trace	trace	trace	trace
S	trace	trace	2.6	52
Total COD	1538	31000	1690	33800
Solid COD	1082	21650	1290	25800
Soluble COD	456	9100	400	8000
Cell nature	rigid ellipsoidal cells		form filaments	
Cell size (μm)	10	-	30	-

[a] Concentration is shown in mg/L for a whole cell algal slurry containing 20 g DW/L (as loaded into all batch digesters);[b,c,d] Sialve et al. (2009); Becker (2007), [e] Samson and LeDuy (1986), note in certain cases a dash has been placed where values could not be found in literature or were experimentally determined as well as when they were not relevant to the phase of the algae.

The C/N ratios for *Spirulina spp.* of 5.33 and *Scenedesmus spp.* of 11.5, are important in predicting the ammonia release into the system (Yen and Brune, 2007). The ratio is low for *Spirulina spp.* due to the high protein content (60%) and low lipid content (3%). This raises concern for possible high ammonia release from digestion of large amounts of nitrogenous matter. Optimum ratios for AD are between 20 and 30 (Yen and Brune, 2007). Both algal species have VS contents in excess of 85%, which makes their applicability to AD very high.

The total VFA concentration in the whole cell algal slurries were higher for *Spirulina spp.* This resulted from cells undergoing disruption, most likely due to osmotic shock. The alkalinity is higher for the *Spirulina spp.* slurries due to the release of intracellular components and from residual media on the unwashed wet biomass. The increased alkalinity can act as a buffer to stabilise the pH and reduce the possible inhibition by VFAs and NH_3 (Samson and LeDuy, 1986).

The difference in cell size and nature of these algae is noted in Table 4.1. Filaments tend to break open, releasing their intracellular contents more easily than small rigid recalcitrant cells.

4.3.2 Dynamic metabolic pathways and effect of COD and VFAs on system parameters

The anaerobic digestion process comprises four key stages. Hydrolysis, acido- and aceto-genisis and finally methanogenisis occur to achieve the conversion of biomass to methane. The complexity of modeling AD has been studied for many years and a number of possible models have been proposed (Lyberatos and Skiadas, 1999). The metabolism of organics within the system is dependent on the type of substrate and the concentration of specific nutrients supplied to the anaerobic microbial consortia (Zehnder, 1998). Therefore, this study aims to present and discuss the data using a basic fundamental approach rather than attempting to develop a new process model.

Formulating a generic approach to system profiling

In analysing the feasibility of AD using specific complex substrates, it is essential to consider the compound in terms of its key components and review the reactants and products of each stage of digestion. Angelidaki et al. (1999) use a simple first principle approach in modeling anaerobic bioconversion of complex substrates to biogas. Considering the substrate in terms of key components (carbohydrates, lipids, proteins) allows the degradation to be explained using generic compounds that represent each of these components.

Degradation pathways for these compounds can then be used to estimate the expected product mix. Table 4.2 depicts the generic degradation of these substances by enzyme aided hydrolysis and acid forming bacteria (Angelidaki et al., 1999).

Table 4.2: Degradation of key components (Carbohydrates, Lipids, Proteins) using generic compounds as a basis (Angelidaki et al., 1999).

Component	Basis	Degradation reactions	Eqn	Conversion mechanism
Carbohydrates	$(C_6H_{10}O_5)_{s/in}$	$(C_6H_{10}O_5)_{in} \rightarrow Y_c(C_6H_{10}O_5)_s +$ $(1\text{-}Y_c)(C_6H_{10}O_5)_{in}$	1	Enzymatic hydrolysis
		$(C_6H_{10}O_5)_s \rightarrow$(VFAs) + (Biomass)	2	Acid forming bacteria
Lipids	Glycol trioleate ($C_{57}H_{104}O_6$)	$C_{57}H_{104}O_5 + 3H_2O \rightarrow C_3H_8O_3 + 3C_{18}H_{34}O_2$	3	Enzymatic lipolysis
		$C_3H_8O_3 + 0.04071\ NH_3 + 0.0291\ CO_2 \rightarrow$ $0.04071\ C_5H_7NO_2 + 0.9418\ C_3H_8O_2 + 1.09305$ H_2O	4	Glycerol fermenting bacteria
		$C_{18}H_{34}O_2 + 15.24H_2O + 0.25CO_2 + 0.17\ NH_3 \rightarrow$ $0.1701\ C_5H_7NO_2 + 8.6998\ C_2H_4O_2 + 14.500\ H_2O$	5	LCFA degrading acetogens
		$14.500\ H_2 + 3.8334\ CO_2 + 0.0836\ NH \rightarrow$ $0.0836\ C_5H_7NO_2 + 3.4139\ CH_4 + 7.4997\ H_2O$	6	Hydrogen utilisation
Proteins	Gelatin ($CH_{2.03}O_{0.6}N_{0.3}S_{0.001}$)	$(Protein)_{in} \rightarrow Y_p(Amino\ acids) + (1\text{-}Y_p)$ $(Protein)_{in}$	7	Enzymatic hydrolysis
		$CH_{2.03}O_{0.6}N_{0.3}S_{0.001} + 0.3006\ H_2O \rightarrow 0.017013$ $C_5H_7NO_2 + 0.29742\ C_2H_4O_2 + 0.02904\ C_3H_6O_2 +$ $0.022826\ C_4H_8O_2 + 0.013202\ C_5H_{10}O_2 + 0.07527$ $CO_2 + 0.28298\ NH_3 + 0.001\ H_2S$	8	Acid forming bactetria

The generic degradation reactions can be described as follows:

1. Insoluble carbohydrates are hydrolysed to soluble carbohydrates with Y_c being the degradation yield coefficient of carbohydrates. The remaining non-degradable fraction is determined as (1-Y_c) times the initial insoluble concentration.

2. The solubilised carbohydrates are converted by acidogenic bacteria to biomass ($C_5H_7NO_2$) and VFAs.

3. Lipids undergo degradation by enzymatic lipolysis to form glycerol ($C_3H_8O_3$) and oleate ($C_{18}H_{34}O_2$, basis for long chain fatty acids (LCFA's)).

4. The glycerol is then consumed by glycerol fermenting bacteria to produce biomass, propionate and water.

5. The LCFA's are consumed by acetate forming bacteria to produce biomass, acetate and hydrogen.

6. The final step in lipid degradation is hydrogen utilisation by acidogenic bacteria to produce biomass, methane and water.

7. Similar to carbohydrates, the insoluble proteins are solubilised by enzymatic hydrolysis to form amino acids according to the protein degradation coefficient (Y_p), leaving (1-Y_p) times the initial concentration of insoluble protein.

8. Soluble proteins (amino acids) are consumed by acidogenic bacteria to produce biomass, acetate, propionate, butyrate, valerate, CO_2, ammonia (NH_3) and sulphide (H_2S).

In the next phase of the digestion model the VFAs are metabolised. Degradation stoichiometry of VFAs formed from the complex organics within the system can be explained using the reaction system, depicted in Table 4.3.

Table 4.3: Reaction pathways for fatty acid degradation (Pind et al., 2003)

VFA	Reaction	Eqn number
Acetate	$CH_3COOH \rightarrow CH_4 + CO_2$	1
Propionate	$CH_3CH_2COOH + 2H_2O \rightarrow CH_3COOH + CO_2 + 2H_2$	2
n-Butyrate	$CH_3CH_2CH_2COOH + 2H_2O \rightarrow 2CH_3COOH + 2H_2$	3
Iso-butyrate	$CH_3(CHCH_3)COOH + 2H_2O \rightarrow 2CH_3COOH + 2H_2$	4
n-Valerate	$CH_3CH_2CH_2CH_2COOH + 2H_2O \rightarrow CH_3COOH + CH_3CH_2CH_2COOH + 2H_2$	5
Iso-valerate	$CH_3(CHCH_3)CH_2COOH + CO_2 + 2H_2O \rightarrow 3CH_3COOH + H_2$	6

The reactions are described as follows:

1. Acetate is consumed by methanogens (archae-acetoclastic microorganisms) to produce methane and carbon dioxide (reaction 1).
2. Propionate is consumed by acetogenic bacteria to produce acetate, CO_2 and Hydrogen (H_2) (reaction 2).
3. Both n-butyrate and iso-butyrate are consumed by acetic acidogenic bacteria to produce acetate and hydrogen (reactions 3 and 4). The butyrate will undergo reciprocal isomerisation between its n-and iso- forms by the migration of the carboxyl group to the adjacent carbon (Wang et al., 1999). The rate and direction of isomerisation is dependent on the bacteria present in the digester and the amount of specific enzyme available to catalyse the isomerisation (Wang et al., 1999).
4. n-Valerate is degraded via β-oxidation to produce acetate, propionate and hydrogen (reaction 5).
5. iso-Valertae does not generally undergo β-oxidation and so will only degrade to acetate and hydrogen (reaction 6) (Wang et al., 1999).

Trends in solid and soluble COD concentrations

The progress of digestion was monitored through solid and soluble COD concentrations. The COD of the solid biomass represented oxygen demand by complex organics comprising the cell wall and intracellular content of the algae. The soluble COD represented the demand for oxygen from organic compounds in the aqueous phase of the digesters.

For the *Spirulina spp.* digesters a large initial decrease in solid COD was followed by an increase in soluble COD (days 0 to 4). This result indicated that insoluble organics in the solid biomass were liberated by hydrolytic enzymes and bacteria (Table 4.2, reactions 1, 3 and and 7). *Spirulina spp.* has a soft cell wall made of complex sugars and proteins, unlike the cellulosic walls of most other algae, hence is easily disrupted and digested (Kozenko and Henson, 1996). This was emphasised by the solid COD concentration significantly decreasing on digestion from day 0 to 30, after which it stabilised. The soluble COD decreased

from day 4 to stabilise at the same time point, 30 days. At this point minimal solubilisation of solid biomass resulted in minimal production of soluble organics and so VFAs.

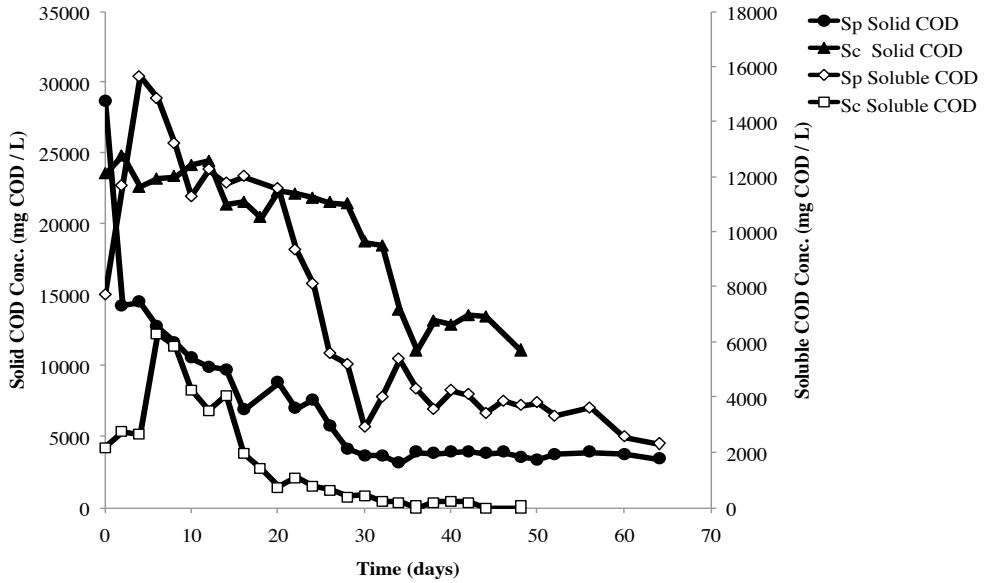

Figure 4.1: Solid and soluble COD concentration profiles of whole cell *Spirulina spp.* and *Scenedesmus spp.* batch digestion (n=3)

The solid COD in the *Scenedesmus spp.* digesters only decreased significantly at a later stage (day 26) indicating lower biodegradability. The cell walls of *Scenedesmus spp.* are composed of highly resistant, non-hydrolysable aliphatic biopolymers. The biopolymers are composed of long-chain even-carbon-numbered o9-unsaturated o-hydroxy fatty acid monomers. The polyether nature of these algaenans makes them highly resistant against degradation (Blokker et al., 1998). The cell walls also are composed of large amounts of hemicellulose, characterised by slow hydrolysis (Yen and Brune, 2007). The soluble COD concentration of the *Scenedesmus spp.* digesters was, as expected, decreased to the detection limit. This related directly to the slow biomass degradation, which was the rate limiting step.

Biomass production, due to microbial growth (acidogenic and methanogenic), also contributes to an increase in solid COD. However, in AD systems the contribution rarely exceeds 0.5 g/L and so the impact on the COD is low (Lyberatos and Skiadas, 1999).

Primary VFA Profiling

The largest source of methane production in AD is through the microbial conversion of acetate formed from consumption of longer chain fatty acids (butyrate and propionate). Therefore, monitoring these key volatile fatty acids informs the final feasibility analysis. Trends in VFA metabolism have been used as process indicators in many laboratory, pilot and industrial scale digesters (Ahring et al., 1995; Boltes et al., 2008; Buyukkamaci and Filibeli, 2004; Hickey and Switzenbaum, 1991). The real time analysis of VFAs

allows digester stability to be monitored and, if necessary, actions taken to control the system. For batch digestion the acidogenic (including acetogenisis) and methanogenic stages should be clearly identifiable from changes in the key VFAs within the digester (Boltes et al., 2008).

For both *Spirulina spp.* (Figure 4.2 (a)) and *Scenedesmus spp.* (Figure 4.2 (b)), large amounts of VFAs were produced from day 0 to 4. The most significant VFAs produced were acetic, butyric and propionic acids. A consequence of the high VFA production was a decrease in pH. The *Spirulina spp.* culture decreased from pH 6.5 to 6.1 and the *Scenedesmus spp.* culture from pH 6.6 to 6.2. The additional alkalinity in the *Spirulina spp.* substrate buffered the system and, despite the high VFAs production, the pH did not drop excessively. After this initial decrease in pH, active control using 5 M NaOH was initiated to maintain the pH above 7.0 and ensure maximum methanogen activity.

The accumulation of these acids indicated that the system was in the acido- and aceto-genisis phases of AD. The acids formed at a higher rate than the acetic acid consumption by the methanogenic microbes. After the initial high rate of production of these specific acids, the total VFA concentration stabilised. The high concentration of VFAs affects the activity of the microbial consortia, requiring it to acclimatise to the new environment and stabilise (Angelidaki et al., 1999). The anaerobic microbial consortia can also be sensitive to the hydrogen partial pressures (pH_2) (Lyberatos and Skiadas, 1999). Whilst acetate production is independent of hydrogen partial pressure, the degradation of carbohydrates to butyrate and propionate cannot proceed at high hydrogen partial pressures (Lyberatos and Skiadas, 1999). A high pH_2 will thus lead to inhibition of butyrate and propionate leading to their accumulation.

The difference in the AD of the two unruptured algal species is clearly visible. VFA generation was greater when the reactors were loaded with *Spirulina spp.* (8000 mg Total VFAs/L) compared to being loaded with *Scenedesmus spp.* (2800 mg Total VFAs/L). The ratio at which the key acids (acetate:butyrate:propionate) were produced also varied: 8:4:1 for the *Spirulina spp.* system and 3:2:1 for the *Scenedesmus spp.* system at maximum total VFA concentrations. The higher concentration of VFAs produced is related directly to the availability of easily fermentable organics and simply degradable biomass within the digesters (Angelidaki et al., 1999). In their general model for AD, Moletta et al. (1986) proposed that an organic substrate is comprised of non-easily fermentable organics (non-soluble proteins, lipids etc.) and easily fermentable organics (glucose equivalent), which are fermented by acidogenic bacteria to produce organic acids (acetate equivalent). This model follows the reactions presented in Tables 4.2 and 4.3. The high acid production relates directly to the high rate of fermentation. *Spirulina spp.* cells disrupt due to osmotic shock releasing a larger amount of organic compounds for hydrolysis and fermentation. Osmotic shock resulted from the sudden change in the solute concentration around the cells, causing a rapid change in the movement of water across the cell membranes and so osmotic pressure. *Scenedesmus spp.* has a strong cell wall made up of complex biopolymers resistant to hydrolysis. Along with this the growth media is of a lower ionic strength (roughly 2 mS/cm) and so the cells are not as prone to experience osmotic shock. Hence less readily available organics were present in the aqueous phase of the slurry for conversion to VFAs during the initial stages of digestion. Degradation of the cellulosic cell wall is required to liberate organics and since the enzymatic degradation of cellulose is slow (Samson and LeDuy (1983b)) the lower amount of VFAs on AD of *Scenedesmus spp.* was expected.

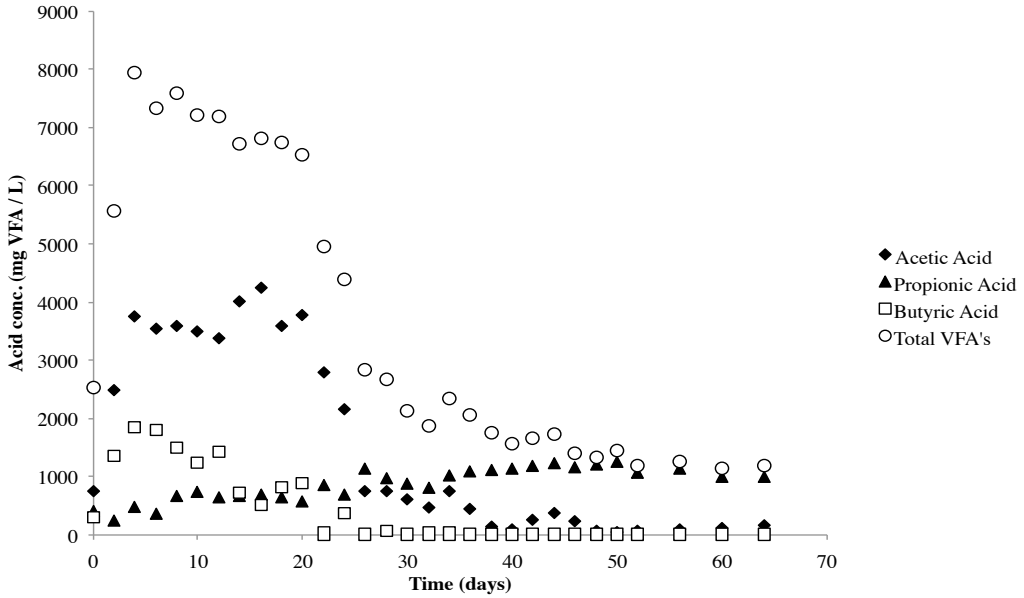

(a) *Spirulina spp.* substrate loaded digesters

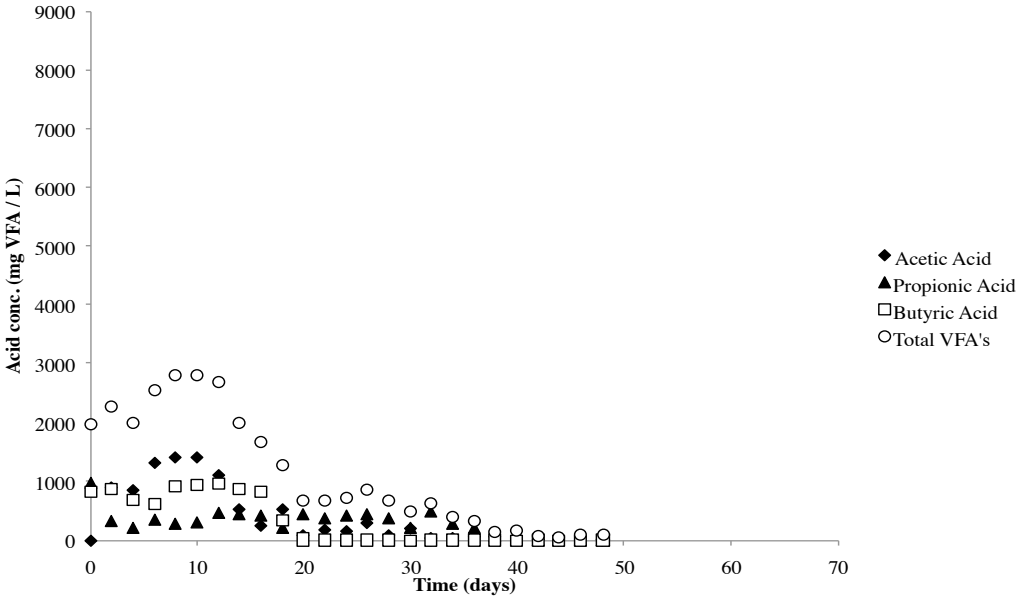

(b) *Scenedesmus spp.* substrate loaded digesters

Figure 4.2: Total and specific VFA concentration profiles of whole cell *Spirulina spp.* and *Scenedesmus spp.* batch digestion (n=3)

After the microbial consortia adapted to the high VFA concentration, their activity increased and the methanogenic activity increased such that the rate of consumption of acetate exceeded production of butyrate, propionate and acetate. This is illustrated by a rapid decrease in the concentration of these specific acids (Figure 4.2). The methanogenic activity increased after a shorter period (10 days) for the *Scenedesmus spp.* digesters than the *Spirulina spp.* digesters (18 days). The latter produced three times the total VFA concentrations in the initial stages of digestion, resulting in a longer stabilisation or acclimatisation period.

The profile of these three key VFAs (Figure 4.2) was similar to the studies conducted by Boltes et al. (2008) and Vavilin et al. (2000), depicted in Figure 4.3. In the Vavilin (2000) study, an initial high rate of VFA production was followed by a period of minimal microbial activity (small fluctuations in VFA concentrations). Thereafter, linear consumption of VFAs followed until the concentrations tended towards zero. The profile from Boltes et al. (2008), in which acetic, butyric and propionic acids were used as substrates, also showed a period of linear consumption until concentrations tended towards zero.

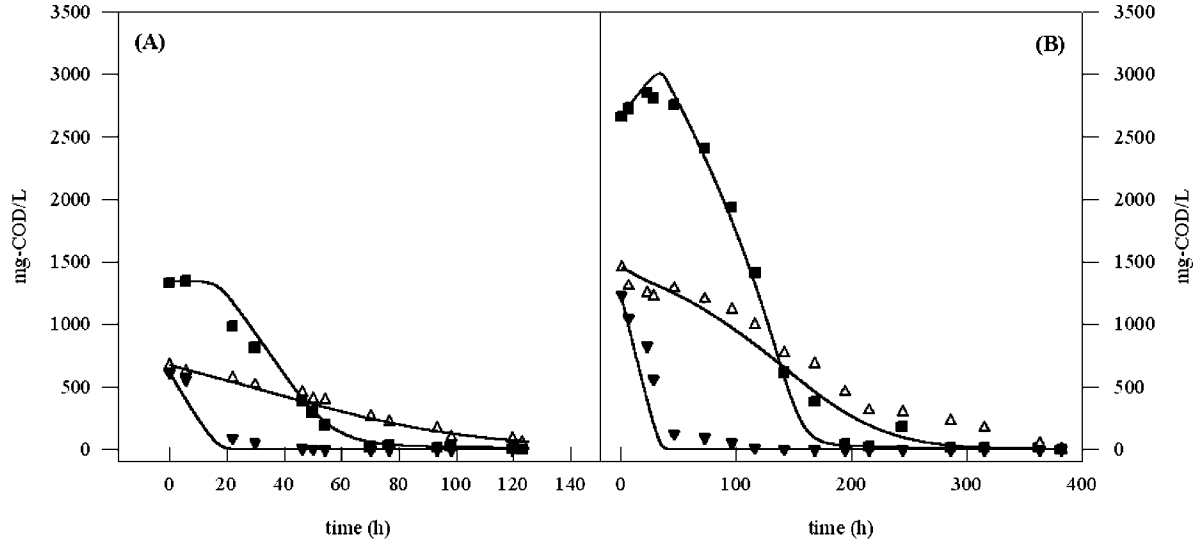

(a) Experimental and predicted values for acetic, butyric and propionic acids in two batch digestion assays: (A) 2682 mg of COD/L initial loading; (B) 5351 mg of COD/L initial loading (Boltes et al., 2008).
* acetic acid (■), butyric acid (▼) and propionic acid (△)

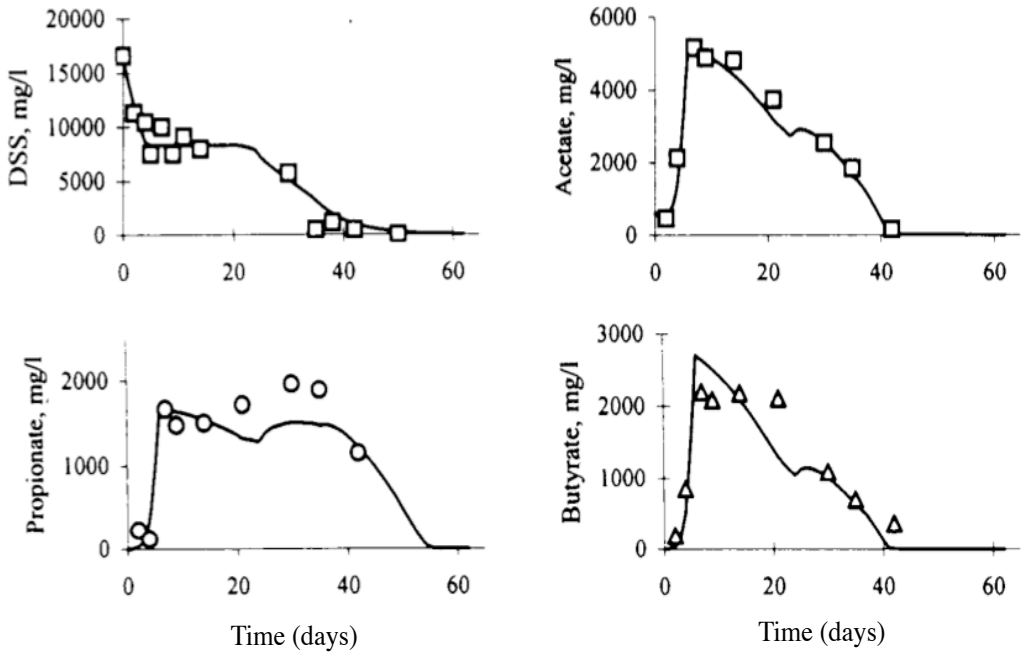

(b) Experimental and predicted values for acetic, butyric and propionic acids as well as degradable suspended (DSS) solids in batch assays, expressed in mg/L (Vavilin et al., 2000).

Figure 4.3: Experimental and predicted values for acetic, butyric and propionic acids during batch studies conducted by (a) Boltes et al. (2008) and (b) Vavilin et al. (2000)

The VFA profiles (Figure 4.2) show that *Spirulina spp.* contained more degradable biomass. This is backed by the higher concentration of VFAs produced initially and the extended period of activity of the anaerobic consortia. Propionic acid, reported as the most resistant to degradation by Boltes et al. (2008), remained at significant concentrations throughout the digestion period. The profile for propionic acid presented by Vavilin et al. (2000) is consistent with this. The degradation of propionate results in the production of acetate, CO_2 and H_2. Wang et al. (1999) reported that this specific degradation reaction required specific enzymes and the oxidation of propionate was not thermodynamically favourable under anaerobic digester conditions. The degradation is sensitive to hydrogen partial pressure. Buyukkamaci and Filibeli (2004) suggest that the propionic acid to acetic acid ratio can be used as an indicator of digester imbalance with a propionic acid to acetic acid ratio greater than 1.4 indicating a digester failure. This was consistent with trends in the *Spirulina spp.* digesters where methanogenic activity decreased when the ratio increased. The higher concentrations of propionic acid experienced in *Spirulina spp.* digesters most likely originate from the high concentration of protein and so amino acids degraded (Table 4.3.2 reaction 8).

Indicator VFAs

A complete VFA profile for the digestion of both *Spirulina spp.* and *Scenedesmus spp.* was developed by tracking all VFAs identified in the reaction sets of Tables 4.2 and 4.3. Nakakubo (2008) showed that accumulation of iso-butyric, iso-valeric or valeric acids could be a useful indication for ammonia inhibition within the system. Since *Spirulina spp.* has a high protein content (60%) the potential of ammonia inhibition is higher.

Pind et al. (2003) indicate that iso-valeric acid is a metabolite from amino acid (leucine) digestion and degrades into acetate and hydrogen according to reaction 6 in Table 4.3. Pind et al. (2003) recommended monitoring indicator acid concentrations hourly even though digestion retention times may be in the order of days. An accumulation of this acid is consistent with methanogenic inhibition, as reduced consumption of acetate allows for accumulation of iso-valerate (Pind et al., 2003; Wang et al., 1999). The maximum amounts of iso-valerate present during the digestion of *Spirulina spp.* and *Scenedesmus spp.* respectively were 1650 mg/L and 130 mg/L (Figure 4.4). The iso-valeric acid steadily decreased across the digestion period for the *Spirulina spp.* digesters until only trace amounts remained.

Iso-butyric acid was the most resistant to degradation during the period of maximum microbial activity. Along with propionic acid its degradation is characterised as difficult. In AD systems it is typically converted from iso-butyrate to n-butyrate by isomerisation (Wang et al., 1999). All the indicator acids fell to below detectable concentrations towards the end of the *Spirulina spp.* digestion period and remained low across the entire *Scenedesmus spp.* digestion period.

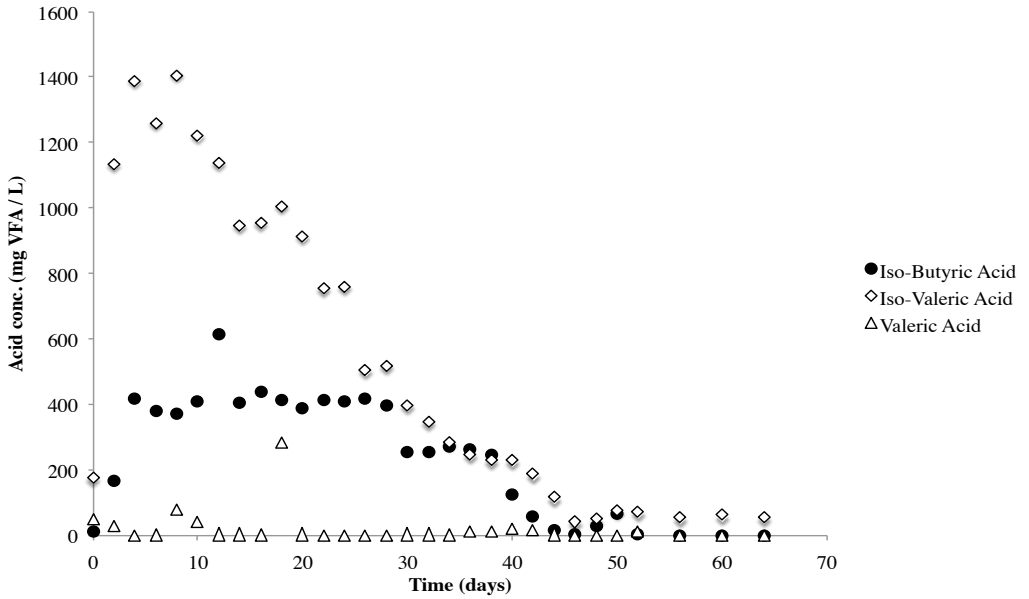

(a) *Spirulina spp.* loaded digester concentration profile for iso-butyric, iso-valeric and valeric acids

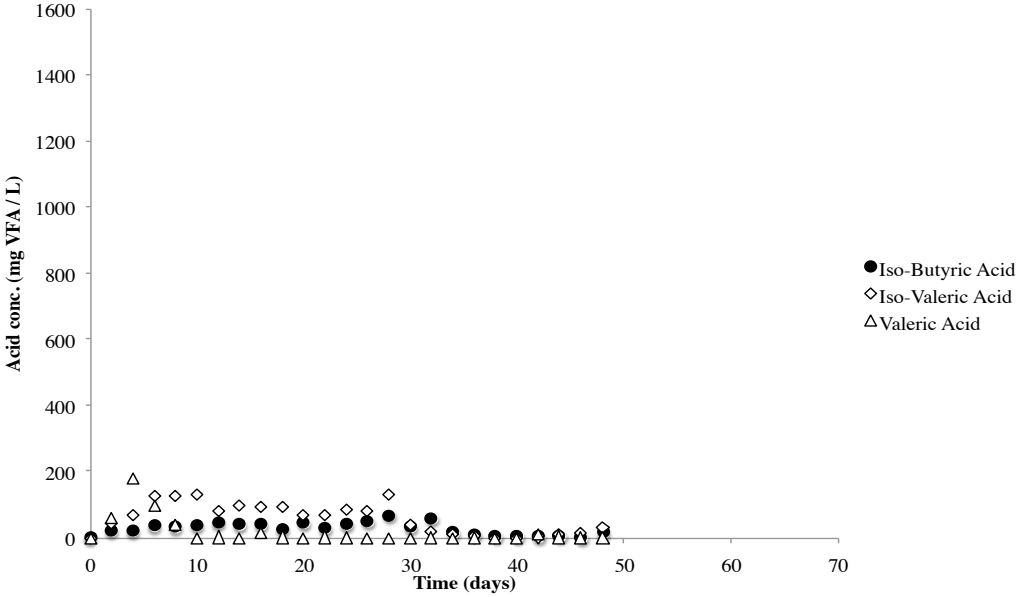

(b) *Scenedesmus spp.* loaded digester concentration profile for iso-butyric, iso-valeric and valeric acids

Figure 4.4: Specific concentration profiles of key indicator VFAs for whole cell *Spirulina spp.* and *Scenedesmus spp.* batch digestion (n=3)

The concentrations of the indicator acids did not accumulate to concerning levels. This suggests that the amount of nitrogenous matter degraded did not cause ammonia inhibition within the systems. At this point is should be noted that lactic acid was also monitored throughout digestion. Since the concentration levels were on average less than 10 mg/L, the data were not presented.

Soluble COD concentration profiling

The soluble chemical oxygen demand of the digester contents was, for the most part, governed by the concentration of VFAs in the system (Figure 4.5).

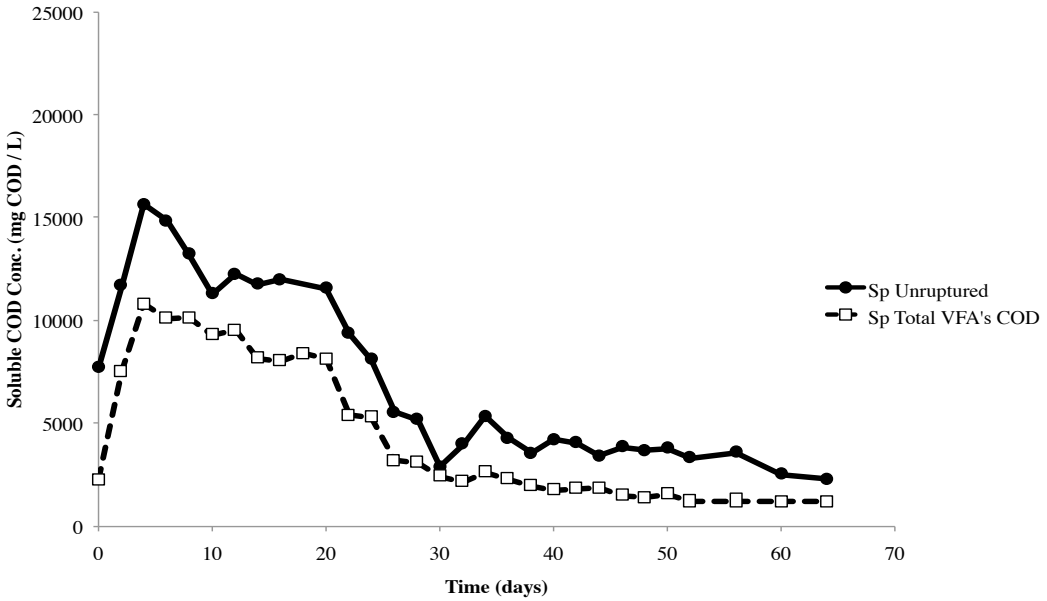

(a) *Spirulina spp.* whole cell substrate loaded digesters

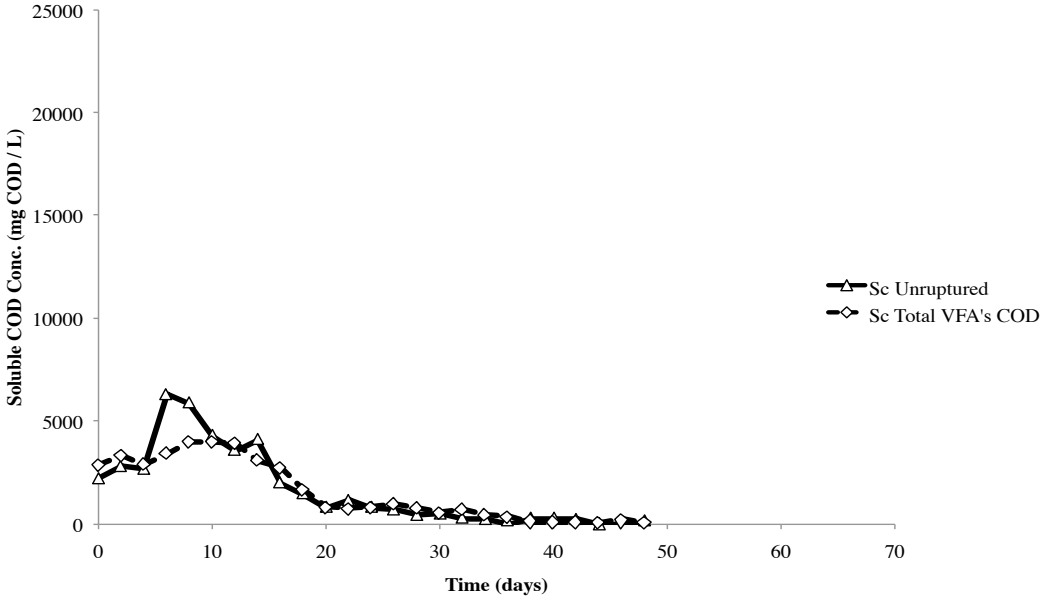

(b) *Scenedesmus spp.* whole cell substrate loaded digesters

Figure 4.5: Soluble COD and VFA COD destruction profiles for whole cell *Spirulina spp.* and *Scenedesmus spp.* batch digestion (n=3)

Initially, for the *Spirulina spp.* digesters, the contribution of VFAs to the soluble COD was low as complex organics (carbohydrates, proteins and lipids) hydrolysed from the solid biomass were present in high concentrations. Once the acidogenic bacteria had converted these organics and VFA production increased, the percentage contribution to soluble COD increased. This trend was more pronounced in the *Spirulina spp.* digesters compared to the *Scenedesmus spp.* digesters, as *Scenedesmus spp.* was more resistant to

hydrolysis. This further suggested than any complex organics that were solubilised were rapidly converted to VFAs. Towards the end of digestion the soluble COD in both sets of digesters was mainly comprised of the residual acids that resisted degradation. This indicated that the degradation of complex soluble organics or solid biomass was no longer occurring.

During the high VFA production phase the total soluble COD of the *Spirulina spp.* digesters increased from 7 500 mg COD/L to ca. 16 000 mg COD/L, however the total VFA contribution increased from 2800 mg/L to 11 000 mg/L. One would expect to see a much larger increase in total soluble COD with this high VFA COD production as well as from biomass hydrolysis. However, simultaneous to this high production of VFAs was a high release of CO_2 and moderate release of CH_4. Since CO_2 is the most oxidised form of carbon, the release of this out of the system is a consequence of a decrease in COD, which balances out the contribution to COD by the VFAs. The release of biogas, and so COD, from the system during the initial stages of digestion accounted for the fact that the solid COD decreased more than the soluble COD increased (Figure 4.1). The *Scenedesmus spp.* digesters had a lower soluble COD concentration through digestion as less VFAs could be produced since degradation of the solid biomass was limited.

A linear decrease in COD coincided with a linear decrease in VFA concentration. Towards the end of digestion the *Spirulina spp.* digesters still had a relatively high soluble COD (2300 mg COD/L). This COD was attributed to the residual propionic acid. In all previous studies conducted on digestion of *Spirulina spp.* the propionic acid concentrations, when reported, were significant (Samson and LeDuy, 1982, 1983b).

4.3.3 Biogas and methane production

Biogas Productivity

The biogas productivity profiles (Figure 4.6) for both *Spirulina spp.* and *Scenedesmus spp.* followed a similar trend. Within the first two days after inoculation, the biogas production was at a maximum. During this phase of digestion, the active culture of inoculated microorganisms immediately consumed any easily available resource and produced VFAs. The VFA profiles (Section 4.3.2) confirm this. From the reactions proposed it can be seen that CO_2 is formed in all the stages where acidogenic bacteria are active. Since the pH dropped with the production of LCFA's and VFAs the CO_2 speciation will favour the release of CO_2 gas over the formation of soluble bicarbonate (Wang et al., 1999).

After this period of maximum productivity, biogas production stopped. This was consistent with the VFA concentration profiles that showed a "lag" period where minimal changes in VFA concentration occurred. When VFAs are produced and consumed by acidogenic bacteria and methanogens, CO_2, H_2, CH_4, NH_3 and H_2S gases are released (Table 4.3 reactions (1)-(6)). Since there was minimal microbial activity biogas productivity was negligible.

When microbial activity began to increase, biogas production increased simultaneously. The subsequent peak in biogas productivity related directly to the maximum rate of consumption of VFAs. The higher

maximum biogas productivity of the *Spirulina spp.* digesters (0.21 L Biogas/ $L_{reactor}$.day) exceeded that of the *Scenedesmus spp.* digesters (0.15 L Biogas/$L_{reactor}$.day), and was consistent with the greater change in VFA concentrations.

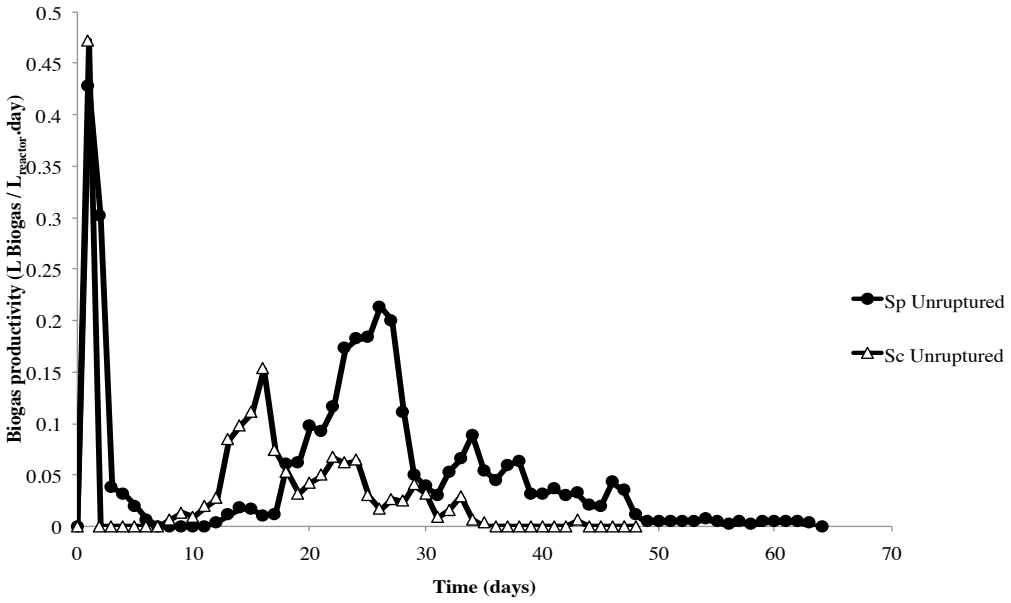

Figure 4.6: Biogas productivity profiles for whole cell *Spirulina spp.* and *Scenedesmus spp.* batch digestion (n=3)

Methane productivity

Many studies (Sanchez and Travieso, 1993; Gunaseelan, 2009) conducted on batch phase AD have only measured the composition of the biogas produced at distant intervals. Furthermore, average values are used to calculate all methane production parameters resulting in overestimates of efficiency. In this study, biogas composition was measured daily (Figure 4.7). The data show that the composition of biogas varied significantly, with changes from 20% CH_4 to 80% CH_4 seen in the space of two days. This emphasises the importance of regular sampling in the generation of a complete data set.

For both algal species, the biogas produced during the initial phase had a relatively low CH_4 content. This was expected as biogas resulted from the conversion of easily fermentable organics into VFAs by acidogenic bacteria and not from the consumption of acetate by methanogens. The production of these VFAs resulted in the release of predominantly CO_2 as well as NH_3 and H_2 (Table 4.3 reactions (1) - (8)). The biogas did contain CH_4 (10-20%), which suggested some methanogenic activity. However this activity decreased due to inhibition from the VFA production and the subsequent decrease in pH.

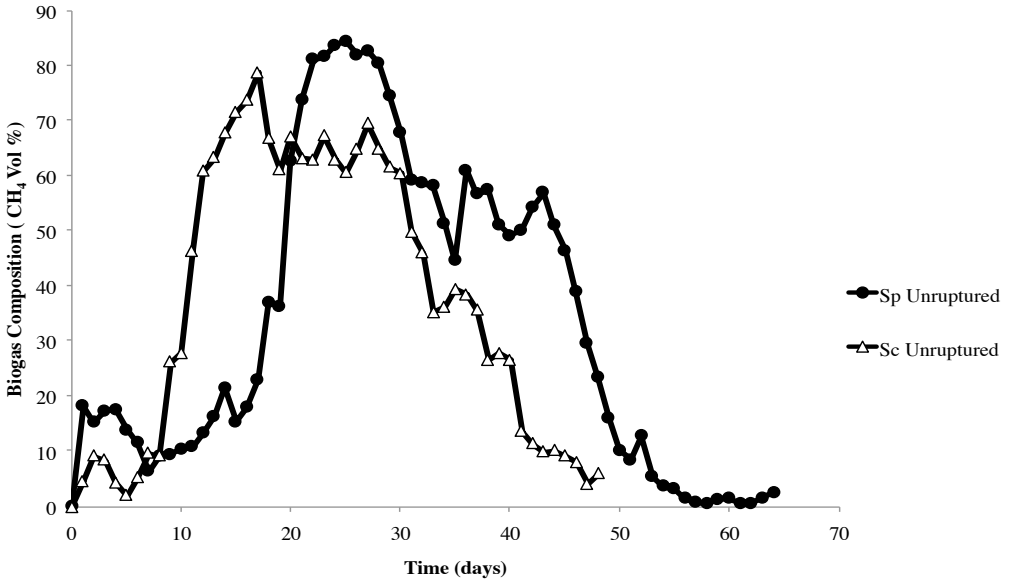

(a) Biogas methane composition profiles for whole cell *Spirulina spp.* and *Scenedesmus spp.* batch digestion (n=3)

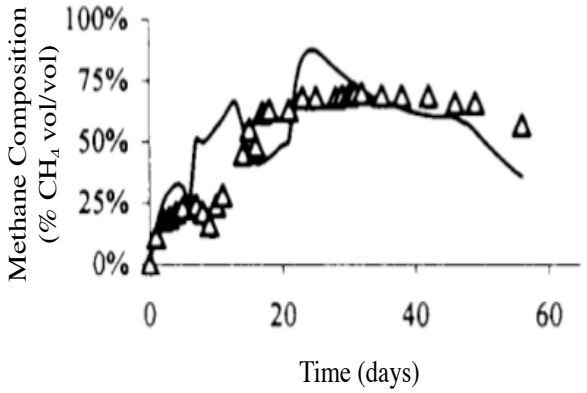

(b) Predicted and experimental biogas methane composition profiles of solid poultory slaughter house waste (SSW) substrate loaded batch digesters (Vavilin et al., 2000)

Figure 4.7: Biogas methane composition profiles for batch digestion, expressed in% CH_4 (vol/vol)

Applying the methane content to the biogas productivity yielded the methane productivity of the AD systems. The methane composition profile for *Spirulina spp.*, showed that after 15 days the methane content started to increase. This related closely to the production of biogas (Figure 4.6) and to the consumption of acetate (Figure 4.2). After 18 days the biogas productivity started to increase substantially, reaching a peak after 27 days at 0.23 L biogas/$L_{reactor}$.day. At this same point the methane content was at a maximum of 81%. The combination of these two variables resulted in a maximum methane productivity of 0.177 L CH_4/ $L_{reactor}$.day. After this period, both the methane content and biogas productivity steadily decreased resulting in lower methane productivities. The *Scenedesmus spp.* digesters followed this same trend. The key difference, which related directly to the biogas productivity, was that the maximum methane production occurred earlier (16 days) and at a lower rate (0.125 L CH_4/ $L_{reactor}$.day).

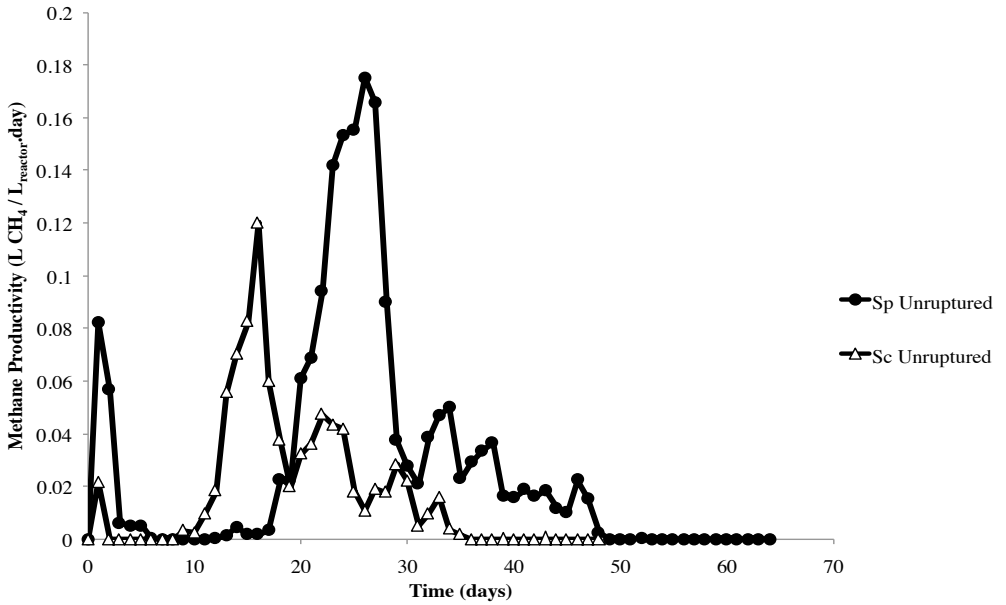

Figure 4.8: Methane productivity profiles for whole cell *Spirulina spp.* and *Scenedesmus spp.* batch digestion (n=3)

The relationship between methane production rates and methane composition was consistent with the progression of the digestion. At the stage where both acidogenic bacteria and methanogens were active the pH of the system increased. At a certain time in the process, the pH of the system became more favourable to the methanogenic microbes and their activity increased to levels greater than that of the acido-and aceto-genic bacteria. This resulted in a decrease in acetic acid concentrations and an increase in methane composition as well as productivities (Figures 4.7 and 4.9).

The data suggests that acetate metabolism is the most important controlling factor in the feasibility of digesting the investigated algal substrates. Vavilin et al. (2000) conducted batch phase digestion studies on solid poultry slaughterhouse wastes and demonstrated a similar result. They used the <METHANE> model developed by their group to simulate the results. The model is based on similar degradation reactions to those presented in the beginning of Section 4.3.2. By assigning rates of reactions to the degradation of these compounds, the amount of gas and composition can be predicted over time. The profile obtained from the model (Figure 4.7 (b)) clearly demonstrates the initial low CH_4 content (20%), increasing to a maximum (70%) and then decreasing back down to 20% towards the end of digestion.

The high methane content measured for both *Spirulina spp.* (84%) and *Scenedesmus spp.* (80%) digesters suggested some retention of CO_2 in the system. During the period of maximum methane productivity the pH increased. The increase in pH favoured the speciation of dissolved CO_2 to bicarbonate (HCO_3^-) in the aqueous phase of the digester (Wang et al., 1999). Methane is sparingly soluble in aqueous solutions so would evolve into the gaseous phase (Lyberatos and Skiadas, 1999).

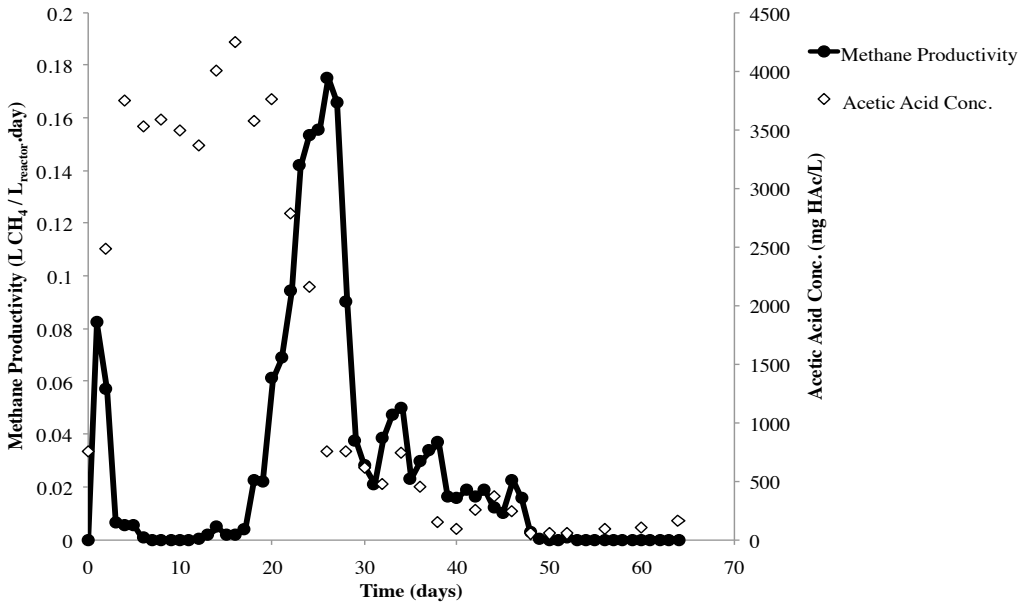

(a) Whole cell *Spirulina spp.* substrate loaded digesters

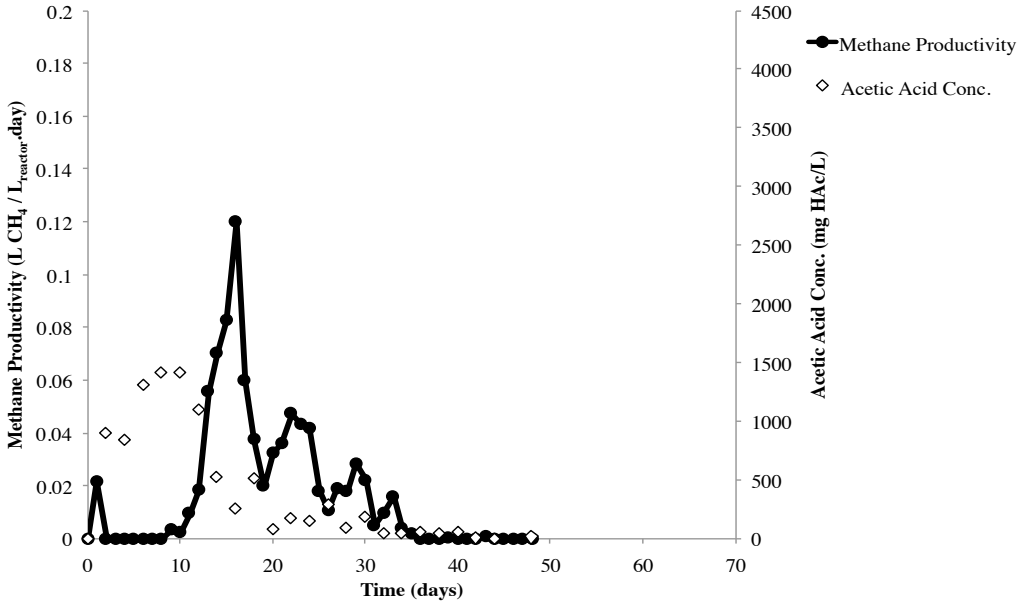

(b) Whole cell *Scenedesmus spp.* substrate loaded digesters

Figure 4.9: Methane productivity as a function of acetate concentration for whole cell *Spirulina spp.* and *Scenedesmus spp.* batch digestion (n=3)

The maximum methane contents, in excess of 80% vol/vol, achieved in this study were higher than most published results. The majority of literature studies present the average methane content or stoichiometrically predicted methane content, so underestimating the maximum values achievable. With appropriate pH control CO_2 speciation can be manipulated and a methane content of over 80% can be maintained.

Methane yields

The final derived parameter investigated was the methane yield. Generally the final methane yield is given as methane produced per kilogram/gram of volatile solids (VS) fed into the digester or per kilogram/gram

of total COD consumed through digestion (Sialve et al., 2009). This study presents both these values and tracks them over the period of digestion. The methane yield is closely related to system parameters and it becomes difficult to compare between different studies. The development of the biomethane potential (BMP) assay for determination of ultimate yield in batch digestion has attempted to minimise the influence of these parameters and allow a reasonable comparison to be made between substrates (Braun et al., 2010).

For both *Spirulina spp.* and *Scenedesmus spp.* digesters the initial DW loading was 20 g/L, which corresponded to 16.8 g VS/L for *Spirulina spp.* and 16.3 g VS/L for *Scenedesmus spp.*. The 's' shaped curve produced related to the inverse of total VFA consumption and was representative of the cumulative methane produced during digestion. Three key stages occurred: an initial lag phase, a linear rate of increase and an eventual tailing off to yield the final methane yield.

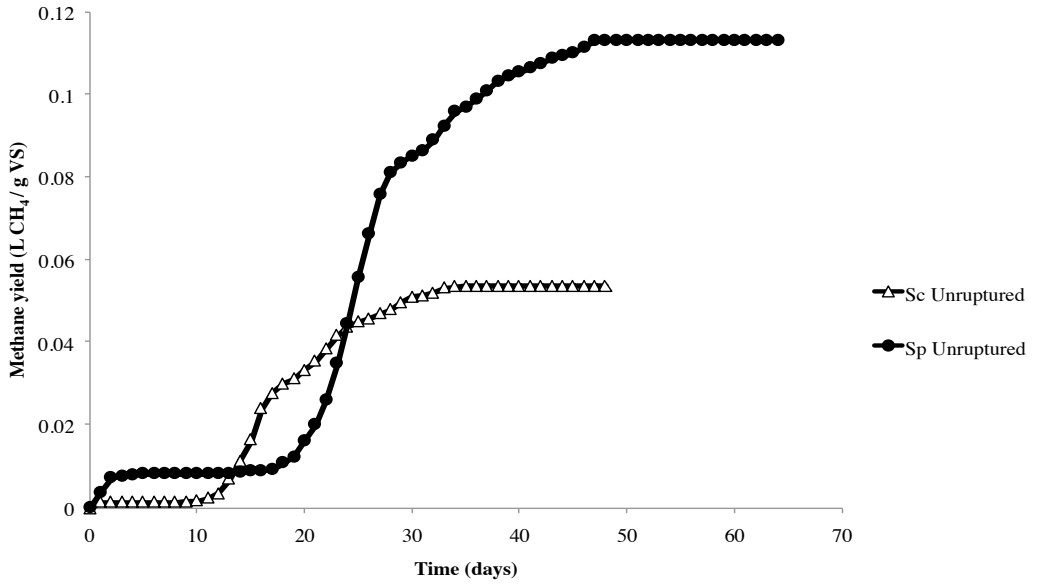

Figure 4.10: Specific Methane Yield (SMY) in terms of volatile solids loaded for whole cell *Spirulina spp.* and *Scenedesmus spp.* batch digestion (n=3)

The ultimate yield for the *Spirulina spp.* digesters (0.11 L CH_4 /g VS loaded) was greater than that of the *Scenedesmus spp.* digesters (0.06 L CH_4/g VS loaded). This overall yield represented the high biomethane potential of *Spirulina spp.* as an AD substrate. The 's' shape trend for the methane production and so yield has been reported in numerous batch phase digestion studies using various substrates. In the study conducted by Vavilin et al. (2000), the predicted methane production curve based on the <METHANE> model as well as the experimentally obtained profile show this trend (Figure 4.11). The operating conditions of the reactor were not presented in the study, as focus was made on the effectiveness of the model in predicting the AD system progress. The result can still be compared for the impact of VFA concentrations on methane yields. The VFA profiles (Figure 4.3) presented by Vavilin et al. (2000) were similar to the current study.

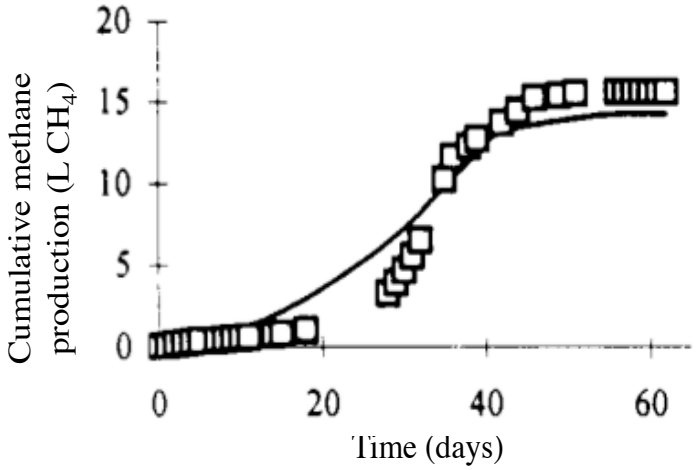

Figure 4.11: Cumulative methane production (L), predicted and experimental profiles obtained by Vavilin et al. (2000)

The ultimate methane yield can also be presented in terms of the total COD that was destroyed during digestion. It is often difficult to obtain accurate results for volatile solids degradation due to the inaccuracies of the analytical method (Samson and LeDuy, 1986). For this reason the ultimate yield is also determined by using the COD destruction as a measure of organic consumption across digestion. Table 4.4 presents the results in terms of total methane produced, total COD consumed and the ultimate yield after the duration of digestion.

Table 4.4: Methane yield of whole cell digesters, expressed in L CH_4/ g COD destroyed (n=3)

Substrate	Total methane produced (L CH_4)	Total COD destroyed[a] (g)	Methane yield (L CH_4/ g COD destroyed)
Whole cell *Spirulina spp.*	1.81	30.28	0.06
Whole cell *Scenedesmus spp.*	0.86	14.05	0.06

[a]Total COD was calculated by addition of soluble and solid COD

The methane yields per gram of COD destroyed were the same for the two algal species. This yield represents the efficiency which methanogens convert available COD (acetate equivalent) to CH_4. Even though more COD was destroyed in the *Spirulina spp.* digesters, the efficiency that this was converted into methane was equal to that of the *Scenedesmus spp.* digesters.

4.3.4 Efficiency of digestion

The efficiency of AD can also be represented by the overall destruction of COD (both solid and soluble), VFAs and VS's. In systems such as wastewater digesters, there is often more focus on this side of the process than the gaseous product (Speece, 1983; Parkin et al., 1983; Ghosh et al., 1975; Burton et al., 2008). Regulations imposed by water boards set limitations on COD levels that wastewaters must meet before they are returned to the watercourse. In the case of this study, the decrease in the above mentioned parameters

over the digestion period represented the efficiency and biodegradability of the chosen substrates. The profiles are presented in Figure 4.12.

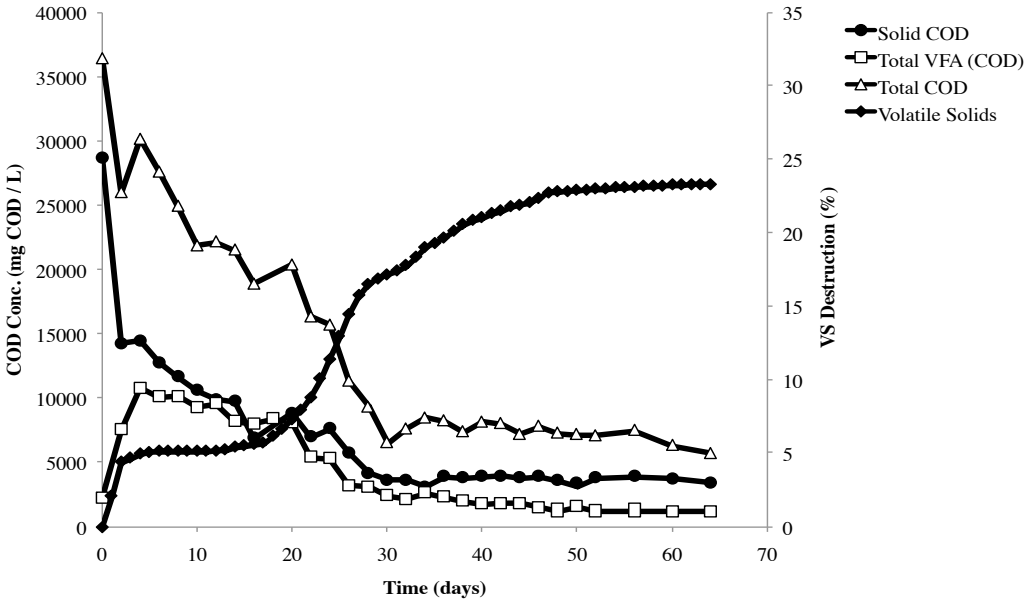

(a) *Spirulina spp.* substrate loaded digesters

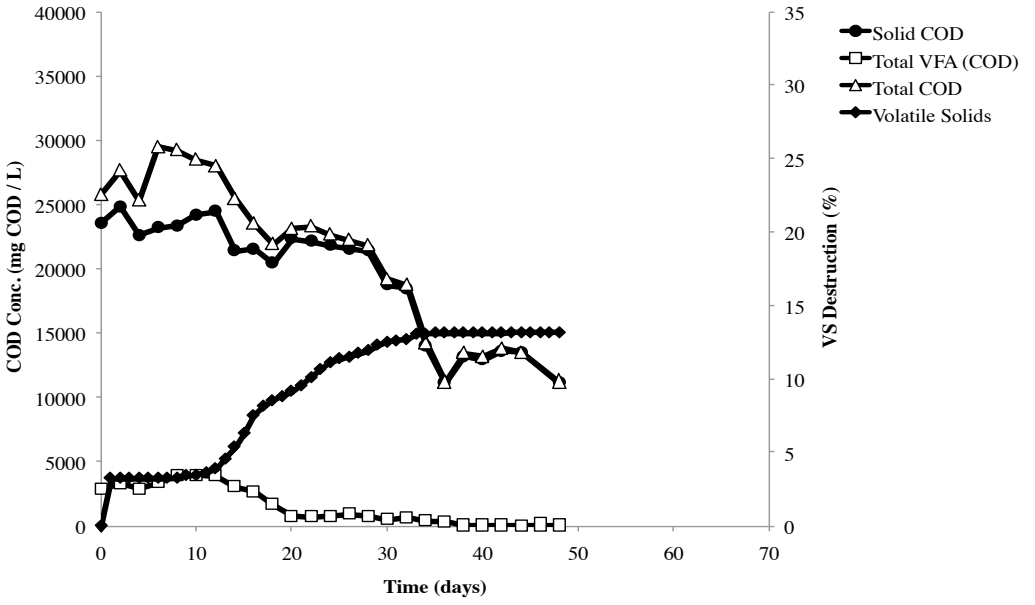

(b) *Scenedesmus spp.* substrate loaded digesters

Figure 4.12: Solid COD, Total COD, Total VFA and VS destruction profiles for whole cell *Spirulina spp.* and *Scenedesmus spp.* batch digestion (n=3)

Both solid and total COD decreased as a function of time. The rate of solids COD destruction was controlled by the digestibility of the remaining substrate. The hydrolytic and acidogenic organisms need complex molecules for energy. Therefore, when microbial activity slowed so to did the degradation of algal biomass. This result was confirmed by the stable VFA concentrations towards the end of the digestion period. The consumption of total COD confirmed that there was no significant inhibition of acidogenic bacteria, since soluble COD made available by the degradation of complex organics was converted into VFAs which were further consumed to produce biogas. The significant results from these profiles for the

full 64 and 48 day digestion periods are summarised in Table 4.5.

Table 4.5: Efficiency of AD in the destruction of COD, VFAs and VS 's for whole cell *Spirulina spp.* and *Scenedesmus spp.*

Substrate	Solid COD Destruction[a] (%)	Total COD Destruction[b] (%)	VFA Destruction[c] (%)	VS Destruction[d] (%)
Whole cell *Spirulina spp.*	88	85	89	23
Whole cell *Scenedesmus spp.*	53	56	98	13

[a] :⇒Calculated from the difference in final and initial solid COD concentrations.

[b] :⇒Additive destruction of both solid and soluble COD

[c] :⇒ Calculated by taking point of maximum VFA conc. as the initial conc.

[d] :⇒ Calculated using Varel's eq: VS destroyed(g) = (mol CO_2 +mol CH_4)X(12/(carbon content of biomass))

These results confirm that *Spirulina spp.* degraded more easily than *Scenedesmus spp.*. The larger consumption of both total and solid COD as well as the total destruction of VS supported this result. It becomes clear that using Varel's equation to calculate the percentage of VS destroyed to produce biogas may result in a misinterpretation of the COD destruction results. Taking *Spirulina spp.* as an example, with an 88% destruction of total COD, one would assume that this would result in a higher VS destruction. However, Varel's equation calculates the percentage of the VS in the biomass that were degraded and released in the form of biogas, not what percentage of total VS degraded. It also does not account for CO_2 retained in the aqueous phase as HCO_3^-. Total VS degraded can be calculated using the initial VS concentration and the final VS concentration and calculating the difference obtained.

The higher consumption of VFAs that occurred in the *Scenedesmus spp.* digesters (98% compared to 89%) was due to the lower residual concentrations of propionic acid. The degradation of more fermentable organics (fatty acids, sugars and amino acids) caused a greater release of recalcitrant propionic acid in the *Spirulina spp.* digesters.

4.4 Impact of mechanical pre-treatment

4.4.1 Efficiency of bead milling as a method for physical disintegration of algal cells

Bead milling was selected as the physical pre-treatment method to disrupt both *Spirulina spp.* and *Scenedesmus spp.* cells prior to digestion. The focus of this study was not on optimising this method by varying intrinsic parameters nor by determining the most energy efficient approach. The focus was to ensure complete disruption was achieved, such that the importance or lack there of in terms of AD efficiency could be determined.

Spirulina spp.

To evaluate the extent of disruption, samples were taken every half an hour and investigated by light microscopy (Figures 4.13 and 4.14). With the chosen operating conditions of the bead mill (40 g DW/L, impeller speed 900 rpm, 35% 4 mm diameter glass bead loading) complete disruption was achieved after 3.5 hours of milling. In a previous study by Cisneros and Rito-Palomares (2004), batch bead milling of *Spirulina maxima* cells was conducted to release *c-phycocyanin*. The study reported that extent of disruption decreased with increasing initial wet weight concentration when operating for a constant time period. With the specific operating conditions; impeller speed 800-1100 rpm, 38% 5mm glass bead loading, initial wet weight concentration of 12 g/L; an 85% disruption was achieved after 30 minutes of milling. Considering the images in Figure 4.14, it can be seen that after 2 hours of bead milling the algal cells were almost completely disrupted. At this point an estimated 90% disruption of cells was achieved.

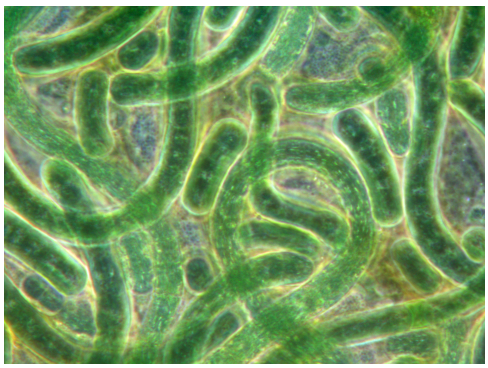

(a) *Spirulina spp.* algal cells at Time = 0 of bead milling

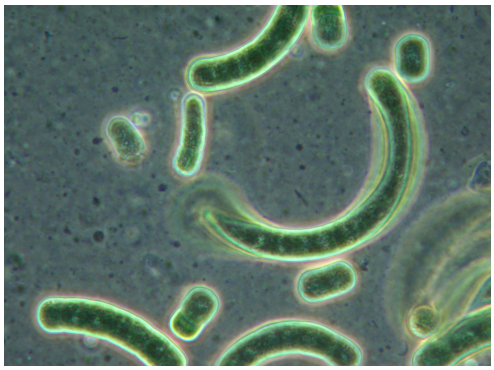

(b) *Spirulina spp.* algal cells at Time = 0.5 hrs of bead milling

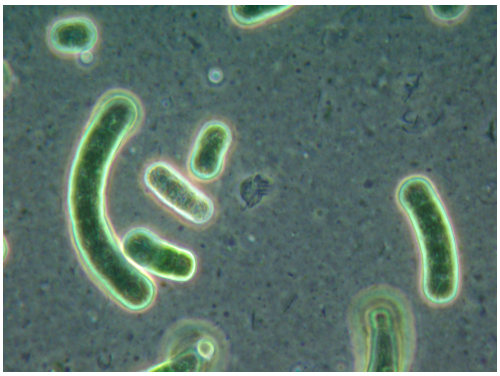

(c) *Spirulina spp.* algal cells at Time = 1 hrs of bead milling

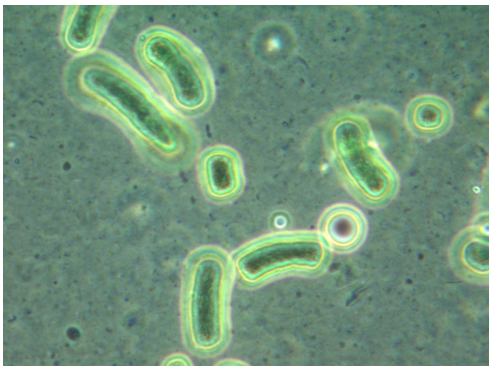

(d) *Spirulina spp.* algal cells at Time = 1.5 hrs of bead milling

Figure 4.13: Microscopy of mechanical disruption of *Spirulina spp.* algal cells through bead mill operation (hours 0-1.5 of operation). All images taken using a 100X objective lens

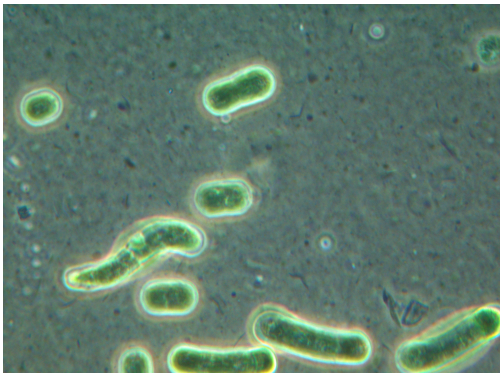

(a) *Spirulina spp.* algal cells at Time = 2 hrs of bead milling

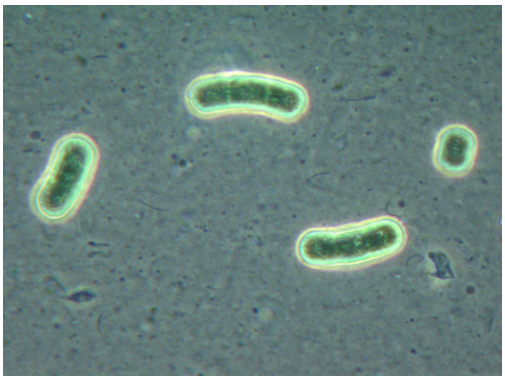

(b) *Spirulina spp.* algal cells at Time = 2.5 hrs of bead milling

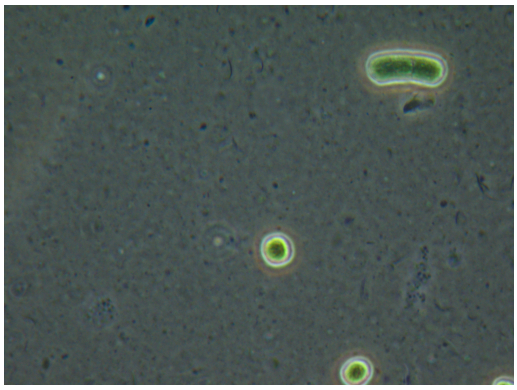

(c) *Spirulina spp.* algal cells at Time = 3 hrs of bead milling

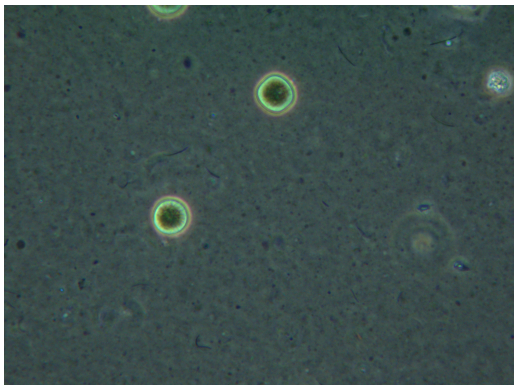

(d) *Spirulina spp.* algal cells at Time = 3.5 hrs of bead milling

Figure 4.14: Microscopy of mechanical disruption of *Spirulina spp.* algal cells through bead mill operation (hours 2-3.5 of operation). All images taken using a 100X objective lens

The main purpose for performing a mechanical pre-treatment was to release the intracellular contents, such that digestion was not limited by hydrolysis (Samson and LeDuy, 1983b). The disruption efficiency was determined by quantifying the increase in soluble COD of the slurry.

The majority of work done on rupturing algal cells focuses on the release of a high-value end product that can be physically or chemically extracted form the aqueous phase of the ruptured slurry (Doucha and Livansky, 2008; Cisneros and Rito-Palomares, 2004; Mandal and Mallick, 2009). Generally these high value end products are long chain organics, such as proteins or lipids.

Figure 4.15 demonstrates a significant increase in soluble COD (18250 mg COD/L to 41250 mg COD/L), over the period of milling. This was accompanied by a significant decrease in solid COD (46400 mg COD/L to 24 400 mg COD/L). These values corresponded to an increase in soluble COD of 126% and a decrease in solid COD of 48%.

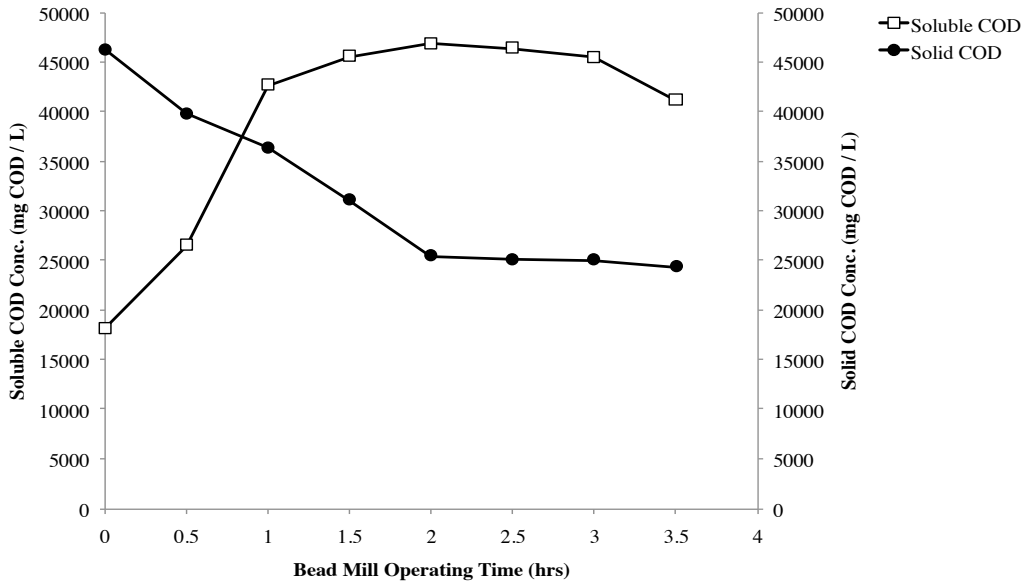

Figure 4.15: Solid and Soluble COD concentration profiles of *Spirulina spp.* algal slurry through bead mill operation

The cell contents include certain VFAs, which are further degraded during digestion to produce methane, so it was important to quantify their release during milling. Figure 4.16 presents the VFA profile over the duration of bead milling. There was an increase in total VFAs (2400 mg/L to a maximum of 4700 mg/L) during milling. Investigating the individual acids profile it can be seen that lactic (110% increase) and propionic (70% increase) acids increased significantly. Propionic acid is of particular importance as it degrades to acetate, a key electron donor in the conversion to methane (Boltes et al., 2008).

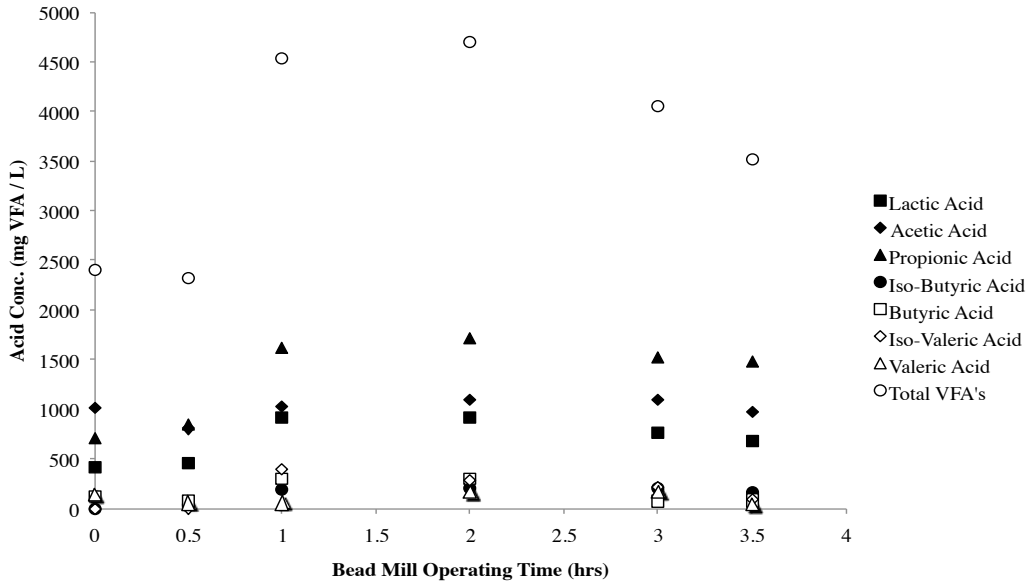

Figure 4.16: Total and specific VFA concentration profiles of *Spirulina spp.* algal slurry through bead mill operation

In summary, *Spirulina spp.,* is a filamentous alkaliphilic cyanobacteria, which is sensitive to osmotic shock when exposed to a medium with low ionic strength and ruptures easily. The ease of rupturing was

emphasised by the following: After 30 minutes of milling (Figure 4.13 (b)) a large fraction of the cells had ruptured. The soluble COD increased to 42700 mg COD/L whilst the solid COD decreased to 36 000 mg COD/L after 1 hour of milling (Figure 4.15) and the total VFA concentration was 4550 mg VFA/L after 1 hour of milling (Figure 4.16).

Scenedesmus spp.

Figure 4.18 (a) -(e) shows images taken using light microscopy over the duration of milling operation. It was expected that an extended period of bead milling would be required due to previous experimental experience and since *Scenedesmus spp.* has a strong, cellulosic cell wall (Sialve et al., 2009). Cell disruption, characterised by cells that had released their intracellular contents and appeared clear under the microscope, was observed during the first hour of milling (Figure 4.18 (b)). Some intact whole cells and partially disrupted cells, not all intracellular contents released, were still clearly visible. This was also the case in Figure 4.18 (c) and (d), but on a decreasing scale. After four hours of milling (Figure 4.18 (e)) no whole cells or partially disrupted cells appeared whilst a significant decrease in the mean size of cell debris was observed. At this point complete disruption had been achieved.

The soluble COD of the algal slurry increased significantly (5700 to 10300 mg COD/L) whilst that of the solid matter decreased (43300 to 39000 mg COD/L) during milling (Figure 4.17). The values represented an increase of soluble COD of 80% and a decrease in solid COD of 10%. The lower destruction of solid COD through milling was an expected result, since the volume ratio of cell wall to cell contents is higher for *Scenedesmus spp.* than *Spirulina spp.* Therefore, the residual cell debris contributed to a higher solid COD even when complete disruption had occurred.

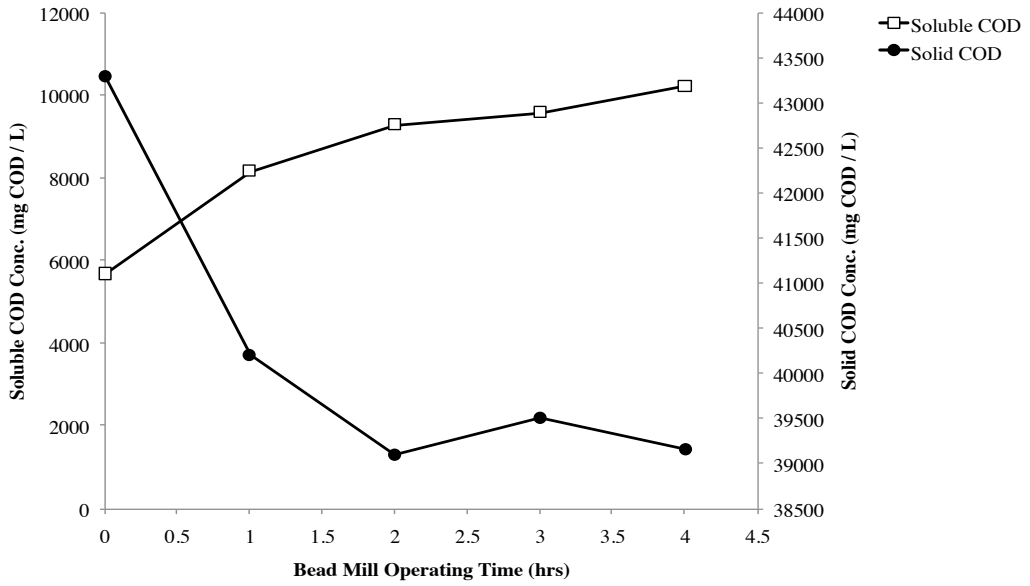

Figure 4.17: Chemical Oxygen Demand (COD) concentration profile of *Scenedesmus spp.* algal slurry through bead mill operation

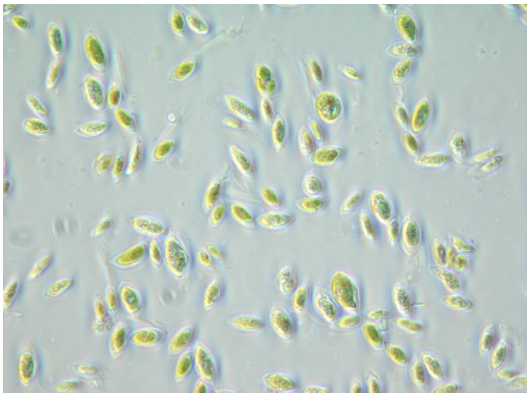

(a) *Scendedesmus spp.* algal cells at Time = 0 of bead milling

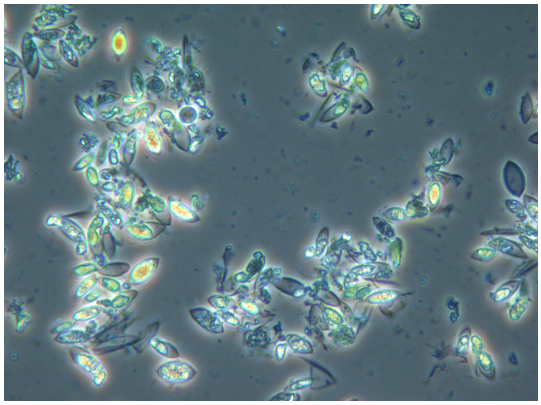

(b) *Scenedesmus spp.* algal cells at Time = 1 hrs of bead milling

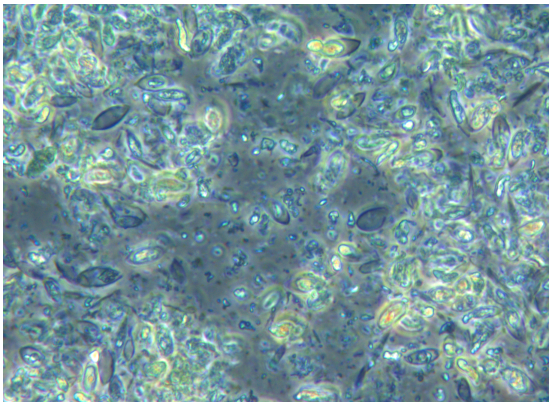

(c) *Scenedesmus spp.* algal cells at Time = 2 hrs of bead milling

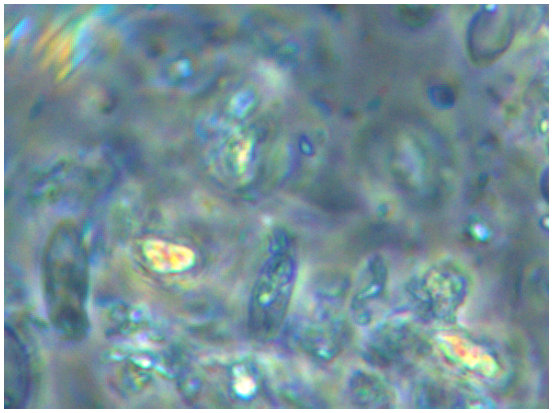

(d) *Scenedesmus spp.* algal cells at Time = 3hrs of bead milling

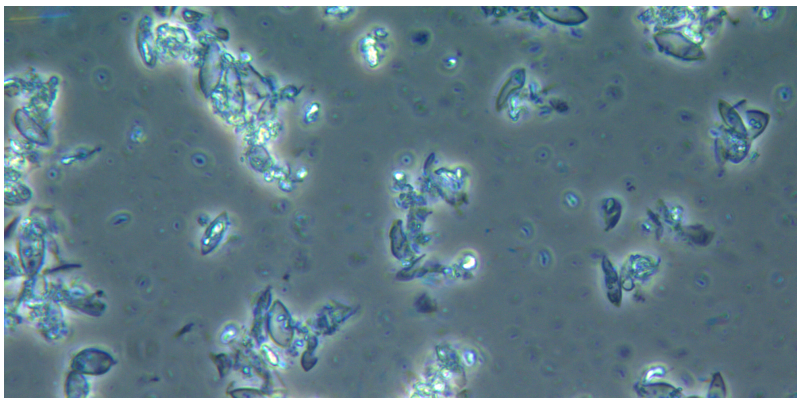

(e) *Scenedesmus spp.* algal cells at Time = 4hrs of bead milling

Figure 4.18: Microscopy of mechanical disruption of *Scenedesmus spp.* algal cells through bead mill operation. Image (a) taken using a 20X objective lens, images (b)-(e) taken using a 100X objective lens.

The total VFA content in the aqueous phase of the algal slurry increased substantially (4000 mg VFA/L to 6300 (52% increase)) during milling (Figure 4.19). Of particular significance were the increase in lactic (150% increase) and propionic (80% increase) acids. These specific acids are derived from three major components within the algal cell: membrane components, storage components and metabolites (Chang et al., 2010).

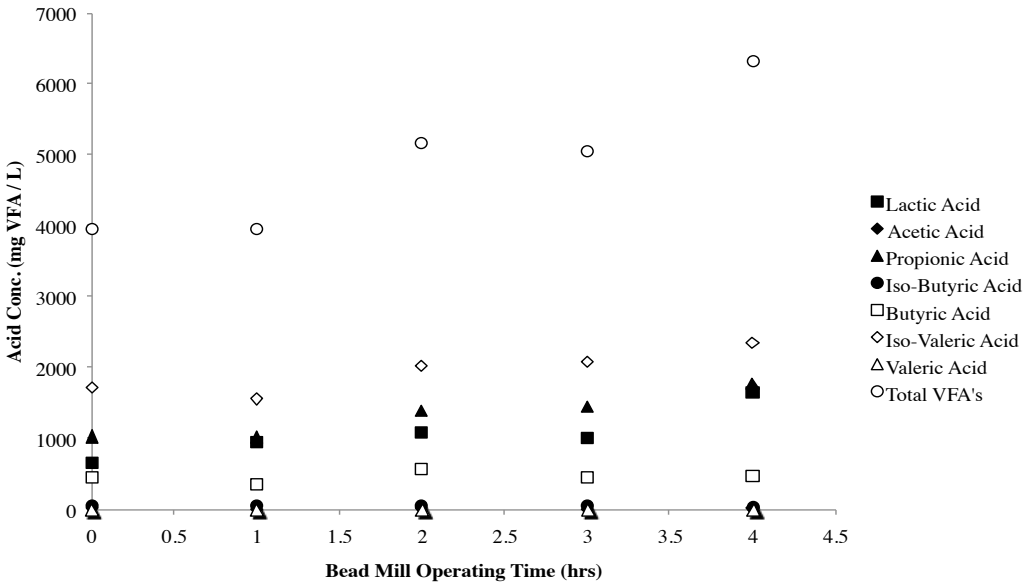

Figure 4.19: Total and specific VFA concentration profiles of *Scenedesmus spp.* algal slurry through bead mill operation

4.4.2 Influence on key anaerobic digestion parameters

VFA dynamics

The detailed analysis of the key variables observed in batch digestion of whole cell algae emphasised the importance of VFAs in the AD process. The production and consumption of these VFAs provides a means to predict the expected methane yields and productivities, as well as the overall efficiency of digestion. Figures 4.20 and 4.21 show the three key acids as well as total acids profile for both unruptured and ruptured cell digesters.

The initial production of VFAs in the ruptured *Spirulina spp.* digesters resulted in a maximum total VFA concentration of ca. 8000 mg/L, which was similar to levels obtained in the whole cell digesters (Figure 4.20 (a) and (b)). In a study by Samson and LeDuy (1983b), the impact on VFA production when an ultrasonic (mechanical disintegration) pre-treatment was applied was far more significant. The semi-continuous AD system had an average VFA concentration of 8 685 mg $CH_3OOH_{equivalent}$/L when digesting the ruptured substrate compared to 3 249 mg $CH_3COOH_{equivalent}$/L for the whole cell biomass. The discrepancy may be a result of the retention time (20 days) and VS loading rate (2 kg VS/m^3.day) not allowing for the whole cells to degrade and further be converted into VFAs.

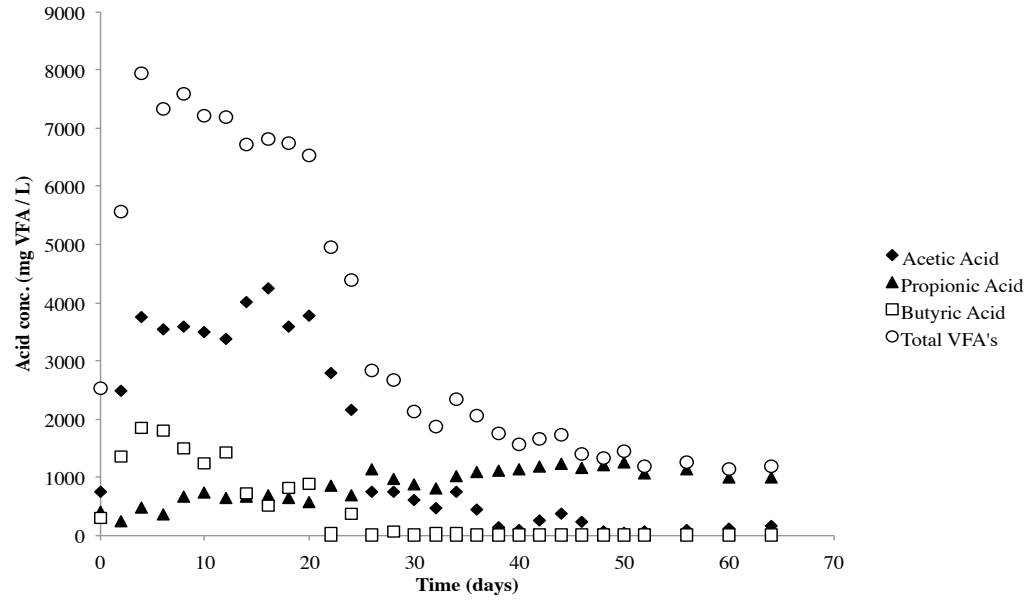

(a) *Spirulina spp.* whole cell substrate loaded digesters

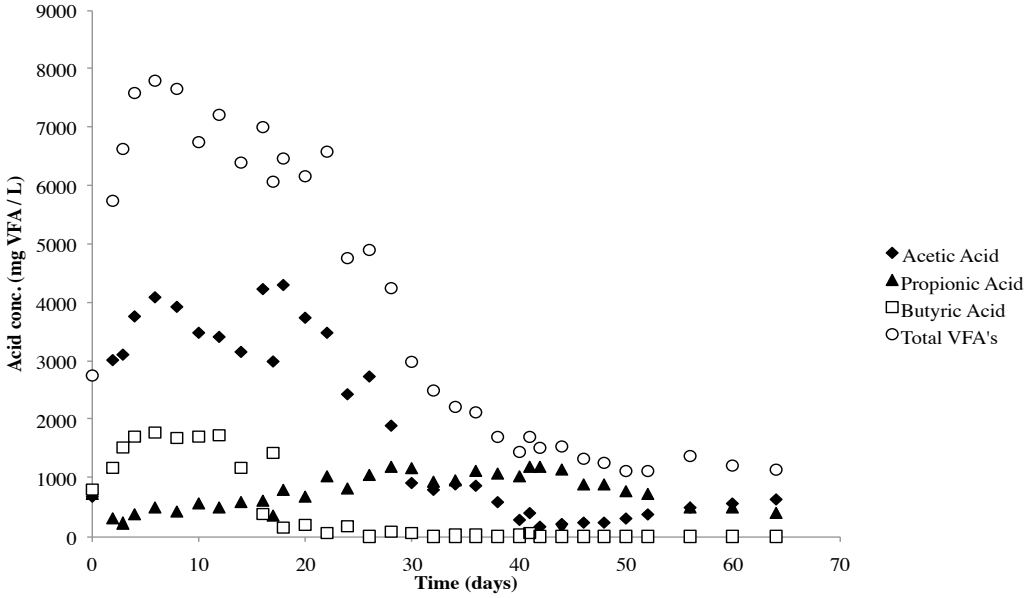

(b) *Spirulina spp.* ruptured cell substrate loaded digesters

Figure 4.20: Total and specific VFA concentration profiles for whole cell and ruptured cell *Spirulina spp.* batch digestion (n=3)

After the initial high VFA production a period of low microbial activity within the system continued until day 20 when the rate of acetic acid consumption exceeded production from propionic and butyric acids. This resulted in sharp linear decrease of acetic and butyric acids and so total acids within the system, similar to whole cell digesters. Propionic acid resisted degradation and maintained a relatively constant concentration until the latter stages of digestion. Towards the end of the linear phase of VFA consumption, the propionic to acetic acid mass concentration ratio increased to above one, however returned to less than one after day 50. This was a good indication that there was no imbalance within the system at that stage. The fact that all the *Spirulina spp.* unruptured cell digesters (n=3) suffered from the propionic to acetic acid imbalance can be assigned to the higher degradation of proteins that occurred (Table 4.2 reaction 8).

The result of the imbalance not affecting the ruptured cell digesters is supported by the increased period of microbial activity and so VFA concentration dynamics during the course of digestion. The difference in ratios for ruptured and whole cell digesters having such a significant impact on the system dynamics has no obviously apparent explanation and is worth additional investigation.

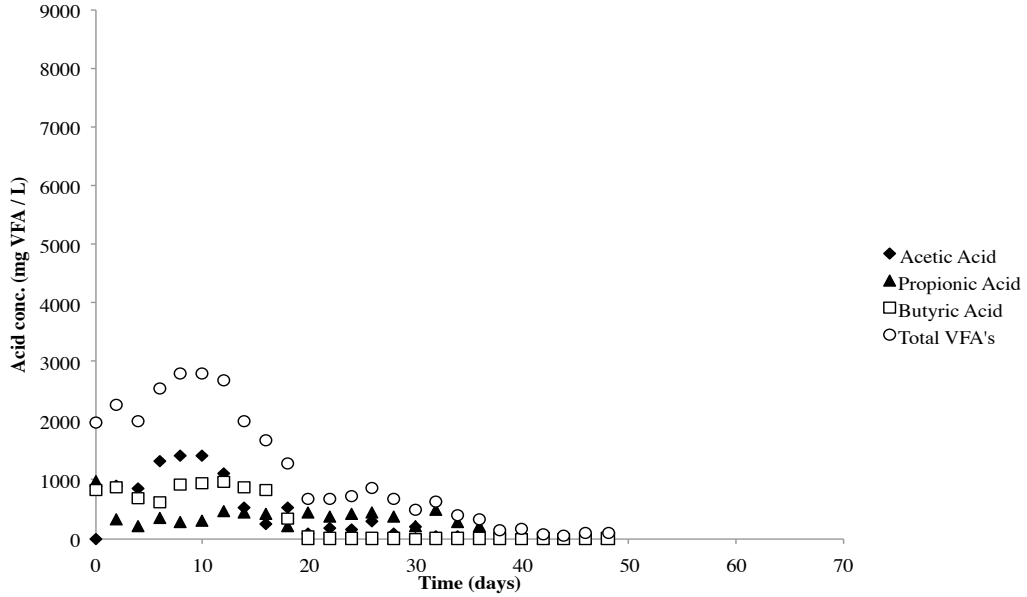

(a) *Scenedesmus spp.* whole cell substrate loaded digesters

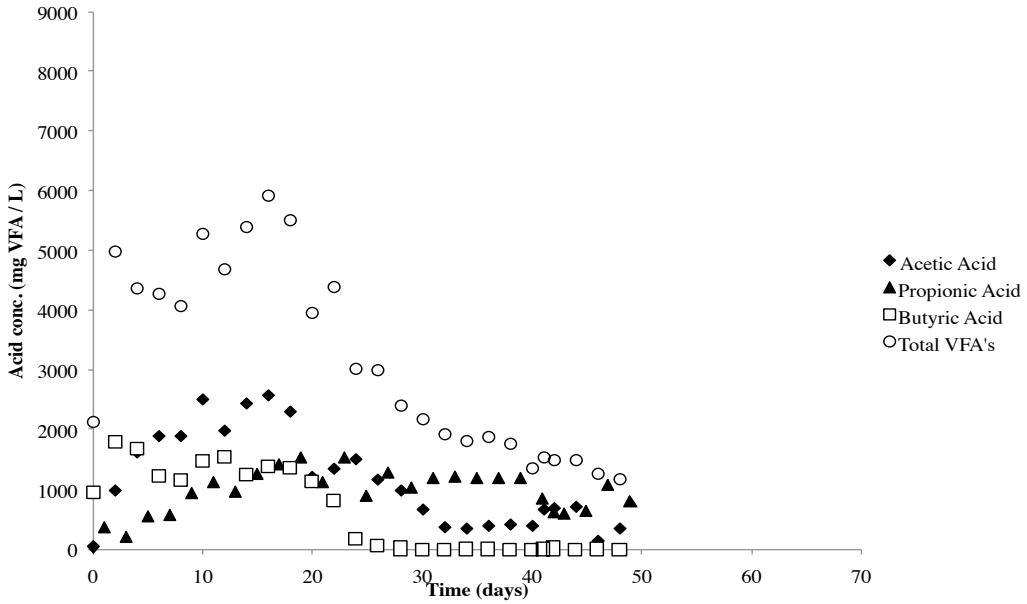

(b) *Scenedesmus spp.* ruptured cell substrate loaded digesters

Figure 4.21: Total and specific VFA concentration profiles for whole cell and ruptured cell *Scenedesmus spp.* batch digestion(n=3)

AD of the ruptured *Scenedesmus spp.* cells resulted in a significantly different VFA profiles (Figure 4.21 (c) and (d)) compared to whole cell digestion. After the initial high activity period, the ruptured cell digesters averaged ca. 5600 mg Total VFA/L whereas the whole cell digesters averaged ca. 2800 mg Total VFA/L. This emphasised the benefit of disruption in allowing for hydrolysis of key organic compounds and so conversion to VFAs. Of particular importance was that of the acetic acid concentration, which

was almost double that of the whole cell digesters (2600 mg/L vs. 1430 mg/L) at the maximum level. This immediately increased the BMP of the system. The higher initial VFA production resulted in an extended lag phase (18 days compared to 10 days) since more time was needed for the microbial consortia to acclimatise to the change in environment. A pH drop (6.6 to 4.59) confirmed this. The *Spirulina spp.* digesters did not suffer from a pH drop since residual alkalinity buffered the pH, however an imbalance did still occur from high VFA concentrations.

Impact on key indicator VFAs

Similar to the whole cell digesters, key indicator acids were monitored through the course of digestion.

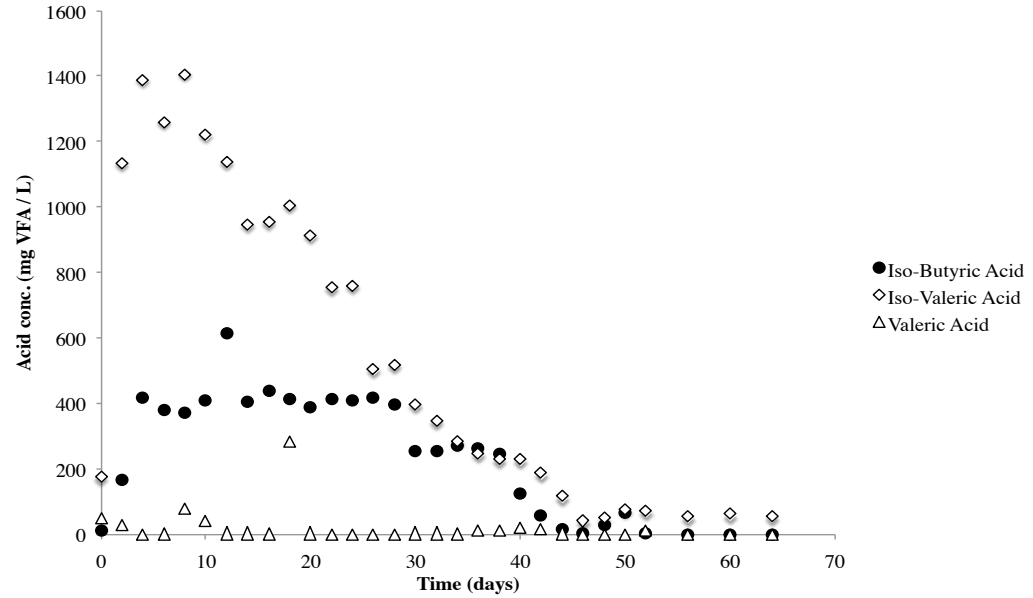

(a) *Spirulina spp.* whole cell substrate loaded digesters

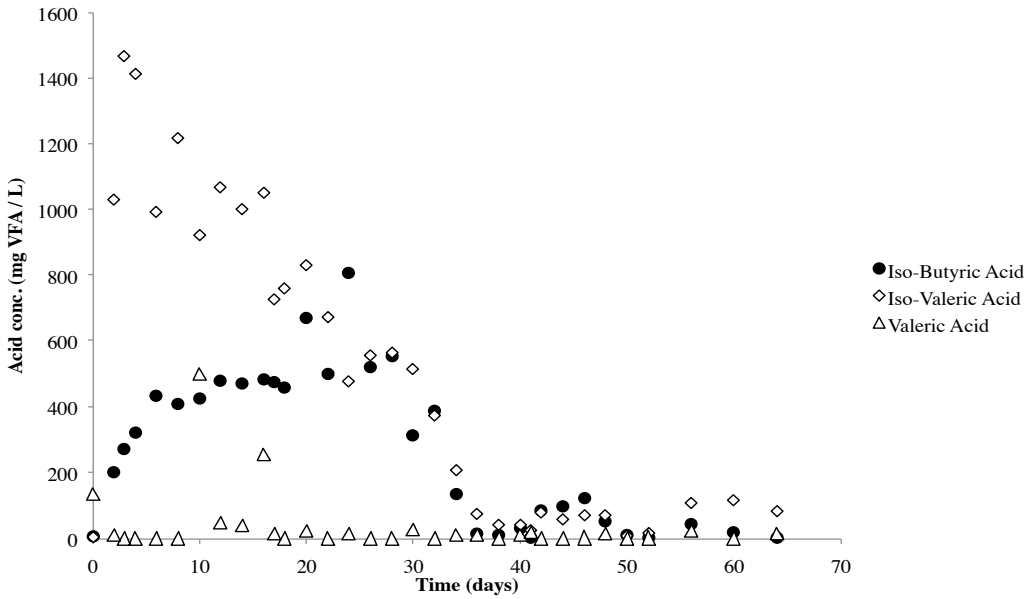

(b) *Spirulina spp.* ruptured cell substrate loaded digesters

Figure 4.22: Indicator VFA concentration profiles for whole cell and ruptured cell *Spirulina spp.* batch digestion (n=3)

At no stage for either algal species did accumulation of any indicator acid occur. Rupturing the cells prior to digestion had no impact on the specific indicator VFAs for *Spirulina spp.* digesters but did increase the production by two fold for that of the *Scenedesmus spp.* digesters. Iso-valeric acid was the most resistant to degradation, maintaining the highest concentration through the linear degradation phase, until eventually being consumed to trace concentrations.

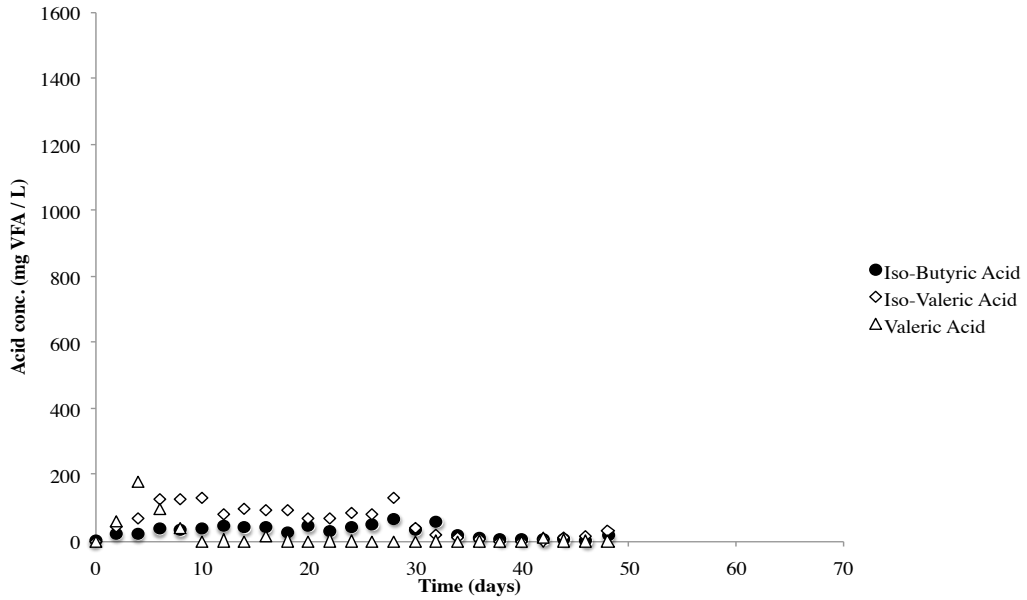

(a) *Scenedesmus spp.* whole cell substrate loaded digesters

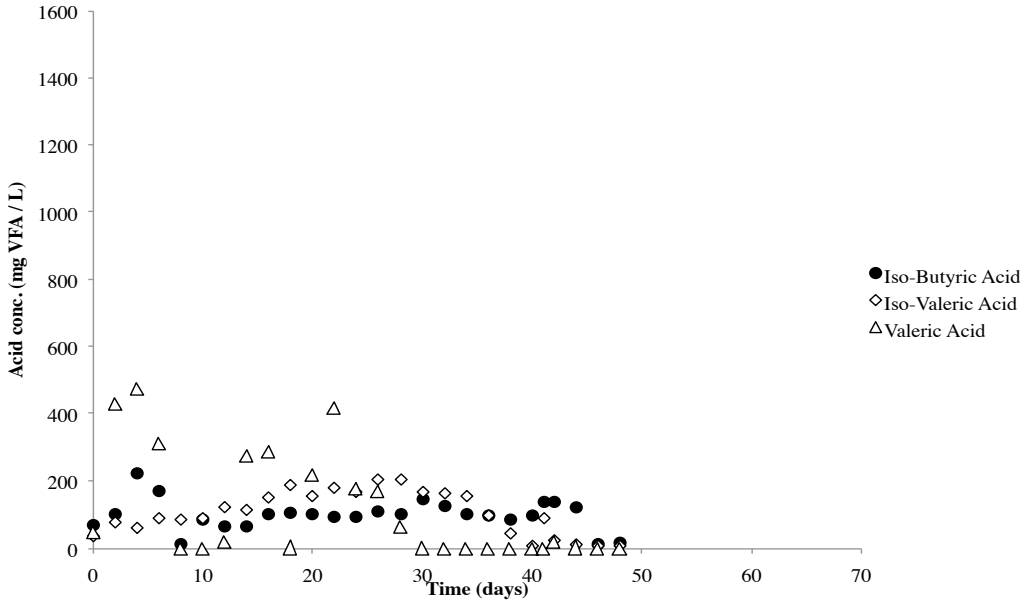

(b) *Scenedesmus spp.* ruptured cell substrate loaded digesters

Figure 4.23: Indicator VFA concentration profiles for whole cell and ruptured cell *Scenedesmus spp.* batch digestion (n=3)

Impact on soluble COD and contribution by VFAs

The total soluble COD in the aqueous phase of the digesters was once again governed, to a large extent, by the VFA concentrations. The higher initial soluble COD concentrations confirmed the efficiency of mechanical disruption of the algal cells prior to digestion. With the exception of the first few days the COD profiles for *Spirulina spp.* ruptured cell digesters were comparable to that of the whole cell digesters. The concentration for the *Scenedesmus spp.* ruptured cell digesters (average maximum 14500 mg COD/L decreasing to $<$ 1500 mg/L) was significantly greater than the whole cell digesters (average maximum 6500 mg COD/L decreasing to $<$ 200 mg COD/L).

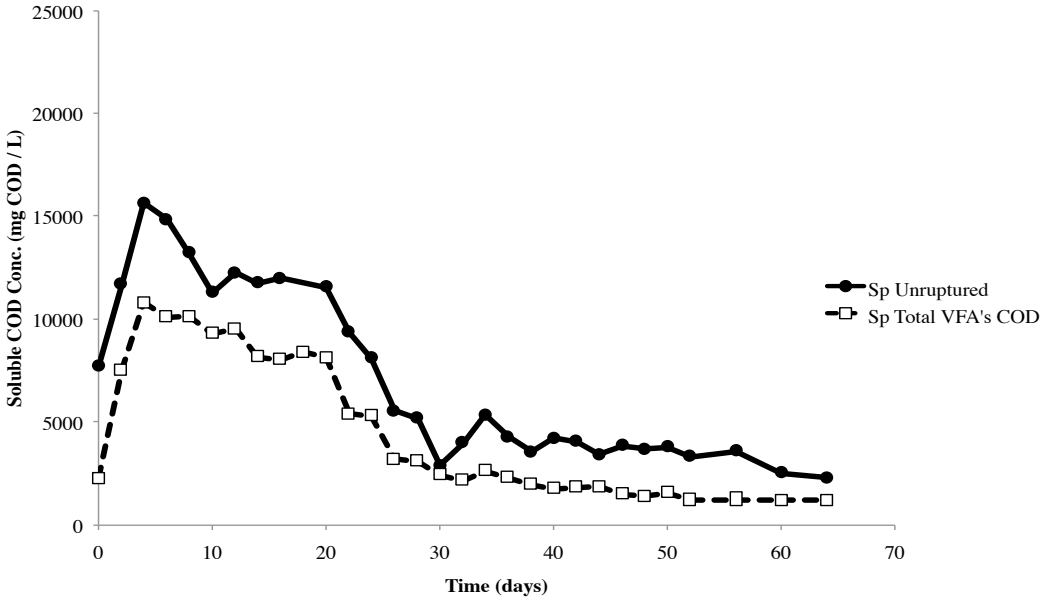

(a) *Spirulina spp.* whole cell substrate loaded digesters

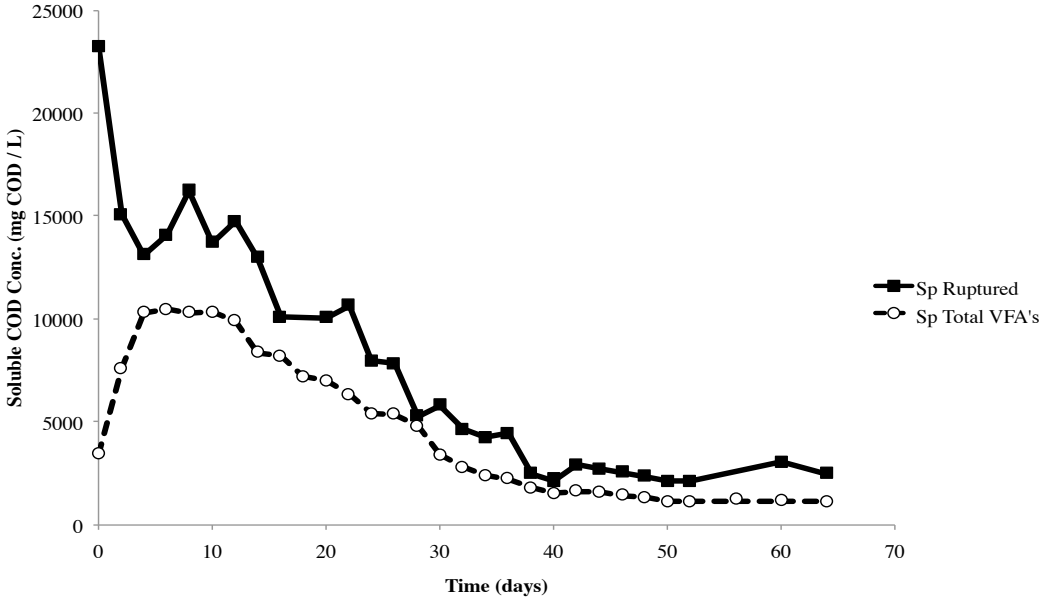

(b) *Spirulina spp.* ruptured cell substrate loaded digesters

Figure 4.24: Soluble COD and Total VFA COD concentration profiles for whole cell and ruptured cell *Spirulina spp.* batch digestion (n=3)

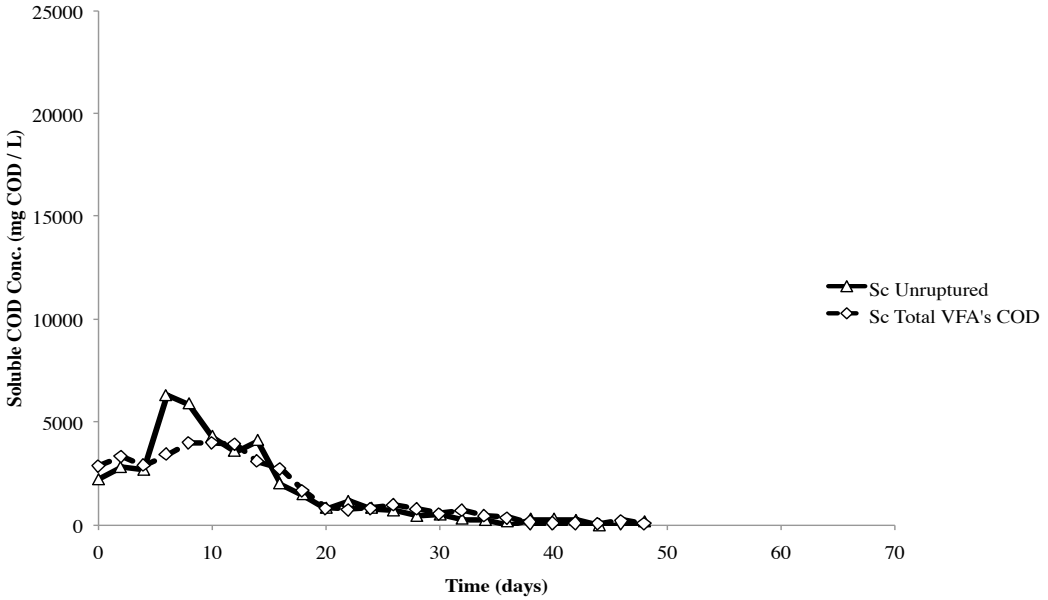

(a) *Scenedesmus spp.* whole cell substrate loaded digesters

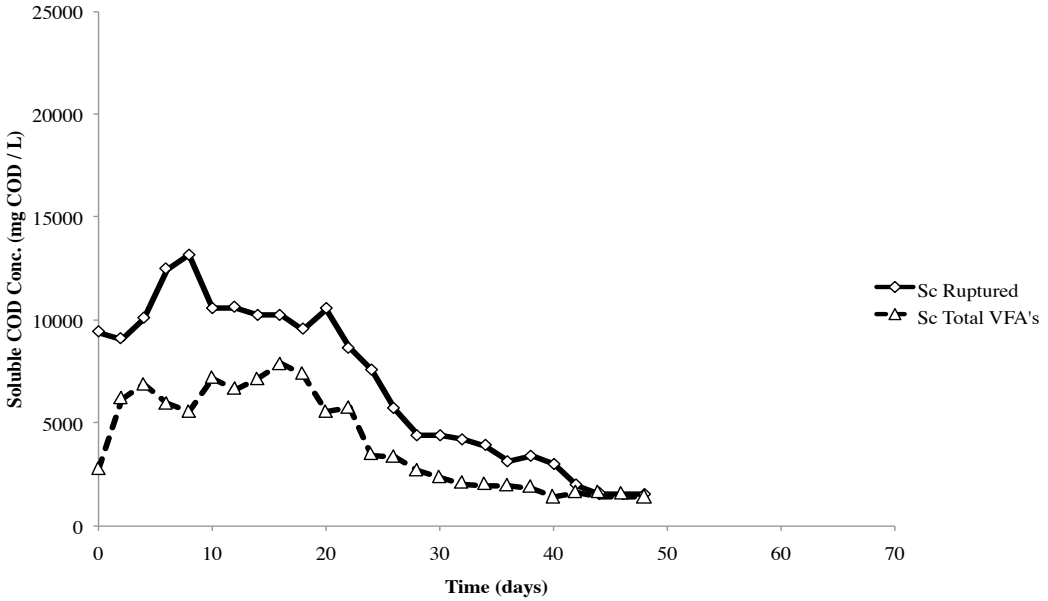

(b) *Scenedesmus spp.* ruptured cell substrate loaded digesters

Figure 4.25: Soluble COD and Total VFA COD concentration profiles for whole cell and ruptured cell *Scenedesmus spp.* batch digestion (n=3)

For both species the ruptured cell digesters showed a decrease in soluble COD during the first few days of digestion. This was attributed to the proportion of the total COD accounted for by the solid biomass. In the whole cell systems the soluble COD increased despite the initial spike in gas production (removal of COD in gaseous phase) because of the hydrolysis reactions. This was not the case for the ruptured cell digesters since solubilisation of complex organics took place during disruption (Figures 4.15 and 4.17).

4.4.3 Influence on biogas production and efficiency of digestion

Methane Productivity

For *Spirulina spp.* the liberation of key organics through disruption resulted in a greater initial methane productivity of 0.23 L CH_4/ $L_{reactor}$.day compared to 0.08L CH_4/ $L_{reactor}$.day for the whole cell digesters. The productivity also rose to a greater maximum of 0.26 L CH_4/ $L_{reactor}$.day compared to 0.175 L CH_4/ $L_{reactor}$.day for the whole cell digesters during the linear VFA consumption phase (Figure 4.26 (a)). With the exception of these two values, rupturing did not significantly alter the profile.

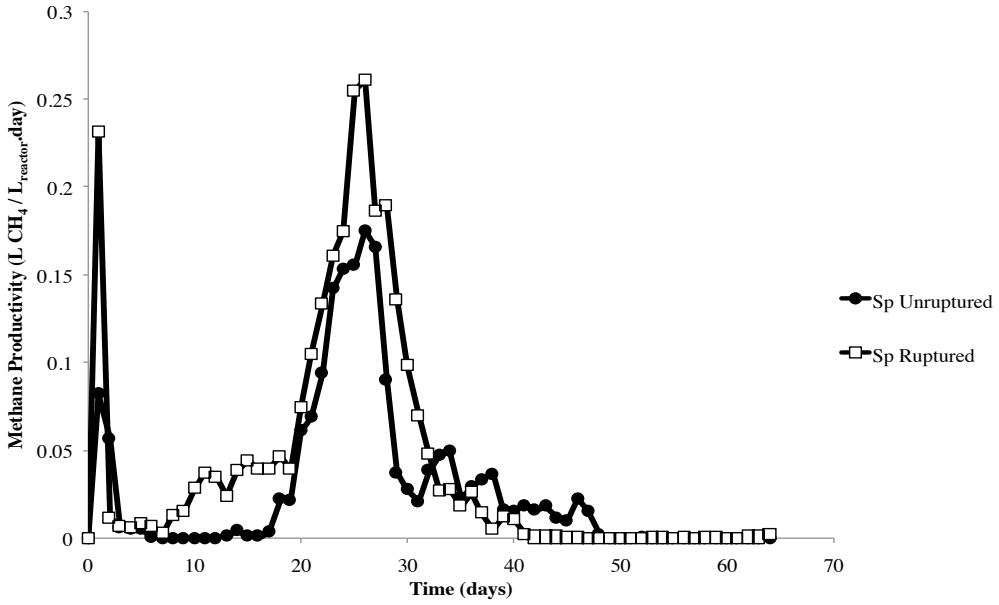

(a) *Spirulina spp.* substrate loaded digesters

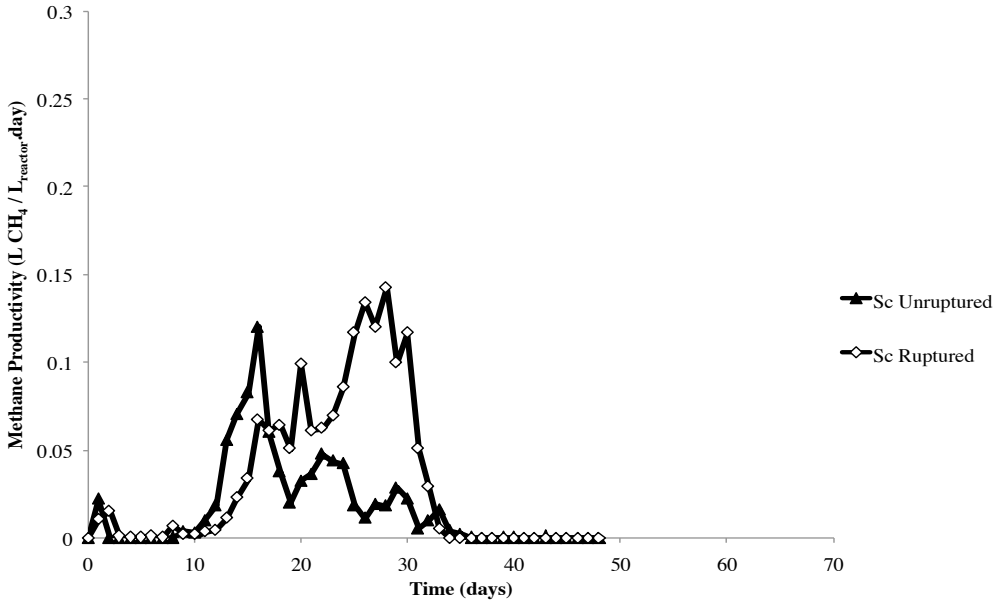

(b) *Scenedesmus spp.* substrate loaded digesters

Figure 4.26: Methane productivity profiles for whole cell and ruptured *Spirulina spp.* and *Scenedesmus spp.* batch digestion(n=3)

Unlike the whole cell digesters, the initial period of acclimatisation did not affect the ruptured cell digesters to the same extent. The stages that followed the initial high production of VFAs showed signs of some microbial activity and so methane productivity (average of 0.025 L CH_4/ $L_{reactor}$.day for days 3-20). This suggested that even with the imbalance created in the system from the sudden increase in VFAs, rupturing of the cells allowed for easily fermentable and readily available organics to be consumed.

The methane productivity profiles for the *Scenedesmus spp.* digesters indicated that the disruption of the algal cells resulted in a significant rise in methane production across digestion (Figure 4.26 (b)). The productivities did not rise to similar levels as the *Spirulina spp.* digesters, with the maximum for ruptured *Scenedesmus spp.* digesters at 0.15 L CH_4/ $L_{reactor}$.day and for *Spirulina spp.* digesters at 0.26 L CH_4/ $L_{reactor}$.day.

The methane productivity related to the amount of acetic acid that was produced from the degradation of VFAs by acetogenic bacteria. This was further controlled by the availability of easily fermentable organics. Even with rupturing, the digestibility of the remaining biomass was still lower than for that of *Spirulina spp.* The destruction profiles indicated that *Spirulina spp.* degraded more easily than *Scenedesmus spp.*

At the stage in digestion where the solubilised organics from disruption were completely consumed, the degradation of *Scenedesmus spp.* cell debris was once again influential in biomethanation process. This reiterated the fact that a large portion of the organic constituents that make up the algal cell were found within the degradation resistant cellulosic cell wall and emphasised the importance that the cell wall composition had on system progress.

Methane yields

The results obtained for the methane productivity profiles relate directly to the final derived parameter, the methane yields (Figure 4.27). The final methane yield for *Spirulina spp.* increased from 0.113 L CH_4/ g VS to 0.166 L CH_4/ g VS with the inclusion of mechanical pre-treatment. The increase of 47% was attributed to increased microbial activity during the early stages of digestion, as well as to the extended period of methane production without the negative impact of high propionic to acetic acid ratios.

Samson and LeDuy (1983b) reported that the mechanical pre-treatment of *Spirulina maxima* positively influenced acidogenic bacteria, but did not increase methane production. The results shown in the current study indicate that an increase in VFA production results in a greater consumption of acetic acid by methanogens and so a greater methane yield. Unless the concentrations become inhibitory, this should always be the case. Samson and LeDuy (1983b) reported similar total VFA concentrations, which were not inhibitory. The sensitivity of the AD process to a range of parameters makes it difficult to attribute the apparent contradiction to a particular parameter.

The methane yield from *Scenedesmus spp.* digestion increased from 0.054 L CH_4/ g VS to 0.096 L CH_4/ g VS with disruption. The substantial increase related to the greater amount of acetic acid produced and consumed. This originated from the release of key organic compounds (glucose equivalent) during disruption, which allowed for greater production of key VFAs.

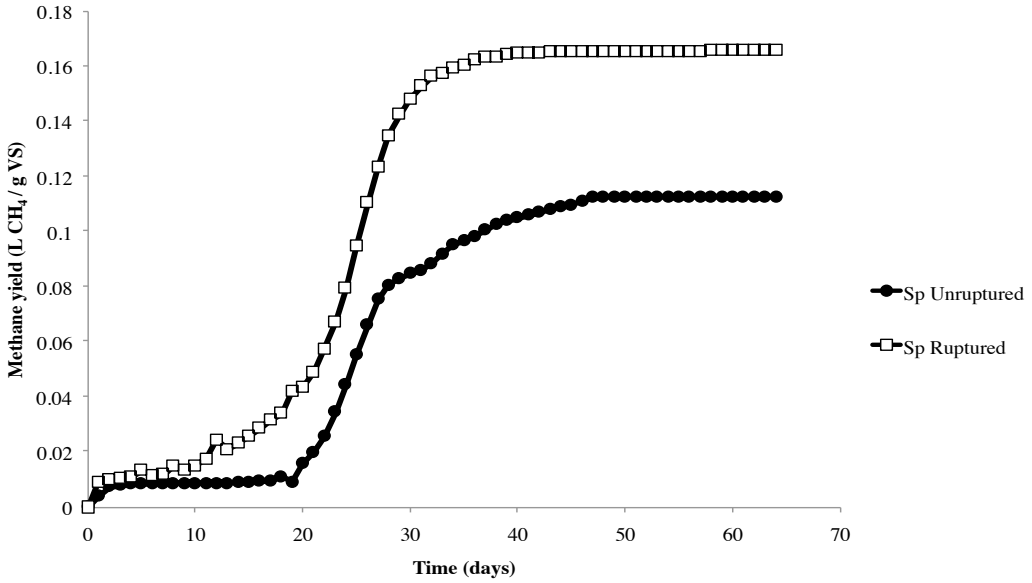

(a) *Spirulina spp.* substrate loaded digesters

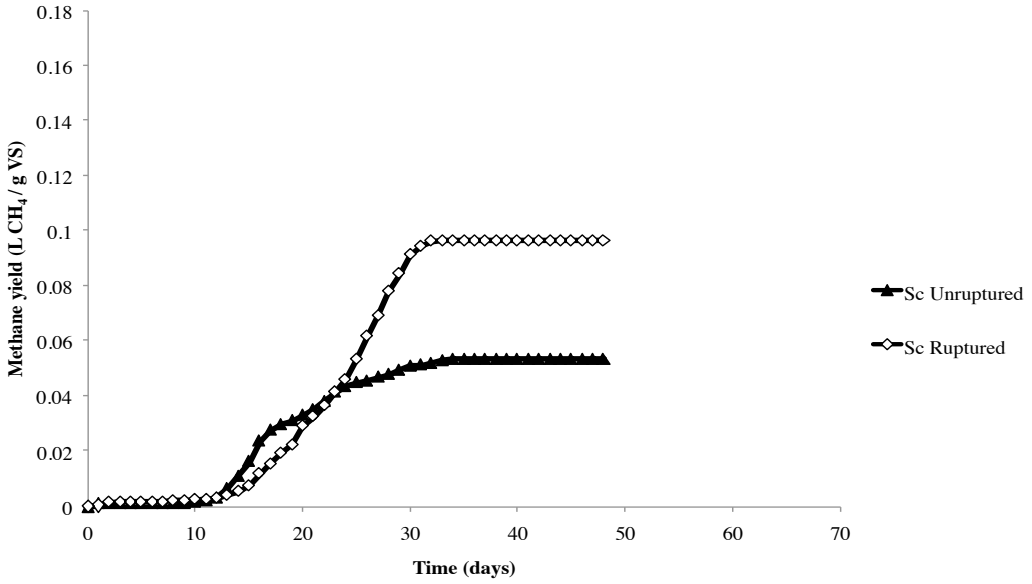

(b) *Scenedesmus spp.* substrate loaded digesters

Figure 4.27: Methane yield profiles for whole cell and ruptured *Spirulina spp.* and *Scenedesmus spp.* batch digestion (n=3)

The yield of methane in terms of total COD destroyed was interesting for the whole cell digesters, where the final yield was the same for both species. This was not the case for the ruptured cell digesters (Table 4.6).

Table 4.6: Methane yield of whole cell digesters, expressed in L CH_4/ g COD destroyed (n=3)

Substrate	Total methane produced (L CH_4)	Total COD Destroyed [a] (g)	Methane yield (L CH_4/ g COD destroyed)
Whole cell *Spirulina spp.*	1.81	30.28	0.06
Ruptured cell *Spirulina spp.*	2.66	29.10	0.09
Whole cell *Scenedesmus spp.*	0.86	14.05	0.06
Ruptured cell *Scenedesmus spp.*	1.55	21.84	0.07

[a] :⇒Calculated by subtracting the final and initial total COD values

An increase in the methane yield per COD consumed indicates a more efficient conversion of COD into methane. The *Spirulina spp.* yield was greater in the case of the ruptured cell digesters, 0.09 compared to 0.06 L CH_4/ g COD destroyed for the whole cell digesters, which was attributed the imbalance suffered from the propionic to acetic acid ratio in the whole cell digesters.

The inhibition due to this high propionic acid to acetic acid ratio has, as already mentioned, been reported in previous anaerobic digestion studies. However, no mechanistic description of the complex metabolism of fermentable organics to propionic acid has been provided and so a robust discussion can not be completed.

Digestion efficiency

The final measure of the influence of mechanical pre-treatment on the overall AD process was determined by the destruction profiles. During the initial stages of AD the solid COD of the whole cell *Spirulina spp.* digesters dropped to levels comparable to that of the ruptured cell digesters (ca. 15000 mg COD/L (Figure 4.28)). This was due to the disruption of cells and release of the intracellular contents due to osmotic shock.

The ruptured cell digester solid COD did not drop in these stages of digestion, suggesting that the mechanical pre-treatment was successful in maximising the disruption of the cells. The total COD, which was the summation of solid and soluble COD, destruction profiles for both the unruptured and ruptured *Spirulina spp.* digesters were similar in terms of trends observed and quantities of COD destroyed.

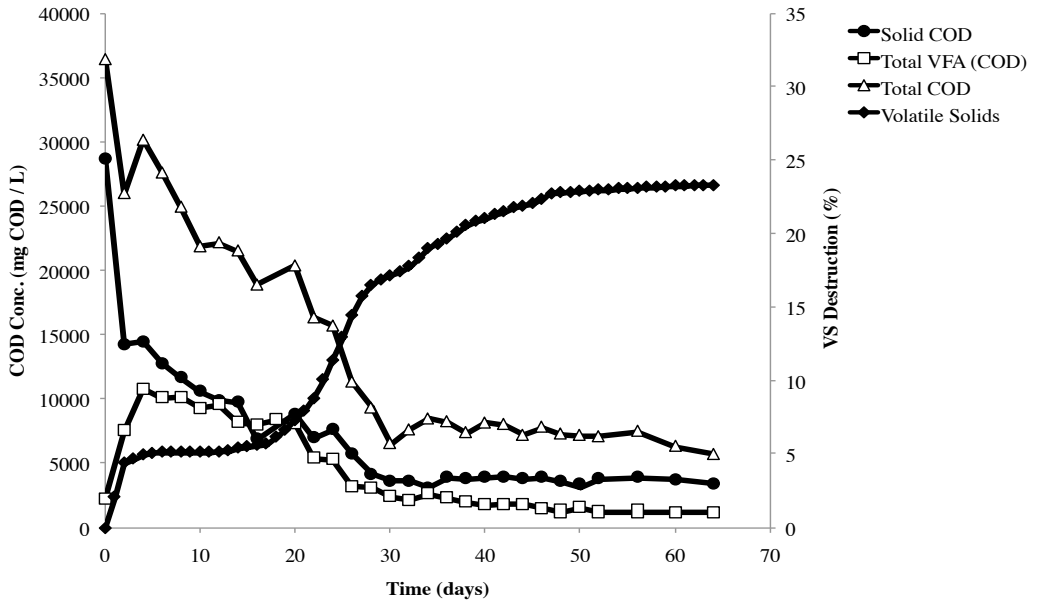

(a) *Spirulina spp.* whole cell substrate loaded digesters

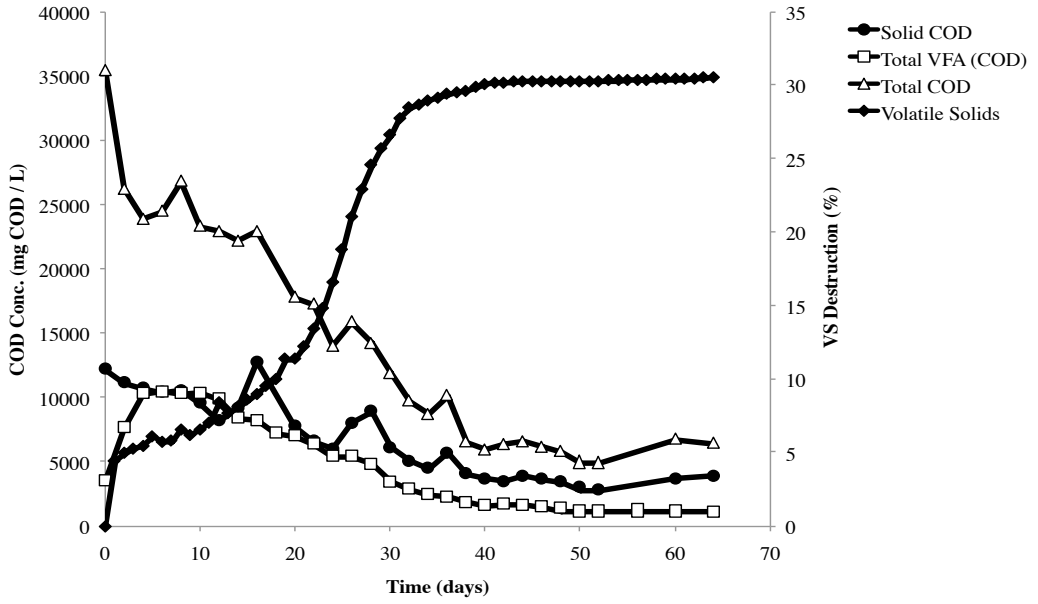

(b) *Spirulina spp.* ruptured cell substrate loaded digesters

Figure 4.28: Solid COD, Total COD, Total VFA and VS destruction profiles of whole and ruptured cell *Spirulina spp.* batch digestion (n=3)

The destruction profiles for the *Scenedesmus spp.* whole cell and ruptured cell digesters revealed that mechanical disruption of the cells allowed more of the original solid COD to be consumed. The result differs from the *Spirulina spp.* digesters where the residual solid COD was not affected by mechanical pre-treatment. The difference is largely due to the extent of disruption.

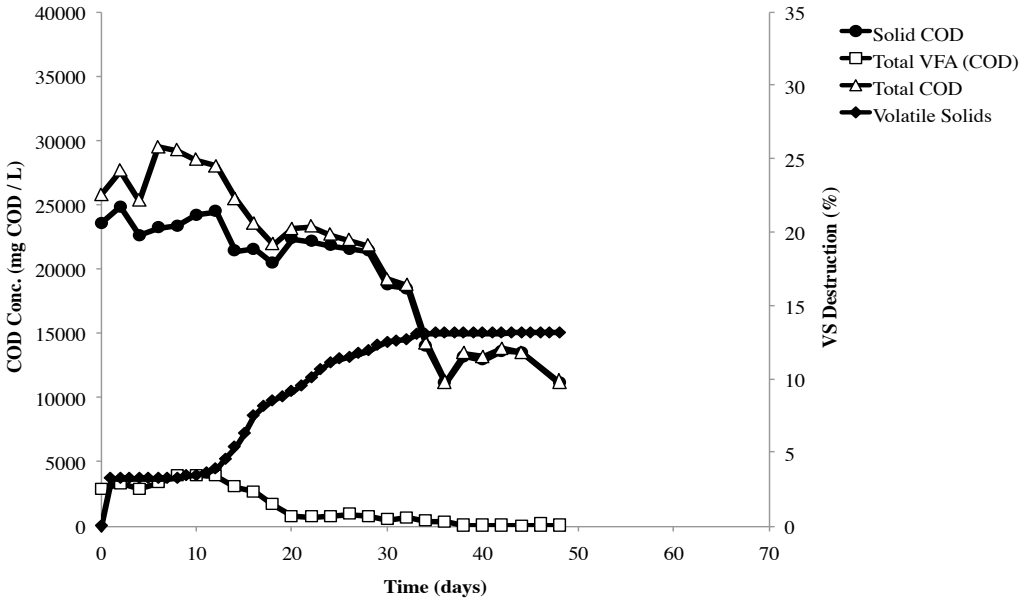

(a) *Scenedesmus spp.* whole cell substrate loaded digesters

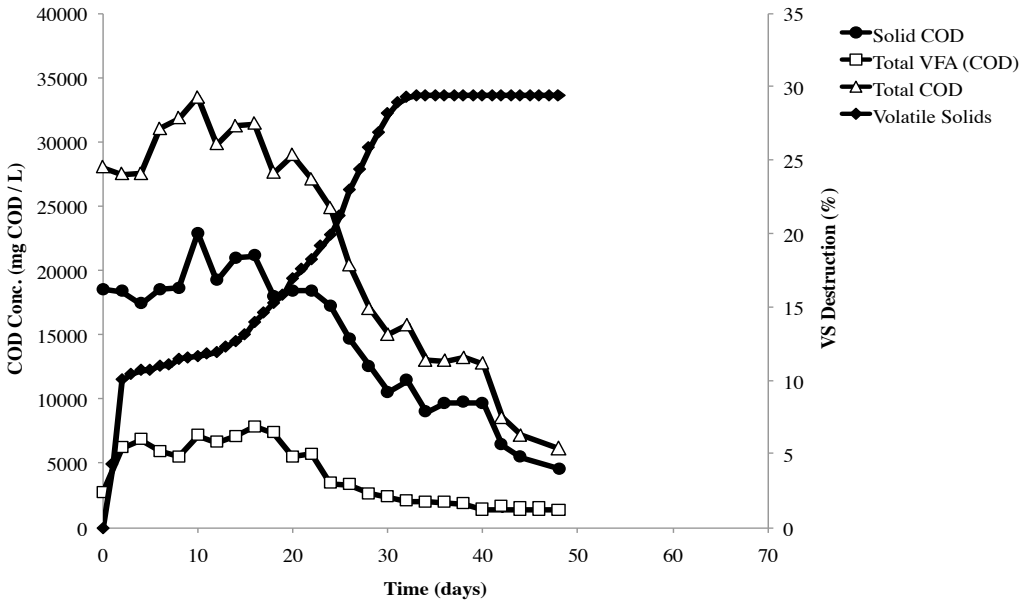

(b) *Scenedesmus spp.* ruptured cell substrate loaded digesters

Figure 4.29: Solid COD, Total COD, Total VFA and VS destruction profiles of whole and ruptured cell *Scenedesmus spp.* batch digestion (n=3)

From the images taken during milling (Figure 4.18 (a)-(e)) partially disrupted cells were seen after bead mill operation had stopped, which contributed to solid COD. However these cells degrade more easily through digestion, increasing the concentration of soluble organics. This also led to a high net destruction of solid COD. The low destruction of solid COD in the whole cell digesters supported this result and highlighted the resistance of *Scenedesmus spp.* to degradation.This confirmed that break down of COD

in the ruptured cell digesters was most likely not a result of cell fragment degradation. In an intact cell, the soluble intracellular components still count as solid COD because they are trapped in the cell. As the cell walls are not easily digested there were most likely some intact cells left at 50 days in the whole cell system. In the ruptured system this was not the case.

Table 4.7: Impact of mechanical pre-treatment of the efficiency of AD in the destruction of COD, VFAs and VS 's for *Spirulina spp.* and *Scenedesmus spp.* batch digestion (n=3)

Substrate	Solid COD Destruction[a] (%)	Total COD Destruction[b] (%)	VFA Destruction[c] (%)	VS Destruction[d] (%)
Whole cell *Spirulina spp.*	88	86	89	20
Ruptured cell *Spirulina spp.*	68	81	92	27
Whole cell *Scenedesmus spp.*	53	60	98	10
Ruptured cell *Scenedesmus spp.*	75	81	80	24

[a] :⇒Calculated by using the initial solid loading of 20 g/L and a ratio of g DW: kg COD of

[b] :⇒Additive destruction of both solid and soluble COD

[c] :⇒ Calculated by taking point of maximum VFA conc. as the initial conc.

[d] :⇒ Calculated using Varel's eq: VS destroyed(g) = (mol CO_2 +mol CH_4)X(12/(carbon content of biomass))

The most significant result from the destruction profiles have been reported in Table 4.7. The extent to which disruption has increased the digestibility of the algal substrates can be taken directly from these key variable results.

4.5 Anaerobic digestion of direct transesterification reside as the major substrate

4.5.1 Feasibility of AD with the DT residue as a substrate

The most important parameters to be monitored to assess the feasibility of digesting the residue remaining after direct transesterification were derived from the previous experiments. The process of DT required the use of strong acid and base catalysts as well as methanol and hexane. The method used in preparation of the substrate included a centrifugation and evaporation stage to remove the majority of excess hexane and methanol respectively.

However, the catalysts remained, carrying chloride and sodium ions into the digester. Chen et al. (2008), in their review of inhibition in AD, reported that, above threshold limits, these ions inhibit propionic acid utilising bacteria and methanogenic microorganisms.

VFA Profiles

Any inhibition that occurred would be detected in the VFA profiles (Figure 4.30). If unusual trends, such as accumulation of any specific acid, arose it would have indicated that there was inhibition of the anaerobic microbial consortia. Accumulation of specific acids would also have indicated which microorganisms were inhibited and the toxic compounds causing the inhibition.

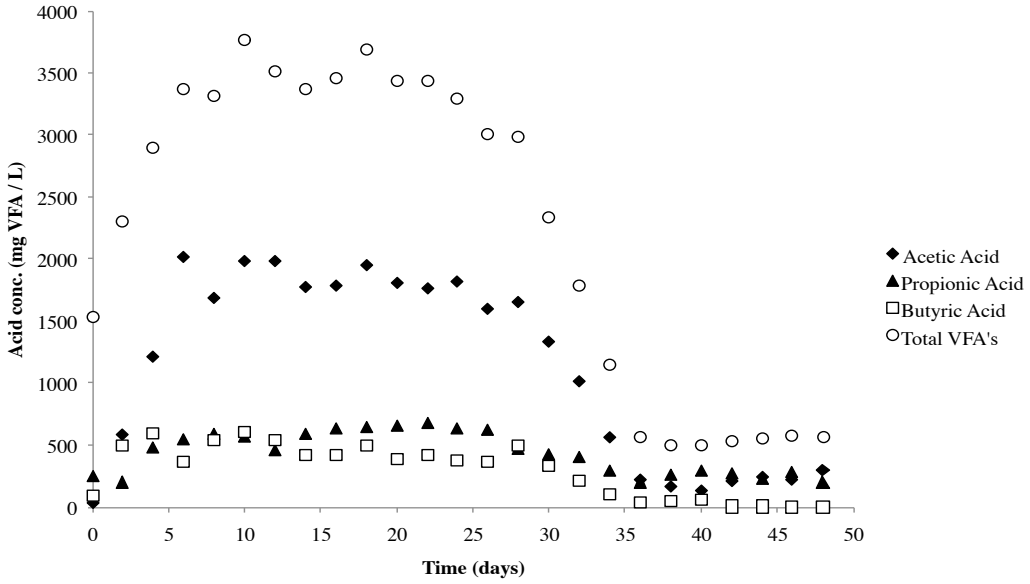

(a) Key VFA profiles

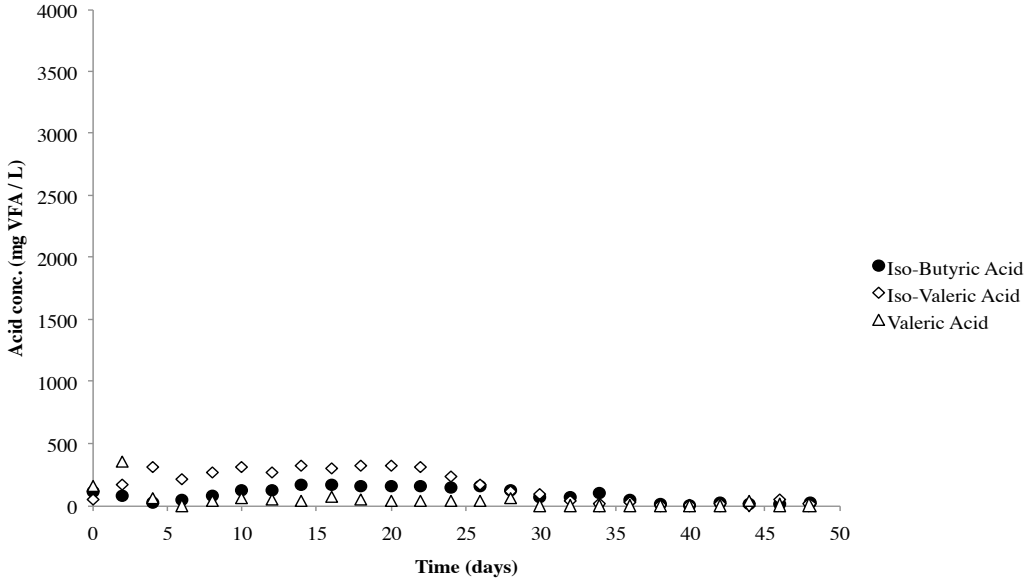

(b) Indicator VFA profiles

Figure 4.30: Total and Specific VFA concentration profiles for *Scenedesmus spp.* DT residue batch digestion (n=1)

The acid forming bacteria were not inhibited by residual catalyst from DT. This was confirmed by the sharp initial increase in key VFAs (acetic, propionic and butyric acids), which was also observed for both the whole cell and ruptured cell digesters. There was a rise in indicator VFAs (iso-butyric, iso-valeric and valeric acids) but no continued accumulation across digestion.

The DT residue had an initial substrate loading of ca. 20 g DW/L, the same as whole cell and ruptured cell digesters, and so yields of VFAs could be compared directly to these reactors. During DT the cells were partially ruptured to release their intracellular contents. This allowed for increased enzymatic hydrolysis of complex organics (carbohydrates, proteins) to simpler organics that were then consumed by acidogenic bacteria to produce VFAs.

The yield of VFAs (average total VFA conc. 3500 mg/L) was higher than that obtained from the whole cell digesters, but lower than that of the ruptured cell digesters. This suggested that the DT process was effective in increasing the amount of easily fermentable organics, but not to the same extent as that of complete cell rupturing. This comparrison could be made as the amount of volatile solids remaining after extraction of the lipid was the same as intially loaded into the whole cell and ruptured cell digesters.

The residual biomass comprised of mainly proteins and carbohydrates. This resulted in a different ratio of key acids formed. The ratio of acetic:propionic:butyric acids was 4:1:1, which differed to the whole cell and ruptured cell digesters where ratio's of 3:2:1 and 5:3:2 were observed. This indicated that a large proportion of the butyric acid formed in the whole cell digesters was a result of lipid degradation.

After the initial high VFA production period there was an extended lag period where the concentration of VFAs in the system remained fairly constant. However, unlike the whole cell and ruptured cell digesters, this lag period continued for an extended time. This indicated that at this point the acidogenic, acetogenic and methanogenic microorganisms were experiencing some form of inhibition by a toxic compound.

After the extended lag period, the expected linear consumption of VFAs did occur. The total VFA concentration decreased from ca. 3500 mg/L to 550 mg/L over a 20-day period. Propionic acid offered the most resistance to degradation and only decreased in concentration by 250 mg/L. All other acid concentrations tended towards zero. This rate of consumption was similar to the whole cell digesters, where the concentration of total VFAs decreased from ca. 2650 mg/L to 600 mg/L over a 20 day time period.

The extended lag period was attributed to both the imbalance caused by the high VFA concentration and to the residual catalyst from DT. The anaerobic microbial consortia loaded into the digesters needed to acclimatise to both of these variables and so the increased stabilisation period was an expected result. The consumption of acetic acid indicated that the methanogenic culture recovered from the initial inhibition, which was a primary concern when experimentation began.

Soluble COD and VFA contribution

The residual organic compounds (hexane and methanol) from DT contributed a large amount to the soluble COD of the digesters (Figure 4.31). This result was confirmed by the difference in soluble COD and total VFA COD experienced. During the lag phase of digestion, the VFA COD was ca. 4500 mg/L whilst the soluble COD was ca. 13 000 mg/L. The difference was also a result of macro-organic compounds (glucose equivalent) solubilised by the degradation of the solid residue. Towards the end of digestion, the soluble COD and VFA COD concentrations did not change significantly. This confirmed that minimal microbial activity occurred and that the maximum amount of possible degradation had taken place. Unlike digestion of whole and ruptured cell biomass, the difference in soluble COD and VFA COD remained high. This suggested that the residual compounds from DT did not degrade across digestion. Methanol has been used as a substrate in AD and was shown to degrade over time (Park and Park, 2003).

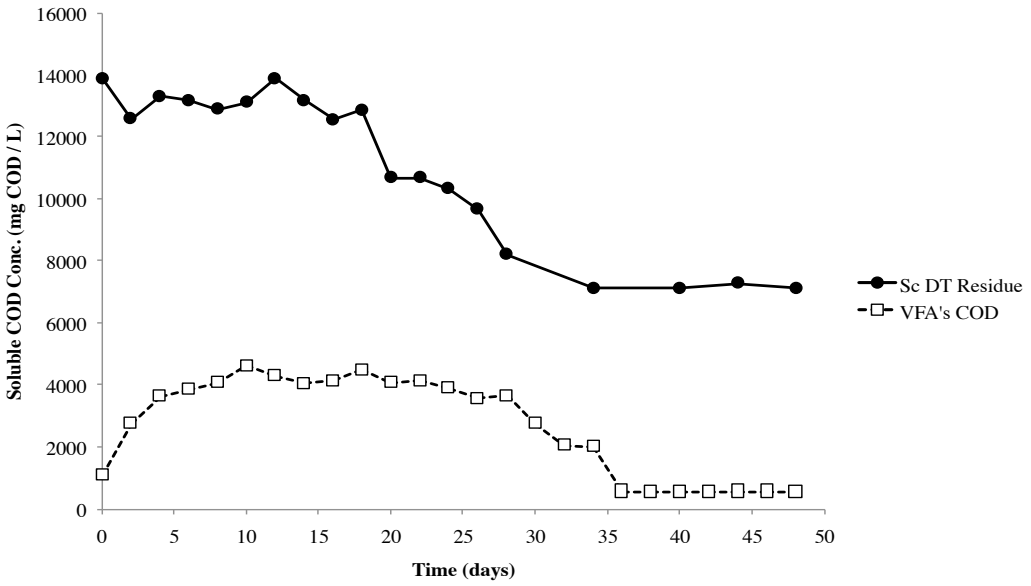

Figure 4.31: Soluble COD and Total VFA COD concentration profiles for *Scenedesmus spp.* DT residue batch digestion(n=1)

4.5.2 Biogas production and efficiency of digestion

Methane productivity and yield

The productivity and yield of methane confirmed what the VFA profiles reported (4.32). Methane productivity was a maximum , 0.11 L $CH_4/L_{reactor}$.day, during the period of linear consumption of VFAs. After 35 days of digestion the productivity decreased towards zero. This was expected as microbial activity and so changes in VFA concentrations slowed at this point. The period of methane productivity (day 19 - day 40) followed closely to the observed changes in VFA concentrations.

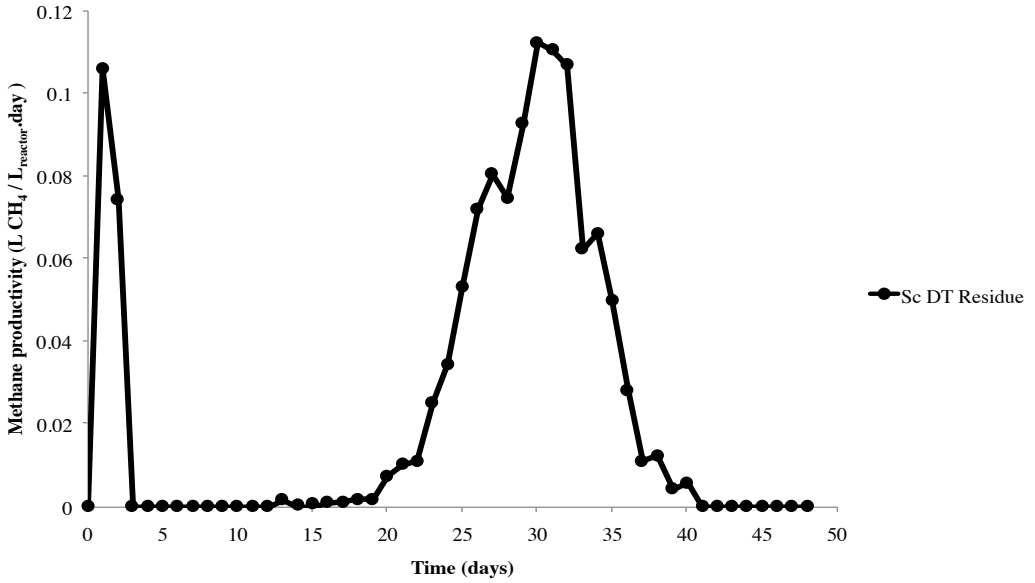

(a) Methane productivity profile

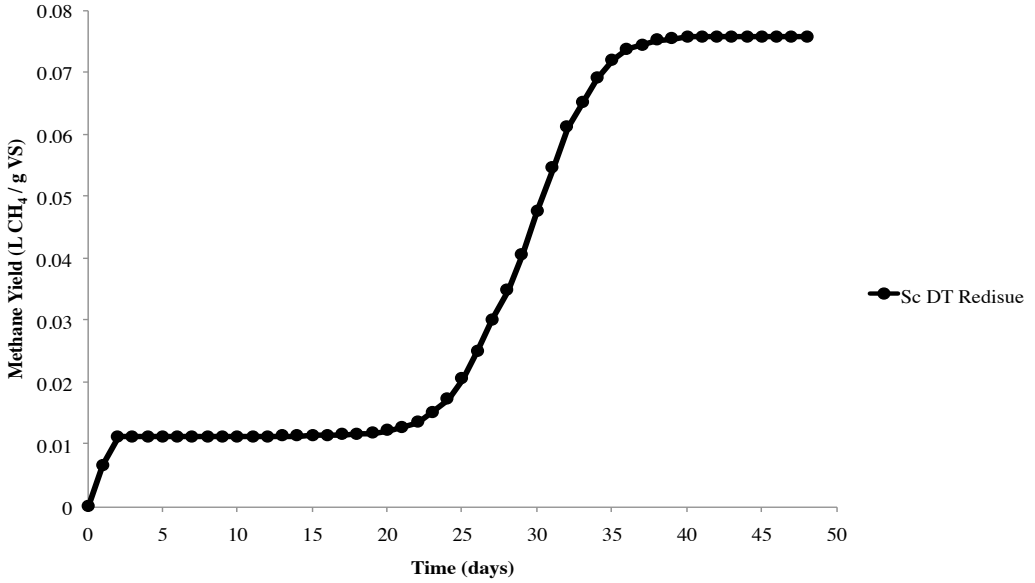

(b) Methane yield profile

Figure 4.32: Methane productivity and yield profiles for *Scenedesmus spp.* DT residue batch digestion (n=1)

The final methane yield of 0.075 L CH_4/ g VS, was greater than that of the whole cell digesters, but less than the ruptured cell digesters. The yield related directly to the cumulative methane produced, which further related to the net consumption of acetic acid. The cumulative methane production and total COD destruction resulted in a methane yield of 0.05 L CH_4/ g COD destroyed. The value was similar to both *Spirulina spp.* and *Scenedesmus spp.* whole cell digesters, indicating equally efficient methane producing systems.

Destruction profiles

Similar to whole and ruptured cell batch digestion, efficiency was determined using the destruction of four key variables (Figure 4.33).

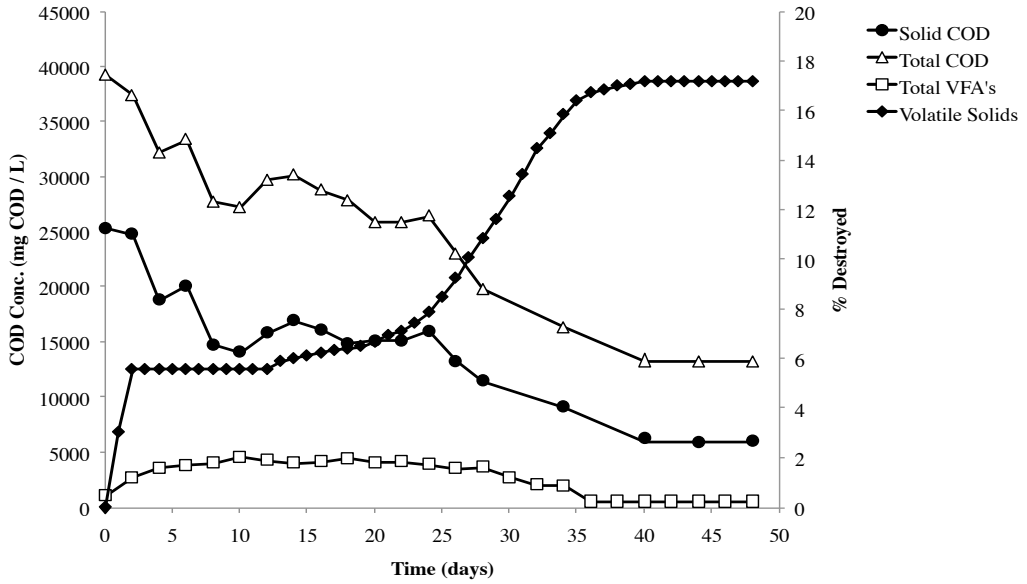

Figure 4.33: Solid COD, Total COD, Total VFA and VS destruction profiles of *Scenedesmus spp.* DT residue batch digestion (n=1)

The ultimate destruction percentages are presented in Table 4.8.

Table 4.8: Efficiency of AD in the destruction of COD, VFAs and VS 's for *Scenedesmus spp.* DT residue (n=1)

Substrate	Solid COD Destruction[a] (%)	Total COD Destruction[b] (%)	VFA Destruction[c] (%)	VS Destruction[d] (%)
Scenedesmus spp. DT residue	75	66	87	17.2

[a] :⇒Calculated by using the initial solid loading of 20 g/L and a ratio of g DW: kg COD of

[b] :⇒Additive destruction of both solid and soluble COD

[c] :⇒ Calculated by taking point of maximum VFA conc. as the initial conc.

[d] :⇒ Calculated using Varel's eq: VS destroyed(g) = (mol CO_2 +mol CH_4)X(12/(carbon content of biomass))

The solid COD destruction of 75% indicated that DT provided a more easily degradable source of biomass than whole cells. This was further emphasised by the pronounced decrease during the first 10 days of digestion. DT partially ruptured the *Scenedesmus spp.* cells. These cells broke down on initiation of digestion hence the drop in solid COD.

The lower total COD destruction, 69%, resulted from the resistance to degradation of the residual compounds from DT. This result was confirmed by the 87% destruction of VFAs produced. The efficiency

of the system in producing biogas from destroyed VS's was 17.2%. The result was expected to be higher than that of the whole cell digesters and less than the ruptured cell digesters, which was the case.

4.6 Conclusions

The feasibility of anaerobically digesting *Spirulina spp.* and *Scenedesmus spp.* whole cell and ruptured cell algal biomass as well as *Scenedesmus spp.* lipid extraction residue was thoroughly investigated and key results discussed. The close monitoring and profiling of liquid phase compounds (VFAs and COD) allowed for important characteristics of each substrate to be identified. A higher production of VFAs was a direct result of the amount of freely available easily fermentable organics released by the degradation of the algal biomass. The biodegradability of *Spirulina spp.* biomass allowed for a greater production of VFAs and so higher concentrations of soluble COD. Across digestion the high COD was converted by the anaerobic microorganisms into biogas, hence greater methane yields for the specific substrate. The higher resistance of *Scenedesmus spp.* to degradation resulted in reduced methane yields.

Mechanical pre-treatment increased the available COD in the *Scenedesmus spp.* digesters to a greater extent relative to the *Spirulina spp.* digesters. *Spirulina spp.* cells ruptured upon initialisation of digestion, most likely from osmotic shock, resulting in an increase in soluble COD. The larger impact on available COD resulted in more significant increases in final methane yields for *Scenedesmus spp.* ruptured cell digesters compared to *Spirulina spp.*. The pre-treatment had a positive effect on both acidogenic and methanogenic microbial activity, which was emphasised by the increase in VFA production and consumption.

AD of the *Scenedesmus spp.* DT residue proved successful and resulted in a higher final methane yield than the whole cell digesters, but lower yield than the ruptured cell digesters. The increased methane yield was attributed to the increased microbial activity due to the more easily degradable source of biomass created during DT. However, the extended lag period and increased COD pose issues as to the potential for the residual compounds from DT to impact large scale digestion.

Chapter 5

Creating an integrated algal anaerobic digestion system for bioenergy production using *Spirulina spp.* as a feed stock

5.1 Introduction

The results from the batch digestion studies indicated that *Spirulina spp.* had the greatest potential for methane production and net energy production. This prompted further investigation into the digestion of *Spirulina spp.* in an integrated algal growth and digestion process. The chapter focuses on the continuous algal growth and harvesting process as well as the semi-continuous AD unit. A detailed analysis of the semi-continuous digester feed and effluent was conducted. Emphasis was placed on the effect of VFA concentrations on the system stability and efficiency of methane production. Potential toxic compounds were monitored and the profiles presented. The characterisation of the AD effluent allowed for recommendations to be made regarding its potential down-stream applications.

The chapter is concluded with a brief overview of the methane potentials from *Spirulina spp.* semi-continuous systems when optimal conditions were applied.

5.2 Methodology

The results presented in this chapter refer to the experimental design expressed in Section 3.5.3. With the given time constraints, optimisation of the integrated system was not the objective of this study, rather evaluation of performance and identification of possible issues. A full work-up of the data presented in this Chapter for the full 56 day operating period can be found in Appendix C.

5.3 Results and Discussion

5.3.1 Algal growth unit

The algal productivity, based on continuous harvesting over 52 day period is presented in Figure 5.1. Harvesting was conducted using simple cloth filtration and biomass harvested measured each 24h. Typically algal productivities are expressed in units of g DW/ m^2.day (Chisti, 2007; Dowling, 2009; Sialve et al., 2009), however to keep with the theme of volatile solids, this study presented productivity in terms of g VS/m^2.day. Depending on growth conditions, VS contents can vary between 60 and 90%. The productivities reported were measured in terms of dry mass and converted using a factor of 0.75 g DW per g VS (Sialve et al., 2009).

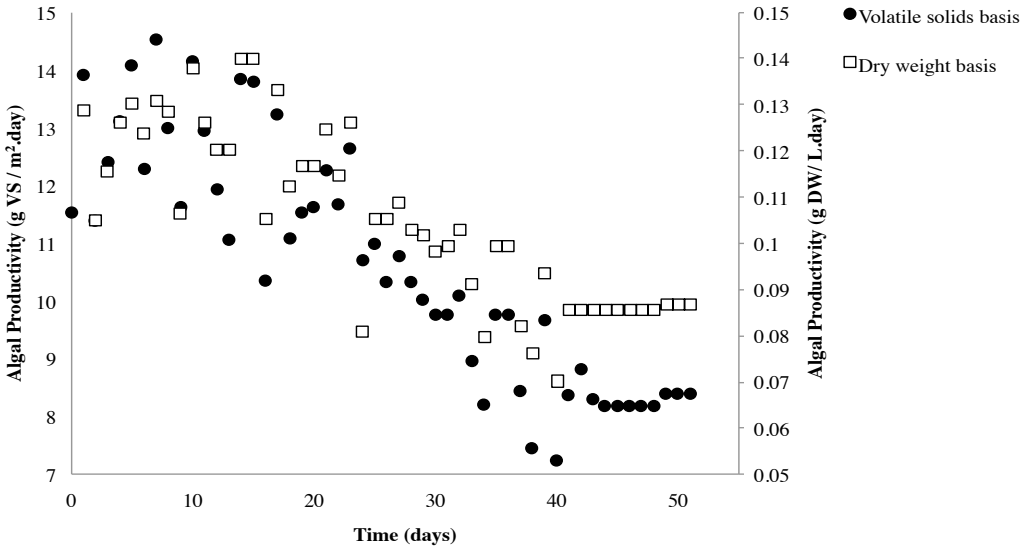

Figure 5.1: Algal productivity for the integrated system as a function of time, expressed in g VS harvested per day specific to one m^2 of reactor space and g DW harvested per day specific to L of the growth unit.

An average productivity of 40.6 ton VS/ha.year (0.11 g DW/L.day) with a maximum of 53.1 ton VS/ha.year (0.14 g DW/l.day) was obtained from the growth unit. These values are based on direct scaling of the productivity from the 65 L growth unit. This approach has been adapted in many studies reporting final algal yields derived from laboratory-scaled units (De Schamphelaire and Verstraete, 2009; Richmond et al., 1990; Jimenez et al., 2003b). The average concentration of algal biomass in the growth unit was 1.33 g VS/L (1.78 g DW/L.) with a maximum of 1.51 g VS/L (2.1 g DW/L). It was postulated that the decrease in productivity observed over the 56 day growth period was a result of accumulation of associated cations from the nitrates, phosphates and salts in the growth media. This originated from the rate of nutrient addition (make-up media) to the unit being greater than the rate of utilisation by the algae. An increase in conductivity (14 to 23 mS/cm) supported this postulation. Both the productivity and algal biomass concentration are extremely dependent on the type of algal species and the operating conditions of the growth unit e.g. irradiance, pH, temperature, reactor design, harvesting routine. The accumulation of cations could be overcome by a bleed of the system, however the growth unit was still providing sufficient biomass for feed to the digester and so this was not performed. Table 5.1 depicts some typical produc-

tivity values reported for in similar *Spirulina spp.* growth units. To enable comparisons between different studies, some of the key system operating conditions are presented with the biomass concentrations and productivities.

Table 5.1: Typical algal biomass concentrations and productivities observed in *Spirulina spp.* growth units

Species	Type of Reactor	Light conditions	Growth Conditions	Biomass concentration (g VS/L)	Biomass productivity (ton VS/ha.year)	Reference
Spirulina spp.	Raceway pond 0.52 m^2 (65 L)	4* 32 Watt fluorescent bulbs	Zarouk media	1.50	53.0	1
Spirulina spp.	Raceway pond	Outdoor	-	-	32.9-40.0	2
Spirulina platentis	Open raceway ponds	Outdoors (over four seasons)	-	-	45.0-52.5	3
Spirulina platentis	Pilot scale raceway pond 450 m^2 (135000 L)	1.7-0.4 (J/m^2.day)	Zarouk media	0.35	22.5-24.0	4
Spirulina platentis	Pilot scale batch raceway pond 45 m^2 (13500 L)	1.7-0.4 (J/m^2.day)	Zarouk media	0.30	29.3	4
Spirulina platentis	Pilot scale batch raceway pond 4.5 m^2 (1350 L)	1.7-0.4 (J/m^2.day)	Zarouk media	0.45	5.5- 38.2	4

[1] Current study; [2] Clement et al. (1980); [3] Richmond et al. (1990); [4] Jimenez et al. (2003b),* Note all productivities were adjusted using the conversion factor of 0.75 for VS:DW

Important results reported from the referred studies were:

1. Richmond et al. (1990) indicated that the temperature of the surrounding environment during daylight hours influenced the biomass productivities of the algal biomass, with hotter climates resulting in significant increases in productivity. Photoinhibition was more pronounced during summer, where growth almost ceased after midday. Contamination by other microorganisms, particularly *S. minor* and *Chlorella sp.* reduced the biomass yield by at least 15 to 20%. Harvesting in the evening resulted in a significant increase in the biomass recovery relative to morning harvesting. The productivity reported in Table 5.1 was only possible when the optimal temperature for *Spirulina* was maintained throughout daylight hours, photoinhibition was controlled, biomass harvested in the evening during summer and contamination by other cyanobacteria or microalgae was kept low. Pronounced daily fluctuations in the output rate at peak productivity in summer suggested that when environmental limitations of growth were minimal, other limitations became dominant.

2. Jimenez et al. (2003b), who investigated the feasibility of large-scale cultivation of *Spirulina platentis*, showed that the productivity was dependent on biomass concentration, temperature, dissolved oxygen concentration, pH and irradiance. Testing was conducted at a maximum level of 135 000 L, which allowed the most relevant comparisons with yields of agricultural crops and other second generation energy crops.

The sensitivity of productivity to parameters associated with large-scale production (contamination, photoinhibition, temperature, night-day cycles etc.) indicate that the direct scaling of laboratory data may not be valid and may provide an over estimation.

5.3.2 Batch phase acclimatisation of the integrated anaerobic digestion unit

The reactor was operated in batch phase for a period of 6 weeks to allow acclimatisation of the culture and reduction of VFAs to desired concentrations for semi-continuous operation. Table 5.2 summarises the most important results gathered from the acclimatisation period.

Table 5.2: Results obtained from batch phase acclimatisation of the integrated algal system's AD unit

Parameter	Amount	Units
Initial VS loading	16.4	g VS / $L_{reactor}$
Total VS destruction	25.1	%
Total COD destruction	59.3	%
Solid COD destruction	85.1	%
Total VFA production	4810	mg Total VFA / L
Final pH	7.9	
Final ionised sulphide conc.	2.30	mg HS^- / L
Final non-ionised sulphide conc.	18.6	mg H_2S / L
Final ionised ammonia conc.	612	mg NH_4^+ / L
Final free ammonia conc.	26.2	mg NH_3 / L
Final alkalinity conc.	9.5	mg $NaHCO_3$ / L
Cumulative biogas production	3.2	L
Final biogas CH_4 content	67	% CH_4 (vol/vol)
Average methane productivity	0.011	L CH_4 /$L_{reactor}$.day
Final methane yield	0.068	L CH_4 / g VS_{fed}

5.3.3 Semi-continuous operation of the integrated anaerobic digestion unit

OLR and operating temperature

The OLR, a critical parameter, was varied during the four retention periods. The OLR has been shown to have a large impact on digester performance (Samson and LeDuy, 1986). The OLR was varied from an initial high rate of 1.72 g VS/$L_{reactor}$.day to a medium rate of 1.2 g VS/$L_{reactor}$.day. Following this between days 34 and 42 the feed rate was stopped due to poor digester performance. Upon recommencing of feed to the digester a new lower OLR of 0.48 g VS/$L_{reactor}$.day was established.

The temperature of operation was ambient (approximately 25°C)) for retention period 1 and 2 (up to day 28). Following this, for retention period 3 and 4, the entire digester was placed in a temperature control room at 37±2℃. A full analysis of why the changes to the OLR and temperature were made is presented and discussed in the following section of this Chapter. It should be noted that for all Figures presented in this Chapter, the time scale reflects the semi-continuous operation.

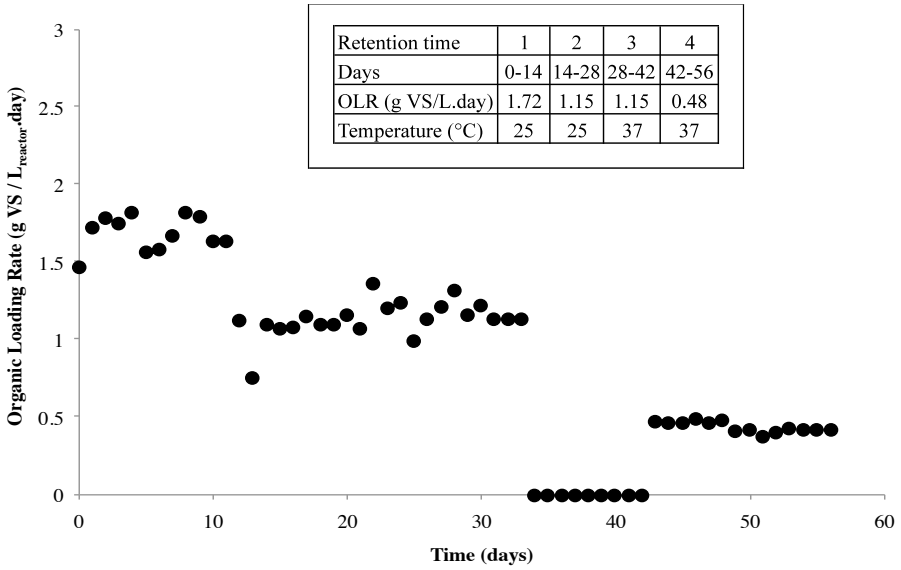

Figure 5.2: Organic Loading Rate (OLR) as a function of time, expressed in g VS per L of reactor liquid volume per day.

VFA dynamics

The value of VFA tracking was established in the batch digestion studies and was conducted on the effluent of the semi-continuous digestion unit. In addition to providing information on process efficiency it was essential that the AD effluent was fully characterised to inform decisions on potential downstream applications. The total and specific VFA concentration profiles of the digester effluent are presented in Figure 5.3.

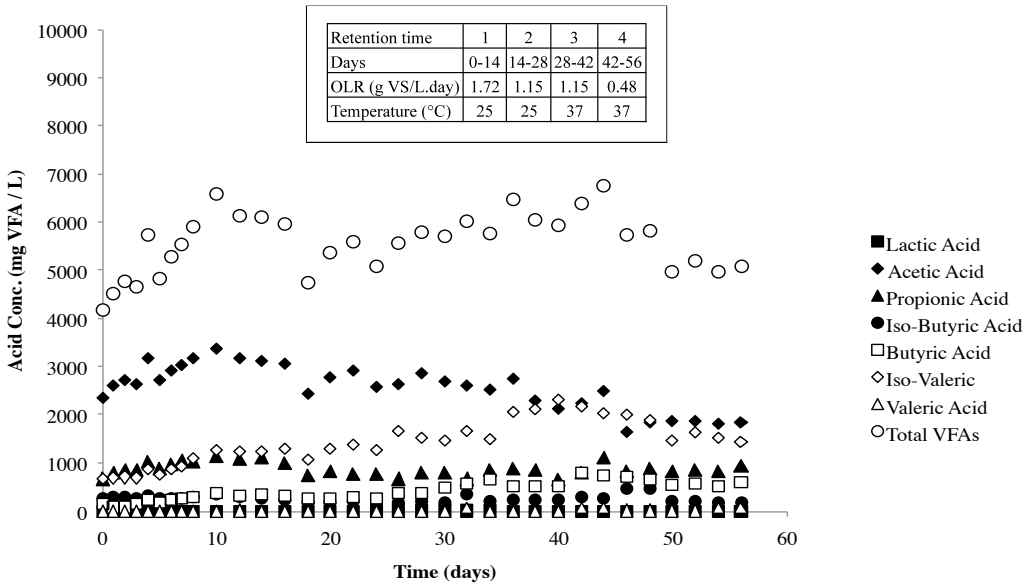

Figure 5.3: Total and specific VFA concentration as a function of time for semi-continuous digestion of *Spirulina spp.*. Data are expressed in mg VFA per L of reactor liquid volume. Note feeding of biomass stopped between days 34 and 42.

As soon as regular feeding was started the total and specific VFA concentrations in the digester increased. In the first 10 days of operation, the concentration of VFAs increased from 4180 mg total VFA/L to 6110 mg total VFA/L whilst the pH dropped from 7.9 to 6.9. The levels of acetic (2350 mg/L - 3200 mg/L), propionic (690 mg/L - 1130 mg/L), butyric (140 mg/L - 333 mg/L) and iso-valeric (688 mg/L - 1230 mg/L) acids increased significantly. The initial accumulation of acids was not a concern as the sharp increase was anticipated. Boltes et al. (2008) presented similar experimental and modelled data showing an initial increase in these three acids at the start of continuous operation (Figure 5.4). However, the continued accumulation observed towards the end of the first retention time (14 days) in this study was a cause for concern.

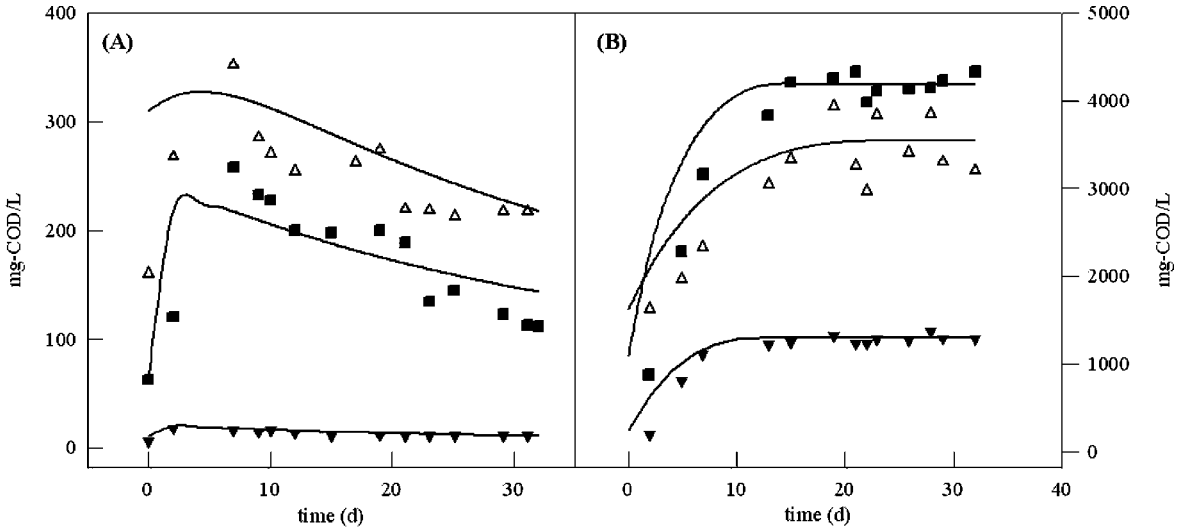

Figure 5.4: Experimental and predicted values for acetic, propionic, and butyric acids in two continuous reactors with the organic loading rate: (A) 0.151 mg of COD/mg of VSS · L; (B) 0.634 mg of COD/mg of VSS.L (Boltes et al., 2008).

* Note the scale for figure A is differnent to that of B. * acetic acid (■), butyric acid (▼) and propionic acid (△)

In the Boltes et al. (2008) study, the sharp initial increase was followed by a period of linear consumption, when the OLR was low. A comparison of the data suggested that the OLR in the current study was too high resulting in excessive provision of easily fermentable organics (glucose equivalent). Consequently the acid forming bacteria had an excess of readily available substrate. The increased acidogenic and acetogenic activity caused the methanogenic stage of digestion to be rate limiting, leading to accumulation of VFAs. Based on this result it was decided to reduce the OLR to 1.15 g VA/$L_{reactor}$.day for the second residence time.

The concentration of acids recorded (4000 - 7000 mg/L) was higher than those reported by Samson and LeDuy (1986). They reported a total VFA concentration of 2600 mg/L when digesting *Spirulina maxima* at an initial substrate loading of 20 g VS/L with an OLR of 2 g VS/$L_{reactor}$.day and a retention period of 20 days. Only acetic and propionic acid concentrations were significant, whilst butyric and valeric acids concentrations were less than 10 mg/L. At higher initial substrate loadings (40 g VS/L) the concentrations of VFAs (7420 mg/L) became more comparable to the current study. Samson and LeDuy did not track the VFAs through each retention time so the dynamic concentration profile could not be determined. Many studies reporting on semi-continuous or continuous AD do not present full VFA profiles, but rather report

the average concentrations across a number of retention times. Table 5.3 presents a summary of VFA concentrations reported for a number of algal biomass digesters operated across a range of residence times and biomass loading rates.

Table 5.3: A review of VFA production during semi-continuous and batch AD of algal biomass

Species	S_0 (kg VS/m^3)	HRT (d)	OLR (g VS/$L_{reactor}$.day)	Total VFAs (mg/L)	Valeric Acid (mg HVa/L)	Added Comments	Ref
Spirulina maxima	5	33	0.97	3000	-	-	1
Spirulina maxima	40	20	2	3250	-	-	2
Spirulina maxima	40	20	2	8690	-	A	2
Spirulina maxima	40	20	batch	14 000	-	B	3
Spirulina maxima	20	10	2	3570	trace	-	4
Spirulina maxima	20	20	2	2590	0	-	4
Spirulina maxima	20	40	2	890	0	-	4
Spirulina maxima	40	10	2	7420	1940	-	4
Spirulina maxima	40	20	2	2240	0	-	4
Spirulina maxima	40	40	2	1110	0	-	4
Spirulina spp.	20	20	2	2000- 5000	-	-	5
Chlorella and Scenedesmus	20	10	2	1300	-	-	6
Chlorella and Scenedesmus	20	10	4	4980	-	-	6
Chlorella and Scenedesmus	20	10	6	5860	-	-	6

[1] Samson and LeDuy (1982); [2] Samson and LeDuy (1983b); [3] Samson and LeDuy (1983a); [4] Samson and LeDuy (1986); [5] Jimenez et al. (2003b); [6] Yen and Brune (2007), A: mechanical pre-treatment, B: co-digestion

From this analysis of VFA formation in semi-continuous systems the following relationships can be identified:

1. Increased OLR's lead to increased VFA concentrations.
2. A short retention period can result in accumulation of VFAs
3. A high initial substrate loading can result in very high VFA concentrations, and depending on the OLR, accumulation could occur.

The decision to decrease the OLR after the first retention time prevented further accumulation of the acids within the digester. During the second retention period (OLR of 1.15 g VS/$L_{reactor}$.day), the total VFA concentration averaged 5450 mg/L. OLR's of 2 g VS/$L_{reactor}$.day have been reported to be satisfactory in several studies conducted on AD of *Spirulina spp.*, (Samson and LeDuy, 1982, 1983b,a, 1986). However the digesters were typically operated at temperatures greater than 35℃, which improved methanogenic activity (Angelidaki and Ahring, 1993). The ambient conditions at which the AD unit operated reduced the methanogenic activity and contributed towards the accumulation of VFAs. During the second retention period, the acetic acid concentration averaged 2750 mg HAc/L whilst methanogenic activity remained low. Therefore, after the second retention period (day 28), the AD unit was moved into a temperature

controlled environment at 37±2℃ to favour increased methanogenic activity.

The VFA concentration profile across the digestion time is presented in Figure 5.3. Similar to the batch studies, the key indicator acids iso-butyric, iso-valeric and valeric acids were tracked across digestion. At no stage, during batch digestion, did these acids accumulate to significant concentrations. However, in the semi-continuous AD unit iso-valeric acid did accumulate. The concentration increased as follows: from 680-1230 mg/L in the first retention period, from 1230-1510 mg/L in the second retention period, from 1510-2350 mg/L in the third retention period and decreased from 2350-1400 mg/L in the final retention period. The accumulation of this acid served as a possible indicator of ammonia toxicity (Ahring et al., 1995; Nakakubo, 2008). Samson and LeDuy (1986) showed that by increasing the initial substrate loading (S_0) and OLR as well as having shorter retention periods i.e. increasing loading rate, higher concentrations of total VFAs occurred. At no stage in their study was mention made of accumulating iso-valeric or valeric acids. The results (Table 5.3) indicated that only one set of operating conditions (S_0 40 kg VS/m^3 with an OLR of 2 g VS/$L_{reactor}.day$ and retention time of 10 day) resulted in a high valeric acid concentration (1940 mg/L). The methane yield obtained from this set of conditions (0.15 L CH_4/ g VS) was comparable to those achieved across all other conditions tested. This indicated that the higher concentration of valeric acid did not inhibit the methanogenic, acido- or aceto-genic microorganisms.

In the batch studies of whole cell *Spirulina spp.* the concentration of iso-valeric acid increased to 1650 mg/L during the initial stages of digestion. As the digestion progressed the acid was consumed to trace concentrations. Therefore, the high concentration of iso-valerate in the semi-continuous digester was an expected result. During the final retention time, substantial consumption of iso-valeric acid was observed. With the lower OLR a net consumption of VFAs occurred and the imbalance caused by the initial high OLR decreased, increasing methanogenic activity. The VFA profile for the final retention time was similar to the profile obtained by Boltes et al. (2008) (Figure 5.4 (a)). The lower feeding rate of organics was adopted which resulted in an initial VFA accumulation followed by a slow linear consumption.

Ammonia release through digestion

The monitoring of free ammonia levels (Figure 5.5) suggested that ammonia inhibition did not occur. The concentrations of dissolved free ammonia were below previously stated inhibitory levels (1.7 g/L - 14 g/L (Chen et al., 2008)) and did not increase. The high concentration of VFAs in the digester resulted in an average pH of pH 7.17, which was low relative to the pKa of ammonia (9.23). This minimised the non-ionised ammonia concentration in the aqueous phase of the digester and maximised the ionised ammonia (NH_4^+) concentration (Vavilin et al., 1995a).

With the decreasing OLR in the later retention times, the amount of nitrogenous matter degraded decreased. This was confirmed by the steady decrease observed for both ionised and non-ionised ammonia concentrations.

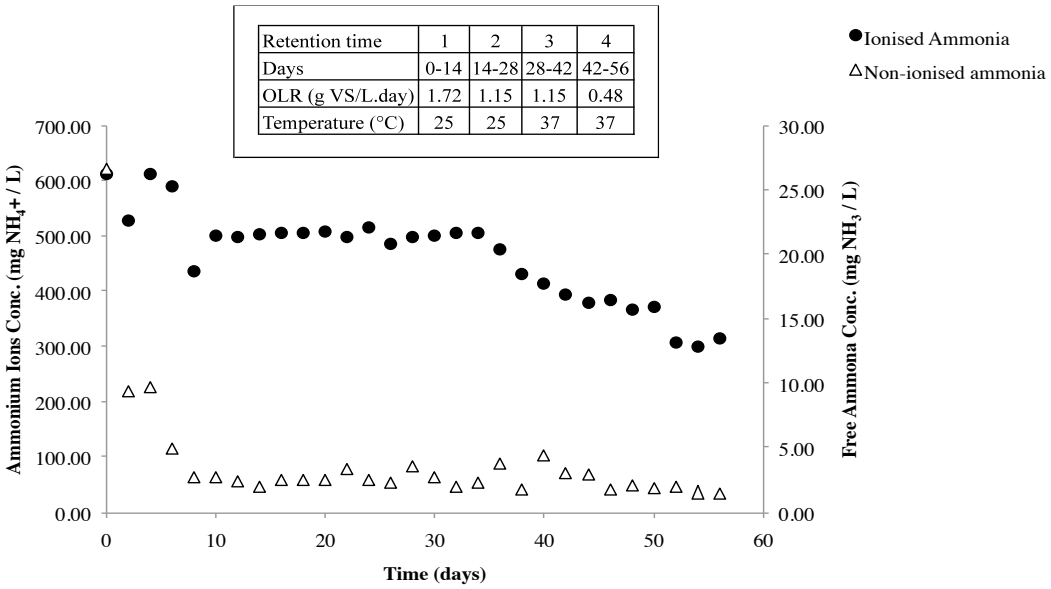

Figure 5.5: Ionised and non-ionised ammonia concentration as a function of time , expressed in mg NH_4^+ and $NH_3 - N$ per L reactor liquid volume. Note feeding of biomass stopped between days 34 and 42.

The dissolved NH_3 concentrations were calculated using the Equation 5.1:

$$NH_{3\ dissolved} = \frac{(NH_3 + NH_4^+)K}{(H^+)} \tag{5.1}$$

where (H^+) is the hydrogen concentration; (NH_3 + NH_4^+) is the dissolved ionised ammonia concentration; and K is the ionisation constant of NH_4^+ at 35 ℃ = 5.12 x 10^{-10}.

Sulphide release through digestion

After ammonia, sulphide is the most likely inhibitory product, particularly where the substrate has a high protein content (Vavilin et al., 1995b). Methanogens are particularly sensitive to sulphide inhibition. If the partial pressure of CO_2 in the gaseous phase is high, dissolved CO_2 reduces the pH and the non-ionised sulphide concentrations in the aqueous phase increase (Vavilin et al., 1995a). The non-ionised H_2S concentration was determined thermodynamically using the experimentally measured value and the solution pH and is presented in Figure 5.6.

During the first retention period, the non-ionised sulphide concentration in the digester effluent increased from an initial value below 18 mg H_2S/L to a maximum of 99 mg H_2S/L with an average of 60 mg H_2S/L (Figure 5.6). The increase in non-ionised sulphide concentration was expected, as the pH of the system dropped from 7.9 to 6.9 during this period. The pKa of hydrogen sulphide is 7.04 so at a pH of 6.9 approximately 47% of the total dissolved sulphide is present in the non-ionised form.

With the aim of the second retention period to mitigate the impact that the high OLR rate had on

the VFA accumulation, it was expected that the non-ionised sulphide concentration would decrease. After 24 days (towards the end of retention time 2) seven grams of sodium molybdate was added to the digester to inhibit the sulphate reducing bacteria (SRB). This proved to be effective as after the addition of molybdate, the concentration of dissolved sulphide decreased significantly.

Published values for sulphide inhibition vary somewhat, but concentrations in a range of 50 - 250 mg H_2S/L have been reported as inhibitory (Chen et al., 2008; Burton et al., 2008). This suggested that sulphide inhibition may have occurred during the first two retention periods where the concentration exceeded 75 mg/L. The high sulphide concentration in the digester originated from the degradation of proteins. This was supported by high concentrations of iso-valeric acid in the digester.

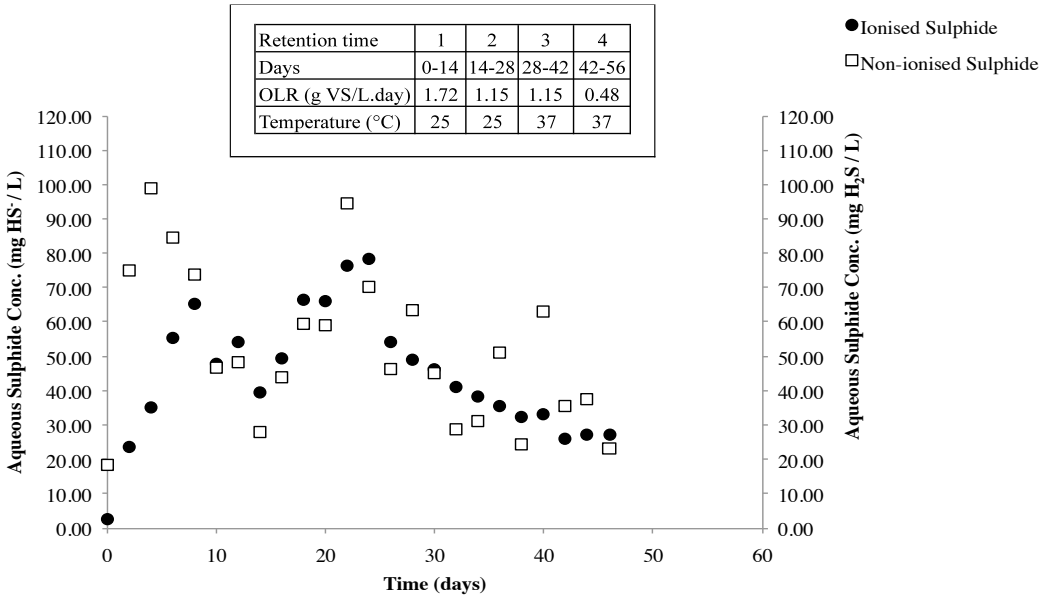

Figure 5.6: Ionised and non-ionised sulphide concentration as a function of time, expressed in mg HS^- and H_2S per L reactor liquid volume. Note feeding of biomass stopped between days 34 and 42.

Soluble COD Dynamics

The VFA concentration in the digester effluent can be monitored by determining the soluble COD concentration. Figure 5.7 indicates the close relationship which was obtained between soluble COD concentration and the total contribution of VFAs to this COD. The contribution to soluble COD by the VFAs became more significant after day 34. At this time feeding of the digester was stopped to decrease the total VFA concentration and increase methanogenic activity. Once feeding stopped, the complex organics (glucose equivalent) were degraded to VFAs so the difference between soluble COD and VFA COD decreased. When feeding recommenced (day 42) the OLR rate was decreased to 0.5 g VS/$L_{reactor}$.day. At the lower loading rate the complex organics could be metabolised within the given retention period. This was supported by the difference in soluble COD and VFA COD remaining small throughout the final 14 day retention period.

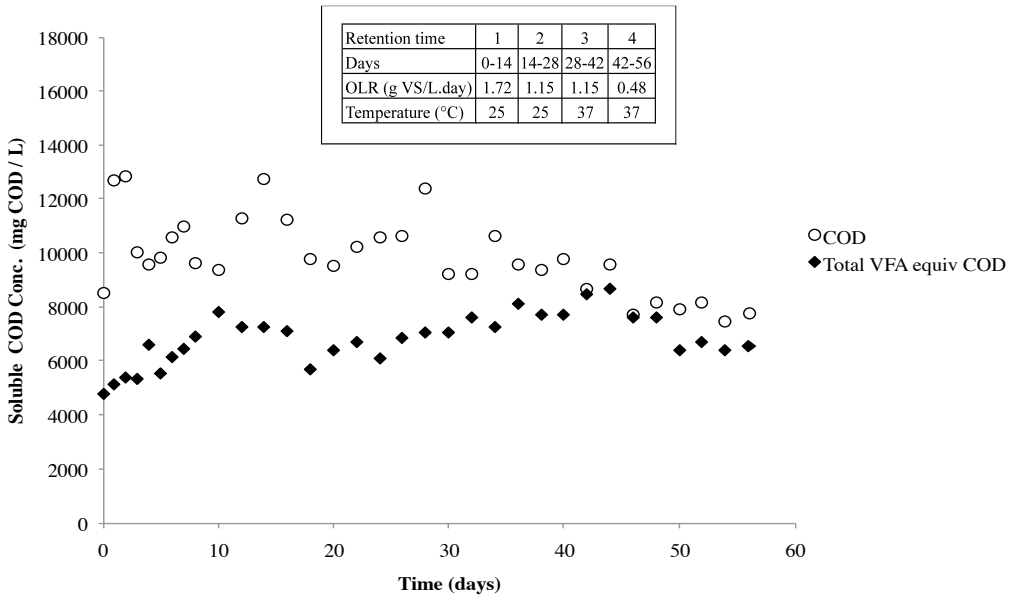

Figure 5.7: Soluble COD and total VFA COD concentration profiles during digestion, expressed in mg soluble COD/L. Note feeding of biomass stopped between days 34 and 42.

5.3.4 Biogas and methane production from anaerobic digestion

In parallel to the analysis of the liquid AD effluent, a robust analysis of the evolved gas phase was conducted. The evolved gas was collected on a daily basis. The OLR had a significant impact on the biogas productivity. The OLR was varied across the four retention periods to address inhibitory indicators in the aqueous phase of the digester effluent. The gaseous product was also used as an indication of performance by tracking the biogas productivity, methane content, methane productivity and methane yields.

Biogas Productivity

As soon as feeding commenced (day 0), the biogas productivity started to rise in accordance with the increase in VFAs. As discussed in the batch phase analysis, the break down of soluble organics to intermediates (LCFAs, amino acids, glucose etc.) and then to VFAs results in the release of various gases (Section 4.3.3). The productivity increased to a maximum of 0.166 L Biogas/$L_{reactor}$.day after day 11 but decreased sharply to 0.11 L Biogas/$L_{reactor}$.day towards the end of the retention period. This was in accordance with an accumulation of VFAs affecting the microbial activity. During the first retention period the OLR averaged 1.72 g VS/$L_{reactor}$.day, which was then decreased to 1.15 g VS/$L_{reactor}$.day once accumulation of VFAs occurred. The lower feed rate caused a decrease in biogas productivity since less easily fermentable organics were freely available for VFA production and so gas release.

However, after the end of the second retention period there was still limited methanogenic activity, as discussed in Section 4.2.3. This was further addressed by moving the unit into a controlled temperature (37 $\pm$ 2°C) environment (day 29) with a continued feed of 1.1 g VS/$L_{reactor}$. This resulted in an increased biogas productivity to 0.16 L Biogas/$L_{reactor}$.day compared to an average of 0.06 L Biogas/$L_{reactor}$.day

experienced at ambient conditions (Figure 5.8). However, the activity of the methanogenic culture did not increase.

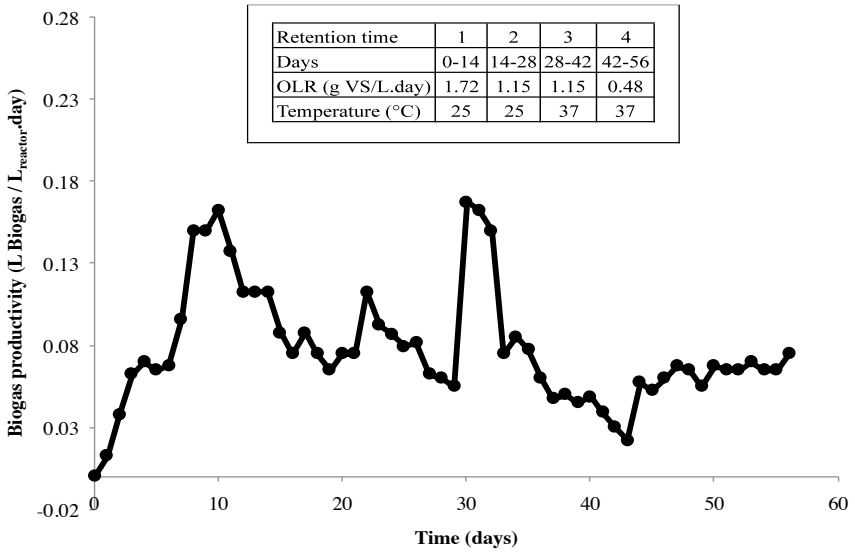

Figure 5.8: Biogas productivity for the semi-continous anaerobic digestion unit, expressed in L biogas produced per L of reactor liquid volume per day

The OLR was only maintained until four days into the third retention period, at which point decreasing methanogen activity became a concern. As the aqueous sulphide concentration was under control, it was decided that the high VFA concentration was once again the primary cause of the low activity.

In a further attempt to improve the methangencic activity, 286 ml of SAB inoculum (high methanogen content) was fed into the reactor whilst the feeding of biomass stopped. The aim was to allow for maximum consumption of acetic acid, stimulating the metabolism of the other key VFAs (propionic, butyric and iso-valeric). With a low concentration of easily fermentable organics in the system the acidogenic bacteria activity was expected to become lower than the methanogens. Once the feeding of harvested biomass was stopped the biogas productivity decreased.

During the final retention period (OLR of 0.5 g VS/$L_{reactor}$) the biogas productivity was lower than previously seen. The lower organic loading resulted in lower gas yields (on a reactor volume basis). However, if the methane productivity was comparable or higher than during previous retention periods it could be concluded that methanogenic activity had increased.

Methane Productivity

During the first two retention periods the methane content (Figure 5.9) of the gaseous product averaged 40% CH_4 vol/vol, which was well below the expected and previously seen averages of 70% (Samson and LeDuy, 1982, 1983b,a, 1986). This emphasised the low methanogenic activity within the system.

The decreased OLR of 1.1 g VS/$L_{reactor}$.day in retention period 2 and 3 resulted in the methane content increasing from 43% to 48%. This positive result justified the decrease in organic loading , even though the overall productivity of methane decreased. With a lower OLR the VFA concentrations decrease and so to the amount of acetic acid produced. A much higher increase in methane content was expected to confirm that the imbalance in the system was reduced.

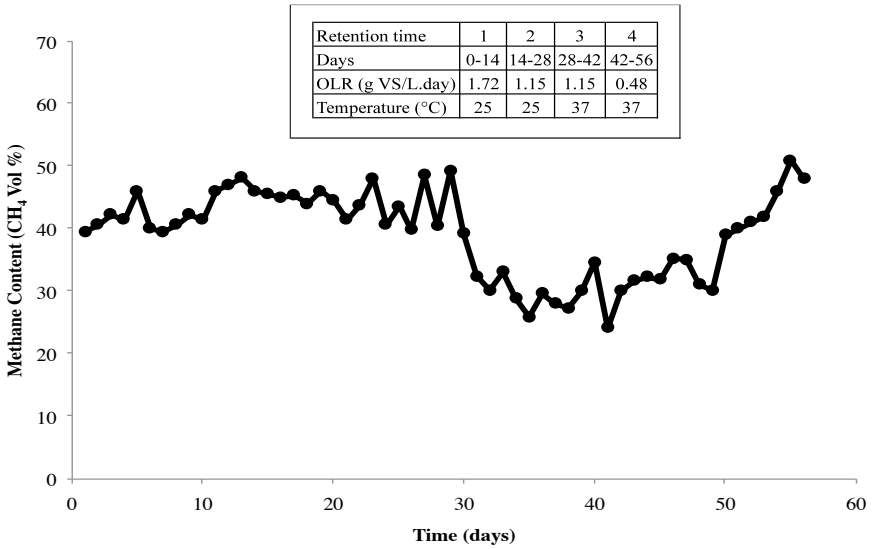

(a) Methane content of biogas produced by AD unit, expressed in CH_4 vol/vol%

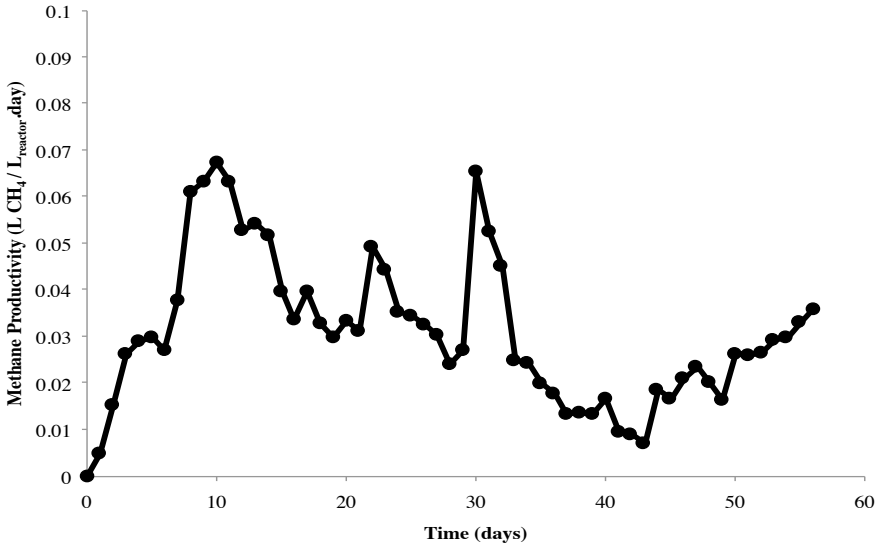

(b) Methane productivity of AD unit, expressed in litres CH_4 produced per L of reactor reactor liquid volume per day

Figure 5.9: Methane content and productivity of semi-continuous anaerobic digestion unit

Biogas production increased significantly when the AD unit was moved into the temperature controlled environment. However, after the initial increase both biogas production and methane content decreased lowering methane productivity. The biogas production was a direct reult of easily fermentable orgaincs breaking down into VFAs. The increased concentrations of VFAs produced reintroduced an imbalance within the digester. Increased temperature has shown to favour methanogens in many previous studies

(Chen, 1987), however these studies had a methanogenic culture that was well adapted to the specific operating conditions. Therefore stopping the addition of harvested biomass to the digester and allowing the methanogenic culture to become acclimatised to the new environment was a justified decision. Upon reintroduction of harvested biomass at the reduced OLR of 0.5 g VS/$L_{reactor}$.day methane content began to increase steadily. At the end of the this period the content had risen to ca. 52% CH_4 vol/vol.

Methane Yields

The methane yields (Figure 5.10) experienced in this study were much lower than seen in previous investigations on semi-continuous AD of *Spirulina spp.* biomass.

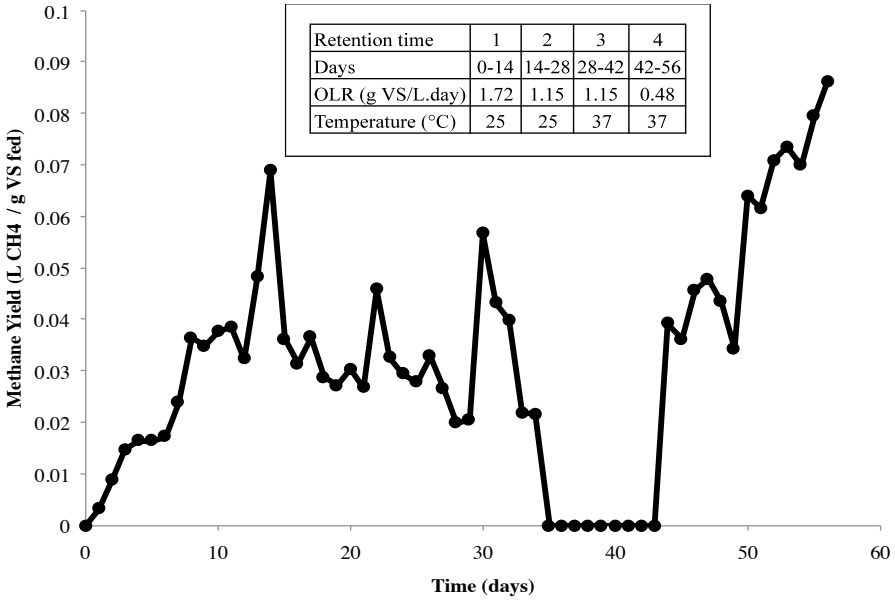

Figure 5.10: Methane yield profiles of the semi-continuous anaerobic digestion unit, expressed in L CH_4 per g VS fed per L reactor per day. * Note zero yield represents period where no biomass was fed to the digester and does not represent zero gas evolution.

During the first retention period the methane yield increased steadily but at very slow rates and so remained in an undesirable range ($<$ 0.2 L CH_4/ g VS). Towards the end of the retention period it had decreased to 0.032 L CH_4/ g VS. Across the second and most of the third retention period the yield steadily decreased to levels less than 0.03 L CH_4/ g VS indicating low relative methanogenic activity. As mentioned reactor feeding was stopped (period where methane yield is zero) during the third retention period to try and limit the accumulation of VFAs within the system. The methane yield increased steadily during the final retention period. The final value of just under 0.09 L CH_4/ g VS was similar to that of the *Spirulina spp.* whole cell batch digestion. The positive results obtained indicate how real time monitoring of the AD unit was essential for the evolution of operating conditions that promoted efficient digestion.

Table 5.4 presents the key previous investigations in digestion of whole cell *Spirulina*. Since the obtainable yields are very dependent on key operating conditions they have been highlighted for each study.

Table 5.4: A review of methane yields obtained during semi-continuous and batch AD of algal biomass

Species	S_0 (kg VS/m^3)	Retention time (days)	OLR (g VS/$L_{reactor}$.day)	CH_4 (%)	Methane Yield (L CH_4/g VS)	Reference
Spirulina maxima	5	33	0.97	70	0.26	1
Spirulina maxima	40	20	2	70	0.2	2
Spirulina maxima	40	20	2	75	0.17	2
Spirulina maxima	40	20	batch	70	0.35	3
Spirulina maxima	20	10	2	76	0.2	4
Spirulina maxima	20	20	2	74	0.3	4
Spirulina maxima	20	40	2	76	0.35	4
Spirulina maxima	40	10	2	64	0.15	4
Spirulina maxima	40	20	2	72	0.18	4
Spirulina maxima	40	40	2	74	0.24	4
Chlorella spp. and Scenedesmus spp.	20	10	2	69	0.09	5
Chlorella spp. and Scenedesmus spp.	20	10	4	69	0.11	5
Chlorella spp. and Scenedesmus spp.	20	10	6	69	0.136	5

[1] Samson and LeDuy (1982); [2] Samson and LeDuy (1983b); [3] Samson and LeDuy (1983a); [4] Samson and LeDuy (1986); [5] Yen and Brune (2007)

An increase retention time resulted in a greater yield of methane per gram of VS fed. This related directly to the amount of time allowed for degradation of the algal biomass. In the batch studies conducted on whole cell digesters there was a decrease in solid COD as the experiment progressed, in particular during the linear phase of gas production and VFA consumption. A long retention time in a semi-continuous digester will allow for maximum biomass degradation and so VFA production. The result is dependent on the initial substrate loading and OLR. If the initial loading of substrate was high and the retention period long, there was a large degradation of solid biomass and so production of VFAs. The increased VFA concentration begins to negatively impact the methanogenic culture (Chen et al., 2008). As seen in the batch studies after a certain period of time the rate of consumption of VFAs starts to become greater than production and a net decrease in VFA concentration is observed. Thus the retention time of a semi-continuous system can be such that the rate of VFA consumption is greater than production. Then, even with high OLR and initial loading, the VFA concentration will not impact the system.

The more efficient degradation of *Spirulina spp.* biomass results in substantial protein metabolism, which increases the release of ammonia in the system. When levels of ammonia release from this degradation become high the methanogens will become inhibited from ammonia toxicity (Nielsen and Angelidaki, 2008). The ideal operating conditions for a *Spirulina spp.* whole cell algal digester would be a low initial substrate loading, with a moderate OLR and retention period.

5.3.5 Efficiency of semi-continuous digestion

The total solids (TS), VS, solid COD and total COD of the digester effluent were monitored across the digestion period. This allowed for the analysis of the efficiency the digester had in breaking down solids in the given retention periods.

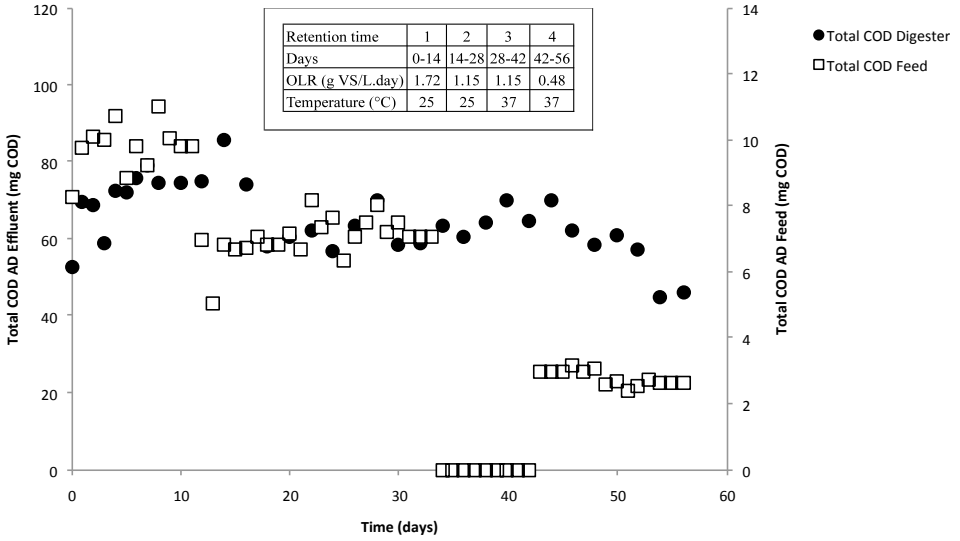

(a) Total COD, expressed in mg COD

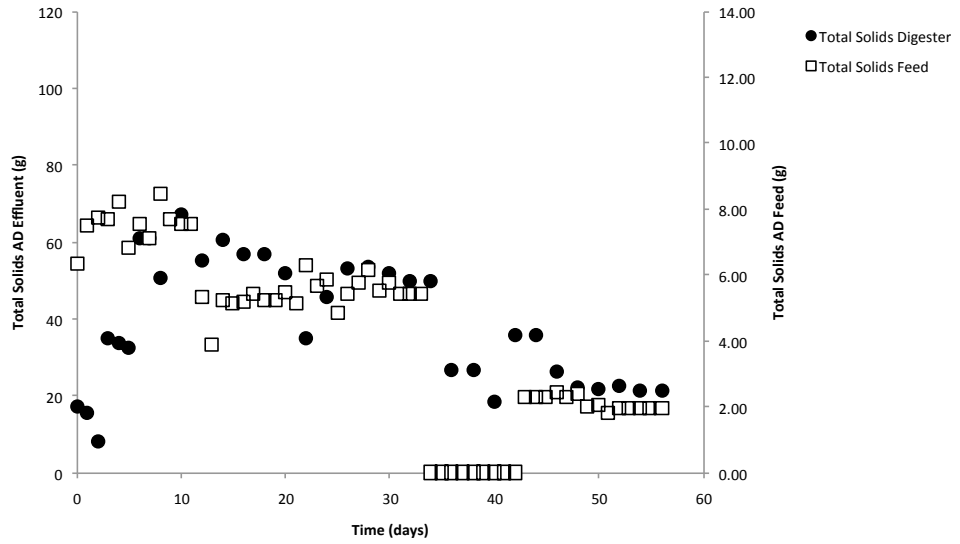

(b) Total solids, expressed in g TS

Figure 5.11: Total COD and TS profiles for semi-continuous digestion, expressed mg COD and g TS

A continual increase in any of these variables indicated that the OLR and retention time were such that the biomass was not degrading fast enough. Using the total COD fed to the digester in terms of mg COD and total COD of the digester contents (obtained from effluent concentration and shown in Figure 5.11) the difference was used to determine the total destruction observed. Similarly this was done for the other three variables (TS, VS and solid COD) (Table 5.5).

Table 5.5: Efficiency of AD in the destruction of COD, TS and VS 's for *Spirulina spp.* during semi-continuous operation

Substrate	Solid COD Destruction[a] (%)	Total COD Destruction[b] (%)	TS Destruction[c] (%)	VS Destruction[d] (%)
Retention period 1	83	68	78	7.9
Retention period 2	97	75	111	8.1
Retention period 3	81	43	73	12.3
Retention period 4	155	136	145	13.2

[a,b,c] :$\Rightarrow \%\, Destruction_i = \frac{M_{i,fed}-(M_{i,effluent}-M_{i-1,effluent})}{M_{i,fed}} * 100$, where M= Solid COD, Total COD or TS

[d] :$\Rightarrow$ Calculated using Varel's eq: VS destroyed(g) = (mol CO_2 +mol CH_4)X(12/(carbon content of biomass fed))

*Note: Destruction % greater than 100% indicates that all COD fed was destroyed as well as some of the initial loaded COD

The percentage destruction was directly controlled by the OLR and retention time allowed for degradation of the biomass. A negative percentage destruction indicated an accumulation of biomass within the reactor. During the first three days of the first retention period, the concentration of solid and total COD as well as TS of the digester increased (Figure 5.11), which suggested that more solids were loaded into the digester than were degraded. However after this initial rise, a steady COD and TS concentration was obtained. This indicated that no further accumulation was occurring and that the biomass was degrading with the high OLR and short retention period.

When the OLR decreased the concentration of total COD and TS adjusted to reach a lower steady state of degradation. Decreasing OLR (retention times 2, 3, and 4) resulted in the percentage destruction of all variables to increase. With a greater percentage destruction the overall efficiency of digestion increased. The destruction efficiencies during retention time 3 dropped significantly when the feeding stopped after 3 days. This meant that the destruction values were calculated using the final concentration before feeding stopped and so destruction of only digester contents occurred, not of feed stock. A percentage destruction of greater than 100%, retention time 4, indicated that degradation of all the solids fed as well as a portion of residual solids not degraded occurred. The increased VS destruction across the four retention times emphasised the increasingly efficient biogas production system.

5.3.6 Possible uses of the anaerobic digestion effluent

Nutrient supply or fertiliser manufacturing

Table 5.6 shows that there were a high concentrations of nitrogen and phosphorous containing compounds in the effluent. Nitrogen, phosphorous and sulphur are key nutrients required for algal growth (Benemann and Oswald, 1994; Chaumont, 1993). Therefore, this stream could be recycled directly into the growth unit to supply the necessary make-up of nutrients consumed during cell growth. Recycling of the digester effluent has been conducted successfully in two previous studies that investigated closed-loop algal growth and digestion systems (Golueke and Oswald, 1959; De Schamphelaire and Verstraete, 2009). The compounds in the effluent are also integral in the production of industrial fertilisers. It has been widely

reported that the effluent of anaerobic digestion can be used directly as a soil fertiliser or an additive compound in fertiliser production (Beurskens et al., 2010).

Microbial Fuel Cell (MFC)

In a MFC a reduced compound is oxidised by electrogenic bacteria in an anode chamber. This process delivers the electrons to the anodic electrode. The electrons pass through an external circuit, generating electrical current, and are released at the cathode to reduce an oxidant such as oxygen (De Schamphelaire and Verstraete, 2009). The residual compounds from the degradation of *Spirulina spp.* can be further oxidised at the anode of a MFC, while living algae from the growth unit can pass over the cathode to supply oxygen as the electron acceptor. Residual compounds such as VFAs, nitrate ions and phosphate ions can all be oxidised by bacteria so releasing electrons. Table 5.6 summarises the average concentration of each of these compounds in the effluent of the digester across the four retention periods.

Table 5.6: Average nitrate, phosphate and VFA concentrations of AD unit effluent for each retention time, expressed in mg per L reactor liquid volume

Time Period	Average [VFA] (mg/L)	Average $[NO_3^-]$ (mg/L)	Average $[PO_4^{3-}]$ (mg/L)
retention time 1	5360	32	553
retention time 2	5450	21	550
retention time 3	6050	17	476
retention time 4	5500	12	356

The high residual concentrations of each compound can result in a large cell potential when used in a MFC. An added benefit of the MFC is that it degrades these compounds further polishing the stream and making its return into the algal growth less toxic. In the study conducted by De Schamphelaire and Verstraete (2009) total COD destruction across the anode was 37%.

5.4 Conclusions

The concept of anaerobically digesting *Spirulina spp.* as part of an integrated system in the production of bioenergy was proven. The close monitoring of liquid phase compounds (VFAs, free ammonia and aqueous sulphide) allowed for actions to be taken to address imbalances in the degradation reactions or inhibition from accumulation of toxic compounds before complete reactor failure occurred. Key parameters that impacted the efficiency of the semi-continuous digester were also highlighted. The OLR, retention time and initial substrate concentration influenced the total amount of solid biomass degradation, which in turn controlled the amount of methane produced. Through optimisation of these operating conditions a stable digestion unit was obtained. These parameters also controlled the characteristics of the AD effluent and could be manipulated to obtain an effluent with certain desired compounds in high or low concentrations.

Chapter 6

Perspectives and opportunities for bioenergy production by anaerobic digestion of algal biomass

6.1 Introduction

Chapters 4 and 5 focussed on the fundamental data obtained through batch and semi-continuous digestion of *Spirulina spp.* and *Scenedesmus spp.* biomass. In this chapter the final methane yields obtained from these studies are used together with potential and reported algal productivities to calculate the theoretical energy production. Comparisons with traditional agricultural and second generation energy crops are made to evaluate the feasibility of using algae as a feed stock for bioenergy production by anaerobic digestion. Using the methane yields obtained from the batch digestion of residual *Scenedesmus spp.* following biodiesel extraction, the efficiency of AD as a stand-alone technology, compared with as part of an integrated biodiesel-biogas production system, was investigated.

6.2 Algal productivity compared to traditional energy crops

It has been widely reported (Gunaseelan, 1997; Samson and LeDuy, 1986; De Schamphelaire and Verstraete, 2009; Sialve et al., 2009) that one of the major benefits of using algae as a substrate for biofuel production is that it can be cultivated using non-arable land and non-potable water. In addition, productivity and annual biomass yield are suggested to far exceed those obtained for traditional energy crops. A comprehensive review of a wide range of energy crop productivities (ton DW/ha.year) was conducted (Table 6.1) and compared to the algal biomass investigated in this study. Fuels derived from biomass are classified according to the nature of the organic substrate. First-generation biofuels are derived from sugar, starch, vegetable oil, or animal fats using conventional conversion technology. The feed stocks are often plant seeds, grains or rapeseeds. Second generation biofuels use feed stocks from non-food crops or waste biomass, such as corn stalks, wood and special energy crops (*e.g. Jatropha curcus*, *Miscanthus*,

reed). Third generation biofuels are from low-input, high yield feed stocks such as algae and genetically modified plants (Chang et al., 2010).

Table 6.1: A review of annual productivities obtained from various energy crops, expressed in ton DW per hectare of land every year

Crop	Biomass productivity (ton DW/ha.year)	Reference
Food Plant Crops (1^{st} generation)		
Maize (whole crop)	9-30	1
Wheat (grain)	3.6-11.75	1
Oats (grain)	4.1-12.4	1
Rye (grain)	2.1	1
Barley (grain)	3.6-4.1	1
Triticale (grain)	3.3-11.9	1
Sorghum	8-25	1
Red clover	5-19	1
Alfalfa	7.5-16.5	1
Sudan grass	10-20	1
Hemp	8-16	1
Nettle	5.6-10	1
Ryegrass	7.4-15	1
Sunflower	6-8	1
Oilseed rape	2.5-7.8	1
Jerusalem artichoke	9-16	1
Peas	3.7-4.7	1
Rhubarb	2-4	1
Turnip	5-7.5	1
Kale	6-45	1
Potatoes	10.7-50	1
Sugar beet	3-16	1
Fodder beet	8-34	1
Non-Food Plant Crops (2^{nd} generation)		
Jatropha curcus (seeds)	3.75 - 4.05	2, 3
Grass	12-14	1
Miscanthus	8-25	1
Flax	5.5-12.5	1
Reed canary grass	5-11	1
Algal Biomass (3^{rd} generation)		
Kelp	7-16	4
Spirulina spp.[a]	75	-
Spirulina platentis	30-70	5,6
Scenedesmus spp.[a]	30	-
Scenedesmus obliquus	70	7

[1]Braun et al. (2010), [2]Gunaseelan (2009), [3]Chandra et al. (2006), [4]Chang et al. (2010), [5]Jimenez et al. (2003a), [6]Richmond et al. (1990), [7]Hartig et al. (1988),[a] Maximum achieved in current study

Annual biomass yield per hectare (also termed biomass productivity) is dependent on local climatic conditions, the availability of irrigation water and resistance to disease (Braun et al., 2010). This dependency is evident by the large variation in recorded productivities (Table 6.1). The results illustrated the potential superiority, in terms of productivity of algae relative to other agricultural and non-food energy crops. Only maize, potatoes and fodder beet had annual growth yields comparable to the lower range of algal productivities. Maize, beet and potatoes are staple food crops and their utilisation on a large-scale for biofuel generation fuels the food security debate, particularly in developing countries. Potatoes and beet, in particular, are difficult substrates for AD as carry over of soil can lead to sand accumulation in the digesters (Braun et al., 2010).

Second generation energy crops have medium to low productivities and in some cases *(Jatropha curcus)* are classified as undesirable alien plants. In many countries restrictions are imposed on the importation of these plants. Alien plants compete with the indigenous plants for available resources, making their introduction into indigenous environments undesirable with potential impact on biodiversity. Grasses also experienced medium to low biomass productivities, but are commonly used in digestion processes on account of their wide availability and their modest growth requirements (Braun et al., 2010).

6.3 Feasibility of AD of algae for bioenergy production

Specific methane yields of energy crops

The International Energy Agency (IEA) conducted methane production tests on numerous plants and plant materials. The tests were done as part of Task 37, which aims to harness energy from biogas and landfill gas. The study concluded that, in principle, many varieties of grass, clover, cereals and maize as well as rape and sunflower were feasible substrates for methane production. The most important results from this study are included in Table 6.2, which reports the methane yields achieved from various food, non-food and algal biomass resources.

The ultimate methane yields varied between 80 and 660 m^3 CH_4/ ton VS over the range of energy crops. Harvest time resulted in large variations in specific methane yields for several crop species. Late harvests are associated with higher cellulose contents in the biomass, leading to slower degradation and lower methane yields (Braun et al., 2010). Five different results were presented for algal biomass. Macroalgae (kelp) had a lower average methane yield relative to many of the plant crops, but higher than that of the microalgal species investigated. The methane yields for *Spirulina spp.* and *Scenedesmus spp.*, based on the data generated in this study, were at the lower end of the range. However, the current study did not focus on digestion optimisation and higher yields have been reported in literature for these species.

Table 6.2: A review of methane yields and productivities obtained from various energy crops, expressed in m^3 CH_4 per ton VS and per hectare

Crop	Biomass productivity (ton DW/ha.year)	Methane yield (m^3 CH_4/ ton VS)	Methane productivity (m^3 CH_4/ ha.year)	Reference
Food Plant Crops (1^{st} generation)				
Maize (whole crop)	9-30	397-618	3570-18540	1
Wheat (grain)	3.6-11.75	384-426	1380-5000	1
Oats (grain)	4.1-12.4	350-365	1030- 4530	1
Rye (grain)	2.1	283-492	590-1030	1
Barley (grain)	3.6-4.1	353-658	1270-2700	1
Triticale (grain)	3.3-11.9	337-555	1120-6600	1
Sorghum	8-25	295-372	2360-9300	1
Red clover	5-19	300-350	1500-6650	1
Alfalfa	7.5-16.5	340-500	2550-8250	1
Sudan grass	10-20	213-303	2130-6060	1
Hemp	8-16	355-409	2840-6540	1
Nettle	5.6-10	120-420	670-4200	1
Ryegrass	7.4-15	390-410	2890-6150	1
Sunflower	6-8	154-400	930-3200	1
Oilseed rape	2.5-7.8	240-340	600-2650	1
Jerusalem artichoke	9-16	300-370	2700-5920	1
Peas	3.7-4.7	390	1440-1830	1
Rhubarb	2-4	420-490	640-1960	1
Turnip	5-7.5	314	1570-2360	1
Kale	6-45	240-334	1440-15000	1
Potatoes	10.7-50	276-400	2950-20000	1
Sugar beet	3-16	236-381	710-6100	1
Fodder beet	8-34	401-500	3210-17000	1
Non-Food Plant Crops (2^{nd} generation)				
Jatropha curcus (seeds)	3.75 - 4.05	400-610	1500-2470	2, 3
Grass	12-14	298-467	3580-6540	1
Miscanthus	8-25	179-218	1430-5450	1
Flax	5.5-12.5	212	1170-2650	1
Reed canary grass	5-11	340-430	1700-4730	1
Algal Biomass (3^{rd} generation)				
Kelp	7-16	200	1400-3200	4
Spirulina spp.[a]	75	113	11250	-
Spirulina platentis	30-90	350	10500-31500	5
Scenedesmus spp.[a]	15-45	55	1200-3600	-
Scenedesmus spp.	75	136	10200	6,7
Microalgae[b]	150-350	500	75000-175000	8

[1]Braun et al. (2010), [2]Gunaseelan (2009), [3]Chandra et al. (2006), [4]Chang et al. (2010), [5]Jimenez et al. (2003a), [6]Yen and Brune (2007), [7]Yen and Brune (2007), [8]Chisti (2008),[a] Maximum achieved in current study, [b] Highest reported theoretical yields

The lower methane yields for algal biomass achieved in this study are not a major concern as the focus was on feasibility of digestion rather than optimisation. Higher yields could be obtained through manipulation of the process operating conditions. A model of potential methane productivity, as a function of biomass productivity and specific methane yield is presented in Figure 6.1.

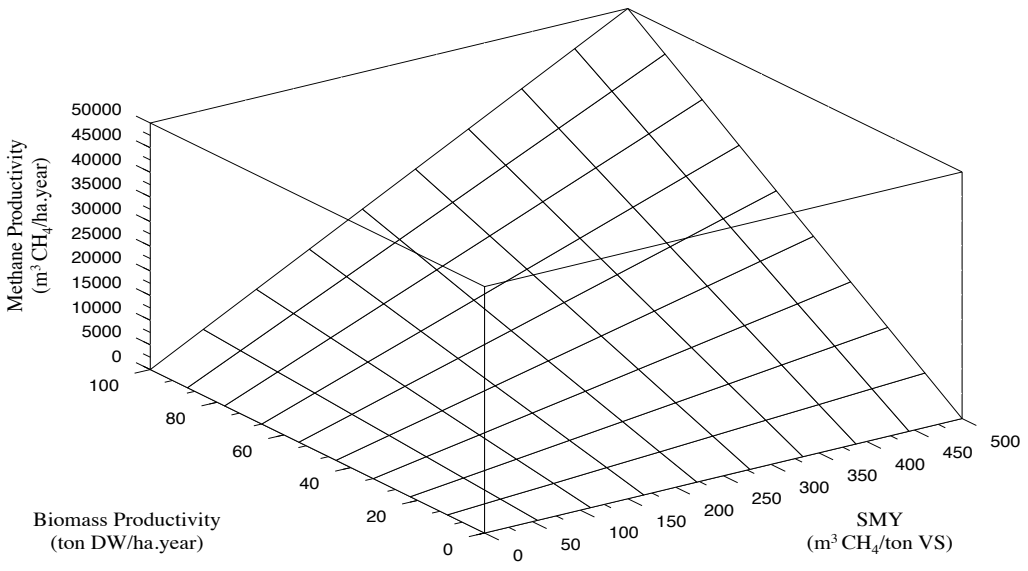

Figure 6.1: Methane productivities of algal biomass as a function of biomass productivity and specific methane yields, expressed in m^3 CH_4 per hectare per year

Methane yields as high as 400 m^3 CH_4/ton VS have been reported for algae (Sialve et al., 2009; Yen and Brune, 2007). Methane production of up to 50000 m^3 CH_4/ ha.year is not an unrealistic prediction if biomass productivity in excess of 90 ton DW/ha.year is achieved. A benchmark value for methane productivity of 20 000 m^3 CH_4/ ha.year would allow for competitiveness with the best of the traditional energy crops. This benchmark can be achieved by increasing the SMY or biomass productivity.

Net energy production from energy crops

As reported by Braun et al. (2010), the annual energy production per hectare of land presented in Table 6.2 was determined based on the annual biomass productivity and specific methane yields. This energy productivity was based entirely on the product and did not account for the energy required for the process. Plant crops require energy for ploughing, seedbed cultivation, fertilising, pesticide and herbicide application, harvesting and transport. Furthermore, large amounts of energy are required for the production of fertilisers, pesticides and herbicides (Braun et al., 2010). These energy requirements are grouped into direct energy consumed in the crop production process (e.g. labour, fossil fuels), and indirect energy required for products and machinery integral to the crop production process (e.g. fertiliser, pesticides/herbicides and machinery). A full sample calculation, using maize as the standard crop, of the energy input required per hectare can be found in Appendix E, Table 8.40. The majority of energy required for algal production has traditionally been assigned to the harvesting of biomass (Chisti, 2007; Mandal and Mallick, 2009; Sialve et al., 2009), and more recently, to the supply of aeration (compressed gases) to closed growth units (Richardson, 2011). In literature, the energies associated with mass production of algal biomass are usually exemplary estimates, such as those presented by Chisti (2008). This is due to the fact that algal production on an industrial scale is uncommon. This is particularly true for a commodity product, such as energy, where the return is significantly lower than that for current products derived from microalgae (pigments, food supplements etc.) The estimations result in a large range of potential energy requirements.

Therefore, rather than of making an inaccurate assumption or using unrealistically attractive estimations the energy requirements were treated as an unknown and the net energy was determined across a range of energy inputs. This allowed the estimation of the maximum energy requirements of the algal process yielding positive results, and their comparison to those obtained for agricultural energy crops.

Table 6.3: Energy requirements for production of energy crops

Crop	Energy Input (GJ/ha.year)	Reference
Food Plant Crops (1^{st} generation)		
Potatoes	24.2	1
Beets	16.8-23.9	1
Wheat, barely, maize	14.5-19.1	1
Non-Food Plant Crops (2^{nd} generation)		
Jatropha curcus	14.5-19.1	2
Algal Biomass (3^{rd} generation)		
Kelp	0-100	3
Spirulina spp.	0-100	3
Scenedesmus spp.	0-100	3

[1]Braun et al. (2010), [2]Chang et al. (2010), [3] The tested range incorporates lower and higher energies than food and non-food plant crops

In addition to the energy associated with biomass production, further energy is required for the digestion step. This depends on the operating conditions of the anaerobic digester. Braun et al. (2010) define typical process energy requirements as:

1. Transport or upgrading of digestate and biogas.
2. Electrical energy demand.
3. Energy transfer losses during utilisation of biogas.
4. Process heat demand depending on the design of the digester.

As an exemplary assumption a relatively lower overall process demand of 15% of the energy generated from methane production for the digestion process was calculated. The IEA study made the same assumption, allowing for a comparison to be made between the various energy crops. To obtain the final annual net energy production in GJ per hectare per year for a specific energy crop, the specific methane yield (m^3 CH_4/ton VS) is multiplied by the calorific value of methane (0.0358 GJ/m^3 CH_4) and the crop productivity (ton DW/ha.year) to get the annual energy production. Process energy (15 % of the energy produced) and energy input (based on literature values for specific crop) were subtracted from the energy produced to obtain the net energy.

Table 6.4: Net energy production for plant energy crops, expressed in GJ per hectare per year

Crop	Methane productivity (m^3 CH_4/ ha.year)	Methane energy production (GJ/ ha.year)	Energy Inputs (GJ/ha.year)	Process energy demand for digestion (GJ/ha)	Net energy production (GJ/ha.year)	Reference
Food Plant Crops (1^{st} generation)						
Potatoes	10250	367.3	24.2	55.1	287.9	1
Beets	9450	338.4	16.8	50.7	267.2	1
Wheat, barely, maize	9880	353.9	16.8	53.1	284.0	1
Non-Food Plant Crops (2^{nd} generation)						
Jatropha curcus	2500	89.5	10.0	13.4	66.1	2

[1]Braun et al. (2010), [2]Gunaseelan (2009)

The data presented in Table 6.4 indicate that net energy productivities in excess of 300 GJ/ha.year are required for algal biomass in order for it to be considered as a better feed stock option, on a purely energetic basis, than plant energy crops. The methane yields obtained in this study, 113 and 55 m^3 CH_4/ ton VS for *Spirulina spp.* and *Scenedesmus spp.* respectively, were used to determine the maximum energy input, below which the net energy produced exceeded 300 GJ/ha.year (Figures 6.2 and 6.3). The permissible energy input could be increased if biomass productivities are improved. The energy productivities are conservative as they do not represent an optimised system.

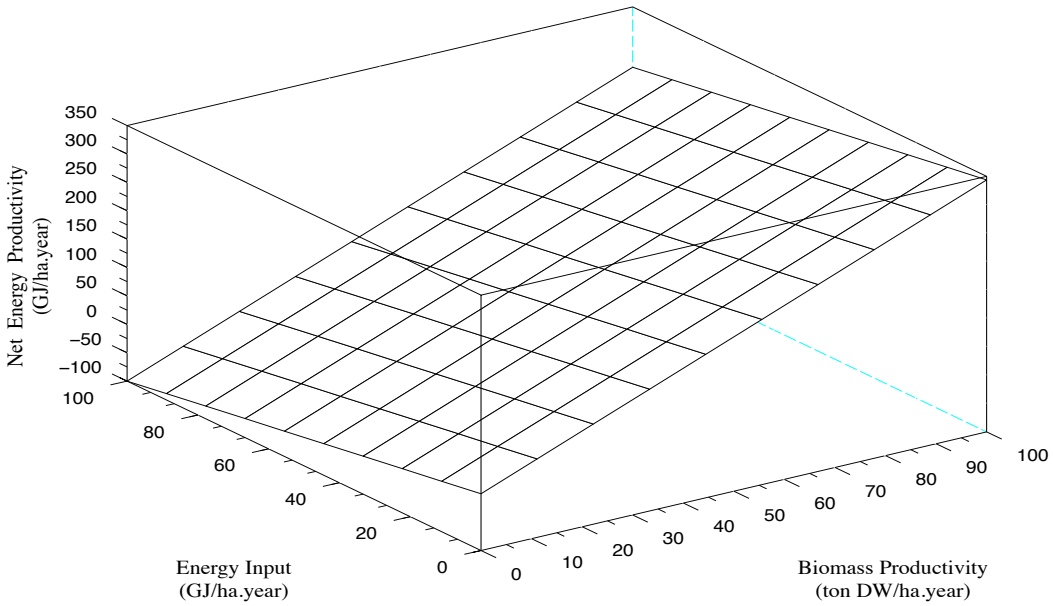

Figure 6.2: Net energy productivity from digestion of *Spirulina spp.* as a function of biomass productivity and energy input for biomass generation, expressed in GJ per hectare

To compete with first generation energy crops, *Spirulina spp.* productivity needed to exceed 75 ton DW/ha.year at an energy input less than 20 GJ/ha.year. These figures are not unrealistic as productivities in excess of 90 tons DW/ha.year have been reported. Energy inputs of less than 20 GJ/ha.year appear feasible by comparison with maize. Maize cultivation requires large amounts of fertiliser, pesticide, herbicide and mechanical input (tractors etc). Its energy inputs have been calculated at 16.8 GJ/ha.year.

Spirulina spp. cultivation in open raceway ponds requires less energy than closed photobioreactors. In addition, the filamentous nature of *Spirulina spp.* allows for simple and energetically efficient harvesting methods such as nylon cloth filtration (Jimenez et al., 2003a).

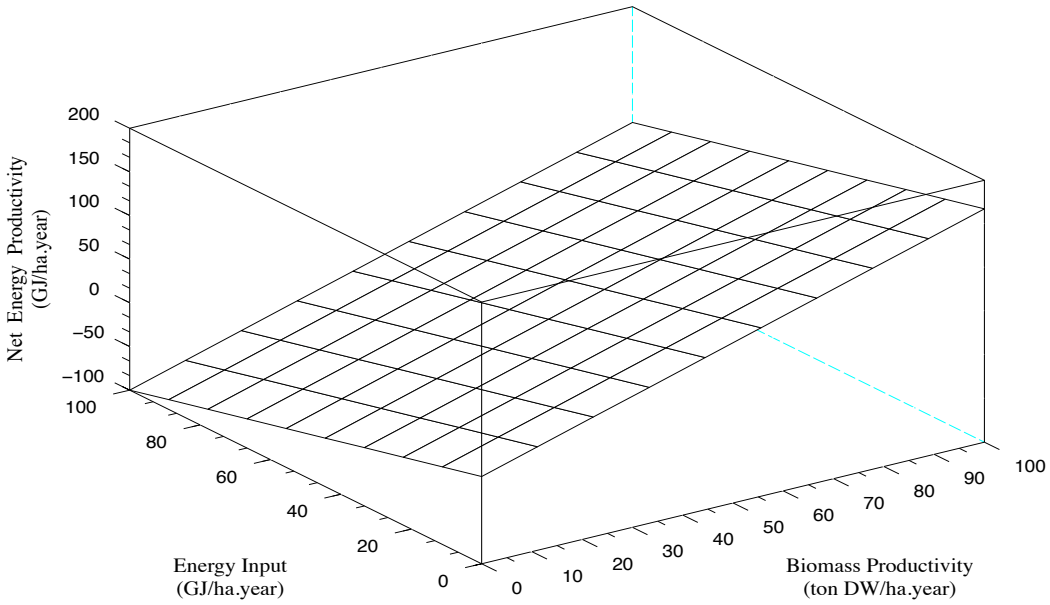

Figure 6.3: Net energy productivity from digestion of *Scenedesmus spp.* as a function of biomass productivity and energy input for biomass generation, expressed in GJ per hectare per year

The profile for *Scenedesmus spp.* was less encouraging. A net energy productivity of 180 GJ/ha.year is theoretically possible when biomass productivities approach 100 ton DW/ha.year and energy inputs are less than 1 GJ/ha.year. These values are improbable, particularly given the challenges associated with harvesting unicellular organisms as well as CO_2 provision through direct gas liquid mass transfer. This suggests bioenergy production through AD of whole cell *Scenedesmus spp.* is not energetically favourable. However, microalgae offer several additional benefits associated with their intrinsic characteristics (CO_2 fixation, use of non-arable land etc., (Sialve et al., 2009)). These properties may allow for lower net energy productivities to be acceptable.

6.4 Mechanical pre-treatment; net energy gain or loss?

For the batch digestion studies, mechanical pre-treatment resulted in a clear improvement on the methane yields per kg VS. To determine the effect of pre-treatment on the net energy of the system, the energy gain was compared to the added energy required for the pre-treatment process. The aim of this study was not to optimise the pre-treatment process in terms of energy input vs. disruption efficiency, but rather to ensure total disruption of the algal cells had occurred. Using the same calculation as in Section 6.3 for net energy produced, the relationship for maximum energy input, still yielding an overall net energy gain, from the pre-treatment was established (Figures 6.4 (a) and 6.5 (a)).

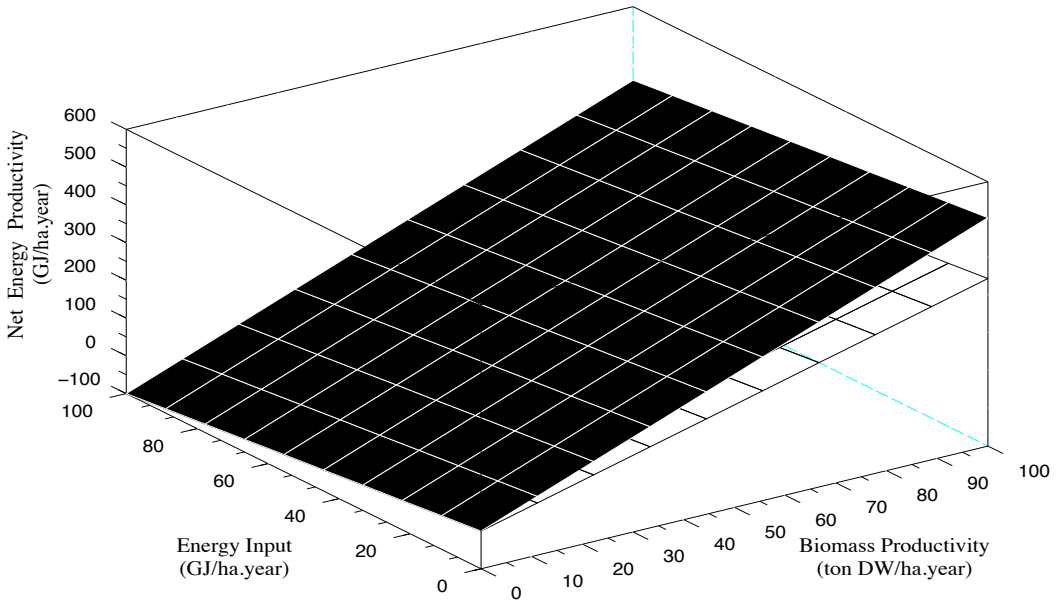

(a) Impact of mechanical pre-treatment on net energy productivity for *Spirulina spp.* as a function of biomass productivity and energy input, expressed in GJ/ha.year. Black plane represents the ruptured digesters, whilst the white plane represents the whole cell digesters.

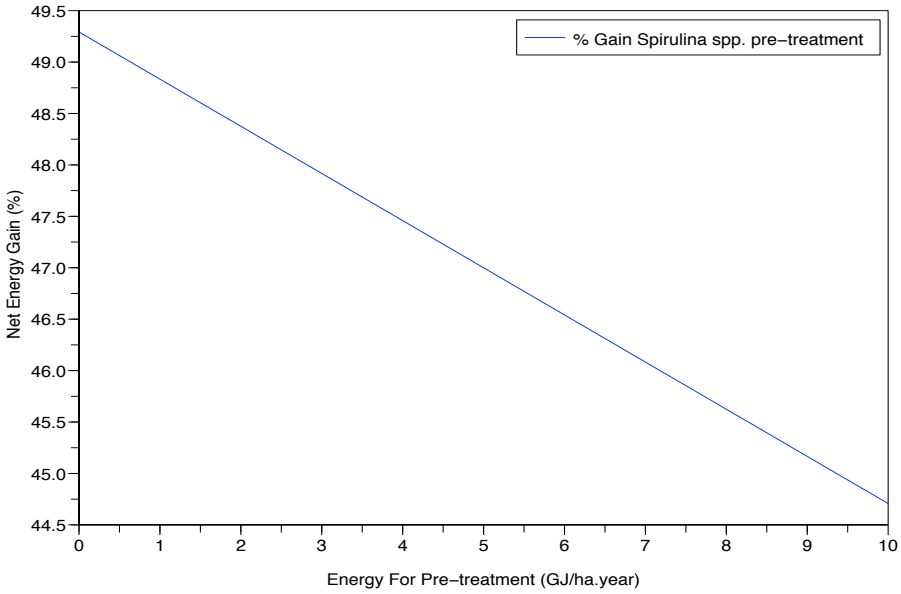

(b) % Net energy gains for various pre-treatment energy requirements when digesting *Spirulina spp.* algal biomass, expressed in % using 70 ton DW/ha.year and a cultivation energy requirement of 10 GJ/ha.year

Figure 6.4: Total and relative % net energy gains for various pre-treatment energy requirements when digesting algal biomass, expressed in % and GJ/ha

At higher biomass productivities (75 ton DW/ha.year) the positive increase on the net energy for *Spirulina spp.* exceeded 200 GJ/ha.year. This suggested that if the pre-treatment energy requirement was less than this, a net energy gain would be obtained. As an example, if the energy requirement for pre-treatment of *Spirulina spp.,* at a biomass productivity of 70 ton DW/ha.year, was 5 GJ/ha.year a 47% increase in net energy could be achieved (Figure 6.4 (b)). This gain resulted in a net energy production in excess of 430 GJ/ha.year, which exceeds those reported for plant energy crops. With the added benefits associated with

a third generation substrate, the high net energy potential points to AD of *Spirulina spp.* as an attractive option for bioenergy production.

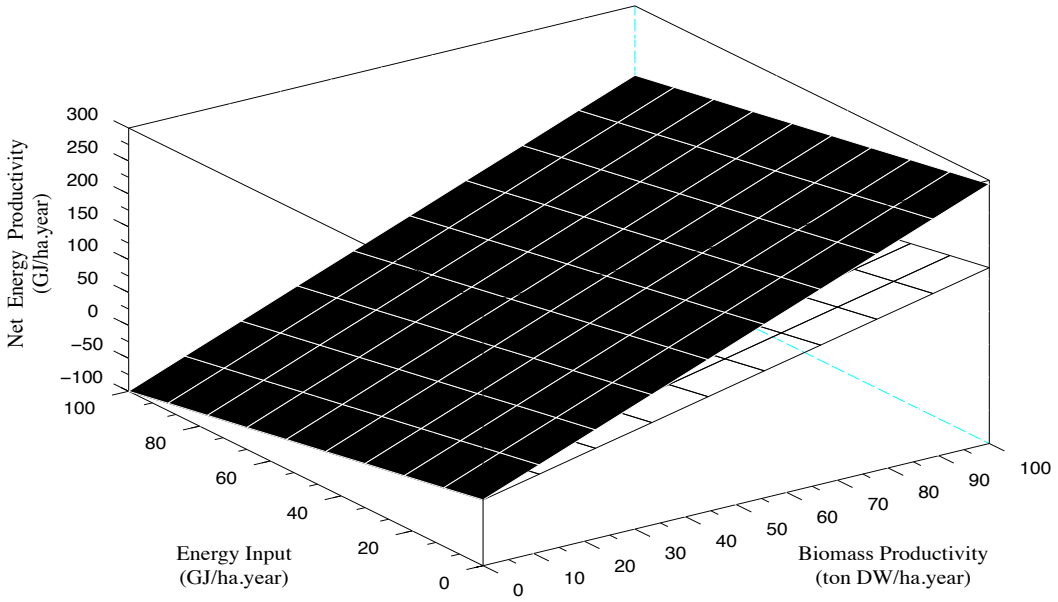

(a) Impact of mechanical pre-treatment on net energy production for *Scenedesmus spp.* as a function of biomass productivity and energy input, expressed in GJ/ha. Black plane represents the ruptured digesters, whilst the white plane represents the whole cell digesters.

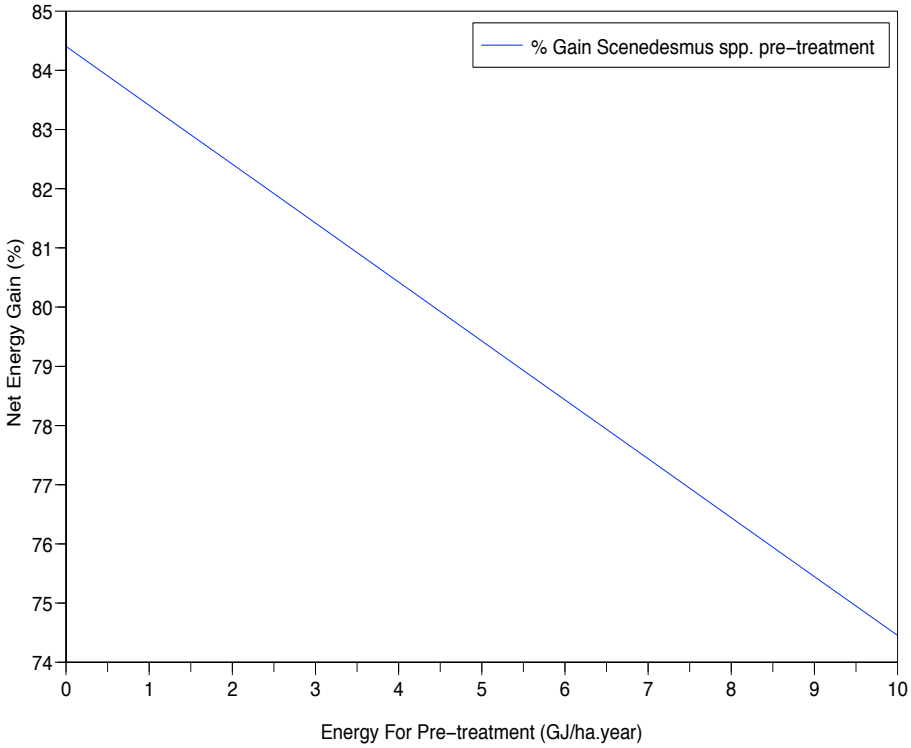

(b) % Net energy gains for various pre-treatment energy requirements when digesting *Scenedesmus spp.* algal biomass, expressed in % using 70 ton DW/ha.year and a general energy requirement of 20 GJ/ha.year

Figure 6.5: Total and relative net energy gains for various pre-treatment energy requirements when digesting algal biomass, expressed in % and GJ/ha

Mechanical pre-treatment had a more significant impact on the net energy gain for digestion of *Scenedesmus spp.* (Figure 6.5). An increase in net energy of more than 250 GJ/ha.year is possible with the incorporation of pre-treatment. As an estimation the amount of energy required for pre-treatment was double that of *Spirulina spp.*. The lower energy requirement for *Spirulina spp.* results from the ease at which cells were disrupted. A longer period of milling was required to completely disrupt *Scenedesmus spp.* compared to *Spirulina spp.* (Section 4.4.1). Despite the higher energy requirements for the bead milling, the net energy gain was significant. For a biomass productivity of 70 ton DW/ha.year and a general energy requirement of 20 GJ.ha.year, a 50% increase in energy input due to bead milling still resulted in a 72% net energy gain (Figure 6.5 (b)). With the inclusion of a pre-treatment the annual net energy production achievable was comparable to that of first generation energy crops where energy inputs were at or below 20 GJ/ha.year. It is postulated that with the difficulty in harvesting unicellular *Scenedesmus spp.* cells and the need for aeration (compression) this will most likely not be a feasible value.

6.5 Comparison of anaerobic digestion as a stand-alone technology or integrated with microalgal biodiesel production

To determine whether or not AD is more beneficial as a stand-alone process or integrated with the microalgal biodiesel production process, an energy account was conducted for three scenarios.

1. Anaerobic digestion of whole cell *Scenedesmus spp.*
2. Anaerobic digestion of *Scenedesmus spp.* with the inclusion of a mechanical pre-treatment
3. Biodiesel production from *Scenedesmus spp.* integrated with anaerobic digestion of the oil extraction residue

This analysis was only conducted for *Scenedesmus spp.*, as its high lipid productivities has identified it as a possible resource for biodiesel production (Mandal and Mallick, 2009). *Spirulina spp.* does not accumulate substantial amounts of lipid, even under stress conditions. A similar approach to that of Chisti (2008) was used to calculate the final net energy production of the microalgal AD and biodiesel processes (Table 6.5).

At this point it should be noted that the basis for which the calculations were made was per kg oil produced. This assumption cannot be applied in certain cases. For example the energies associated with cultivation become dependent on the oil content of the biomass. Clearly the oil content of the algae should not determine how much energy goes into cultivation rather the amount of biomass produced determines this number. However, for the purpose of comparison between the systems this approach was acceptable. For biogas production on its own, the value associated with oil recovery was omitted and the rest of the input energies remained the same as for the integrated system.

Table 6.5: Energy account of algal oil production (adapted from Chisti (2008))

Energy Balance	
Input/output	Energy (MJ/kg oil)
Energy in fertiliser[a]	14.12
Energy for cultivation	8.77
Energy for harvesting[b]	0.3
Energy for oil recovery[c]	3.17
Energy for biogas production	0.88
Energy for construction (entire facility including maintenance)[d]	4.00
Energy embodied in equipment (including maintenance)[e]	62.8 X 10^{-6}
Energy in algal oil[f]	37.90
Energy in biogas from residual biomass[g]	35.8
Biomass productivity	ton/ha.year
$P_{biomass}$	10 -100
X_{oil}	0.1 -1
$P_{residue}{}^{i}$	10 -100
Energy Inputs	GJ/ha.year
$E_{input\ Biodiesel+Biogas}$=$P_{biomas}$*$X_{oil}$*($E_{Fertilizer}$+$E_{Cultivation}$+$E_{Harvesting}$ +$E_{Oil\ recovery}$ + $E_{Biogas\ prod}$ + E_{Constr} + E_{equip}	
$E_{input\ Biogas}$= P_{biomas}*X_{oil}*($E_{Fertilizer}$+$E_{Cultivation}$+$E_{Harvesting}$ + $E_{Biogas\ prod}$ + E_{Constr} + E_{equip}	
Energy Productivities	GJ/ha.year
$Y_{E\ Biodiesel+Biogas}$ = $E_{oil}P_{oil}$ + $E_{biogas}P_{residue}SMY_{residue}{}^{j}$	
$Y_{E\ Biogas}$ = $E_{Biogas}P_{Biomass}SMY_{Biomass}{}^{j}$	
Net Energy Productivities	GJ/ha.year
$Y_{N\ Biodiesel+Biogas}$ = $Y_{E\ Biodiesel+Biogas}$ - $E_{input\ Biodiesel+Biogas}$	Figure 6.6
$Y_{N\ Biogas}$ = $Y_{E\ Biogas}$ - $E_{input\ Biogas}$	Figure 6.7

[a] Estimated as 22.85 MJ/kg of urea and 2.94 MJ/kg of diammonium phosphate; [b] Using sedimentation followed by continuous vacuum belt filtration; [c] Approximate only in the view of the developmental nature of algal oil recovery; [d] Estimated as 90.4 MJ/m^2 of facility area divided by a 20 year working life and the mass of oil produced annually; [e] Estimated as fossil energy requirement of 27.2 MJ/t of machinery (including equipment for biogas production) divided by the 20 year working life of equipment and the mass of oil produced, [f] Assuming the same energy content in algal oil as in rapeseed oil; [g] Energetic value of methane 35.8 MJ/m^3; [j] Specific methane yield of the extraction residue.

Three dependent variables influenced the possible net energy productivity in the combined biodiesel and biogas production system. These were the final biomass productivity, oil content of the biomass and the specific methane yield (SMY) of the lipid extraction residue. To assess the impact of algal production variables on the final net energy, the experimental SMY obtained for the extraction residue (75 m^3/ton VS) was kept constant whilst the biomass productivity and oil content were varied. The minimum requirements for the two unknown variables to result in net energy production comparable to those obtained from digestion of first generation substrates were determined. Using these values, the SMY of the residue was varied to quantify its impact on final energy production. This staged approach allowed for the significance of each of the three variables to be evaluated (Figure 6.6).

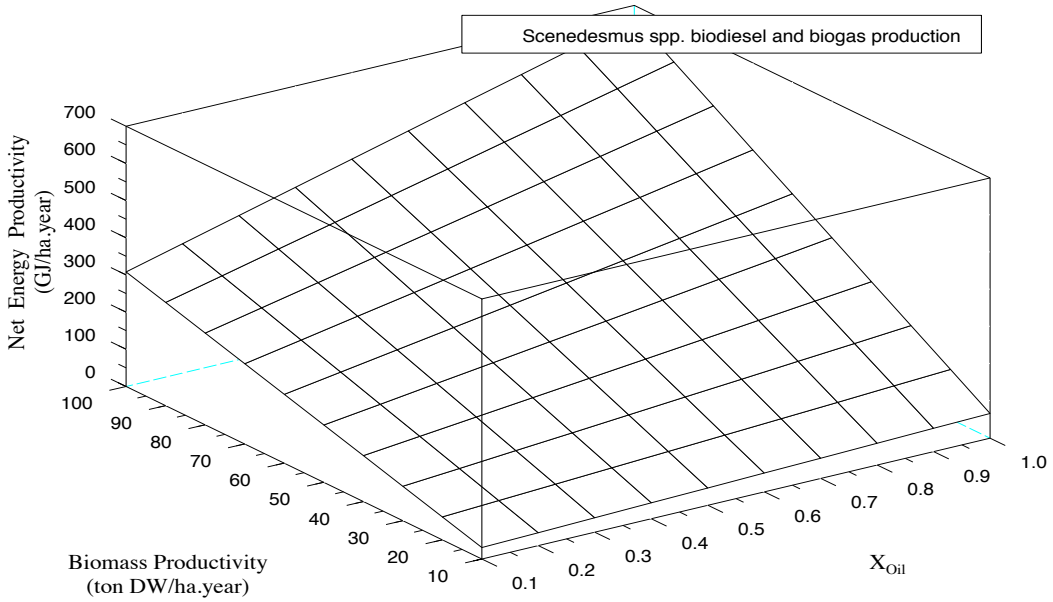

(a) *Scenedesmus spp.* biodiesel and biogas production, calculated at a SMY of 75 m^3/ton VS

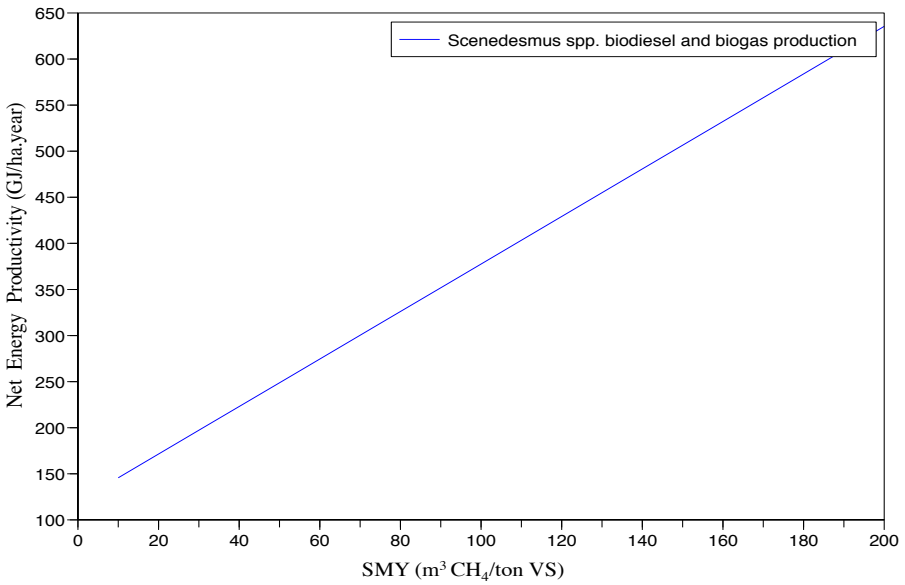

(b) *Scenedesmus spp.* biogas production, calculated for biomass productivity of 90 ton DW/ha.year and an oil content of 20 %

Figure 6.6: Net energy productivity for biodiesel and biogas production as a function of fractional oil contents, biomass productivity as well as specific methane yields, expressed in GJ/ha.year

An increasing oil content resulted in a greater energy production from biodiesel (37.9 MJ/kg Oil) than energy required for the process (cumulative 31.24 MJ/kg Oil) and so an increase in net energy produced. Similarly the net energy produced increased more significantly with a higher biomass productivity. The rate at which net energy increased was greater with an increase in biomass productivity than with an increase in oil content. This suggested that the final biomass productivity contributed more than the oil content to the net energy productivity. The greatest net energy productivity was obtained when oil content and biomass productivity were high. To have greater net energy productivities than first generation energy crops (300 GJ/ha.year) an oil content of at least 10% was required with an annual biomass

production of 100 ton DW/ha, or an oil content exceeding 20% with an annual biomass productivity of 80 ton DW/ha. It is important to determine the percentage of the total net energy resulting from biogas production compared to biodiesel production. At 10% oil, the contribution to net energy from methane is estimated as 40%, whereas 20% oil this contribution decreases to 23%. These results illustrate the opportunity to increase the net energy gain of the microalgal biodiesel process with the inclusion of biogas production from residual oil extraction biomass. This result is consistent with the review conducted by Sialve et al. (2009), who suggested AD of microalgae was a necessary step in making microalgal biodiesel production feasible on an economical and energetic basis.

In Section 6.3 it was determined that the two most important variables that impact the net energy productivity of biogas production were the annual biomass productivity and process energy input requirement. To allow a reasonable comparison between the two systems, a similar approach was used to calculate the energy inputs for the stand-alone process as the integrated system. The added energy inputs for oil production were omitted. With a biomass dependent method for calculating the energy requirements, it became a significant variable in potential energy productivities. Therefore the impact on net energy from biomass productivities and SMY's were assessed in Figure 6.7.

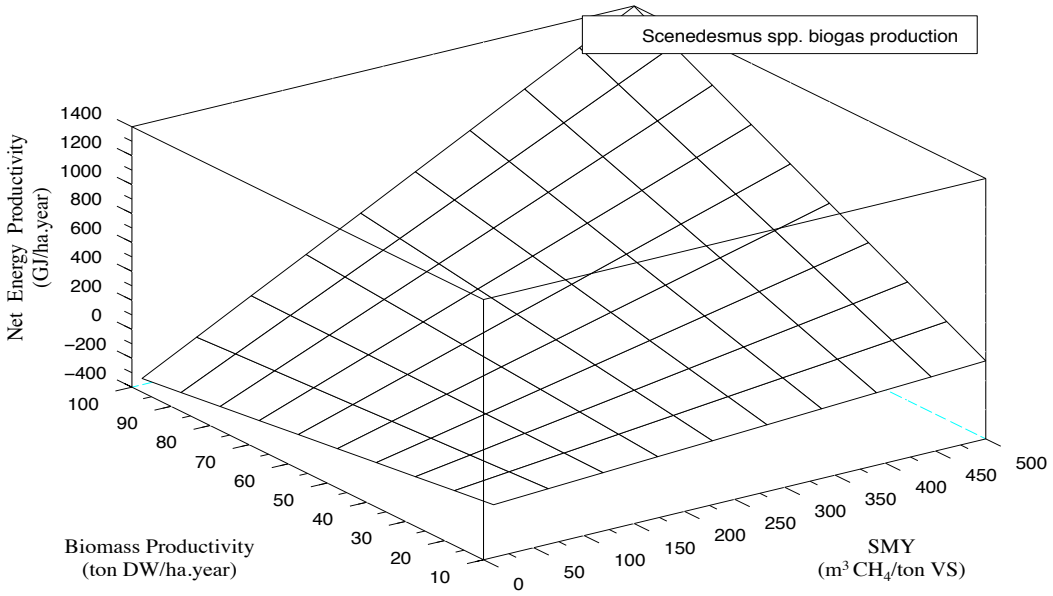

Figure 6.7: Net energy productivity as a function of biomass productivity and as specific methane yield for biogas production as a stand-alone technology. Calculated with an assumed oil content of 14 %.

A minimum methane yield of more than 230 m^3 CH_4/ ton VS, with a biomass productivity greater than 70 tons DW/ha.year, was required to exceed net energies of 300 GJ/ha.year. The reason behind the low efficiency of the biogas production process was the high energy inputs associated with production of the biomass with an estimated 14% oil content. With the production of biodiesel, the added energy gained from the oil product resulted in a higher net energy even when oil contents were low. Since the energy of the oil extracted is 37.9 MJ/kg Oil and that of biogas at 35.8 MJ/m^3CH_4 the lower energy productivities were expected.

6.6 Conclusions

Both the experimentally obtained and previously reported algal biomass productivities were far greater than those achievable by plant energy crops. The result was expected as algae, a third generation biofuel feed stock, is defined by its low input high output production. Specific methane yields reported for traditional energy crops were on average higher than the experimentally obtained values for the algae investigated in study. However, yields reported in literature were comparable to the plant crops ($>$ 300 m^3/ton VS).

The analysis of the net energy production through digestion of plant crops indicated that a net energy of more than 300 GJ/ha.year would be required by the algal biomass to be significant. With this the maximum energy requirement for the production of the biomass was determined. Using the experimental methane yield and productivity, digestion of *Spirulina spp.* needed to have an energy input of less than 20 GJ/ha.year to provide an appropriate net energy gain. Using the experimental values for whole cell *Scenedesmus spp.* did not allow for comparable energy productivities with realistic energy requirements, owing to its poor digestibility.

Mechanical pre-treatment resulted in positive net energy gains for both algal species. The energy gain associated with disruption was greater for *Scenedesmus spp.* since the pre-treatment had a more significant impact on digestibility hence the methane productivity of the AD process. This gain resulted in more desirable net energy productivities, which exceeded those achievable by traditional plant energy crops.

The analysis of AD as a stand-alone technology and as an integrated unit in biodiesel production indicated that the combination of biodiesel and biogas production was more favourable in terms of net energy production. The high energy inputs associated with the process resulted in less favourable biogas energy productivities. A clear comparison for final net energy productivities between anaerobic digestion of whole cell and ruptured cell *Scenedesmus spp.* as well as with the integrated biodiesel process was not practical. Unless a productivity and oil content of *Scenedesmus spp.* was assumed and a theoretical methane yield used the calculation would be bias. The approach taken whereby benchmark values needed to make the processes competitive with traditional energy crops provided a more sound analysis.

Chapter 7

Closing remarks and recommendations

7.1 Introduction

Detailed conclusions are drawn at the end of the sub-studies presented in Chapters 4, 5 and 6. In this chapter, the findings are integrated and general conclusions made, based on the hypotheses presented in Chapter 2. Accompanying the conclusions are recommendations, which suggest further investigation and, where applicable, propose an experimental approach to completing the investigation.

7.2 Batch digestion studies

7.2.1 Whole cell studies

Anaerobic digestion of whole cell *Spirulina spp.* resulted in a higher productivity and final yield of methane (maximum yield 113 m^3 CH_4/ton VS and productivity 0.175 L $CH_4/L_{reactor}$.day) than the digestion of whole cell *Scenedesmus spp.* (max yield 55 m^3 CH_4/ton VS and 0.067 L $CH_4/L_{reactor}$.day). This was a result of the hydrolysis and fermentation to produce acetic acid. The increased amount of acetic acid available for consumption by methanogens in the *Spirulina spp.* digesters was due to the degradability of the algal biomass, resulting in more freely available organics to be converted by the acidogenic bacteria. This finding is in accordance with the hypothesis that the ease at which *Spirulina spp.* cells undergo hydrolysis would provide a more readily available and so consumable source of organic compounds.

Further investigation into optimising the propionic to acetic acid ratios for digestion of whole cell *Spirulina spp.* should be conducted to maximise methane production and define use of indicator VFAs. All three replicate digesters suffered from high propionic to acetic acid ratios, which have been reported as undesirable and a sign of poor digester performance.

7.2.2 Mechanical pre-treatments and the effect thereof

From the mechanical disruption studies conducted, it was shown that *Spirulina spp.* cells disrupted more easily than *Scenedesmus spp.* cells. This was attributed the sensitivity of *Spirulina spp.* cells to osmotic

shock, the low cell wall strength and the filamentous nature of the biomass. *Scenedesmus spp.* cells needed an extended period to disrupt as the small rigid cell has a thick recalcitrant cell wall made up of biopolymers which are resistant to degradation.

The final methane yields (m^3 CH_4/ton VS) obtained from digestion following mechanical pre-treatment showed a 47% increase for *Spirulina spp.* (166 m^3 CH_4/ton VS) compared to 76% increase for *Scenedesmus spp.* digesters (96 m^3 CH_4/ton VS). The greater increase observed for *Scenedesmus spp.* was expected due to the resistance to degradation whole cells offered. These findings are in accordance with the hypotheses that rupturing of algal cells prior to digestion enhances the efficiency of AD as it will allow for an increased concentration of soluble organic compounds for consumption by the anaerobic microflora.

7.2.3 Digestion of DT residue

Batch digestion of the residue remaining after biodiesel extraction showed limited reproducibility. Only one of the triplicate reactors produced consistent data and was used to provide preliminary results. The sensitivity of the digestion was a result of the toxic chemicals used in the direct transesterification process.

The methane yield obtained from the DT residue digester (75 m^3/ton VS) was lower than the ruptured cell digesters but higher than the whole cell digesters. This resulted from the partial disruption of cells during DT allowing for a more easily degradable source of biomass and so concentration of freely available organics for conversion to methane. These findings are in accordance with the hypotheses that rupturing of algal cells prior to digestion enhances the efficiency of AD as it will allow for an increased concentration of soluble organic compounds for consumption by the anaerobic microflora.

It is recommended that further investigation be conducted into the feasibility of digesting the residual biomass after direct transesterification has been conducted. The digestion of the residual biomass is critical to make microalgal biodiesel production energetically feasible and so attention needs to be paid to obtaining a full understanding of all potential issues that relate to its digestion. Investigation into the digestion of residues from typical oil extraction techniques should be done. This will inform of appropriate oil extraction approaches for integration with AD.

7.3 Integrated algal anaerobic digestion system

The concept of creating an integrated algal anaerobic digestion system using *Spirulina spp.* as the only feed stock was demonstrated. The final retention period showed a steadily improving AD system. As a suggestion the following conditions are recommended for semi-continuous digestion of *Spirulina spp.* : S_0 = 5 kg/m^3, retention period 30 days and OLR 0.8 g VS/$L_{reactor}$.day. Under these conditions, a low production of VFAs will be expected, but for an extended period of time. This would minimise the possibility of VFA accumulation and excessive ammonia and sulphide release, hence reducing inhibition of the methanogenic consortia. The temperature should also be maintained in the mesophilic range as thermophilic anaerobic microbial consortia have been reported to be very sensitive and so relatively more

prone to inhibition (Angelidaki and Ahring, 1993). With the number of possible sources of inhibition resulting from the digestion of *Spirulina spp.* a very stable set of methanogens will be essential.

7.4 Energy production analysis

The net energy productivity in terms of GJ/ha.year from anaerobic digestion of whole cell *Spirulina spp.* were greater than that of *Scenedesmus spp.*. This originated from the higher methane yields (113 m^3 CH_4/ ton VS), faster productivity (75 tons DW/ ha.year) as well as the ease at which *Spirulina spp.* can be harvested (low energy input for biomass generation estimated at less than 20 GJ/ha.year). These findings are in accordance with the hypothesis that the net energy production from open pond algal cultivation and digestion of *Spirulina spp.* will be greater than that of *Scenedesmus spp.*.

The net energy productivity in terms of GJ/ha.year for anaerobic digestion of ruptured *Spirulina spp.* would be greater than that of ruptured *Scenedesmus spp.* This originated from the higher methane yields (m^3 CH_4/ ton VS), the faster productivity (tons DW/ ha.year) and from the ease at which the cells are disrupted. The ease of disruption indicates a less energy intensive process.

The total net energy productivity in terms of GJ/ha.year of anaerobic digestion of *Scenedesmus spp.* as a stand-alone technology was lower than that of the integrated biodiesel-AD system. This resulted from the method used in approaching the energy input calculation. This was not in accordance with the initial hypothesis that the fewer operational steps of the AD process compared the integrated one would result in significant decreases in input energies and so increases in net energy productivities. As no specific energy inputs could be found in literature for the two processes, a very broad estimation was made, based on the biomass productivity and oil contents of *Scenedesmus spp.* biomass. This calculation resulted in a more favourable energy balance for biodiesel production than biogas. It is recommended that a full experimental analysis be conducted on the two processes and a detailed energy evaluation be made to arrive at a final conclusion as to whether or not biodiesel and biogas production should be integrated or whether biogas production should stand-alone as bioenergy production process. Along with this is should be noted that the final choice of technologies will be informed by both the energy recovery and the form of energy required i.e. liquid fuel or electricity.

Bibliography

Ahring, B., Sandberg, M., Angelidaki, I., 1995. Volatile fatty acids as indicators of process imbalance in anaerobic digestors. Applied Microbiology and Biotechnology 43, 559–565.

Amin, S., 2009. Review on biofuel oil and gas production processes from microalgae. Energy Conversion and Management 50 (7), 1834 – 1840.

Angelidaki, I., Ahring, B. K., 1993. Thermophilic anaerobic digestion of livestock waste: the effect of ammonia. Applied Microbiology and Biotechnology 38 (4), 560–564.

Angelidaki, I., Ellegaard, L., Ahring, B. K., 1999. A comprehensive model of anaerobic bioconversion of complex substrates to biogas. Biotechnology and Bioengineering 63 (3), 363–372.

Angelidaki, I., Sanders, W., 2004. Assessment of the anaerobic biodegradability of macropollutants. Reviews in Environmental Science and Biotechnology 3 (2), 117–129.

Anrderson, G., Donnelly, T., McKeown, K. J., 1982. Identification and control of inhibition in the anaerobic treatment of industrial wastewaters. Process Biochemistry (United Kingdom) 17:4, 28–32.

Antonopoulou, K. S. G., Lyberatos, G., 2009. Potential to produce methane from extration by-products through anaerobic digestion, deliverable 2.3, Sustoil.

Asinari Di San Marzano, C. M., Legros, A., Naveau, H. P., Nyns, E. J., 1982. Biomethanation of the marine algae tetraselmis. International Journal of Solar Energy 1 (4), 263–272.

Becker, W., 2007. Microalgae in human and animal nutrition. In: Richmond, A. (Ed.), Handbook of Microalgal Culture. pp. 312–351.

Benemann, J. R., Oswald, W. J., 1994. Systems and economic analysis of microalgae ponds for conversion of co2 to biomass. NASA STI/Recon Technical Report N 95, 19554.

Beurskens, J., Faaij, A., Fraenkel, P., Fridleifsson, I., Lysen, E., Mills, D., Moreira, J. R., Nilsson, L. J., Schaap, A., Sinke, W. C., 2010. Renewable energy technologies. Tech. rep., World Energy Assessment.

Blokker, P., Schouten, S., van den Ende, H., de Leeuw, J. W., Hatcher, P. G., Damste, J. S. S., 1998. Chemical structure of algaenans from the fresh water algae tetraedron minimum, scenedesmus communis and pediastrum boryanum. Organic Geochemistry 29 (5-7), 1453 – 1468.

Boltes, K., Leton, P., Garcia-Calvo, E., 2008. Volatile fatty acid anaerobic degradation: Kinetic modeling with an inoculum under controlled conditions. Industrial & Engineering Chemistry Research 47 (15), 5337–5345.

Braun, R., Weiland, P., Wellinger, A., 2010. Biogas fom energy crop digestion. In: IEA Bioenergy.

Bridgwater, A. V., 2003. Renewable fuels and chemicals by thermal processing of biomass. Chemical Engineering Journal 91 (2-3), 87 – 102.

Buekens, A., 2005. Energy recovery from residual wastes by means of anaerobic digestion technologies. In: The future of residual waste managment in Europe.

Burton, S., Cohen, B., Harrison, S., Pather-Elias, S., Stafford, W., van Hille, R., et al.l, 2008. Energy from wastewater- a feasability study. Water Research Commission.

Buyukkamaci, N., Filibeli, A., 2004. Volatile fatty acid formation in an anaerobic hybrid reactor. Process Biochemistry 39 (11), 1491 – 1494.

Carlsson, A., van Beilen, J., Moller, R., Clayton, D., 2007. Micro- and macro- algae. utility for industrial applications. In: Bowles, D. (Ed.), Outputs from the EPOBIO project. CPL press, UK, p. 82.

Chandra, R., Vijay, V., Sunnaroa, P., 2006. A study on biogas generation from non-edible oil seed cakes: potential and propects in india. In: Second joint International conference on sustainable energy and environmnet (SEE 2006). Bangkok, Thailand.

Chang, H., Kim, N.-J., Kang, J., Jeong, C., 2010. Biomass-derived volatile fatty acid platform for fuels and chemicals. Biotechnology and Bioprocess Engineering 15, 1–10.

Chaumont, D., 1993. Biotechnology of algal biomass production: a review of systems for outdoor mass culture. Journal of Applied Phycology 5, 593–604.

Chen, P., 1987. Factors influencing methane fermentation of micro-algae. Ph.D. thesis, California Univ., Berkeley.

Chen, P. H., Oswald, W. J., 1998. Thermochemical treatment for algal fermentation. Environment International 24 (8), 889 – 897.

Chen, Y., Cheng, J. J., Creamer, K. S., 2008. Inhibition of anaerobic digestion process: A review. Bioresource Technology 99 (10), 4044 – 4064.

Cheng, L., Zhang, L., Chen, H., Gao, C., 2006. Carbon dioxide removal from air by microalgae cultured in a membrane-photobioreactor. Separation and Purification Technology 50 (3), 324 – 329.

Chisti, Y., 2007. Biodiesel from microalgae. Biotechnology Advances 25 (3), 294 – 306.

Chisti, Y., 2008. Response to reijnders: Do biofuels from microalgae beat biofuels from terrestrial plants? Trends in Biotechnology 26 (7), 351 – 352.

Choi, E., R. J. M., 1991. Competition and inhibition of sulfate reducers and methane producers in anaerobic treatment. Water Science and Technology 23, 1259–64.

Ciferri, O., 1983. Spirulina, the edible microorganism. Microbiological Reviews. 47 (4).

Cisneros, M., Rito-Palomares, M., 2004. A simplified strategy for the release and primary recovery of c-phcocyanin produced by spirulina maxima. Chemical and biochemical engineering quarterly 18(4), 385–390.

Clement, C., Lonchamp, D., Rebeller, M., Landeghem, H. V., 1980. The development of spirulina algae cultivation. Chemical Engineering Science 35 (1-2), 119 – 126.

Colleran, E., Pender, S., 2002. Mesophilic and thermophilic anaerobic digestion of sulphate-containing wastewaters. Water science and technology 45 (10), 231–235.

De Schamphelaire, L., Verstraete, W., 2009. Revival of the biological sunlight-to-biogas energy conversion systems. Biotechnology and Bioengineering 103 (2), 296–304.

Doucha, J., Livansky, K., 2008. Influence of processing parameters on disintegration of chlorella cells in various types of homogenizers. Applied Microbiology and Biotechnology 81, 431–440, 10.1007/s00253-008-1660-6.

Dowling, S., 2009. Energy from waste as a renewable energy supply to supplement electricity in south africa. Master's thesis, University of Cape Town, Chemical Engineering.

FAO, 2009. Oil production. Accessed 22.09.2010.
URL `www.fao.org/docrep/w7241e/w7241e0h.htm`

Gallert, C., Bauer, S., Winter, J., 1998. Effect of ammonia on the anaerobic degradation of protein by a mesophilic and thermophilic biowaste population. Applied Microbiology and Biotechnology 50 (4), 495–501.

Ghosh, S., , Conrad, J. R., Klass, D. L., 1975. Anaerobic acidogenesis of wastewater sludge. Water Pollution Control Federation 47 (1), 30–45.

Golueke, C. G., Oswald, W. J., 1959. Biological conversion of light energy to the chemical energy of methane. Applid and Environmental Microbiology 7 (4), 219–227.

Golueke, C. G., Oswald, W. J., Gotaas, H. B., 1957. Anaerobic digestion of algae. Applid and Environmental Microbiology 5 (1), 47–55.

Greenwell, H. C., Laurens, L. M. L., Shields, R. J., Lovitt, R. W., Flynn, K. J., 2010. Placing microalgae on the biofuels priority list: a review of the technological challenges. Journal of The Royal Society Interface 7 (46), 703–726.

Griffiths, M., Harrison, S., van Hille, R., 2010. Direct transesterification as an assay for total fatty acid content of microalgae, university of Cape Town, Centre for bioprocess engineering.

Gunaseelan, V. N., 1997. Anaerobic digestion of biomass for methane production: A review. Biomass and Bioenergy 13 (1-2), 83 – 114.

Gunaseelan, V. N., 2009. Biomass estimates, characteristics, biochemical methane potential, kinetics and energy flow from jatropha curcus on dry lands. Biomass and Bioenergy 33 (4), 589 – 596.

Harada, H., Uemura, S., Momonoi, K., 1994. Interaction between sulfate-reducing bacteria and methane-producing bacteria in uasb reactors fed with low strength wastes containing different levels of sulfate. Water Research 28 (2), 355 – 367.

Hartig, P., Grobbelaar, J. U., Soeder, C. J., Groeneweg, J., 1988. On the mass culture of microalgae: Areal density as an important factor for achieving maximal productivity. Biomass 15 (4), 211 – 221.

Heaven, S., Milledge, J., Zhang, Y., 2010. Comments on [']anaerobic digestion of microalgae as a necessary step to make microalgal biodiesel sustainable'. Biotechnology Advances In Press, Corrected Proof, –.

Hickey, R. F., Switzenbaum, M. S., 1991. Thermodynamics of volatile fatty acid accumulation in anaerobic digesters subject to increases in hydraulic and organic loading. Research Journal of the Water Pollution Control Federation 63 (2), 141–144.

Himmel, M., Overend, B. J., 1994. Enzymatic Conversion of Biomass for Fuels Production. American Chemical Society, Ch. Pretreatment of lignocellulosic biomass, pp. 292–324.

Illman, A. M., Scragg, A. H., Shales, S. W., 2000. Increase in chlorella strains calorific values when grown in low nitrogen medium. Enzyme and Microbial Technology 27 (8), 631 – 635.

Jenkins, B. M., Baxter, L. L., Miles, T. R., Miles, T. R., 1998. Combustion properties of biomass. Fuel Processing Technology 54 (1-3), 17 – 46.

Jimenez, C., Cossio, B. R., Labella, D., Niell, F. X., 2003a. The feasibility of industrial production of spirulina (arthrospira) in southern spain. Aquaculture 217 (1-4), 179 – 190.

Jimenez, C., Cossio, B. R., Niell, F. X., 2003b. Relationship between physicochemical variables and productivity in open ponds for the production of spirulina: a predictive model of algal yields. Aquaculture 221 (1-4), 331 – 345.

Kayhanian, M., Rich, D., 1995. Pilot-scale high solids thermophilic anaerobic digestion of municipal solid waste with an emphasis on nutrient requirements. Biomass and Bioenergy 8 (6), 433 – 444.

Keenan, P. J., Iza, J., Switzenbaum, M. S., 1993. Inorganic solids development in a pilot-scale anaerobic reactor treating municipal solid waste landfill leachate. Water Environment Research 65 No: 2, 181–188.

Kozenko, R., Henson, R. H., 1996. The study of spirulina; effects on the aids virus, cancer and the immune systems.

Kube, N., 2006. The integration of microalgae photobioreactors in a recirculation system for low water discharge mariculture. Ph.D. thesis, Christian-Albrechts Univeritat.

Langley, N., Harrison, S., van Hille, R., 2010. A critical evaluation of co2 supplementation to algal systems by direct injection, biotechnology and Bioenegineering (Submitted).

Lau, A., 2008. Anaerobic digestion of agr-food wastes for methane vs. hydrogen. Tech. rep., The University of British Columbia, Department of Chemical & Biological Engineering.

Lyberatos, G., Skiadas, I., 1999. Modelling of anaerobic digestion-a review. Global Nest. The International Journal 1(2), 63–76.

Mandal, S., Mallick, N., 2009. Microalga scenedesmus obliquus as a potential source for biodiesel production. Applied Microbiology and Biotechnology 84, 281–291.

McKendry, P., 2002a. Energy production from biomass (part 2): conversion technologies. Bioresource Technology 83 (1), 47 – 54.

McKendry, P., 2002b. Energy production from biomass (part 3): gasification technologies. Bioresource Technology 83 (1), 55 – 63.

Meyen, F., 1820. Beobachtungen iiber einige niedere algenformen. Naturae 14, 768–778.

Miao, X., Wu, Q., Yang, C., 2004. Fast pyrolysis of microalgae to produce renewable fuels. Journal of Analytical and Applied Pyrolysis 71 (2), 855 – 863.

Moheimani, N., Borowitzka, M., 2006. The long-term culture of the coccolithophore pleurochrysis carterae (haptophyta) in outdoor raceway ponds. Journal of Applied Phycology 18 (6), 703–712.

Moletta, R., Verrier, D., Albagnac, G., 1986. Dynamic modelling of anaerobic digestion. Water Research 20 (4), 427 – 434.

Nakakubo, R., 2008. Ammonia inhibition of methanogenesis and identification of process indicators during anaerobic digestion.

Nielsen, H. B., Angelidaki, I., 2008. Strategies for optimizing recovery of the biogas process following ammonia inhibition. Bioresource Technology 99 (17), 7995 – 8001.

Nussbaumer, T., 2003. Combustion and co-combustion of biomass: Fundamentals, technologies, and primary measures for emission reductionÊ. Energy and Fuels 17 (6), 1510–1521.

Oilgae, 2010. Energy products from algae. eBook.
URL `www.oilgae.com`

Okuda, K., 2002. Structure and phylogeny of cell coverings. Journal of Plant Research 115 (4), 283–288.

Park, J.-H., Park, J.-K., 2003. Fate of methanol in an anaerobic digester. Korean Journal of Chemical Engineering 20, 509–516.

Parkin, G. F., Owen, W. F., 1986. Fundamentals of anaerobic digestion of wastewater sludges. Journal of Environmental Engineering 112 (5), 867–920.

Parkin, G. F., Speece, R. E., Yang, C. H. J., Kocher, W. M., 1983. Response of methane fermentation systems to industrial toxicants. Water Pollution Control Federation 55 No.1, 45–53.

Pernet, F., Tremblay, R., 2003. Effect of ultrasonication and grinding on the determination of lipid class content of microalgae harvested on filters. Lipids 38 (11), 1191–1195.

Pind, P. F., Angelidaki, I., Ahring, B. K., 2003. Dynamics of the anaerobic process: Effects of volatile fatty acids. Biotechnology and Bioengineering 82 (7), 791–801.

Poulsen, T. G., 2003. Anaerobic digestion. Aalborg University, Ch. 5, pp. 93–115.

Rajvanshi, A. K., 1986. Alternative energy in agricultural. CRC Press, Ch. 4, pp. 83–102.

Renaud, S. M., Luong-Van, T., Lambrindis, G., Parry, D., 2002. Effect of temperature on growth, chemical composition and fatty acid composition of tropical australian microalgae grown in batch cultures. Aquaculture 211 (1-4), 195–214.

Richardson, C., 2011. Life cycle analysis of microalgal biodies production facilities. Master's thesis, University of Cape Town.

Richmond, A., Lichtenberg, E., Stahl, B., Vonshak, A., 1990. Quantitative assessment of the major limitations on productivity of spirulina platensis in open raceways. Journal of Applied Phycology 2, 195–206.

Samson, R., LeDuy, A., 1982. Biogas production from anaerobic digestion of spirulina maxima algal biomass. Biotechnology and Bioengineering 24 (8), 1919–1924.

Samson, R., LeDuy, A., 1983a. Improved performance of anaerobic digestion of spirulina maxima algal biomass by addition of carbon-rich wastes. Biotechnology Letters 5 (10), 677–682.

Samson, R., LeDuy, A., 1983b. Influence of mechanical and thermochemical pretreatments on anaerobic digestion of spirulina maxima algal biomass. Biotechnology Letters 5, 671–676.

Samson, R., LeDuy, A., 1986. Detailed study of anaerobic digestion of spirulina maxima algal biomass. Biotechnology and Bioengineering 28 (7), 1014–1023.

Sanchez, E. P., Travieso, L., 1993. Anaerobic digestion of chlorella vulgaris for energy production. Resources, Conservation and Recycling 9 (1-2), 127 – 132.

Sialve, B., Bernet, N., Bernard, O., 2009. Anaerobic digestion of microalgae as a necessary step to make microalgal biodiesel sustainable. Biotechnology Advances 27 (4), 409 – 416.

Speece, R. E., 1983. Anaerobic biotechnology for industrial wastewater treatment. Environmental Science & Technology 17 (9), 416A–427A.

Stefanie, J., Oude, E., , Visser, A., Pol, L. W., Hulshoff, W., Stams, J. M. A., 1994. Sulfate reduction in methanogenic bioreactors. FEMS Microbiology Reviews 15 (2-3), 119–136.

Sterritt, R., Lester, J., 1980. Interactions of heavy metals with bacteria. Science of The Total Environment 14 (1), 5 – 17.

Sun, Y., Cheng, J., 2002. Hydrolysis of lignocellulosic materials for ethanol production: a review. Bioresource Technology 83 (1), 1 – 11.

Symons, G. E., Buswell, A. M., 1933. The methane fermentation of carbohydrates1,2. Journal of the American Chemical Society 55 (5), 2028–2036.

Uzun, B. B., Putun, A. E., Putun, E., 2006. Fast pyrolysis of soybean cake: Product yields and compositions. Bioresource Technology 97 (4), 569 – 576.

van Langerak, E., Gonzales-Gil, G., van Aelst, A., van Lier, J., H Hamelersand G Lettinga, G., 1998. Effects of high calcium concentrations on the development of methanogenic sludge in upflow anaerobic sludge bed (usab) reactors. Water resource technology 32 (4), 1255–63.

Vavilin, V., Lokshina, L., Rytov, S., 2000. The <methane> simulation model as the first generic user-friendly model of anaerobic digestion. Vestn Mosk Univ Khim Supp 41, 22–26.

Vavilin, V. A., Vasiliev, V. B., Rytov, S. V., 1995a. Modelling of gas pressure effects on anaerobic digestion. Bioresource Technology 52 (1), 25 – 32.

Vavilin, V. A., Vasiliev, V. B., Rytov, S. V., Ponomarev, A. V., 1995b. Modeling ammonia and hydrogen sulfide inhibition in anaerobic digestion. Water Research 29 (3), 827 – 835.

Venkataraman, L., 1997. Review of spirulina platensis (arthrospira): Physiology, cell biology and biotechnologym, edited by avigad vonshak. Journal of Applied Phycology Volume 9 (3), 295–296.

Ververis, C., Georghiou, K., Danielidis, D., Hatzinikolaou, D., Santas, P., Santas, R., Corleti, V., 2007. Cellulose, hemicelluloses, lignin and ash content of some organic materials and their suitability for use as paper pulp supplements. Bioresource Technology 98 (2), 296 – 301.

Wang, Q., Kuninobu, M., Ogawa, H. I., Kato, Y., 1999. Degradation of volatile fatty acids in highly efficient anaerobic digestion. Biomass and Bioenergy 16 (6), 407 – 416.

Werther, J., Saenger, M., Hartge, E. U., Ogada, T., Siagi, Z., 2000. Combustion of agricultural residues. Progress in Energy and Combustion Science 26 (1), 1 – 27.

Wijffels, R. H., Jan. 2008. Potential of sponges and microalgae for marine biotechnology.

Wyman, C. E., Dale, B. E., Elander, R. T., Holtzapple, M., Ladisch, M. R., Lee, Y., 2005. Coordinated development of leading biomass pretreatment technologies. Bioresource Technology 96 (18), 1959 – 1966.

Yang, Y. F., Feng, C. P., Inamori, Y., Maekawa, T., 2004. Analysis of energy conversion characteristics in liquefaction of algae. Resources, Conservation and Recycling 43 (1), 21 – 33.

Yen, H.-W., Brune, D. E., 2007. Anaerobic co-digestion of algal sludge and waste paper to produce methane. Bioresource Technology 98 (1), 130 – 134.

Zehnder, A. J., 1998. Biology of anaerobic microorganisms (Environmental and Applied Microbiology Series). John wiley and Sons.

Chapter 8

Appendices

8.1 Appendix A: Standard curves for analytical techniques

This appendix presents the standard curves obtained for the respective analytical methods. In most cases a number of standard curves were developed and the average standard curve presented.

For the analytical methods that used HPLC analysis, a typical peak profile as well as identifying retention times are presented. Additional information is supplied where necessary.

Ammonium ions assay

The ammonium ion assay was conducted using HPLC analysis. An example of a typical chromatogram (Figure 8.1) and identification of retention times (Table 8.1) are presented as well as the standard curve obtained for varying concentrations of the standard ion solution.

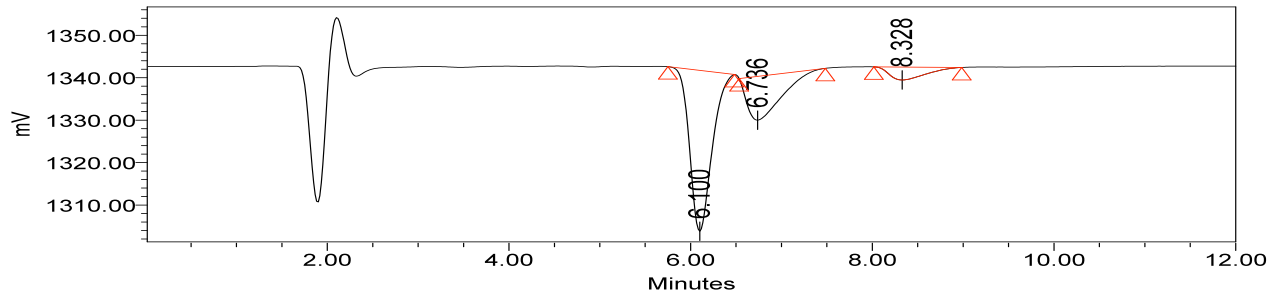

Figure 8.1: HPLC Chromatogram for cation ion peak identification

The inverse or negative peaks observed in Figure 8.1 were due to the polarity of the conductivity detector being positive. This resulted in a drop in conductivity when a positive cation was detected. For the analysis of cations, a strongly conducting acid eluent was used, and all peaks were detected as negative peaks.

Table 8.1: Retention times for cation analysis

Acid	Retention Time (min)
Sodium	6.10
Ammonium	6.74
Potassium	8.33

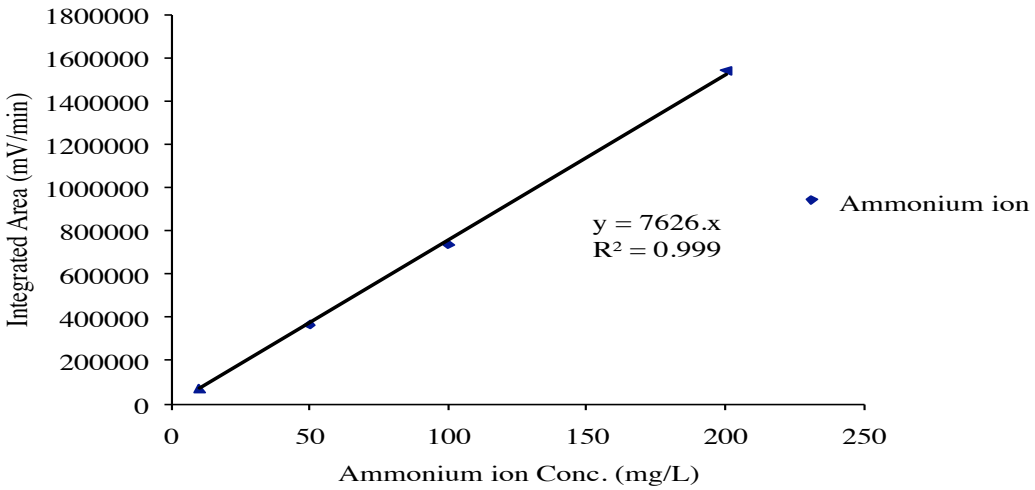

Figure 8.2: Ammonium ion assay standard curve

Aqueous sulphide assay

The aqueous sulphide assay (colorimetric DMDP method) was tested using a standard solution of sulphide. The detection range is from 0.2 mg/L to 1 mg/L.

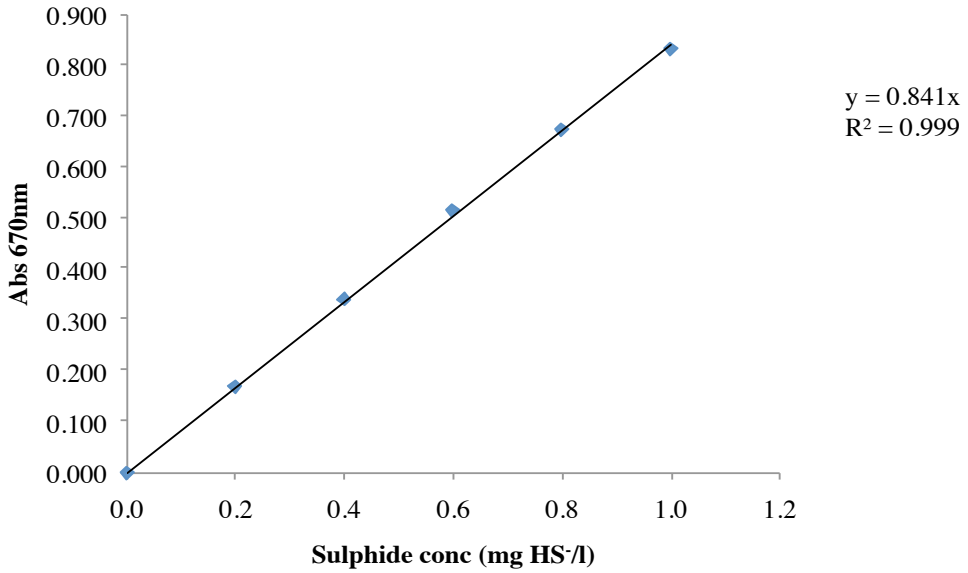

Figure 8.3: Aqueous sulphide assay standard curve

Biomass dry weight assay

Dry weights were measured by filtration and drying, as well as by using optical density at 750 nm. A standard curve for optical density (at 750 nm) as a function of dry weight was developed by using varying concentrations of 2 mL algal samples. These are presented for Spirulina spp. and Scendesmus spp. in Figures 8.3 and 8.5 respectively. The maximum OD above which the correlation is not linear was taken to be 1 and dilutions were made to ensure readings less than this were measured.

Spirulina spp.

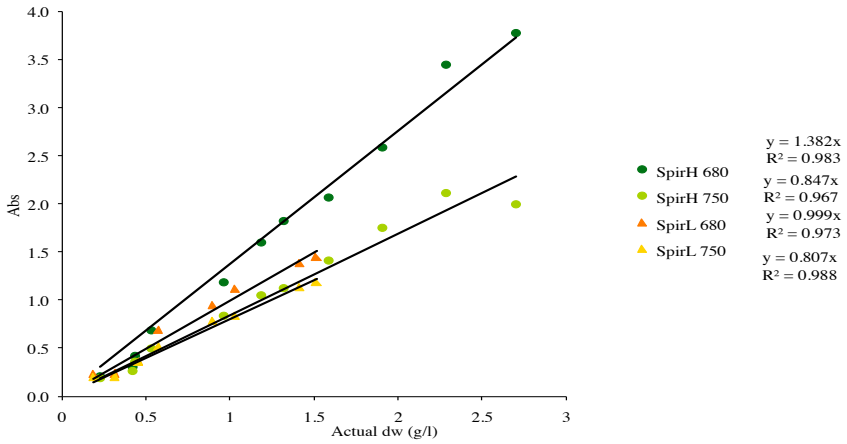

Figure 8.4: *Spirulina spp.* dry weight assay standard curve (Abs at 750 nm, H- high nitrogen media; L= low nitrogen media)

Scenedesmus spp.

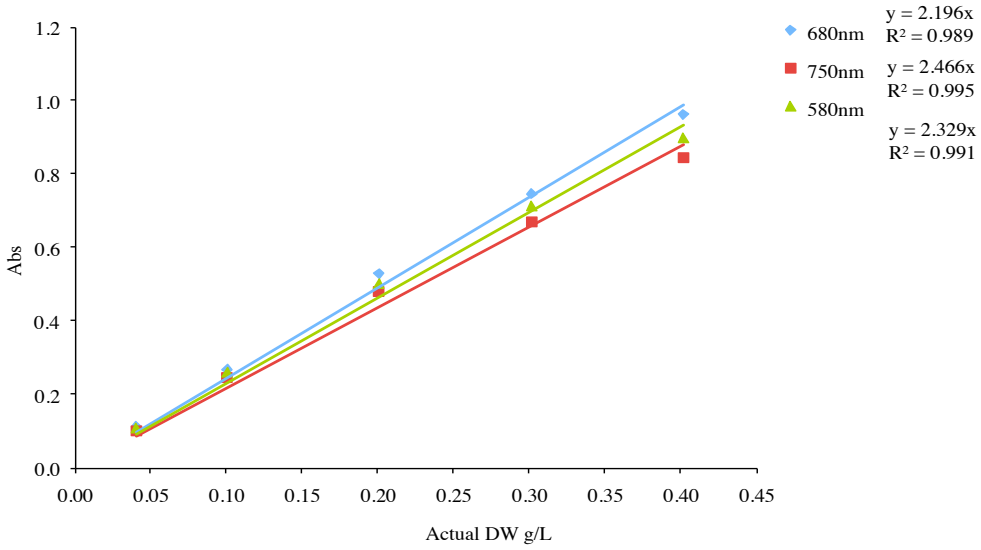

Figure 8.5: *Scenedesmus spp.* dry weight assay standard curve (Abs at 750 nm)

COD assay

The specific method for determining the solid, soluble and total COD concentrations is typically not described in literature so the detailed protocol is described below.

1. Withdraw 1 mL of sample
2. Spin down 0.5 mL of sample at 13 000 RPM using a Hettich MIKRO-RAPID centrifuge for 10 min. Decant the supernatant and dilute 5 times with dH_2O. Add 2 mL dH_2O to the solid pellet and re-suspend by vortex mixing for 3 min.

3. Add 0.5 mL of dH_2O to the other 0.5 mL of sample.
4. Add 2.2 mL of Merk COD solution A and 1.8 mL of solution B to 1 mL of each diluted sample.
5. Mix by inverting and load tubes into a HANN C9800 heating block at 150°C for two hours.
6. After two hours allow samples to cool to 120°C then remove from reactor and mix by inverting.
7. Allow samples to cool to room temperature.
8. Record absorbance using UNICAM, HeλIOSα quant spectrophotometer at a wavelength of 605 nm.

A standard curve for the COD analysis was developed using potassium hydrogen phthalate. This compound is known to have a COD of 10000 mg COD/L at a concentration of 8.5 g/L. So by preparing the 8.5 g/L solution dilutions can be made to test over a range. Since the COD was expected to be high, due to 20 g/L initial substrate loading, a high range was used to develop the standard curve.

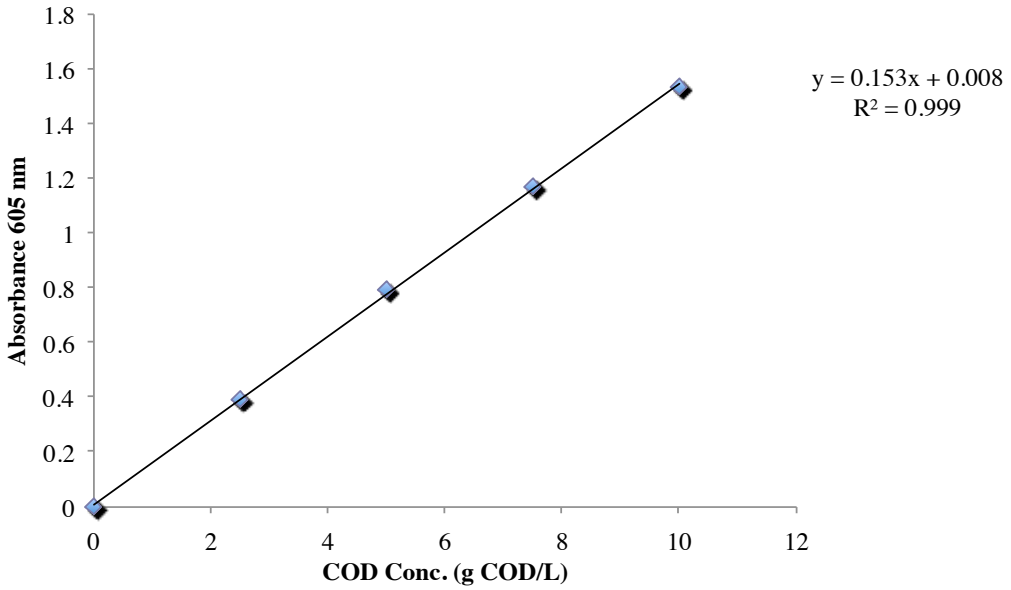

Figure 8.6: Chemical oxygen demand assay standard curve

Molecular analysis assay

The DNA extraction method was adapted from the standard method for extracting DNA from biomining samples and is described below.

1. Spin down $>5\times10^8$ microbial cells in a 1.5 mL Eppendorf at 10 000×g at 4°C for 20 minutes and decant the supernatant.
2. Resuspend the microbes in 1 mL Buffer S (100mM Tris HCL; pH 8.0, 100mM EDTA; pH 8.0, 1.5M NaCl, 1% CTAB) and 5µL Proteinase K (10mg/mL) to lyse cells and inactivate nucleases. Mix well by inverting and add 100µL 10% SDS. Mix well by inverting.

3. Incubate at 65°C in a water bath for 1 hour with regular mixing by inverting. Spin down at 10000×g for 10 min and decant the supernatant.

4. Add 1mL phenol:chloroform (1:1), mix thoroughly by inverting and centrifuge at 13 000 RPM on a desktop centrifuge for 10 minutes. The phenol may turn a violent red colour on addition to the DNA-containing solution; this is an indication of pH and doesn't affect the extraction.

5. Transfer the supernatant to a new tube and add 1/10 volume 3M NaAc (pH 5.2) with gentle mixing. Add two volumes of ice cold ethanol and mix.

6. Spin the samples at 13000 RPM for 10 minutes and decant the supernatant. Resuspend the pellet in 200µL ddH_2O, heat to 60°C to help resuspend the pellet if necessary. Add 800µL ethanol, mix and spin at 13 000 RPM for 10 minutes. Decant the supernatant and allow the DNA pellet to evaporate the ethanol in air or in an oven taking care not to allow the pellet to become completely dry. Resuspend the pellet in 100µL ddH2O or TE buffer and store at -20 or -4°C.

* complete method in triplicates

Nitrate and phosphate ions assay

The nitrates and phosphates assay were measured using HPLC analysis. An example of a typical chromatogram (Figure 8.7) and identification of retention times (Table 8.2) are presented as well as the standard curve obtained for varying concentrations of each standard ion solution.

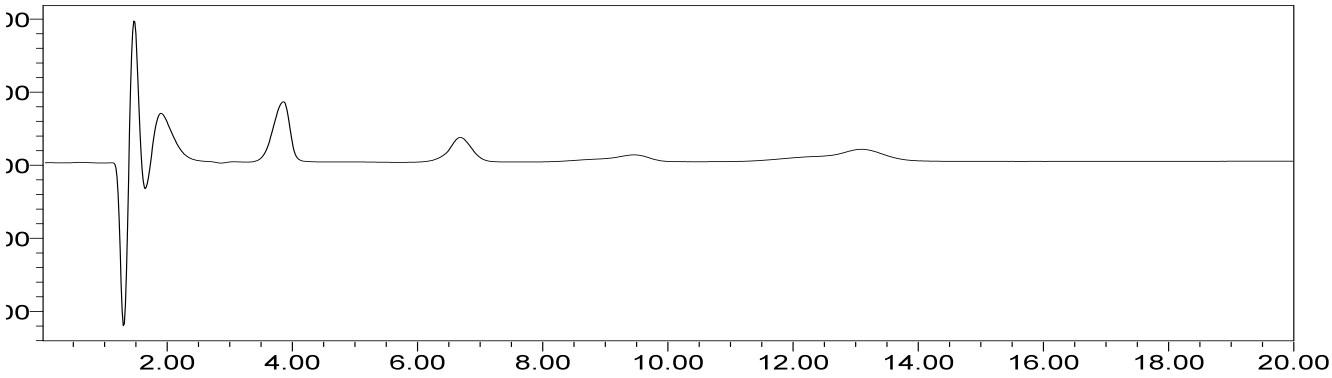

* Each ion 50 ppm

Figure 8.7: HPLC Chromatogram for Nitrate and Phosphate anion peak identification

Table 8.2: Retention times for anion analysis

Anion	Retention Time (min)
Chloride	3.85
Nitrate	6.68
Phosphate	9.46
Sulphate	13.09

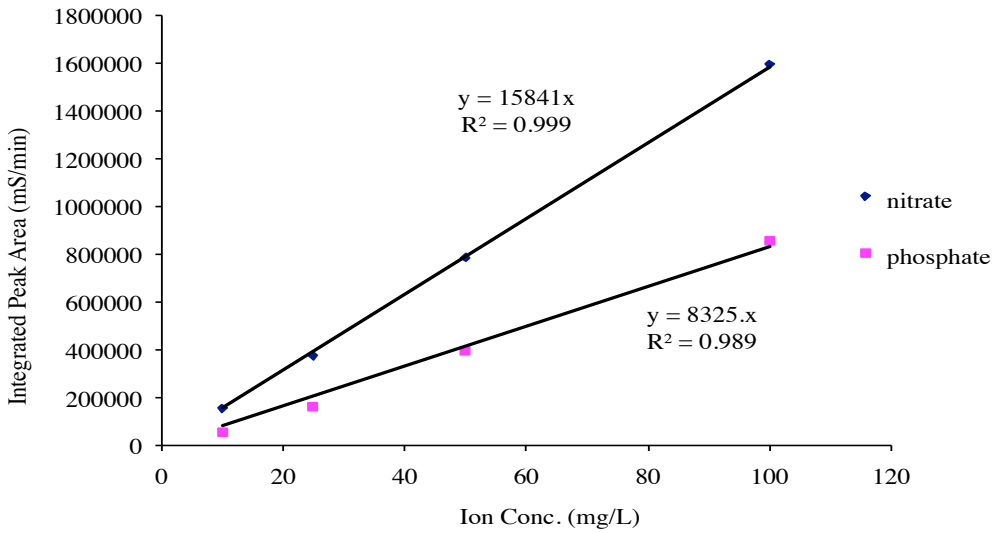

Figure 8.8: Nitrate and phosphate ion assay standard curves

Volatile fatty acids assay

The VFA assay was conducted using HPLC anaylysis. An example of a typical chromatogram is given in Figure 8.9 for identification of retention times (Table 8.3). The standard curve obtained for varying concentrations of each standard acid solution is presented in Figure 8.10.

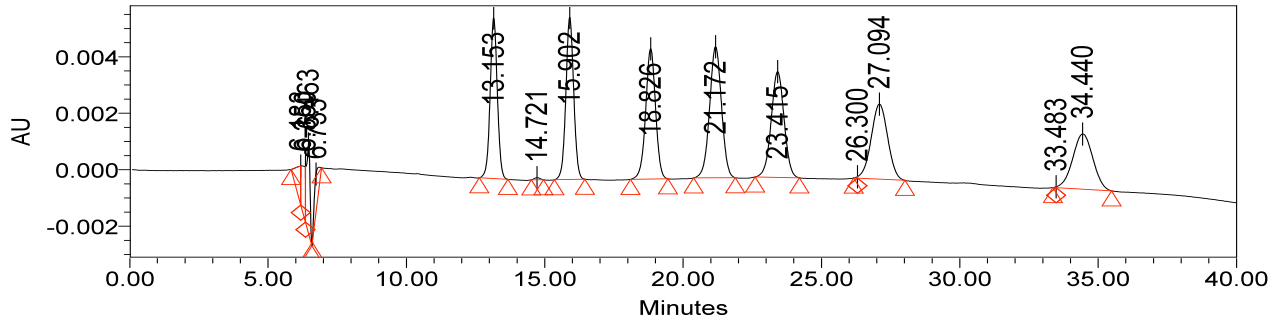

Figure 8.9: HPLC Chromatogram for VFA peak identification

Table 8.3: Retention times for VFA analysis

Acid	Retention Time (min)
Lactic	13.15
Acetic	15.90
Propionic	18.83
Iso-Butyric	21.17
Butyric	23.42
Iso-Valeric	26.91
Valeric	34.45

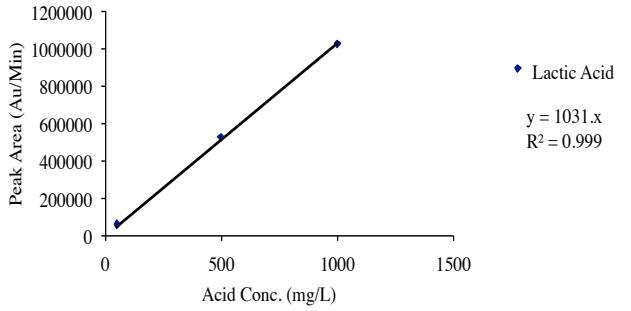

(a) Lactic acid standard curve

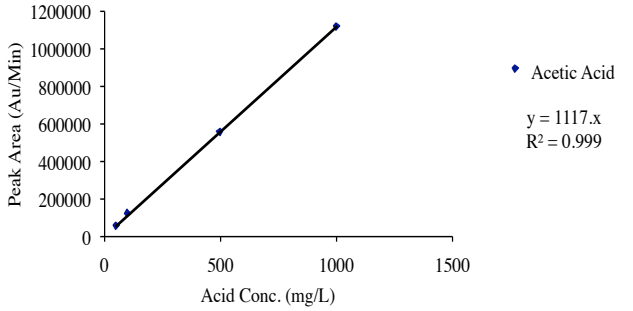

(b) Acetic acid standard curve

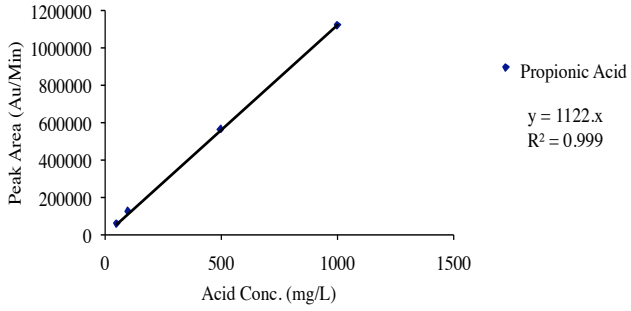

(c) Propionic acid standard curve

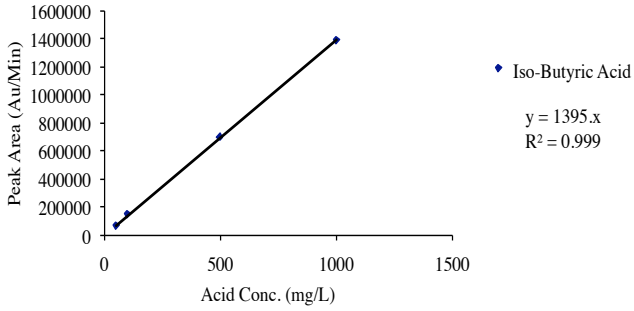

(d) Iso-Butyric acid standard curve

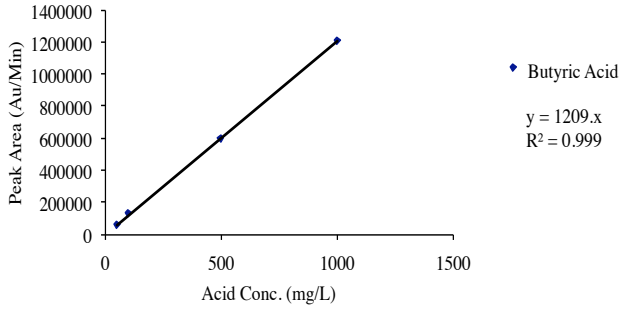

(e) Butyric acid standard curve

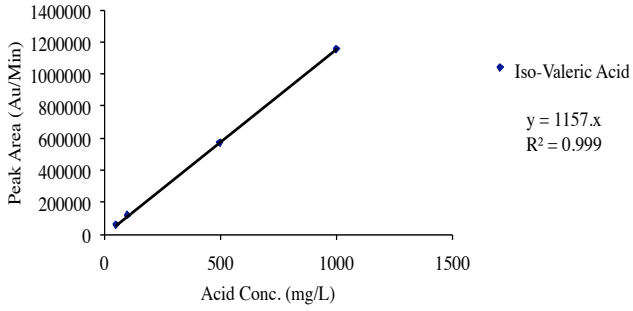

(f) Iso-Valeric acid standard curve

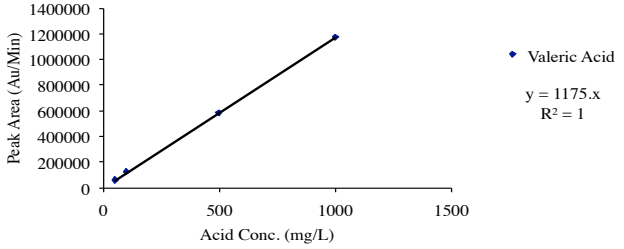

(g) Valeric acid standard curve

Figure 8.10: Volatile fatty acids assay standard curves

8.2 Appendix B: Batch digestion results work-up

Introduction

The following appendix summarises the most important data obtained through the batch digestion studies of this thesis. The approach taken to best represent the data such that a solid understanding of how the data has been worked up was as follows:

1. Present a sample of raw data from one specific digester, in this case a digester loaded with ruptured *Spirulina spp.* algal biomass.
2. Present sample calculations on data manipulation to yield the values in the analysed data set
3. Present the full set of average data and standard deviations for the triplicate digesters run for whole cell and ruptured cell *Spirulina spp.* and *Scenedesmus spp.* substrate loaded digesters as well as *Scenedesmus spp.* DT residue substrate loaded digesters.
4. Using these average data sets, present all the derived variables with sample calculations.

The data presentation is separated into aqueous phase and gaseous phase results.

Aqueous phase data

pH

The pH of all batch digestion bottles was monitored every second day. With the high amount of VFAs produced during the initial stages of digestion, it was essential to control the pH with 5 M NaOH. Generally speaking once the pH was above 6.8, no control was conducted to increase this value. Within each set of digesters, equal amounts of NaOH were added such that a varying result could not be attributed to higher Na concentrations, but rather to differing pH.

Table 8.4: Solid, soluble and total chemical oxygen demand raw data sample sheet for batch digestion

Day	Whole cell *Spirulina spp.* substrate loaded digesters (n=3)		Ruptured cell *Spirulina spp.* substrate loaded digesters (n=3)		Whole cell *Scenedesmus spp.* substrate loaded digesters (n=3)		Ruptured cell *Scenedesmus spp.* substrate loaded digesters (n=3)		*Scenedesmus spp.* DT residue substrate loaded digesters (n=1)
	pH	STDEV	pH	STDEV	pH	STDEV	pH	STDEV	pH
0	6.55	0.07	6.41	0.34	6.64	0.32	6.63	0.25	7.76
2	6.21	0.12	6.40	0.13	6.07	0.18	5.57	0.53	5.24
4	6.58	0.09	6.63	0.06	6.23	0.43	5.93	0.50	7.06
6	6.88	0.07	6.80	0.13	6.41	0.44	6.21	0.56	7.90
8	7.40	0.03	6.93	0.00	6.67	0.15	6.54	0.13	6.97
10	7.59	0.23	7.22	0.04	7.03	0.00	6.86	0.22	7.17
12	7.65	0.14	7.32	0.00	7.56	0.02	6.48	0.52	7.17
14	7.61	0.18	7.43	0.07	7.46	0.01	7.05	0.45	7.37
16	7.72	0.21	7.35	0.01	7.44	0.03	7.18	0.35	7.37
18	7.69	0.11	7.29	0.00	7.43	0.07	7.50	0.02	7.29
20	7.46	0.06	7.45	0.03	7.44	0.15	7.47	0.16	7.33
22	7.70	0.62	7.65	0.06	7.35	0.11	7.40	0.36	7.41
24	7.68	0.45	7.70	0.09	7.30	0.04	7.40	0.32	7.44
26	7.85	0.47	7.95	0.06	7.35	0.11	7.52	0.28	7.45
28	8.01	0.30	8.09	0.11	7.37	0.14	7.61	0.20	7.51
30	8.04	0.20	8.10	0.11	7.36	0.10	7.65	0.11	7.21
32	7.97	0.14	8.10	0.11	7.46	0.11	7.75	0.07	7.40
34	7.91	0.28	8.12	0.25	7.55	0.13	7.79	0.19	7.55
36	8.03	0.20	8.16	0.16	7.60	0.12	7.90	0.21	7.30
38	8.13	0.17	8.25	0.15	7.62	0.09	7.90	0.17	7.45
40	8.13	0.23	8.27	0.17	7.61	0.07	7.87	0.15	7.51
42	8.18	0.32	8.33	0.18	7.60	0.02	7.85	0.11	7.32
44	8.14	0.41	8.32	0.16	7.68	0.08	7.85	0.08	7.52
46	7.97	0.21	8.31	0.11	7.56	0.06	7.94	0.06	7.54
48	8.15	0.25	8.33	0.11	7.58	0.07	7.84	0.17	7.56
50	8.32	0.03	8.32	0.10	-	-	-	-	-
52	8.43	0.22	8.37	0.04	-	-	-	-	-
56	8.26	0.22	8.46	0.02	-	-	-	-	-
60	8.38	0.18	8.52	0.18	-	-	-	-	-
64	8.38	0.13	8.40	0.11	-	-	-	-	-

Solid, soluble and total chemical oxygen demand

The solid, soluble and total COD were determined for every 2^{nd} day of batch digestion. Since the range of the COD assay was 0-10 000 mg/L it was very important to ensure that correct dilutions were made such that the final reading was within these boundaries. Towards the end of digestion, after day 52, the COD fluctuations were not as significant was seen before, hence sampling was done every 4^{th} day.

Table 8.5: Solid, soluble and total chemical oxygen demand raw data sample sheet for batch digestion

Day	Dilution factor	Solid OD (605 nm)	Solid COD (mg/L)	Dilution factor	Soluble OD (605 nm)	Soluble COD (mg/L)	Total COD (mg/L)
0	4	0.454	10669	5	0.717	22481	33150
2	4	0.438	10224	5	0.414	11946	22170
4	4	0.374	8444	3.5	0.623	13449	21893
6	4	0.359	8027	3.5	0.656	14252	22279
8	4	0.393	8972	3.5	0.641	13887	22860
10	4	0.475	11253	3.5	0.608	13084	24337
12	4	0.359	8027	3.5	0.765	16905	24932
14	4	0.4	9167	3.5	0.581	12427	21594
16	4	0.564	13729	2.5	0.59	9033	22762
18	4	0.431	10029	2.5	0.501	7485	17515
20	4	0.264	4571	3.5	0.491	8862	13433
22	4	0.518	5394	3.5	0.554	10211	15606
24	4	0.293	5281	3.5	0.406	7041	12322
26	4	0.298	5403	3.5	0.385	6591	11994
28	4	0.283	5036	3.5	0.346	5756	10792
30	4	0.731	5334	3.5	0.297	4706	10041
32	4	0.278	5088	3.5	0.265	4021	9109
34	4	0.211	3273	3.5	0.223	3121	6395
36	4	0.28	4963	3.5	0.228	3228	8191
38	4	0.276	4865	3.5	0.106	615	5480
40	4	0.211	3273	3.5	0.115	808	4081
42	4	0.186	2661	3.5	0.148	1515	4176
44	4	0.183	2588	3.5	0.138	1301	3889
46	4	0.164	2123	3.5	0.135	1236	3359
50	4	0.179	2490	3.5	0.115	808	3298
52	4	0.169	2245	3.5	0.167	1922	4167
56	4	0.26	4473	3.5	0.2	2629	7102
60	4	0.21	3249	3.5	0.16	1772	5021
64	4	0.215	3371	2.5	0.27	2949	6320

Sample Calculations

The only calculation that was required for calculation of the chemical oxygen demand was to use the standard curve's gradient (m) and intercept (c) and convert the OD (605 nm) readings into COD concentrations in units of mg/L, equation 8.1. Total COD was calculated as the additive COD of soluble and solid COD.

$$COD_{mg/L} = (OD_{reading} - c)/(m) * 1000 * dilution\,factor \tag{8.1}$$

Whole cell digesters

Table 8.6: Solid, soluble and total chemical oxygen demand raw data for batch digestion of whole cell *Spirulina spp.* (n=3)

Day	Solid COD (mg/L)	Standard deviation (mg/L)	Soluble COD (mg/L)	Standard deviation (mg/L)	Total COD (mg/L)	Standard deviation (mg/L)
0	28742	681	7730	2010	36471	2691
2	14285	2911	11701	429	25986	3341
4	14494	3403	15672	3041	30166	6443
6	12783	6766	14870	495	27653	7261
8	11687	2025	13218	2017	24904	4042
10	10590	4912	11293	1476	21883	6388
12	9918	3304	12256	2577	22174	5881
14	9761	7894	11774	3893	21535	11786
16	6918	4990	12015	332	18933	5323
20	8837	3233	11565	3756	20402	6989
22	7008	2030	9369	2639	16377	4669
24	7622	2781	8112	7479	15734	10260
26	5784	3721	5584	2829	11368	6550
28	4177	1629	5201	5351	9379	6980
30	3664	1138	2904	3903	6568	5040
32	3681	2087	4011	3664	7692	5752
34	3147	1609	5385	1846	8532	3455
36	3944	898	4298		8242	898
38	3823	2278	3568	4833	7391	7111
40	3931	399	4251		8183	399
42	3979	1529	4086	3985	8065	5515
44	3820	766	3435		7256	766
46	3946	862	3886	2428	7831	3290
48	3580	735	3704		7284	735
50	3391	981	3796	4666	7187	5647
52	3795	810	3335		7130	810
56	3922	446	3618	3210	7540	3656
60	3787	307	2556		6343	307
64	3443	1026	2319	2969	5762	3995

Table 8.7: Solid, soluble and total chemical oxygen demand raw data for batch digestion of whole cell *Scenedesmus spp.* (n=3)

Day	Solid COD (mg/L)	Standard deviation (mg/L)	Soluble COD (mg/L)	Standard deviation (mg/L)	Total COD (mg/L)	Standard deviation (mg/L)
0	23585	1943	2210	70	25795	2013
2	24890	3754	2778	421	27668	4174
4	22660	2789	2674	991	25334	3780
6	23220	666	6327	1811	29546	2476
8	23354	0	5879	2341	29233	2341
10	24215	3621	4273	207	28488	3827
12	24490	1607	3547	269	28038	1876
14	21420	1042	4078	1652	25499	2695
16	21573	1928	1973	1188	23546	3115
18	20475	374	1437	155	21912	529
20	22377	3306	768	319	23145	3625
22	22173	1271	1119	349	23293	1620
24	21861	1220	785	102	22646	1322
26	21564	1381	658	107	22222	1488
28	21434	1690	411	28	21845	1718
30	18745	2143	460	236	19205	2379
32	18513	2168	241	101	18754	2270
34	14005	3464	221	68	14225	3532
36	11123	4025	103	178	11226	4203
38	13192	1434	230	211	13422	1645
40	12938	712	240	208	13178	919
42	13588	901	213	101	13801	1002
44	13510	541	180	52	13510	593
48	11182	678	169	33	11290	711

Ruptured cell digesters

Table 8.8: Solid, soluble and total chemical oxygen demand raw data for batch digestion of ruptured cell *Spirulina spp.* (n=3)

Day	Solid COD (mg/L)	Standard deviation (mg/L)	Soluble COD (mg/L)	Standard deviation (mg/L)	Total COD (mg/L)	Standard deviation (mg/L)
0	12218	2562	23281	1385	35499	3948
2	11133	2126	15110	3273	26243	5399
4	10734	3967	13146	1524	23880	5490
6	10382	4225	14100	1210	24482	5434
8	10558	2242	16260	3356	26818	5598
10	9543	2419	13753	947	23296	3366
12	8166	197	14775	3012	22941	3209
14	9167	0	13023	843	22190	843
16	12811	1298	10119	1537	22930	2835
20	7736	3501	10080	1891	17816	5392
22	6600	2786	10679	1559	17279	4344
24	6001	626	8002	883	14003	1508
26	7982	4424	7883	1125	15865	5549
28	8902	3348	5328	1378	14230	4727
30	6078	2728	5843	1021	11921	3749
32	5042	450	4691	612	9734	1062
34	4437	1103	4297	1023	8734	2126
36	5653	1120	4480	1135	10133	2255
38	4043	2099	2516	2841	6559	4940
40	3643	1807	2312	2605	5955	4412
42	3439	1902	2954	2064	6394	3966
44	3848	2419	2756	1846	6604	4265
46	3581	2358	2581	2022	6162	4380
48	3385	1651	2409	1651	5795	3302
50	2947	944	2165	1454	5112	2398
52	2784	870	2143	1778	4927	2647
60	3658	0	3107	1458	6765	1458
64	3869	948	2543	2139	6412	3087

Table 8.9: Solid, soluble and total chemical oxygen demand raw data for batch digestion of ruptured cell *Scenedesmus spp.* (n=3)

Day	Solid COD (mg/L)	Standard deviation (mg/L)	Soluble COD (mg/L)	Standard deviation (mg/L)	Total COD (mg/L)	Standard deviation (mg/L)
0	18588	2146	9431	1861	28018	4007
2	18402	2115	9083	3133	27485	5248
4	17447	1567	10091	4648	27539	6214
6	18587	2150	12490	2554	31077	4704
8	18666	3049	13193	120	31860	3169
10	22950	688	10577	654	33527	1342
12	19237	3304	10626	1170	29862	4475
14	20989	4406	10261	654	31250	5060
16	21156	4170	10248	671	31404	4841
18	18027	59	9567	774	27594	833
20	18441	2167	10570	1736	29011	3903
22	18475	5277	8662	2764	27137	8042
24	17318	6561	7608	2394	24927	8955
26	14741	5307	5701	2023	20442	7331
28	12618	3095	4411	1565	17028	4660
30	10615	4084	4403	2298	15018	6381
32	11523	4717	4224	3043	15748	7759
34	9085	3676	3924	3179	13009	6855
36	9761	3421	3171	3326	12932	6748
38	9805	3421	3406	1906	13211	5326
40	9741	3216	3023	1882	12764	5098
42	6530	1008	2001	531	8531	1538
44	5576	1219	1603	299	7179	1518
48	4621	650	1557	101	6178	751

DT Residue digesters

Table 8.10: Solid, soluble and total chemical oxygen demand raw data for batch digestion of *Scenedesmus spp.* DT residue (n=1)

Day	Solid COD (mg/L)	Soluble COD (mg/L)	Total COD (mg/L)
0	25403	13911	39314
2	24819	12597	37416
4	18893	13335	32228
6	20168	13206	33374
8	14855	12913	27769
10	14152	13133	27284
12	15872	13895	29767
14	17003	13189	30193
16	16236	12573	28809
18	14987	12881	27868
20	15229	10715	25944
22	15229	10715	25944
24	16117	10349	26466
26	13354	9691	23045
28	11585	8248	19834
34	9214	7149	16363
40	6386	7169	13555
44	5996	7315	13312
48	6135	7169	13305

Volatile fatty acids

The VFA concentration was determined for every 2^{nd} day of digestion. Samples were analysed using HPLC. The results for the average concentration for each substrate tested have been presented in terms of the key acids; acetic, propionic and butyric; and the indicator acids; iso-butyric, iso-valeric and valeric acids. Lactic acid has been presented with the latter group.

Sample data

Table 8.11: Volatile fatty acids raw data sample sheet for batch digestion of ruptured *Spirulina spp.* (n=1)

Day	Lactic Acid Conc. (mg/L)	Acetic Acid Conc. (mg/L)	Propionic Acid Conc. (mg/L)	Iso-Butyric Acid Conc. (mg/L)	Butyric Acid Conc. (mg/L)	Iso-Valeric Acid Conc. (mg/L)	Valeric Acid Conc. (mg/L)	Total Acid Conc. (mg/L)
0	312	724	849	0	575	0	36	2496
2	33	2861	294	202	1183	989	23	5585
4	0	3524	391	321	1646	2017	0	7899
6	16	3952	501	425	1733	984	0	7612
8	11	3505	421	393	1574	1085	0	6990
10	11	3105	511	486	1765	1001	56	6935
12	0	2929	574	595	1910	1010	133	7152
14	1	2950	571	591	1336	989	124	6562
16	8	3815	602	545	346	959	114	6388
18	7	4089	852	505	162	693	0	6309
20	0	3920	876	453	77	1022	0	6349
22	0	3907	979	492	0	612	0	5991
24	16	2694	907	422	0	451	0	4491
26	0	2238	1054	541	0	538	0	4370
28	10	1502	1207	573	43	541	0	3876
30	0	913	973	325	0	478	0	2689
32	0	1092	981	22	0	484	0	2580
34	0	1280	1023	0	0	38	0	2342
36	19	548	1067	0	0	43	0	1677
38	0	280	959	14	0	45	0	1298
40	0	131	985	21	0	41	0	1178
42	0	161	912	58	0	23	2	1156
44	12	212	623	87	0	43	0	977
46	4	295	498	125	0	63	0	986
48	11	479	518	132	2	85	16	1243
50	0	636	323	9	0	0	0	968
52	0	714	253	0	0	0	0	968
56	0	825	161	41	0	88	45	1160
60	1	837	60	13	0	149	0	1061
64	17	680	64	0	0	81	9	851

Sample Calculations

In order to quantify the amount of specific acid in a sample, the integrated area of the peak on the HPLC chromatograph was used. The standard curve equation was applied with the dilution factor to yield the final concentration of the acid.

Figure 8.11: HPLC Chromatogram example for VFA analyis (day 6 of digestion)

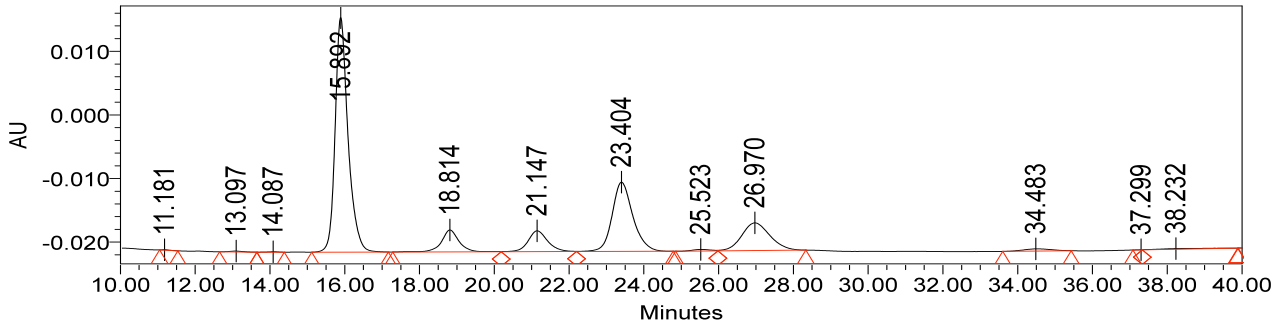

Using the integrated area from the peaks in this profile and the gradient (m) of the specific acid standard curves (Figure 8.10 (a) - (g)) as well as the dilution factor the final concentration of specific acid in a sample was calculated, using Equation 8.2, and is presented in Table 8.13.

$$VFA_{(mg/L)} = (IA)/(m_{specific\,acid}) * dilution\,factor \tag{8.2}$$

The VFA concentration in terms of COD was also calculated. The COD concentration of a 1000 mg/L solution for each acid was calculated. Using this, a ratio relating mg acid/L to mg COD/L was determined and used to convert specific VFA concentration in mg/L to mg COD/L according to Equation 8.3 presented in Table 8.12.

$$VFA\,Conc._{(mg\,COD/L)} = VFA\,Conc._{(mg/L)} * Ratio \tag{8.3}$$

Table 8.12: VFA COD concentrations for standard solutions

Acid	Acid Conc. (mg /L)	COD Conc. (mg COD/L)	Final Ratio (mg COD/L: mg/L)
Lactic	1000	200	0.2
Acetic	1000	1026	1.03
Propionic	1000	1094	1.09
Iso-Butyric	1000	1235	1.24
Butyric	1000	2146	2.15
Iso-Valeric	1000	1412	1.41
Valeric	1000	1345	1.35

Table 8.13: Example of analysis of HPLC data from VFA analysis (day 6 of digesting ruptured *Spirulina spp.* (run=1))

Acid	Retention Time (min)	Integrated Area (Au/min)	Dilution factor	Final Concentration (mg/L)	Final Concentration (mg COD/L)
Lactic	13.1	3258.5	5	15	3
Acetic	15.9	883419.9	5	3952	4070
Propionic	18.8	112523.2	5	501	546
Iso-Butyric	21.1	118697.5	5	425	527
Butyric	23.4	419185.7	5	1733	3726
Iso-Valeric	27.0	227761.0	5	983	1387
Valeric	34.5	0	5	0	0
Toatl	-	-	-	7611	10259

Whole cell digesters

Table 8.14: Key volatile fatty acid raw data for batch digestion of whole cell *Spirulina spp.* (n=3)

Day	Acetic Acid Conc. (mg/L)	STDEV (mg/L)	Propionic Acid Conc. (mg/L)	STDEV (mg/L)	Butyric Acid Conc. (mg/L)	STDEV (mg/L)
0	747	226	404	268	282	146
2	2475	105	248	154	1344	112
4	3745	143	479	163	1852	143
6	3524	174	364	171	1788	13
8	3584	316	649	296	1496	429
10	3495	410	721	157	1230	213
12	3363	88	647	179	1413	649
14	4001	299	654	189	713	13
16	4251	345	676	146	499	29
18	3573	50	644	150	816	709
20	3761	455	576	324	885	661
22	2778	313	843	213	38	212
24	2158	424	676	504	369	521
26	746	434	1140	330	1	0
28	741	395	971	410	57	32
30	602	293	870	289	20	29
32	462	364	799	316	23	33
34	737	118	1023	48	25	10
36	440	60	1094	60	12	16
38	137	49	1112	101	16	23
40	78	102	1123	110	8	12
42	243	303	1172	151	1	1
44	359	449	1234	43	1	2
46	229	101	1149	32	12	1
48	50	29	1207	21	0	0
50	50	21	1259	152	0	0
52	53	43	1051	240	9	1
56	82	54	1126	42	0	0
60	99	30	999	2	0	0
64	154	0	984	59	0	0

Table 8.15: Indicator volatile fatty acid raw data for batch digestion of whole cell *Spirulina spp.* (n=3)

Day	Lactic Acid Conc. (mg/L)	STDEV (mg/L)	Iso-Butyric Acid Conc. (mg/L)	STDEV (mg/L)	Iso-Valeric Acid Conc. (mg/L)	STDEV (mg/L)	Valeric Acid Conc. (mg/L)	STDEV (mg/L)
0	867	388	12	22	174	151	47	82
2	184	43	168	132	1132	109	27	10
4	54	12	419	105	1587	241	0	0
6	10	3	382	6	1409	497	4	6
8	3	4	372	32	1406	365	77	74
10	90	97	410	24	1219	27	42	38
12	7	6	616	299	1136	225	8	10
14	0	0	406	86	945	137	8	11
16	0	0	439	94	952	245	2	3
18	1	1	415	65	1005	269	3	2
20	1	1	387	23	912	117	8	14
22	12	2	413	12	752	105	0	12
24	26	29	408	32	758	270	0	1
26	36	12	419	21	503	88	0	0
28	2	2	396	17	516	80	0	0
30	2	3	255	354	396	215	5	7
32	2	2	253	356	345	265	7	10
34	15	12	272	318	282	335	4	1
36	6	3	262	321	245	332	10	15
38	5	6	248	327	227	322	11	15
40	3	2	125	167	226	292	20	5
42	1	1	59	83	184	201	13	16
44	0	0	16	11	113	72	7	10
46	0	0	4	12	109	23	0	0
48	4	5	30	29	46	2	0	0
50	17	10	68	72	43	11	0	0
52	0	0	2	3	69	9	11	16
56	12	15	1	1	97	82	1	1
60	1	1	0	0	58	28	1	1
64	0	0	0	0	53	8	0	0

Table 8.16: Key volatile fatty acid raw data for batch digestion of whole cell *Scenedesmus spp.* digestion (n=3)

Day	Acetic Acid Conc. (mg/L)	STDEV (mg/L)	Propionic Acid Conc. (mg/L)	STDEV (mg/L)	Butyric Acid Conc. (mg/L)	STDEV (mg/L)
0	0	0	986	0	815	0
2	903	322	326	169	870	97
4	846	0	200	0	675	0
6	1305	283	359	224	617	206
8	1419	12	282	68	907	29
10	1413	62	299	3	930	50
12	1103	370	471	92	973	221
14	533	236	437	23	876	45
16	260	157	424	14	832	25
18	518	250	200	61	342	319
20	91	79	436	107	35	61
22	184	244	375	92	5	7
24	152	69	418	84	11	19
26	294	0	434	0	3	0
28	93	113	363	77	6	10
30	191	287	215	123	0	0
32	47	8	485	17	4	7
34	52	17	286	141	9	14
36	64	27	222	10	5	9
38	52	5	77	35	6	11
40	62	10	102	64	0	0
42	20	12	36	12	1	0
44	7	6	20	8	0	0
46	13	7	18	4	0	0
48	28	7	27	8	2	0

Table 8.17: Indicator volatile fatty acid raw data for batch digestion of whole cell *Scenedesmus spp.* (n=3)

Day	Lactic Acid Conc. (mg/L)	STDEV (mg/L)	Iso-Butyric Acid Conc. (mg/L)	STDEV (mg/L)	Iso-Valeric Acid Conc. (mg/L)	STDEV (mg/L)	Valeric Acid Conc. (mg/L)	STDEV (mg/L)
0	165	0	0	0	0	0	0	0
2	52	46	22	17	45	26	59	26
4	7	0	21	0	70	0	181	0
6	11	16	36	19	125	62	97	103
8	9	10	32	1	127	5	40	24
10	0	0	38	2	132	106	0	0
12	1	0	46	7	82	24	7	3
14	10	12	40	1	99	3	0	0
16	12	9	40	1	95	8	13	19
18	103	144	26	7	93	104	5	6
20	2	4	46	26	68	55	0	0
22	0	0	29	1	69	20	5	8
24	0	0	41	27	87	58	3	6
26	1	0	50	0	82	0	0	0
28	4	3	68	1	133	26	0	0
30	20	16	32	12	40	21	0	0
32	0	0	59	20	21	11	3	4
34	10	9	16	22	13	18	0	0
36	9	7	10	16	8	7	3	5
38	10	12	5	4	0	0	0	0
40	3	4	4	0	0	0	0	0
42	0	0	3	1	9	7	10	3
44	11	3	13	2	11	3	11	2
48	7	1	5	1	7	4	5	3

Ruptured cell digesters

Table 8.18: Key volatile fatty acid raw data for batch digestion of ruptured cell *Spirulina spp.* (n=3)

Day	Acetic Acid Conc. (mg/L)	STDEV (mg/L)	Propionic Acid Conc. (mg/L)	STDEV (mg/L)	Butyric Acid Conc. (mg/L)	STDEV (mg/L)
0	686	268	726	354	804	257
2	3008	208	293	1	1167	23
4	3756	202	377	12	1708	53
6	4080	110	487	12	1787	47
8	3915	355	430	7	1679	91
10	3485	0	561	0	1001	81
12	3410	416	480	82	1739	148
14	3147	171	572	1	1159	153
16	4222	353	595	6	384	33
18	4311	315	784	96	149	19
20	3735	1055	681	462	198	187
22	3487	1521	1036	80	37	53
24	2440	1528	814	271	169	233
26	2737	707	1060	8	0	0
28	1888	546	1184	33	60	24
30	920	644	1160	162	43	48
32	789	516	929	206	12	20
34	894	363	949	207	14	25
36	861	328	1127	68	15	27
38	583	323	1062	167	7	13
40	295	270	1033	45	23	39
42	177	114	1178	364	1	2
44	209	108	1135	379	0	0
46	240	112	887	386	3	5
48	231	219	882	359	6	8
50	311	294	772	425	0	0
52	374	312	728	432	0	0
56	495	327	496	294	4	7
60	571	309	488	510	12	14
64	628	266	118	67	7	12

Table 8.19: Indicator volatile fatty acid raw data for batch digestion of ruptured cell *Spirulina spp.* (n=3)

Day	Lactic Acid Conc. (mg/L)	STDEV (mg/L)	Iso-Butyric Acid Conc. (mg/L)	STDEV (mg/L)	Iso-Valeric Acid Conc. (mg/L)	STDEV (mg/L)	Valeric Acid Conc. (mg/L)	STDEV (mg/L)
0	395	87	5	8	6	10	135	164
2	17	24	202	0	1031	59	12	16
4	0	0	321	0	1414	532	0	0
6	22	6	435	8	994	9	0	0
8	15	3	408	13	1217	114	0	0
10	0	0	367	0	875	71	502	706
12	0	0	478	101	1066	49	46	76
14	3	2	471	103	1000	9	41	71
16	5	2	484	52	1051	80	254	121
18	4	5	458	66	760	94	0	0
20	13	14	671	368	831	171	24	40
22	7	9	500	12	675	89	0	1
24	33	36	809	647	478	85	13	20
26	13	18	523	26	558	29	0	0
28	5	7	555	25	564	32	0	0
30	9	9	314	308	518	62	27	47
32	5	7	389	333	376	273	0	0
34	0	1	137	221	209	292	10	18
36	7	11	14	24	74	31	11	18
38	2	3	11	10	44	2	0	0
40	2	3	30	24	41	22	11	19
42	0	0	86	56	81	63	2	1
44	36	51	99	74	61	21	0	0
46	3	3	123	98	72	44	6	6
48	5	5	53	69	70	31	14	13
50	0	0	12	14	10	18	0	0
52	0	0	0	0	17	29	4	7
56	3	5	244	327	109	76	24	23
60	6	9	18	21	119	57	3	4
64	8	9	1	2	84	25	15	19

Table 8.20: Key volatile fatty acid raw data for batch digestion of ruptured cell *Scenedesmus spp.* digestion (n=3)

Day	Acetic Acid Conc. (mg/L)	STDEV (mg/L)	Propionic Acid Conc. (mg/L)	STDEV (mg/L)	Butyric Acid Conc. (mg/L)	STDEV (mg/L)
0	35	30	363	211	944	339
2	977	322	214	112	1807	624
4	1624	595	553	380	1680	649
6	1900	548	583	260	1218	289
8	1881	814	946	117	1149	75
10	2508	486	1120	249	1476	241
12	1970	17	954	2	1548	216
14	2446	708	1250	278	1238	213
16	2584	591	1414	310	1390	283
18	2290	155	1544	466	1364	59
20	1206	617	1117	627	1143	42
22	1344	936	1534	492	825	436
24	1492	797	903	459	172	37
26	1166	623	1290	111	52	14
28	966	335	1023	606	38	37
30	646	321	1189	567	4	6
32	358	267	1206	505	2	3
34	342	59	1181	491	11	18
36	379	40	1197	486	8	14
38	401	161	1187	545	0	0
40	392	362	840	278	0	1
42	686		602		31	
44	695		650		0	
48	344		605		5	

Table 8.21: Indicator volatile fatty acid raw data for batch digestion of ruptured cell *Scenedesmus spp.* (n=3)

Day	Lactic Acid Conc. (mg/L)	STDEV (mg/L)	Iso-Butyric Acid Conc. (mg/L)	STDEV (mg/L)	Iso-Valeric Acid Conc. (mg/L)	STDEV (mg/L)	Valeric Acid Conc. (mg/L)	STDEV (mg/L)
0	629	439	69	42	40	31	49	86
2	1377	1117	103	71	77	37	431	359
4	5	5	225	2	63	89	476	602
6	1	2	169	92	91	40	313	296
8	1	1	10	9	87	31	0	0
10	1	0	84	63	90	21	0	0
12	2	2	66	26	124	17	20	8
14	12	10	65	35	116	11	277	208
16	1	0	100	32	152	18	286	209
18	5	1	107	9	188	20	10	14
20	6	9	100	31	157	43	218	249
22	2	2	94	6	181	32	416	359
24	12	20	92	34	167	51	177	189
26	2	3	108	36	207	57	169	151
28	14	14	102	38	206	23	64	80
30	19	31	146	56	167	27	4	6
32	59	103	124	43	165	8	0	0
34	15	26	100	40	157	5	0	0
36	110	185	95	46	100	53	0	0
38	42	63	84	37	45	45	0	0
40	19	26	96	80	10	15	0	0
42	0		137		27		19	
44	5		123		16		8	
48	7		11		26		0	

Residue digesters

Table 8.22: Key volatile fatty acid raw data for batch digestion of *Scenedesmus spp.* DT residue (n=1)

Day	Acetic Acid Conc. (mg/L)	Propionic Acid Conc. (mg/L)	Butyric Acid Conc. (mg/L)
0	40	248	91
2	591	204	490
4	1211	486	591
6	2022	547	368
8	1691	588	539
10	1979	565	611
12	1979	457	539
14	1775	585	414
16	1784	630	419
18	1950	651	497
20	1803	659	381
22	1763	684	418
24	1816	637	369
26	1596	619	366
28	1650	473	490
30	1340	421	330
32	1011	401	210
34	1024	395	119
36	221	217	33
38	170	263	40
40	137	292	60
42	214	268	9
44	243	225	12
46	221	285	0
48	298	201	3

Table 8.23: Indicator volatile fatty acid raw data for batch digestion of *Scenedesmus spp.* DT residue (n=1)

Day	Lactic Acid Conc. (mg/L)	Iso-Butyric Acid Conc. (mg/L)	Iso-Valeric Acid Conc. (mg/L)	Valeric Acid Conc. (mg/L)
0	836	108	51	154
2	415	75	166	359
4	215	29	309	61
6	164	49	213	4
8	116	83	266	29
10	129	123	312	54
12	92	128	271	49
14	68	168	318	40
16	87	173	303	63
18	73	151	326	43
20	84	158	320	33
22	67	156	314	39
24	61	146	236	29
26	64	162	168	30
28	85	125	112	53
30	85	73	87	0
32	65	66	32	0
34	56	100	108	0
36	16	51	26	0
38	6	14	0	0
40	0	7	0	0
42	5	20	13	0
44	7	14	18	32
46	1	19	41	8
48	12	21	14	12

Gaseous phase data

All gaseous phase data for the 64 day *(Spirulina spp.)* and 48 day *(Scenedesmus spp.)* digestion periods were recorded daily. Due to the size of the data sets from the 64 day digestion periods, the results are only presented for every second day.

Table 8.24: Gaseous phase raw data sample sheet for batch digestion of ruptured *Spirulina spp.* (n=1)

Day	Time (hrs)	Time (min)	Biogas Production (mL)	Biogas Productivity (L Biogas /$L_{reactor}$.day)	Cumulative Biogas produced (L)	Biogas Methane Content (% CH_4 vol/vol)	Methane Productivity (L CH_4 / $L_{reactor}$.day)	Methane Yield (L CH_4 /g VS)
0	18	0	0	0.000	0.000	0.000	0.000	0.000
2	8	35	84	0.082	0.754	21.616	0.018	0.014
4	17	20	48	0.041	0.848	30.000	0.012	0.015
6	8	0	41	0.042	0.910	39.970	0.017	0.017
8	8	10	42	0.042	0.965	49.333	0.021	0.019
10	9	20	64	0.068	1.082	66.407	0.045	0.023
12	8	20	50	0.055	1.216	66.568	0.036	0.029
14	8	30	54	0.055	1.309	68.624	0.038	0.033
16	8	20	61	0.060	1.441	66.688	0.040	0.038
18	13	0	47	0.059	1.570	67.276	0.040	0.044
20	8	15	75	0.075	1.689	70.446	0.053	0.049
22	8	15	91	0.091	1.856	77.168	0.070	0.057
24	12	0	240	0.208	2.286	83.000	0.172	0.079
26	9	0	320	0.349	2.966	82.572	0.288	0.114
28	12	0	250	0.261	3.496	81.191	0.212	0.142
30	8	30	47	0.047	3.643	70.520	0.033	0.149
32	14	30	76	0.065	3.811	78.639	0.051	0.157
34	8	30	74	0.074	3.935	83.500	0.062	0.163
36	8	45	56	0.055	4.041	74.084	0.041	0.168
38	15	30	0	0.000	4.051	57.008	0.000	0.169
40	7	30	80	0.096	4.210	27.610	0.027	0.172
42	9	0	0	0.000	4.230	14.602	0.000	0.172
44	9	0	0	0.000	4.230	16.602	0.000	0.172
46	9	0	0	0.000	4.230	18.602	0.000	0.172
48	9	0	0	0.000	4.230	20.602	0.000	0.172
50	9	0	0	0.000	4.230	22.602	0.000	0.172
52	9	0	0	0.000	4.230	18.602	0.000	0.172
54	9	0	0	0.000	4.230	15.320	0.000	0.172
56	9	0	0	0.000	4.230	12.160	0.000	0.172
58	9	0	0	0.000	4.230	9.320	0.000	0.172
60	9	0	0	0.000	4.230	8.980	0.000	0.172
62	9	0	0	0.000	4.230	9.910	0.000	0.172
64	9	0	0	0.000	4.230	8.010	0.000	0.172

* Data only shown for every 2^{nd} day of digestion although sampling was done daily.

Sample calculations

Biogas productivity was calculated by determining the amount of biogas produced (mL) over a specific numberof hours. Unit conversion yielded the final value in terms of L Biogas/ $L_{reactor}$.day as shown in Equation 8.4.

$$Biogas\,productivity_{(L\,Biogas/L_{reactor}.day)} = \frac{Biogas\,produced(L)}{Reactor\,volume(L) * (24hrs + \triangle min/60 + \triangle hrs)} * 24/1000 \tag{8.4}$$

The **biogas methane content** was determined using the comparison of peak area obtained from a standard containing 52.8% CH_4 vol/vol, and the specific sample following GC FID analysis (Equation 8.5).

$$Biogas\,methane\,content_{(\%\,CH_4 vol/vol)} = \frac{Integrated\,peak\,area_{sample}}{Integrated\,peak\,area_{standard}} * 52.8 \tag{8.5}$$

The **methane productivity** was calculated by multiplying the biogas productivity and the methane content of the biogas, according to Equation 8.6.

$$Methane\,productivity_{(L\,CH_4/L_{reactor}.day)} = Biogas\,productivity_{(L\,Biogas/L_{reactor}.day)} * CH_4\,content_{(\%\,CH_4 vol/vol)} \tag{8.6}$$

The **methane yield** in terms of VS was calculated as the quotient of the cumulative methane produced and the total VS loaded into the reactor (equation 8.7)

$$Methane\,Yield_{(L\,CH_4/g\,VS)} = \frac{Cumulative\,CH_4\,produced(L)}{VS\,loaded(g)} \tag{8.7}$$

Using these calculations the sample data set shown in Table 8.24 was developed for each digester. The average results and standard deviations were then calculated for each substrate tested with the number of digesters run n=3 (Table 8.25 to 8.29). It should be noted that for some specific result the average relative error may seem quite significant. Due to the nature of the digestion process, the sensitivity of the anaerobic consortia to system parameters, the gaseous phase results may be distinctly different on a specific day. However, more important to this is the overall trend observed through digestion. For instance, the period for which biogas production is at a maximum or the shape of the cumulative methane yield profile etc.

Whole cell digesters

Table 8.25: Key gaseous phase raw data for batch digestion of whole cell *Spirulina spp.* (n=3)

Day	Biogas Productivity (L Biogas /$L_{reactor}$.day)	STDEV (L Biogas /$L_{reactor}$.day)	Methane Content (% CH_4 vol/vol)	STDEV (% CH_4 vol/vol)	Methane Productivity (L CH_4 / $L_{reactor}$.day)	STDEV (L CH_4 / $L_{reactor}$.day)	Methane Yield (L CH_4 /g VS)	STDEV (L CH_4 / g VS)
0	0.0000	0.0000	0.00	0.00	0.0000	0.0000	0.000	0.000
2	0.3021	0.3269	15.19	6.85	0.0571	0.0703	0.007	0.007
4	0.0325	0.0044	17.61	5.10	0.0056	0.0009	0.008	0.007
6	0.0068	0.0096	11.50	0.39	0.0008	0.0011	0.008	0.007
8	0.0000	0.0000	8.98	1.60	0.0000	0.0000	0.008	0.007
10	0.0000	0.0000	10.35	1.15	0.0000	0.0000	0.008	0.007
12	0.0043	0.0061	13.18	1.89	0.0006	0.0008	0.008	0.007
14	0.0185	0.0261	21.56	8.68	0.0051	0.0072	0.009	0.007
16	0.0109	0.0015	17.93	11.72	0.0020	0.0016	0.009	0.007
18	0.0613	0.0439	37.02	0.73	0.0228	0.0167	0.011	0.006
20	0.0978	0.0007	62.71	6.07	0.0614	0.0064	0.016	0.007
22	0.1162	0.0214	81.23	1.51	0.0946	0.0191	0.026	0.004
24	0.1824	0.0191	83.82	5.18	0.1534	0.0254	0.045	0.001
26	0.2137	0.0339	82.09	0.12	0.1754	0.0275	0.066	0.003
28	0.1118	0.0275	80.48	3.24	0.0904	0.0258	0.081	0.003
30	0.0394	0.0145	67.79	20.96	0.0282	0.0181	0.085	0.002
32	0.0535	0.0615	58.65	24.18	0.0388	0.0490	0.089	0.003
34	0.0894	0.0456	51.36	19.29	0.0503	0.0406	0.096	0.011
36	0.0456	0.0221	61.07	16.49	0.0297	0.0210	0.099	0.012
38	0.0642	0.0082	57.45	3.60	0.0370	0.0070	0.103	0.012
40	0.0315	0.0219	49.21	5.93	0.0161	0.0126	0.105	0.011
42	0.0309	0.0145	54.29	1.58	0.0166	0.0074	0.108	0.010
44	0.0213	0.0233	50.99	11.30	0.0122	0.0143	0.110	0.012
46	0.0435	0.0403	38.99	29.69	0.0229	0.0286	0.112	0.014
48	0.0118	0.0012	23.54	13.49	0.0029	0.0019	0.113	0.016
50	0.0052	0.0073	10.18	13.24	0.0000	0.0001	0.113	0.016
52	0.0060	0.0085	12.77	4.34	0.0010	0.0013	0.113	0.016
54	0.0075	0.0106	3.56	3.45	0.0001	0.0001	0.113	0.016
56	0.0027	0.0038	1.34	0.67	0.0000	0.0001	0.113	0.016
58	0.0024	0.0034	0.50	2.01	0.0000	0.0000	0.113	0.016
60	0.0050	0.0071	1.35	1.21	0.0000	0.0000	0.113	0.016
62	0.0050	0.0071	0.55	0.87	0.0000	0.0000	0.113	0.016
64	0.0000	0.0000	2.46	0.12	0.0000	0.0000	0.113	0.016

* Data only shown for every 2^{nd} day of digestion although sampling was done daily.

Table 8.26: Key gaseous phase raw data for batch digestion of whole cell *Scenedesmus spp.* (n=3)

Day	Biogas Productivity (L Biogas /$L_{reactor}$.day)	STDEV (L Biogas /$L_{reactor}$.day)	Methane Content (% CH_4 vol/vol)	STDEV (% CH_4 vol/vol)	Methane Productivity (L CH_4 / $L_{reactor}$.day)	STDEV (L CH_4 / $L_{reactor}$.day)	Methane Yield (L CH_4 /g VS)	STDEV (L CH_4 /g VS)
1	0.4725	0.0065	4.67	4.66	0.022	0.022	0.001	0.001
2	0.0000	0.0000	9.28	12.71	0.000	0.000	0.001	0.001
3	0.0000	0.0000	8.56	10.95	0.000	0.000	0.001	0.001
4	0.0000	0.0000	4.41	5.78	0.000	0.000	0.001	0.001
5	0.0000	0.0000	2.07	0.14	0.000	0.000	0.001	0.001
6	0.0000	0.0000	5.23	5.56	0.000	0.000	0.001	0.001
7	0.0000	0.0000	9.76	10.43	0.000	0.000	0.001	0.001
8	0.0070	0.0120	9.24	11.62	0.000	0.000	0.001	0.001
9	0.0140	0.0104	26.34	7.52	0.004	0.003	0.001	0.001
10	0.0099	0.0001	27.86	8.15	0.003	0.001	0.001	0.001
11	0.0197	0.0267	46.42	10.54	0.010	0.014	0.002	0.001
12	0.0280	0.0451	60.87	13.57	0.019	0.031	0.003	0.003
13	0.0849	0.0262	63.41	11.03	0.056	0.024	0.007	0.003
14	0.0986	0.0544	67.84	10.73	0.071	0.044	0.011	0.006
15	0.1110	0.0591	71.59	8.28	0.083	0.049	0.016	0.008
16	0.1533	0.0987	73.68	12.17	0.120	0.085	0.024	0.014
17	0.0739	0.0217	78.85	11.61	0.060	0.024	0.028	0.015
18	0.0533	0.0286	66.75	11.52	0.038	0.026	0.030	0.015
19	0.0323	0.0238	61.12	11.81	0.020	0.016	0.031	0.016
20	0.0432	0.0291	67.14	19.99	0.033	0.025	0.033	0.018
21	0.0501	0.0473	63.24	20.15	0.036	0.033	0.035	0.020
22	0.0677	0.0475	62.98	16.23	0.048	0.036	0.038	0.022
23	0.0621	0.0207	67.30	16.22	0.044	0.021	0.042	0.024
24	0.0648	0.0510	62.95	9.75	0.042	0.035	0.044	0.026
25	0.0305	0.0226	60.61	1.08	0.018	0.014	0.045	0.025
26	0.0169	0.0138	64.77	10.45	0.011	0.009	0.046	0.024
27	0.0270	0.0286	69.50	6.56	0.019	0.021	0.047	0.023
28	0.0250	0.0277	64.95	12.65	0.018	0.022	0.048	0.022
29	0.0408	0.0524	61.57	13.67	0.029	0.039	0.050	0.019
30	0.0324	0.0438	60.51	16.80	0.022	0.031	0.051	0.018
31	0.0093	0.0092	49.90	11.85	0.005	0.006	0.051	0.017
32	0.0167	0.0289	46.07	12.71	0.010	0.017	0.052	0.016
33	0.0297	0.0415	35.26	20.96	0.016	0.025	0.053	0.014
34	0.0072	0.0124	36.33	22.12	0.004	0.007	0.054	0.014
35	0.0037	0.0064	39.57	18.74	0.002	0.004	0.054	0.014
36	0.0003	0.0006	38.51	16.41	0.000	0.000	0.054	0.014
37	0.0000	0.0000	35.68	14.42	0.000	0.000	0.054	0.014
38	0.0000	0.0000	26.70	20.65	0.000	0.000	0.054	0.014
39	0.0009	0.0016	27.87	15.80	0.000	0.001	0.054	0.014
40	0.0007	0.0012	26.62	12.67	0.000	0.000	0.054	0.014
41	0.0000	0.0000	13.67	0.58	0.000	0.000	0.054	0.014
42	0.0000	0.0000	11.50	0.71	0.000	0.000	0.054	0.014
43	0.0068	0.0118	10.01	5.01	0.001	0.002	0.054	0.014
44	0.0000	0.0000	10.22	3.67	0.000	0.000	0.054	0.014
45	0.0000	0.0000	9.24	5.32	0.000	0.000	0.054	0.014
46	0.0000	0.0000	8.18	5.41	0.000	0.000	0.054	0.014
48	0.0000	0.0000	5.97	3.84	0.000	0.000	0.054	0.014

Ruptured cell digesters

Table 8.27: Key gaseous phase raw data for batch digestion of ruptured cell *Spirulina spp.* (n=3)

Day	Biogas Productivity (L Biogas /$L_{reactor}$.day)	STDEV (L Biogas /$L_{reactor}$.day)	Methane Content (% CH_4 vol/vol)	STDEV (% CH_4 vol/vol)	Methane Productivity (L CH_4 / $L_{reactor}$.day)	STDEV (L CH_4 / $L_{reactor}$.day)	Methane Yield (L CH_4 /g VS)	STDEV (L CH_4 /g VS)
0	0.0000	0.0000	0.00	0.00	0.0000	0.0000	0.000	0.000
2	0.0701	0.0187	16.58	4.36	0.0119	0.0041	0.010	0.004
4	0.0234	0.0159	24.12	6.36	0.0061	0.0045	0.011	0.005
6	0.0203	0.0189	28.66	15.32	0.0068	0.0052	0.011	0.005
8	0.0292	0.0185	43.77	7.87	0.0135	0.0053	0.015	0.005
10	0.0507	0.0304	48.97	19.85	0.0286	0.0080	0.015	0.008
12	0.0545	0.0000	64.59	2.79	0.0352	0.0063	0.024	0.006
14	0.0597	0.0103	64.39	9.13	0.0389	0.0105	0.023	0.011
16	0.0595	0.0073	66.49	2.17	0.0397	0.0113	0.028	0.011
18	0.0690	0.0108	67.74	1.14	0.0467	0.0110	0.034	0.011
20	0.0991	0.0534	73.01	6.67	0.0747	0.0051	0.043	0.005
22	0.1663	0.1626	77.24	5.31	0.1337	0.0123	0.057	0.012
24	0.2225	0.0737	78.51	4.09	0.1750	0.0231	0.079	0.023
26	0.3204	0.0997	81.03	2.62	0.2613	0.0189	0.110	0.019
28	0.2339	0.1159	80.33	1.76	0.1892	0.0091	0.135	0.009
30	0.1347	0.1093	72.51	1.76	0.0983	0.0092	0.148	0.009
32	0.0864	0.0186	58.62	32.44	0.0480	0.0073	0.156	0.007
34	0.0396	0.0299	59.67	38.72	0.0283	0.0066	0.159	0.007
36	0.0353	0.0306	57.21	29.89	0.0263	0.0065	0.162	0.007
38	0.0103	0.0089	52.30	24.65	0.0052	0.0050	0.164	0.005
40	0.0383	0.0501	35.23	9.58	0.0111	0.0064	0.165	0.006
42	0.0043	0.0075	23.80	12.61	0.0017	0.0065	0.165	0.006
44	0.0051	0.0088	22.26	13.97	0.0019	0.0064	0.165	0.006
46	0.0016	0.0028	23.14	13.34	0.0006	0.0065	0.165	0.006
48	0.0000	0.0000	22.78	7.93	0.0000	0.0065	0.165	0.006
50	0.0000	0.0000	22.28	5.95	0.0000	0.0065	0.165	0.006
52	0.0000	0.0000	21.61	4.71	0.0000	0.0065	0.165	0.006
54	0.0023	0.0040	22.92	5.86	0.0006	0.0065	0.166	0.006
56	0.0033	0.0057	24.59	7.29	0.0009	0.0065	0.166	0.006
58	0.0033	0.0058	26.92	7.61	0.0011	0.0065	0.166	0.006
60	0.0007	0.0012	27.49	6.50	0.0002	0.0065	0.166	0.006
62	0.0044	0.0076	24.67	9.20	0.0015	0.0065	0.166	0.007
64	0.0083	0.0104	28.53	6.24	0.0021	0.0067	0.166	0.007

* Data only shown for every 2^{nd} day of digestion although sampling was done daily.

Table 8.28: Key gaseous phase raw data for batch digestion of ruptured cell *Scenedesmus spp.* (n=3)

Day	Biogas Productivity (L Biogas /$L_{reactor}$.day)	STDEV (L Biogas /$L_{reactor}$.day)	Methane Content (% CH_4 vol/vol)	STDEV (% CH_4 vol/vol)	Methane Productivity (L CH_4 / $L_{reactor}$.day)	STDEV (L CH_4 / $L_{reactor}$.day)	Methane Yield (L CH_4 /g VS)	STDEV (L CH_4 /g VS)
1	0.6582	0.4546	2.53	2.15	0.0104	0.0098	0.001	0.001
2	0.6700	0.1639	2.40	0.53	0.0155	0.0010	0.002	0.000
3	0.0546	0.0739	3.00	1.92	0.0011	0.0015	0.002	0.000
4	0.0272	0.0472	1.62	1.16	0.0002	0.0003	0.002	0.000
5	0.0067	0.0058	1.24	1.12	0.0001	0.0001	0.002	0.000
6	0.0341	0.0591	4.61	5.87	0.0009	0.0015	0.002	0.000
7	0.0066	0.0115	4.38	2.89	0.0002	0.0004	0.002	0.000
8	0.0520	0.0454	8.23	11.91	0.0068	0.0100	0.002	0.001
9	0.0133	0.0115	11.31	16.94	0.0023	0.0034	0.002	0.001
10	0.0100	0.0100	14.70	16.03	0.0019	0.0017	0.002	0.001
11	0.0153	0.0134	20.97	11.01	0.0035	0.0042	0.003	0.002
12	0.0164	0.0234	18.49	10.00	0.0045	0.0070	0.003	0.001
13	0.0305	0.0141	32.16	13.43	0.0111	0.0097	0.004	0.001
14	0.0447	0.0129	47.81	15.17	0.0227	0.0120	0.005	0.002
15	0.0583	0.0382	49.22	19.71	0.0335	0.0336	0.008	0.004
16	0.1017	0.0375	65.62	15.82	0.0675	0.0353	0.012	0.006
17	0.0801	0.0578	71.01	11.50	0.0611	0.0494	0.016	0.008
18	0.0797	0.0231	80.57	1.31	0.0641	0.0182	0.019	0.009
19	0.0684	0.0422	72.54	6.54	0.0509	0.0337	0.023	0.008
20	0.1310	0.0749	71.66	10.97	0.0990	0.0630	0.029	0.004
21	0.0823	0.0168	73.28	7.43	0.0611	0.0176	0.033	0.003
22	0.0842	0.0164	73.17	7.18	0.0623	0.0169	0.037	0.003
23	0.0906	0.0340	75.12	7.72	0.0697	0.0308	0.042	0.002
24	0.1091	0.0623	75.87	9.18	0.0856	0.0538	0.046	0.005
25	0.1732	0.0847	66.27	3.33	0.1165	0.0618	0.053	0.008
26	0.2027	0.0613	67.58	7.17	0.1340	0.0278	0.062	0.009
27	0.1707	0.0713	69.95	13.78	0.1202	0.0608	0.070	0.013
28	0.1871	0.0523	76.48	5.68	0.1429	0.0420	0.078	0.016
29	0.1263	0.0233	78.56	2.41	0.0996	0.0210	0.085	0.016
30	0.1650	0.1255	66.78	16.48	0.1165	0.1101	0.091	0.014
31	0.0840	0.0358	61.15	21.49	0.0507	0.0301	0.095	0.015
32	0.0499	0.0076	55.78	24.86	0.0289	0.0152	0.096	0.014
33	0.0174	0.0129	30.23	1.47	0.0051	0.0037	0.097	0.014
34	0	0	27.52	3.54	0	0	0.097	0.014
35	0	0	24.31	9.90	0	0	0.097	0.014
36	0	0	24.72	16.89	0	0	0.097	0.014
37	0	0	25.42	19.22	0	0	0.097	0.014
38	0	0	18.26	11.36	0	0	0.097	0.014
39	0	0	23.50	4.95	0	0	0.097	0.014
40	0	0	16.28	11.33	0	0	0.097	0.014
41	0	0	15.64	10.74	0	0	0.097	0.014
42	0	0	20.50	4.95	0	0	0.097	0.014
43	0	0	14.33	9.62	0	0	0.097	0.014
44	0	0	14.26	8.13	0	0	0.097	0.014
45	0	0	17.50	4.95	0	0	0.097	0.014
46	0	0	16.50	4.95	0	0	0.097	0.014
48	0	0	12.84	4.52	0	0	0.097	0.014

DT Residue digesters

Table 8.29: Key gaseous phase raw data for batch digestion of *Scenedesmus spp.* DT residue (n=1)

Day	Biogas Productivity (L Biogas /$L_{reactor}$.day)	Methane Content (% CH_4 vol/vol)	Methane Productivity (L CH_4 / $L_{reactor}$.day)	Methane Yield (L CH_4 /g VS)
0	0.000	0.00	0.000	0.000
2	0.400	13.68	0.074	0.011
4	0.000	6.36	0.000	0.011
6	0.000	5.77	0.000	0.011
8	0.000	5.29	0.000	0.011
10	0.000	6.14	0.000	0.011
12	0.000	3.78	0.000	0.011
14	0.020	25.59	0.000	0.011
16	0.016	26.76	0.001	0.011
18	0.012	28.93	0.002	0.012
20	0.033	35.07	0.007	0.012
22	0.024	40.40	0.011	0.014
24	0.062	49.64	0.034	0.017
26	0.120	52.93	0.072	0.025
28	0.122	47.36	0.075	0.035
30	0.146	56.25	0.112	0.048
32	0.164	51.36	0.107	0.061
34	0.127	45.75	0.066	0.069
36	0.052	54.00	0.028	0.074
38	0.022	56.00	0.012	0.075
40	0.018	32.00	0.006	0.076
42	0.000	12.00	0.000	0.076
44	0.000	12.00	0.000	0.076
46	0.000	8.00	0.000	0.076
48	0.000	4.00	0.000	0.076

Derived variables

Sample calculations

Volatile Solids Destruction

As mentioned in the text, volatile solids destruction was calculated using Varel's equation. The following equations were used to arrive at the final % destruction presented in the text.

Firstly convert the total cumulative volume of methane and biogas produced through digestion to mols using the fact that at STP 1 mol of gas occupies 22.4 L. Using this the total mols of CO_2 can be calculated from the difference.

$$mol\,CH_4 = L\,CH_4/22.4 \tag{8.8}$$

$$mol\,Biogas = L\,Biogas/22.4 \tag{8.9}$$

$$mol\,CO_2 = mol\,Biogas - mol\,CH_4 \tag{8.10}$$

Then using the carbon percentage in the solid biomass and the cumulative mols of carbon released in the biogas, calculate the total mass (g) of initial carbon that was released in the biogas.

$$VS\,destroyed\,(g) = (molCO_2 + molCH_4)\,X\,(12/(carbon\,content\,of\,biomass)) \tag{8.11}$$

Finally the percentage of total carbon (or volatile solids) released in the biogas can be calculated by using the total initial loading

$$\%\,VS\,destruction = \frac{VS\,destroyed\,(g)}{VS\,loaded\,(g)} \tag{8.12}$$

Solid COD Destruction

The solid COD destruction was calculated as the ratio of final and initital solid COD concentration according to Equation 8.22.

$$\%\,Solid\,COD\,destruction = \frac{Solid\,COD_{final}}{Solid\,COD_{initial}} * 100 \tag{8.13}$$

Total COD Destruction

Similarly the total COD destruction was calculated as the ratio of the final and initial total COD concen-

tration according to Equation 8.24.

$$\%Total\,COD\,destruction = \frac{Total\,COD_{final}}{Total\,COD_{initial}} * 100 \tag{8.14}$$

VFA Destruction

The total VFA destruction was calculated as the ratio of the final and initial total VFA concentration concentration experienced at any point during digestion according to Equation 8.15.

$$\%Total\,VFA\,destruction = \frac{Total\,VFA_{final}}{Total\,VFA_{maximum}} * 100 \tag{8.15}$$

COD Yields

The COD yield was calculated as the quotient of cumulative methane yield over digestion and the total COD destroyed over digestion according to Equation 8.16.

$$COD\ Methane\,Yield_{(L\,CH_4/g\,COD)} = \frac{Cumulative\,CH_4(L)\,produced}{Total\,COD\,destroyed(g)} * 100 \tag{8.16}$$

The derived variables were calculated for each set of digesters and an average value presented in the text. Table 8.30 presents the average value.

Table 8.30: Derived variables for all batch digestion with standard deviations (n=3)

Digester substrate	VS destruction (%)	Solid COD Destruction (%)	Total COD Destruction (%)	Total VFA Destruction (%)	COD Yield (L CH_4/ g COD destroyed)
Spirulina spp. whole cells	20	86	86	89	0.06
Scenedesmus spp. whole cells	16	53	60	98	0.06
Spirulina spp. ruptured cells	27	69	81	92	0.09
Scenedesmus spp. ruptured cells	24	75	81	80	0.07
Scenedesmus spp. DT residue	17	75	66	87	0.05

8.3 Appendix C: Integrated algal anaerobic digestion system results work-up

Introduction

The following appendix summarises the most important data obtained through the semi-continuous digestion studies and continuous algal growth and harvesting of this thesis. The approach taken to best represent the data to provide a solid understanding of the data was as follows:

1. Present a full set of results obtained from the algal growth unit over time, with sample calculations.
2. Present the full set aqueous and gaseous phase raw data results from the AD unit, with sample calculations.
3. Using this data set, present all the derived variables with sample calculations.

Algal growth unit data

The productivity was calculated based on a harvest every 24 hours. The total wet weight collected was determined in terms of DW and VS harvested by using the dry weight and volatile solids contents of the wet biomass. A specific productivity (Table 8.31) in terms of m^2 was calculated by dividing by this amount by the surface area of the growth unit, equation 8.17.

$$Algal\,growth\,productivity_{(g\,VS/m^2.day)} = \frac{Total\,DW\,(g) * VS_{content}(\%)}{Surface\,Area\,(m^2)} \tag{8.17}$$

Table 8.31: Alagal productivity for continuous growth of *Spirulina spp.* raw data sheet

Day	WW Harvested (g)	Productvity (g VS/m^2.day)
0	0	11.5
2	90	11.4
4	108	13.1
6	106	12.3
8	110	13.0
10	118	14.1
12	103	11.9
14	120	13.8
16	90	10.4
18	96	11.1
20	100	11.6
22	98	11.7
24	69	10.7
26	90	10.3
28	88	10.3
30	84	9.7
32	88	10.1
34	68	8.2
36	85	9.7
38	65	7.5
40	60	7.2
42	73	8.8
44	73	8.2
46	73	8.2
48	73	8.2
50	74	8.4

* Data shown for every second day of harvesting and up until day 50 of continuous operation

Semi-continuous AD unit

Aqueous phase data

The **organic loading rate** fed to the semi-continuous AD unit, was determined by the VS concentration in the 286 mL fed to the digester. A sample of the feed was taken, filtered and dried at 105 ℃ overnight and then at 550 ℃ for 2 hours to ensure the desired OLR was obtained (Table 8.32).

Table 8.32: OLR for semi-continuous AD of *Spirulina spp.* raw data sheet

Day	WW Harvested (g)
0	1.5
2	1.8
4	1.8
6	1.6
8	1.8
10	1.6
12	1.1
14	1.1
16	1.1
18	1.1
20	1.2
22	1.4
24	1.2
26	1.1
28	1.3
30	1.2
32	1.1
34	0.0
36	0.0
38	0.0
40	0.0
42	0.0
44	0.5
46	0.5
48	0.5
50	0.4
52	0.4
54	0.4

* Data shown for every second day of harvesting and up until day 54 of semi-continuous operation

The **Nitrate and phosphate ions** were all calculated using the respective assays. That is using the integrated peak areas obtained from the chromatogram produced by the HPLC and then adapting the standard curves equation with the dilution factor to arrive at the final concentration in the respective sample.

Table 8.33: Nitrate and phosphate ion concentrations raw data for semi-continuous digestion of *Spirulina spp.* algal biomass

Day	Nitrate ion conc. (mg/L)	Phosphate ion Conc. (mg/L)
0	25	376
2	16	550
4	3	454
5	5	449
6	9	556
7	8	607
8	2	651
10	1	706
12	12	638
14	3	618
16	2	626
18	4	502
20	9	563
22	9	563
24	2	521
26	6	570
28	44	505
30	10	575
32	19	415
34	16	466
36	15	501
38	18	468
40	14	465
42	19	465
44	8	397
46	10	401
48	12	365
50	14	345
52	10	332
54	19	301
56	11	298

Soluble, solid and total COD concentrations were determined in a similar fashion as to the batch digestion studies.

Table 8.34: Solid, soluble and total chemical oxygen demand raw data for semi-continuous digestion of *Spirulina spp.* algal biomass

Day	Solid COD (mg/L)	Soluble COD (mg/L)	Total COD (mg/L)
0	4633	8508	13141
1	4661	12670	17331
2	4327	12865	17192
3	4744	9993	14737
4	8555	9555	18110
5	8249	9798	18047
6	8333	10553	18885
7	8778	10991	19768
8	8945	9626	18571
10	9195	9380	18575
12	7443	11275	18718
14	8722	12736	21458
16	7282	11241	18522
18	4661	9780	14441
20	5579	9519	15098
22	5321	10197	15518
24	3632	10563	14194
26	5189	10615	15804
28	5042	12405	17447
30	5348	9209	14557
32	5501	9209	14710
34	5189	10615	15804
36	5523	9554	15077
38	6664	9380	16044
40	7665	9780	17445
42	7526	8633	16159
44	7875	9572	17447
46	7832	7694	15526
48	6485	8129	14613
50	7263	7903	15166
52	6095	8143	14238
54	3703	7437	11140
56	3814	7729	11543

Alkalinity

Non-ionised ammonia and sulphide were calculated using the respective ionised concentrations, the ionisation constant and hydrogen concentration respectively, equation 8.18 and 8.19. The ionised concentrations of each compound were determined from their respective assays.

$$NH_{3dissolved} = \frac{(NH_3 + NH_4^+)K}{(H^+)} \tag{8.18}$$

$$H_2S_{dissolved} = \frac{(HS^-)K}{(H^+)} \tag{8.19}$$

Table 8.35: Non-ionised sulphide and ammonia raw data for semi-continuous digestion of *Spirulina spp.* algal biomass

Day	pH	HS^- Conc. (mg/L)	H_2S Conc. (mg/L)	NH_4^+Conc. (mg/L)	NH_3 Conc. (mg/L)
0	7.93	2.38	18.57	612.19	26.68
2	7.54	23.53	74.89	528.69	9.39
4	7.49	34.93	99.10	613.20	9.70
6	7.22	55.49	84.54	589.73	5.01
8	7.09	65.23	73.67	437.63	2.76
10	7.03	47.65	46.87	501.00	2.75
12	6.99	53.94	48.39	497.87	2.49
14	6.89	39.45	28.11	503.85	2.00
16	6.99	49.19	44.13	506.10	2.53
18	6.99	66.42	59.59	506.10	2.53
20	6.99	66.06	59.27	509.08	2.55
22	7.13	76.40	94.61	498.76	3.44
24	6.99	78.54	70.46	515.28	2.58
26	6.97	54.06	46.32	487.00	2.33
28	7.15	48.95	63.48	498.00	3.60
30	7.03	46.10	45.35	501.00	2.75
32	6.89	40.90	29.15	505.21	2.01
34	6.95	38.30	31.34	505.21	2.31
36	7.20	35.30	51.36	476.00	3.86
38	6.92	32.10	24.51	432.00	1.84
40	7.32	32.90	63.10	415.00	4.44
42	7.18	25.70	35.71	396.00	3.07
44	7.18	27.10	37.65	379.58	2.94
46	6.97	27.10	23.22	386.00	1.84
48	7.05			369.00	2.12
50	7.00			374.00	1.91
52	7.10			310.00	2.00
54	7.06			301.00	1.77
56	6.97			317.00	1.51

VFAs concentrations were determined in the same manner as those in the batch digesters. For specific cases where unexpected results were obtained the samples were rerun and the either the corrected values presented or an average of the two.

Table 8.36: Volatile fatty acid raw data for semi-continuous digestion of *Spirulina spp.* algal biomass

Day	Lactic Acid Conc. (mg/L)	Acetic Acid Conc. (mg/L)	Propionic Acid Conc. (mg/L)	Iso-Butyric Acid Conc. (mg/L)	Butyric Acid Conc. (mg/L)	Iso-Valeric Acid Conc. (mg/L)	Valeric Acid Conc. (mg/L)	Total Acid Conc. (mg/L)
0	13	2359	692	283	140	689	0	4175
1	2	2610	804	299	84	710	25	4533
2	21	2727	852	309	106	738	16	4768
3	28	2647	845	287	145	701	17	4671
4	45	3186	1031	340	233	888	12	5735
5	4	2730	876	274	180	750	14	4829
6	6	2909	963	286	221	874	19	5278
7	2	3040	1045	273	260	933	0	5553
8	10	3173	1039	294	283	1096	4	5900
10	16	3389	1155	359	376	1276	21	6591
12	0	3176	1098	292	313	1231	37	6148
14	6	3127	1124	282	334	1230	9	6112
16	11	3066	1013	244	323	1304	1	5961
18	10	2431	758	197	271	1077	7	4750
20	2	2777	843	185	248	1312	6	5373
22	2	2912	787	211	288	1393	0	5592
24	1	2591	783	162	266	1281	0	5084
26	22	2632	695	201	368	1653	0	5570
28	23	2859	806	211	382	1512	0	5793
30	29	2700	800	202	501	1459	23	5713
32	20	2600	701	355	583	1664	84	6007
34	36	2514	853	207	644	1504	0	5758
36	16	2739	891	249	509	2068	2	6476
38	1	2300	856	251	502	2131	0	6041
40	2	2141	671	257	521	2330	23	5946
42	7	2234	801	297	813	2181	69	6401
44	11	2505	1107	279	744	2027	82	6756
46	11	1659	821	487	719	2001	48	5746
48	13	1839	884	485	658	1903	53	5835
50	0	1873	843	208	534	1475	37	4969
52	3	1867	860	211	565	1637	43	5187
54	1	1820	839	204	525	1521	64	4973
56	0	1847	942	203	589	1432	72	5084

Gaseous phase data

All gaseous phase results were obtained in the same manner as to those from the batch digestion studies. In specific cases where total initial loading was used for batch digestion, the calculationwas manipulated to use total fed in the semi-continuous process. For example the methane yield in terms of VS was calculated using the OLR rather than the initial amount of VS loaded into the reactor.

Table 8.37: Key gaseous phase raw data for semi-continuous digestion of *Spirulina spp.* algal biomass

Day	Biogas Productivity (L Biogas /$L_{reactor}$.day)	Biogas Methane Content (% CH_4 vol/vol)	Methane Productivity (L CH_4 / $L_{reactor}$.day)	Methane Yield (L CH_4 / $L_{reactor}$.day.g VS)
2	0.038	41	0.015	0.009
4	0.070	41	0.029	0.017
6	0.068	40	0.027	0.017
8	0.150	41	0.061	0.037
10	0.163	41	0.067	0.038
12	0.113	47	0.053	0.032
14	0.113	46	0.052	0.069
16	0.075	45	0.034	0.031
18	0.075	44	0.033	0.029
20	0.075	45	0.033	0.030
22	0.113	44	0.049	0.046
24	0.087	41	0.035	0.029
26	0.082	40	0.033	0.033
28	0.060	40	0.024	0.020
30	0.168	39	0.066	0.057
32	0.150	30	0.045	0.040
34	0.085	29	0.024	0.022
36	0.060	30	0.018	-
38	0.050	27	0.014	-
40	0.049	35	0.017	-
42	0.030	30	0.009	-
44	0.058	32	0.019	0.039
46	0.060	35	0.021	0.046
48	0.065	31	0.020	0.044
50	0.068	39	0.026	0.064
52	0.065	41	0.027	0.071
54	0.065	46	0.030	0.070
56	0.075	48	0.036	0.086

* Data only shown for every second day of digestion and only key gaseous phase results presented, - represents period where no substrate was fed.

Derived variables

Sample calculations

Volatile Solids Destruction

As mentioned in the text, volatile solids destruction or destroyed was calculated using Varel's equation. The following equations were used to arrive at the final % destruction presented in the text.

Firslty convert the total volume of methane and biogas produced through digestion, per day, to mols using the fact that at STP 1 mol of gas occupies 22.4 L. Using this the total mols of CO_2 can be calculated from the difference, as shown in eqations 8.8-8.10. Then using the carbon percentage in the solid biomass and the cumulative mols of carbon released in the biogas, calculate the total mass (g) of fed carbon that was released in the biogas.

$$VS\,destroyed\,(g) = (molCO_2 + molCH_4)\,X\,(12/(carbon\,content\,of\,biomass\,fed)) \tag{8.20}$$

Finally the percentage of total carbon (or volatile solids) fed to the reactor and released in the biogas can be calculated by usig the total initial loading

$$\%\,VS\,destruction = \frac{VS\,destroyed\,(g)}{VS\,fed\,(g)} \tag{8.21}$$

Solid COD Destruction

The solid COD destruction was calculated using the amount of solid COD in the digester at time i+1, determined from the concentration in the effluent, and comparing it to the solid COD in the digester at time i. The difference was then divded by the amount of solid COD fed at time i to get a % destruction, shown in equation 8.22.

$$\%\,Solid\,COD\,destruction = \frac{(Solid\,COD_{digester}(mg))_i - (Solid\,COD_{digester}(mg))_{i+1}}{Solid\,COD_{fed}(mg)_i} * 100 \tag{8.22}$$

Total COD Destruction

Similar to solid COD using total COD, shown in equation 8.23.

$$\%Total\,COD\,destruction = \frac{(Total\,COD_{digester}(mg))_i - (Total\,COD_{digester}(mg))_{i+1}}{Total\,COD_{fed}(mg)_i} * 100 \tag{8.23}$$

Total Solids Destruction

Similar to solid COD using TS's, show in equation 8.24

$$\%Total\,Solids\,destruction = \frac{(Total\,Solids_{digester}(mg))_i - (Total\,Solids_{digester}(mg))_{i+1}}{Total\,Solids_{fed}(mg)_i} * 100 \tag{8.24}$$

The derived variables were determined across the total 56 day digestion period and an average value for each retention time was presented in the text, see Table 8.39.

Table 8.38: Raw data for calculation of derived variables in semi-continuous AD of *Spirulina spp.* algal biomass

Day	TS fed (g)	Total COD Fed (mg)	Solid COD Fed (mg)	TS digester (g)	Total COD digester (mg)
0	6	8242	6868	17	52565
1	8	9754	8128	16	69324
2	8	10076	8396	8	68768
3	8	9989	8324	35	58949
4	8	10695	8913	34	72439
5	7	8855	7379	32	72189
6	8	9785	8154	61	75541
7	7	9227	7689	61	79074
8	8	11030	9192	51	74284
10	8	9778	8149	67	74302
12	5	6953	5794	55	74872
14	5	6829	5691	60	85831
16	5	6742	5618	57	74090
18	5	6816	5680	57	57765
20	5	7139	5949	52	60393
22	6	8180	6816	35	62073
24	6	7622	6352	46	56777
26	5	7077	5897	53	63217
28	6	8006	6672	53	69789
30	6	7510	6259	52	58228
32	5	7064	5887	50	58840
34	0	0	0	50	63217
36	0	0	0	27	60310
38	0	0	0	27	64176
40	0	0	0	18	69781
42	0	0	0	36	64635
44	2	2956	2463	36	69788
46	2	3160	2634	26	62104
48	2	3083	2569	22	58453
50	2	2677	2231	22	60664
52	2	2528	2107	22	56952
54	2	2640	2200	21	44560
56	2	2640	2200	21	46174

Table 8.39: Derived variables for all retention times of semi-continuous AD of *Spirulina spp.* algal biomass

Retention period	VS destruction (%)	Solid COD Destruction (%)	Total COD Destruction (%)	Total Solids Destruction (%)
1	7.9	83	68	78
2	8.1	97	75	111
3	12.3	81	43	73
4	13.2	155	136	145

8.4 Appendix D: Energy production analysis results work-up

The final results chapter of this thesis presented results in potential bioenergy production from anaerobic digestion of the specific algal biomass identified as potentially suitable biomass feed stocks. The manner in which the key results were obtained is presented in this appendix.

Energy input requirement for plant energy crops

Table 8.40: Energy input for maize crop production (Braun et al., 2010)

operation	No of operations	equipment	time (h/ha)	energy of equipment MJ/ha	tractor (kW)	fuel used (l/ha)
subsoil	1	subsoiler	1.333	120	90	14.6
plough	1	plough+press	1.333	120	90	17.5
drill/harrow	1	combined drill and harrow	0.62	158	90	3.9
fertiliser	1	fertiliser spreader	0.36	45	55	1.2
spray	2	sprayer	0.54	68	55	2.4
harvest	1	forage harvester	2	420		17.5
cart	1	trailer	2	120	55	7.8
ensile	1	tractor and bucket	1.48	8	55	5.8
tractor		90 kW	3.286	564		
tractor		55 kW	4.38	297		
fuel used (litres)				2785 MJ/ha		70.7
total indirect				1920 MJ/ha		
			hours			
labour			9.7	18.8 MJ/ha		
seed		kg/ha	16	215 MJ/ha		
chemicals			(kg/ha)			
N			150	6045 MJ/ha		
P_2O_5			200	680 MJ/ha		
K_2O			175	1277.5 MJ/ha		
packaging & transport				1362 MJ/ha		
sprays			12.8	2432 MJ/ha		
total energy input to crop production and storage				**16.7 GJ/ha**		